POLYBENZOXAZINE MATERIALS FROM RENEWABLE DIPHENOLIC ACID

Camilo Javier Zúñiga Ruiz

Dipòsit Legal: T.1559-2013

Camilo Javier Zúñiga Ruiz

POLYBENZOXAZINE MATERIALS FROM RENEWABLE DIPHENOLIC ACID

PhD thesis

Supervised by Dr. Virginia Cádiz Deleito and Dr. Joan Carles Ronda Bargalló

Department of Analytical Chemistry and Organic Chemistry

UNIVERSITAT ROVIRA I VIRGILI

Tarragona
2013

UNIVERSITAT ROVIRA I VIRGILI
Departament de Química Analítica i Química Orgànica
C/ Marcel·lí Domingo, s/n
Campus Sescelades
43007, Tarragona
Telf. 977 559 769
Fax. 977 558 446

Virginia Cádiz Deleito y Joan Carles Ronda Bargalló, ambos catedráticos del Departamento de Química Analítica y Química Orgánica de la Universidad Rovira i Virgili,

HACEN CONSTAR que la presente tesis doctoral, titulada "Polybenzoxazine materials from renewable diphenolic acid" presentada por Camilo Javier Zúñiga Ruiz para la obtención del título de Doctor, ha sido realizada bajo nuestra dirección en el Departamento de Química Analítica y Química Orgánica de esta Universidad y que cumple con los requisitos para poder optar a la Mención Europea

Tarragona, 23 de julio de 2013

Dra. Virginia Cádiz

Dr. Joan Carles Ronda

CONTENTS

CHAPTER 1

GENERAL INTRODUCTION AND SCOPE

1.1. GENERAL INTRODUCTION

Undoubtedly the diversity of polymers and the flexibility of their properties are employed to produce a broad variety of products that bring medical, technological advances, energy savings and numerous other societal benefits. Plastics are everywhere and although today most plastic items are banal and uninteresting to the user/consumer, a day without their use would be unthinkable. As a result, the global plastics production has increased substantially over the last decades from around 0.5 million tonnes in 1950 to 280 million tonnes in 2011, with an annually increase of 9%[1] **(Figure 1)**. Almost all aspects of daily life involve plastics *e.g.,* telecommunications, sports, clothing, footwear and as packing materials that facilitate the transport of a wide of goods. For instance, in Europe the plastic application sector is led by packing (39%), followed by building & construction (20.5%), automotive (8.3%) and electrical & electronic equipment (5.4%) of overall demand. Others (26.4%) include various sectors such as consumer and household appliances, furniture, agriculture, sport, health and safety[1].

Despite several and well-known benefits of plastics, concerns about usage and final disposal, sustainability, environment and effects on wildlife and humans are gaining momentum in both academic and scientific fields.

Usually, plastics are additivated to improve their performance with substantial quantities of one or more chemical compounds. Unfortunately, some of them are toxic or could leach out of products being potentially harmful for humans and wildlife[2]. On the other hand, around 4% of world oil and gas production, a non-renewable resource, is used as feedstock for plastics and a further 3-4% is expended to provide energy for their manufacture[3]. Given the depletion of fossil fuels reserves, the dramatic fluctuation in oil prices, and the relationship between the cost/risk to safety, health and the environment, the use of hydrocarbons for producing low-cost plastic with short-lived applications is becoming increasingly not sustainable[4].

In addition to the reliance on finite resources of plastic production, and concerns about additive effects of chemicals, current patterns of usage are generating global waste management problems. In 2011 post-consumer plastic waste generation across the European Union was 25.1 million tonnes[1]. Large quantities of plastic debris have been accumulated in the natural environment by contaminating a wide range of natural terrestrial and freshwater ecosystems.

Without going further, the great pacific garbage patch, a gyre composed of floating waste plastic and other products, is just a simple example of the ill-fated consequences of the accumulation of plastic waste in the natural environment. Apart from the physical problems related to plastic debris, there exist other problems resulting from ingestion and entanglement of debris in wildlife[5,6]. Indeed, there has been much speculation that if they are ingested by humans, plastic has the potential to transfer toxic substances to the food chain[7].

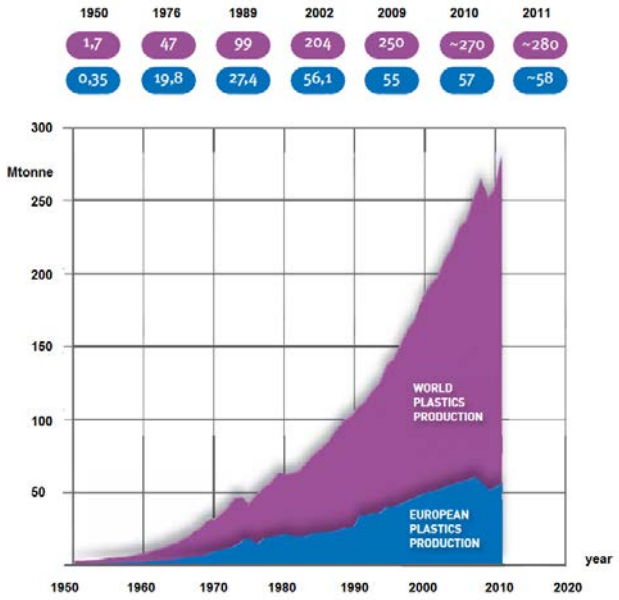

Figure 1. World plastics production from 1950 to 2011[1]

These problems urge to be addressed by several sectors, and also require taking actions beyond a simple awareness campaign. Strategic compromises and agreements on goals of plastic sustainability should be encouraged. For instance, the simple fact for the industry to agree on what a good definition of the term "sustainability" should be in terms of plastics is only a starting point. Not only the development of bio-based or environmentally-friendly plastics but their market penetration supposes new challenges for academic and industrial fields. For their part, the governments need to drive proper regulations in favor of both consumers and producers. Thus, the effectiveness of laws and regulations should be objectively evaluated, and the potential benefits of legal structures not discounted. As regards the media, it is necessary that they stop to frighten people with reports about plastics that are written by journalists with little or no knowledge of chemistry, and sometimes are oversimplified, overgeneralized, or

downright inaccurate. On the contrary, they should try to educate the people honestly about plastics and sustainability and highlight news which are aimed in that direction.

From a waste management perspective, the three R's: Reduce, Reuse, and Recycle are widely advocated to reduce the quantities of plastic that are generated. Together with them, energy Recovery and molecular Redesign are emerging as complementary and potentially important strategies[3]. These approaches have benefits compared with conventional disposal to landfill *i.e.,* some of the energy content is recovered, the environmental impact and resource depletion is reduced, save space when are stored by reducing the amount of packing utilized, the use of biodegradable plastics avoids some separation problems from agricultural applications, among others[3,8].

Precisely, molecular redesign of plastics has become an emerging issue in green chemistry that should be incorporated within the design and life cycle analysis of plastics. In this context, green chemists aspire to design chemical products that are fully effective, yet have little or no toxicity or endocrine-disrupting activity; that break down into innocuous substances if released into the environment after use; and/or that are based upon renewable feedstocks, such as agricultural wastes[3].

In recent years, plastics are becoming less dependent on supplies of fossil fuels. More plastics are being made from renewable resources **(Figure 2)**. The growth rate of bio-based plastics is estimated to be 15-20% in2011, and this growth is expected to continue at multiple times the rate of all plastics growth for the long term (with estimates varying from 12-40% annually)[9].

The use of renewable polymers is not just an academic curiosity. Renewables have the potential to provide a new and sustainable supply of basic chemical building blocks.

Some commercial examples of polymers derived or that integrate renewable resources include the increasingly popular corn ethanol-based polylactic acid (PLA), Nylon 11 Rilsan® based on castor oil, polyesters such as Sorona® and Hytrel® marketed by DuPont and made from corn sugar, polyethylene made from bio-ethanol[10], among many more[11]. Several biological resources are being considered for creating bio-based plastics, ranging from foodcrops to bacteria, and from agricultural wastes to algae. Perhaps some of the most extended examples of the former include the production of cellulose by the *Glucanacetobacter xylinus* strain, which is a remarkably versatile biomaterial

usable in a wide variety of domains, such as papermaking, optics, electronics, acoustics and biomedical devices[12], and the production of polyhydroxyalkanoates (a class of biodegradable polyesters) by various bacteria[13]. Application areas of this kind of polymers include packing, construction, automotive, electrical/electronics, medical and agricultural. These areas show the wide range of ways in which plastics are used, and in which their sustainability is being tested[11].

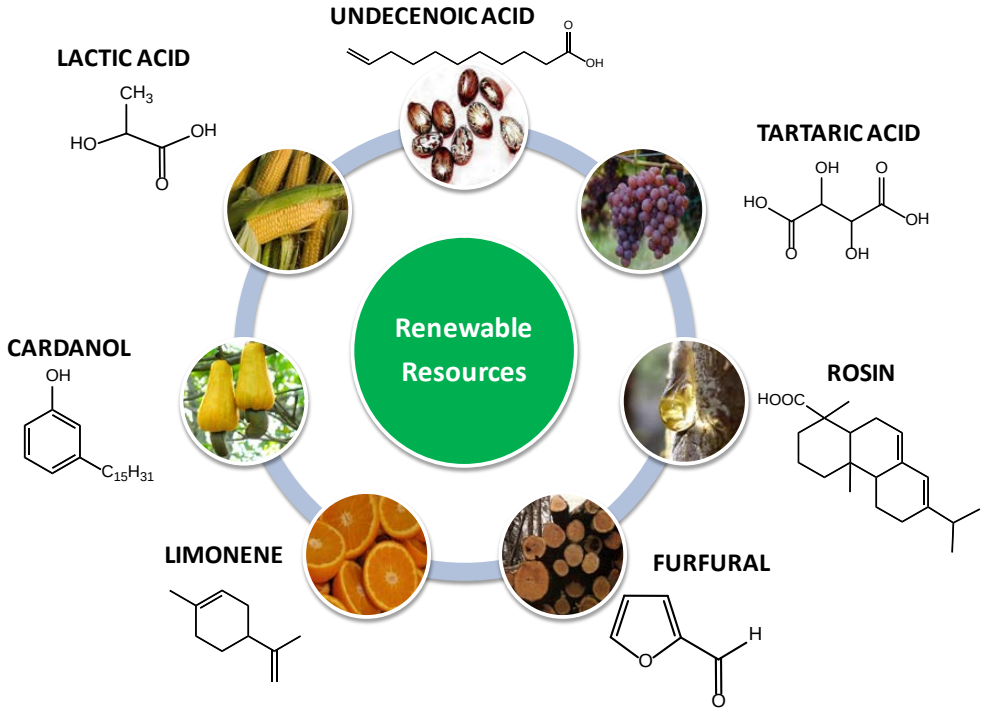

Figure 2. Examples of renewable chemical compounds used for the synthesis of bio-based polymers

Polymeric materials are roughly classified into two main categories: thermoplastics and thermosets. These two have different molecular structures and hence different properties. Thermoset polymers (thermosetting resins) are materials of great interest and a wide versatility in industry due to their excellent electrical, mechanical and thermal properties. They are usually made through a curing reaction from multifunctional precursors of low molecular weight that generate cross-linked polymer networks. The starting point is a group of molecules (monomer or oligomers) that react each other forming chains and branches. As the reaction progresses more molecules join together and various chains linked forming crosslinking points or junctions that finally lead the

formation of a three-dimensional network structure. The properties of the thermosets are strongly determined by the degree of crosslinking of the network. Once thermosets have polymerized, they take a given a permanent shape and become insoluble and infusible, therefore, any part or artifact made of a thermoset requires that the polymerization takes place *in situ*[14]. Epoxy, phenolic, polyurethane, polyimide and polyester resins are the most common high-performance thermosetting polymers.

Polybenzoxazines are considered as a new type of thermosetting phenolic resins that have been developed as an attractive alternative to overcome several shortcomings of epoxies, and traditional resole and novolac phenolic resins while retaining their benefits[15].

Since the first work described by Frederick Holly and Arthur Cope[16] in 1944, polybenzoxazines have prompted a great deal of interest from both a commercial and academic sense worldwide. Benzoxazine is a single benzene ring fused to another six-membered heterocycle containing one atom of oxygen and one of nitrogen. There exist a number of possible isomeric benzoxazines depending upon the relative positions of the two heteroatoms of this oxazine ring system being 1,3-benzoxazine the isomer usually used for polymerization[17].

Typically, benzoxazine monomers are synthesized from phenol, formaldehyde or paraformaldehyde, and amine as starting materials. Precisely, this fact allows a wide range of molecular flexible design because it is possible to introduce several functional groups into their structure[15,18] which in turn can also provide additional crosslinking or post-modifiable sites[19-21]. For the synthesis of benzoxazine monomers, it can be employed the solution or the solventless methods[22]. Among the most organic solvents utilized in the solution approach, are toluene, 1,4-dioxane and chloroform. Their role during the course of a synthesis is to stabilize or destabilize certain species in the reacting pool, thus directly affecting the course of the reaction. Usually, less polar solvents give a higher yield of benzoxazine monomer[23]. Other synthetic methods lie in the use of a triazine precursor compound that render high yields and avoid the formation of oligomers[24,25], the three-step imine method that evolve its formation, reduction and further cyclization with paraformaldehyde[26], and the combination of the three-step approach with the classical one-step synthesis to form unsymmetric bisbenzoxazines *via* tandem reactions[27] (Scheme 1).

Benzoxazines can undergo thermal[19], acid catalyzed[28,29], thiol catalized[30,31] and photo-polymerization[32] through the opening of the oxazine ring.

Polymerization of mono functional benzoxazines renders low molecular weight linear polymers whereas di-functional ones give crosslinked structures. In general, the thermally induced polymerization of benzoxazines gives the corresponding polymers having phenolic moiety bridged by Mannich-type linkage **(Scheme 2a)**. Besides this Mannich-type linkage, there has been reported another type of linkage, N,O-acetal, which can be formed under limited conditions[33] **(Scheme 2b)**. In addition, other studies have demonstrated that the ring opening polymerization does not directly afford the Mannich-type, but provides an intermediary labile polymer having N,O-acetal which undergo a rearrangement reaction in the polymer main chain to give the Mannich-type linkage with generation of phenolic moiety[34,35] **(Scheme 2c).**

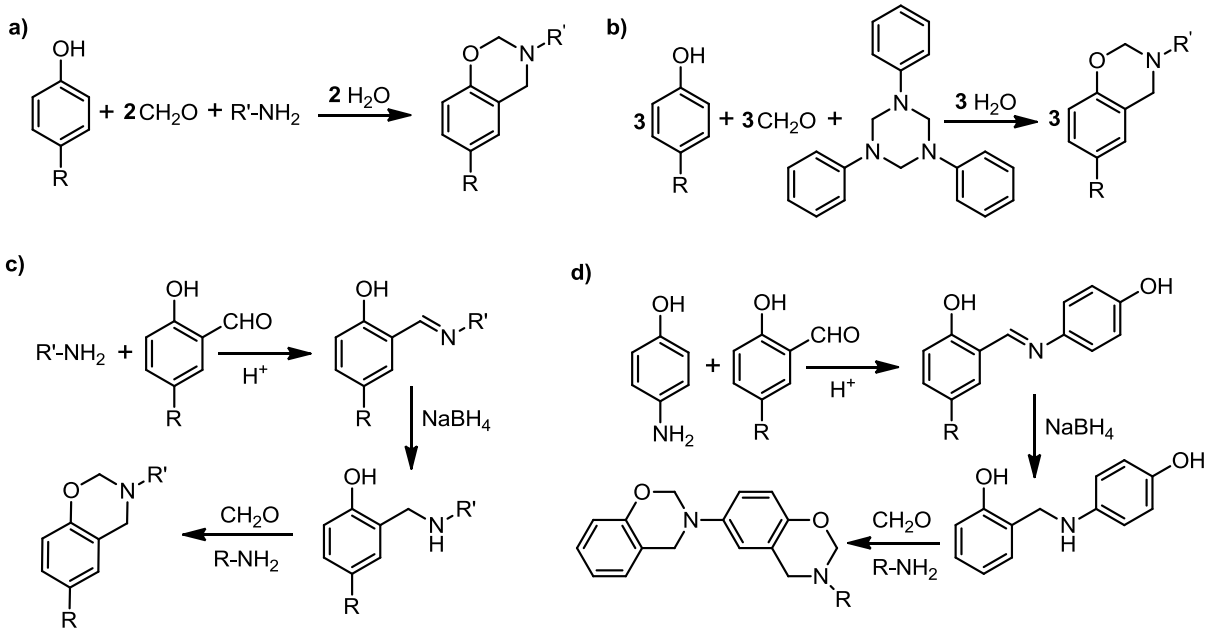

Scheme 1. Pathways of the synthesis of benzoxazines. a) Classical one-step approach, b) triazine approach, c) three-step approach and, d) tandem reactions approach

Polybenzoxazines present unique features such as near zero volumetric change upon polymerization, relatively low melt viscosity, no harsh catalyst required, no volatile release during curing, low water absorption, fast mechanical property build-up as a function of degree of polymerization, high char-yield, low coefficient of thermal expansion, excellent dimensional stability and excellent electrical and flame retardant properties[18,36]. These fascinating characteristics make benzoxazine a promising candidate for various industrial applications,

including electronics, aerospace, composites, coatings, adhesives, and encapsulants manufacturing[37].

Although, polybenzoxazines present a variety of advantages, pure polybenzoxazine-based polymers suffer number of disadvantages too. The disadvantages of the typical polybenzoxazines are the high temperature needed for complete curing, brittleness of the cured materials, and low degree of polymerization that may sometimes limit their potential applications. Moreover, these monomers are usually powders and processing them into thin films is rather difficult. Hence, the enhancement of processability and mechanical properties for polybenzoxazines is indicated. To solve these drawbacks, several strategies have been reported including 1) synthesis of benzoxazine monomers with additional functionality 2) incorporation of benzoxazine groups in a polymer chain and 3) benzoxazine-based composites or alloys[17].

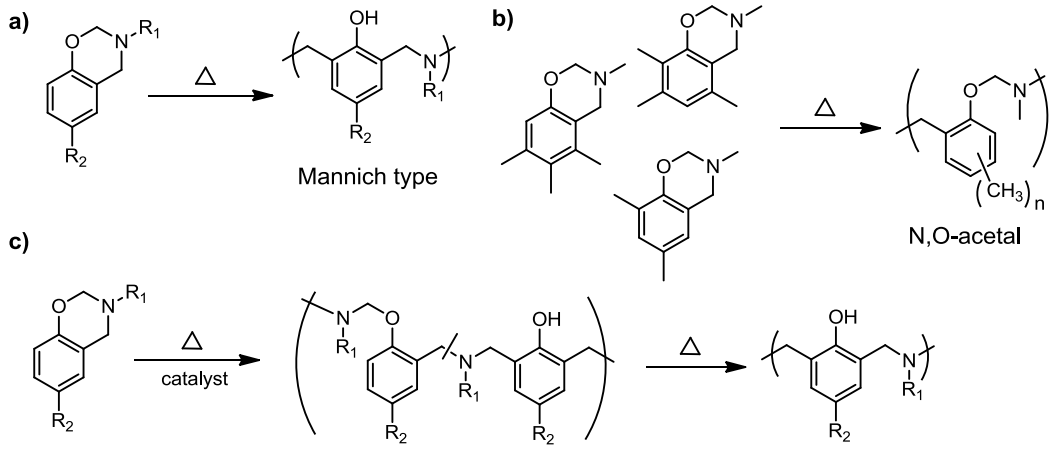

Scheme 2. Ring opening of benzoxazine monomer through a) Mannich-type structure, b) N,O-acetal structure and c) N,O-acetal structure and ulterior rearrangement

As natural resources become scarce, increasing concerns about the environment and sustainability are fueling a growing worldwide research effort devoted for understanding and using renewable materials/feedstocks. Although not many, some successful examples of totally or partially benzoxazine materials derived from renewable resources have been reported in the literature. In **Table 1** are summarized some properties of these renewable polybenzoxazine materials.

Table 1. Characteristics of benzoxazine materials based on natural resources

-based benzoxazine monomers	Natural resource	Starting materials		T_{max}[a] (ºC)	ΔH (ºC)	Tg (ºC)	$T_{5wt\%}$ (ºC)	Char (%) (800ºC)[d]
		Renewables	Non-renewables					
Cardanol	Cashew nuts shell liquid (CNSL)	Cardanol[38]	Formaldehyde, ammonia	243	60.7	36[b]	-	-
		Cardanol[40]	Paraformaldehyde, aniline	263	71.1	-	-	12.0
		Cardanol[39]	Paraformaldehyde, aniline	263	74.0	-	-	-
		CNSL[41]	Paraformaldehyde, methylenediamine	258	83.2	85[b]	343	13.6
		Cardanol-furfural[42]	Formaldehyde, 1,3,5-triazine	275	85.0	80[c]	383	46.2
Terpene	Pine or orange rind	2,8-terpenediphenol[43]	Formaldehyde, aniline	234	-	180[b]	-	-
		1,3-terpenediphenol[43]		245	-	180[b]	-	-
Modified oil	Sunflower oil	Enriched glycerides[44]	Bz-OH, Toluene diisocyanate	215	85.0	-	267	-
Rosin	Pine or conifer	maleopimaric acid imidophenol[45]	Paraformaldehyde, aniline	228	321	-	353	76.9
			Paraformaldehyde, 4'-aminobenzoic acid	232	334	-	321	68.8
Guaiacol	Biomass, wood	Furfurylamine, guaguaiacol[46]	Paraformaldehyde	240	-	148[c]	352	56.0
	Vegetable oils, wood	Stearylamine, guaiacol[46]		-	-	82[c]	329	18.9
Urushiol	Lacquer tree	Urushiol[47]	Paraformaldehyde, aniline	211	141	140[b]	325	-
		Urushiol[48]	Paraformaldehyde, methylenedianiline	212	152	135[b]	350	25.0
Coumaric	Agricultural bagasse, phloretin	Coumaric acid[49]	Paraformaldehyde, 1,3,5-triazine	137	-	119[c]	220	30.0
Ferulic		Ferulic acid[49]		130	-	120[c]	200	34.0
Phloretic		Phloretic acid[49]		212	-	130[c]	293	43.0

[a] peak of polymerization [b] measured by DMTA [c] measured by DSC [d] under nitrogen **Bz-OH:** hydroxyl containing-benzoxazine

Cashew nutshell liquid (CNSL) is one unwanted byproduct of cashew nut industry. It represents nearly 25% of the total nut weight and its production worldwide is estimated to be about 300000 tonnes per year. It is composed of a mixture of anacardic acid, cardanol and traces of cardol and 2-methylcardol[38]. Cardanol is the main component of distilled CNSL and can be considered sustainable, low cost and largely available natural resource. Different cardanol-based benzoxazine monomers (Bz-C) have been synthesized mainly using aniline, formaldehyde, 4,4'-diaminodiphenylmethane, paraformaldehyde, ammonia and cardanol-furfural resin[38-42] **(Scheme 3)**. Cardanol derived polybenzoxazines have technological potential as matrix for natural fiber-reinforced composites[38] and reactive diluents in the synthesis process of bisphenol A (BPA) based benzoxazines[40].

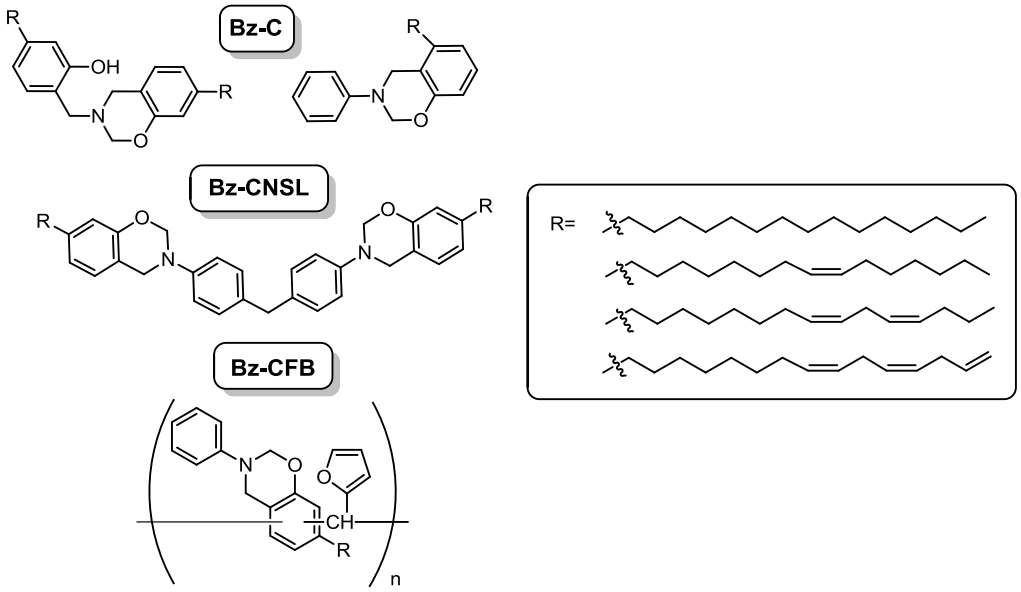

Scheme 3. Chemical structure of CNSL and cardanol-based benzoxazines

Terpenes are important bio-based compounds, widely produced by various plants, typically conifers. They are abundant, inexpensive an ideal starting materials for the synthesis of new important chemicals for the use as fragrances, flavors, pharmaceuticals, solvents, and also chiral intermediates[50]. Terpenediphenol (TP) is one of the most important terpene derivatives and it is synthesized using phenol and terpene compounds from pine or orange rind. With the aim to improve the mechanical properties and water resistance of benzoxazine/epoxy resins, terpenediphenol-based benzoxazine monomers

(Scheme 4) have been synthesized and their curing behavior was studied using mixtures of 50 mol% epoxy (DGEBA) and 50 mol% benzoxazine[43]. It was found that the ring opening of the benzoxazines occurred at a very similar temperature of 240 ºC. The cured resin from terpenediphenol-based benzoxazine (TP-PBz) and epoxy resin had superior heat resistance, electrical insulation, and especially water resistance than those of the cured resin from BPA-based benzoxazine or BPA-type novolac and epoxy resin. Moreover, the inclusion of the rigid hydrocarbon ring on the network structure of TP-PBz increased the glass transition temperatures in comparison to similar BPA-based counterparts.

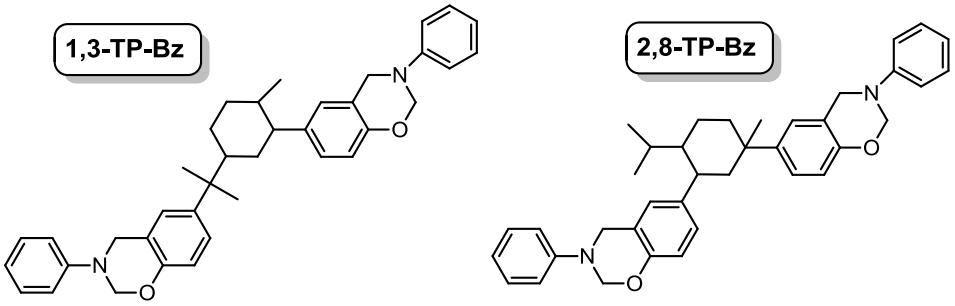

Scheme 4. Chemical structure of terpenediphenol-based benzoxazines

Vegetable oils, such as soybean, castor, sunflower, palm, and rapeseed, are extracted primarily from the seeds of oilseed plants and have a wide variety of applications *e.g.,* foods, fuels (biofuels), lubricants, paints, cosmetics, pharmaceuticals, plasticizers, and construction materials. They are also attractive monomers for polymer chemistry due to their natural abundance and reactive functionality[51]. However, to make well-defined monomers and polymers the triglyceride oils need to be separated and mainly functionalized with hydroxyl, epoxy or carboxyl groups[52]. Recently, it has been carried out the preparation of a benzoxazine-modified vegetable oil (Bz-PGE) by the incorporation of benzoxazine moieties (Bz-OH) into enriched partial glycerides (PGE) through a urethane reaction between diisocyanate and hydroxyl groups of both PGE and Bz-OH[44] **(Scheme 5)**. Thermal curing of Bz-PGE rendered transparent samples with high flexibility and excellent adhesion properties to wood and metal surfaces. Moreover the polybenzoxazines exhibited excellent resistance properties to water, alkali, and acid enabling their use as coatings.

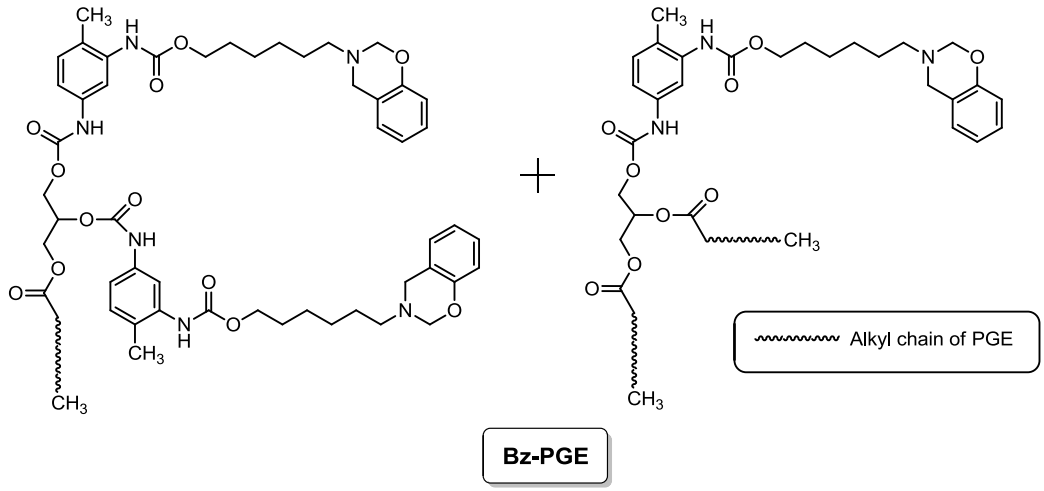

Scheme 5. Chemical structure of Bz-PGE

Lignin is the second most abundant renewable polymer on the earth (making up roughly 25% of vascular plants) after cellulose, with a production estimated in the range of 5-36 x 10^8 tonnes/year[53]. Its structure is not unique and varies according to the plant species, its age and location. Lignin could be considered as a phenolic high molecular mass biopolymer resulting from the oxidative polymerization of *p*-coumaryl, coniferyl and sinapyl alcohols. Vanillin and ferulic acid are apparently the only two small-scale aromatic molecules harvested from lignin[54]. Recently, different benzoxazine monomers derived from ferulic acid, coumaric acid, phloretic acid, and their corresponding esters were described[49] **(Scheme 6)**. Benzoxazines with conjugated unsaturated chains exhibited unusual poor thermal stability and degrade partially at the polymerization temperature making necessary the use of a catalyst to low the polymerization temperature and prevent degradation. The resulting materials presented superior Tg values when compared to those prepared from an unsubstituted monofuctional benzoxazine due to the additional crosslinking through the ester and carboxylic moieties.

Rosin (colophony) is a versatile raw material obtained from pine trees that is made up of a mixture of unsaturated polycyclic carboxylic acids of which, abietic acid is the major representative. The intrinsic acidity and rigidity, coupled with other chemical properties, enable rosin acids to be converted to a large number of downstream derivatives. Applications for these derivatives include their use in the manufacture of adhesives, paper sizing agents, printing inks, solders, and fluxes, surface coatings, insulating materials, and chewing gums[49]. Precisely by using maleopimaric acid imidophenol (MPAIP), a rosin derivative,

paraformaldehyde and aniline or 4-aminobenzoic acid (PABA) it has been synthesized two novel benzoxazine monomers **(Scheme 7)**. The resulting polymers exhibited good thermal stability and char yield due to the incorporation of hydrogenated phenanthrene ring and imide group into the polybenzoxazine structure[45].

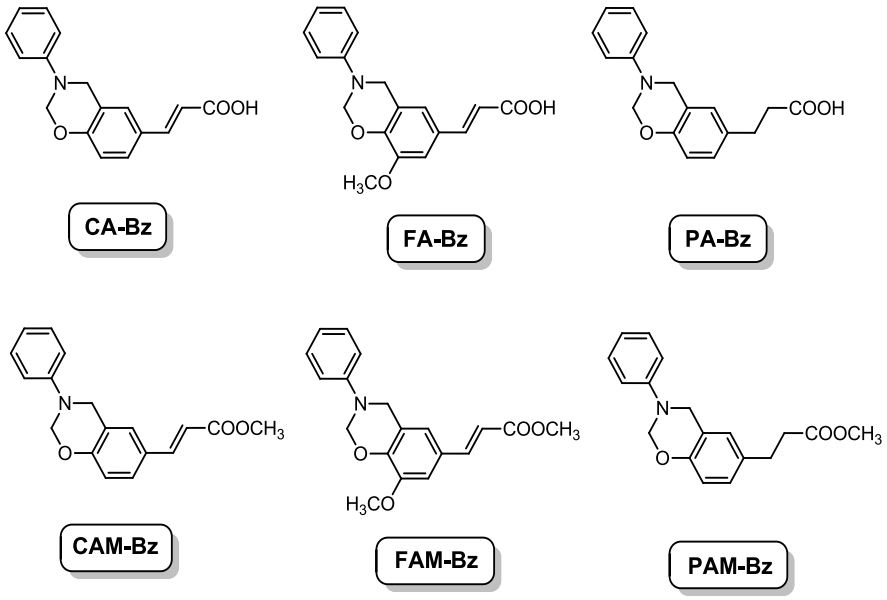

Scheme 6. Chemical structure of ferulic-, coumaric- and phloretic-based benzoxazines and their corresponding esters derivatives

Fully bio-based benzoxazine monomers have been reported using starting materials entirely derived from bio-based feedstocks. The preparation of the monomers was carried out by a solventless method using guaiacol and paraformaldehyde with two different amines, furfurylamine (Bzf) and stearylamine (Bzs) **(Scheme 8)**. Guaiacol is a natural biocide obtained from beechwood. Furfurylamine is obtained from furfural which in turn is prepared by dehydration of C_5 sugars (conventionally xylose) using the Biofine process. Stearylamine can be produced from vegetable oils such as coconut oil and palm oil. Paraformaldehyde can be obtained *e.g.,* from bio-methanol by chemical treatments. These benzoxazines were copolymerized in order to improve the crosslinking density of the resins and therefore enhance their properties such as Tg, thermal stability and char yield[46]. Furthermore, the addition of methyl *p*-toluenesulfonate to Bzf has demonstrated to serve as an efficient promoter of

ring-opening polymerization and significantly enhance the polymerization behavior compared with neat Bzf[55].

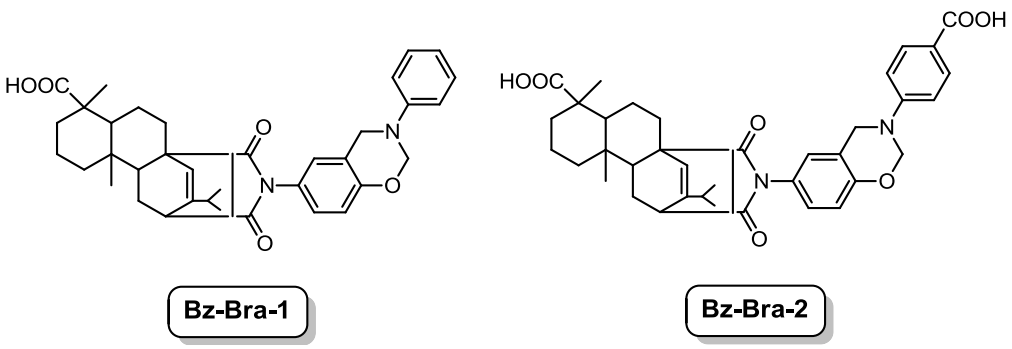

Scheme 7. Chemical structure of rosin based benzoxazines

Urushiol is the major component present in Chinese and Japanese lacquer. It is a mixture of 3-substituted catechol derivatives with n=15 carbon chains and 0–3 double bonds in the side chains. The triene side urushiol makes up 60–70% of urushiol[56]. The synthesis and properties of mono (U-Bz)[47] and bisfunctional (U-da-Bz)[48] urushiol-based polybenzoxazines have been recently reported **(Scheme 9)**. The PU-Bz resins showed extraordinary elongation at break (17.4%) comparing to typical polybenzoxazine but with relatively low Tg (140 ºC), and stress at break (15.3 MPa). This superb toughness property has been attributed to the presence of the long hydrocarbon chains of the urushiol structure. For its part, mixtures of U-da-Bz and a petroleum-based benzoxazine (3,3'-phenylmethanebis(3,4-dihydro-2*H*-1,3-benzoxazine) have been used with the aim to prepare high performance hybrid polybenzoxazines. The resulting mechanical, thermal and dynamomechanical properties of the hybrid materials could be tuned by the monomer content.

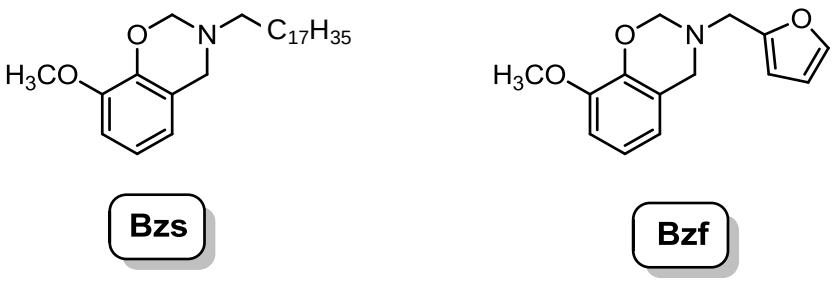

Scheme 8. Chemical structure of fully bio-based benzoxazines

Some of the above-mentioned examples of bio-based compounds are derived from biorefinery processes in which renewable complex raw materials are separated into simpler building blocks that further are converted into marketplace products. Organic acids constitute a significant fraction of those compounds available in a minimum number of steps from biorefinery carbohydrate streams, and as such have received much attention as platform chemicals[57]. Precisely, the levulinic acid (LA) is of interest as a primary biorefinery building block which is why it had been selected as one of the top 10 bio-based products by the US department of energy[57] due to its simple and relatively high yield production from acid hydrolysis of C_6 sugars[58,59]. The production of LA is based on the use of waste biomass (paper, wood, wheat straw and other ligno-cellulosic materials) as feedstock using different approaches such as dehydrative treatment of biomass or carbohydrates, hydrolysis of esters and oxidation of ketones.

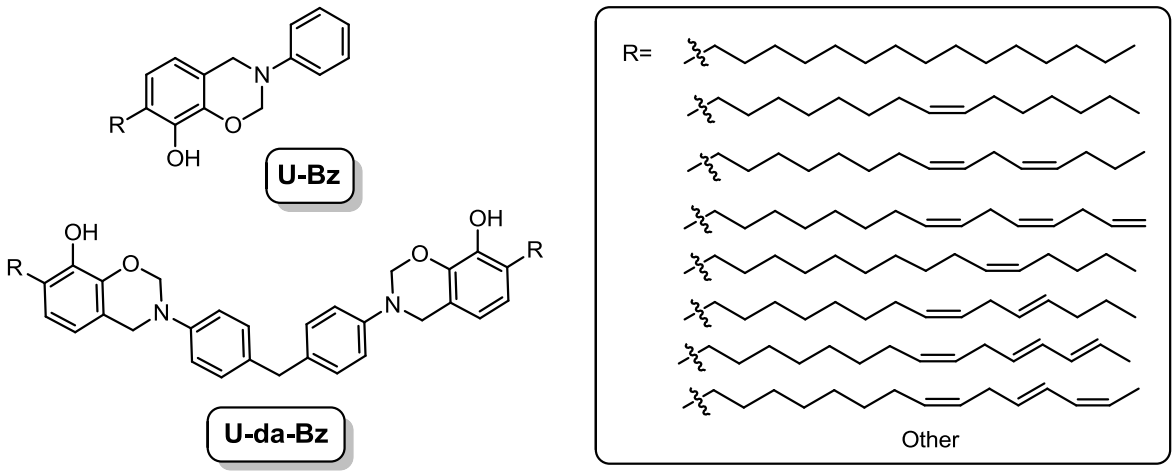

Scheme 9. Chemical structure of urushiol-based benzoxazines

Diphenolic acid (DPA) or 4,4´-bis(4-hydroxyphenyl)pentanoic acid is a chemical compound obtained by the condensation reaction of levulinic acid with phenol **(Scheme 10)** by using a catalyst. Different catalytic systems have been investigated such as Brönsted acid[60], hydrochloric acid, mesoporous $H_3PW_{12}O_4$-silica composite[61], zeolites[62], supported heteropolyacids (HPAs)[63] and most recently sulfonated hyperbranched poly(arylene oxindole)s[64,65].

Thanks to the large-scale commercialization of LA from the Biofine process, in 1999 it was projected a decrease in the market price of DPA from 6 €/kg to

2.4 €/kg promoting its commercialization and use[59,66]. The applications of diphenolic acid cover a huge range of industrial fields being some of interest the production of lubricants[67], paints[68], coatings[69], plasticizers and polymers among others[66]. Specifically in the polymer field, many studies have been focused on the preparation of polyesters[70-73], polycarbonates[74-76], polyamides[77], polysulfone/polyamide blends[78], polyether sulfone[79], polyphenylene ethers[80] and flame retardant polymers[81,82].

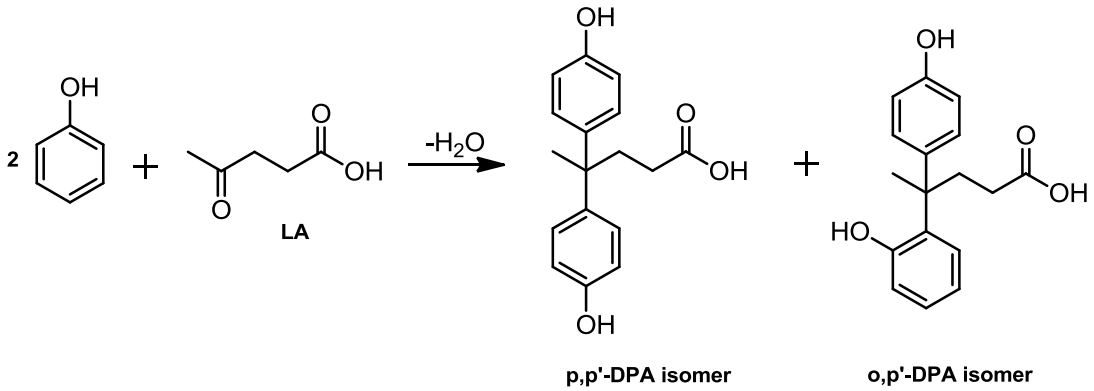

Scheme 10. Synthesis of diphenolic acid

In recent years, the United Nations Environment Programme (UNEP) and the World Health Organization (WHO) have focused their attention on the human health impact of some chemicals compounds as potential endocrine disruptors[83]. Among them is the bisphenol A (BPA), a chemical compound widely used in the production of polycarbonate and epoxy polymers, and additives. In addition, BPA is the starting material for the preparation of the main commercial petroleum-based-benzoxazine product. Inside the human body, studies indicate that BPA can mimic estrogen, a hormone whose proper levels are critical for the sexual development of fetuses and children[84,85]. In addition, other works have shown a significant relationship between urine levels of BPA and a cardiovascular disease, type 2 diabetes and abnormalities in liver enzymes[86], as well as the advance of girls puberty[87], among others[88-90].

1.2. SCOPE AND PURPOSE OF THE THESIS

As above mentioned, the use of renewable feedstocks for the development of polymers is a crucial step towards sustainability. Until now there are few approaches of renewable resources-based benzoxazine materials. For these reasons, the purpose of the thesis was to consider the use of renewable diphenolic acid (DPA) as starting material for the synthesis of new high performance polybenzoxazine materials. DPA is emerging as a potential "green" candidate to displace BPA. DPA has similar chemical structure than BPA, lower price and it contains an extra functionality (carboxylic acid) that can be involved for the polymer synthesis. Several approaches have been developed to explore different applications of these materials and are grouped in different chapters as follows:

Chapter 2 discusses the synthesis of two benzoxazine monomers derived from renewable DPA. The properties of both monomers and polymers are discussed in comparison to the conventional BPA based counterparts. In addition, it was contemplated the use of fiberglass as reinforcement agent of DPA/benzoxazine mixtures. Finally, the preparation of high performance flame retardant polybenzoxazine mixtures using a phosphazene-diphenolic acid derivative was evaluated.

Chapter 3 deals with the preparation and characterization of rigid polybenzoxazine foams using the DPA-based benzoxazine and their corresponding flame retarded foams through the addition of a phosphorus-containing flame retardant compound derived from 9,10-dihydro-9-oxa-10-phosphaphenanthrene-10-oxide (DOPO). Using analytical tools, it is proposed mathematical models for fitting the density and mechanical properties of the flame retardant foams in terms of the foaming variables.

Finally, Chapter 4 describes the preparation of carbon nanotube/polybenzoxazine nanocomposites using a convenient and solventless method and the evaluation of the electrical, thermal, thermomechanical and flammability properties of the materials.

REFERENCES

1. PlasticsEurope *Plastics – the Facts 2012. An analysis of European plastics production, demand and waste data for 2011*; 2012; pp 1-36.
2. Meeker, J. D.; Sathyanarayana, S.; Swan, S. H., Phthalates and other additives in plastics: human exposure and associated health outcomes. *Phil. Trans. R. Soc. B* **2009,** 364, (1526), 2097-2113.
3. Thompson, R. C.; Moore, C. J.; vom Saal, F. S.; Swan, S. H., Plastics, the environment and human health: current consensus and future trends. *Phil. Trans. R. Soc. B* **2009,** 364, (1526), 2153-2166.
4. Tolinski, M., General Introduction. In *Plastics and Sustainability: Towards a Peaceful Coexistence between Bio-based and Fossil Fuel-based Plastics*, John Wiley & Sons, Inc.: 2011; pp 1-30.
5. Gregory, M. R., Environmental implications of plastic debris in marine settings—entanglement, ingestion, smothering, hangers-on, hitch-hiking and alien invasions. *Phil. Trans. R. Soc. B* **2009,** 364, (1526), 2013-2025.
6. Hong, S.; Lee, J.; Jang, Y. C.; Kim, Y. J.; Kim, H. J.; Han, D.; Hong, S. H.; Kang, D.; Shim, W. J., Impacts of marine debris on wild animals in the coastal area of Korea. *Mar. Pollut. Bull.* **2013,** 66, (1–2), 117-124.
7. Teuten, E. L. et al, Transport and release of chemicals from plastics to the environment and to wildlife. *Phil. Trans. R. Soc. B* **2009,** 364, (1526), 2027-2045.
8. Hopewell, J.; Dvorak, R.; Kosior, E., Plastics recycling: challenges and opportunities. *Phil. Trans. R. Soc. B* **2009,** 364, (1526), 2115-2126.
9. Verespej, M. Experts predict boom in bio-based resins. www.prw.com (21/07/2013).
10. de Andrade Coutinho, P. L.; Morita, A. T.; Cassinelli, L. F.; Morschbacker, A.; Werneck Do Carmo, R., Braskem's Ethanol to Polyethylene Process Development. In *Catalytic Process Development for Renewable Materials*, Wiley-VCH Verlag GmbH: 2013; pp 149-165.
11. Tolinski, M., Applications: Demonstrations of Plastics Sustainability. In *Plastics and Sustainability: Towards a Peaceful Coexistence between Bio-based and Fossil Fuel-based Plastics*, John Wiley & Sons, Inc.: 2011; pp 133-167.
12. Pecoraro, É.; Manzani, D.; Messaddeq, Y.; Ribeiro, S. J. L., Bacterial Cellulose from Glucanacetobacter xylinus: Preparation, Properties and Applications. In *Monomers, Polymers and Composites from Renewable Resources*, Belgacem, M. N.; Gandini A., Eds. Elsevier: Amsterdam, 2007; pp 369-383.
13. Chodak, I., Polyhydroxyalkanoates: Origin, Properties and Applications. In *Monomers, Polymers and Composites from Renewable Resources*, Belgacem, M. N.; Gandini A., Eds. Elsevier: Amsterdam, 2008; pp 451-477.
14. Stevens, M. P., *Polymer Chemistry: An Introduction, Third Edition*. Oxford University Press: Oxford, 2009.
15. Ishida, H., Overview and Historical Background of Polybenzoxazine Research. In *Handbook of Benzoxazine Resins*, Hatsuo, I.; Tarek, A., Eds. Elsevier: Amsterdam, 2011; pp 3-81.
16. Holly, F. W.; Cope, A. C., Condensation products of aldehydes and ketones with o-aminobenzyl alcohol and o-hydroxybenzylamine. *J. Am. Chem. Soc.* **1944,** 66, (11), 1875-1879.
17. Yagci, Y.; Kiskan, B.; Ghosh, N. N., Recent advancement on polybenzoxazine—A newly developed high performance thermoset. *J. Polym. Sci., Part A: Polym. Chem.* **2009,** 47, (21), 5565-5576.
18. Ghosh, N. N.; Kiskan, B.; Yagci, Y., Polybenzoxazines—New high performance thermosetting resins: Synthesis and properties. *Prog. Polym. Sci.* **2007,** 32, (11), 1344-1391.
19. Agag, T.; Takeichi, T., Synthesis and characterization of novel benzoxazine monomers containing allyl groups and their high performance thermosets. *Macromolecules* **2003,** 36, (16), 6010-6017.
20. Brunovska, Z.; Ishida, H., Thermal study on the copolymers of phthalonitrile and phenylnitrile-functional benzoxazines. *J. Appl. Polym. Sci.* **1999,** 73, (14), 2937-2949.

21. Kudoh, R.; Sudo, A.; Endo, T., A highly reactive benzoxazine monomer, 1-(2-hydroxyethyl)-1,3-benzoxazine: Activation of benzoxazine by neighboring group participation of hydroxyl group. *Macromolecules* **2010,** 43, (3), 1185-1187.
22. Ishida, H. Process for preparation of benzoxazine compounds in solventless systems. US. Patent 5543516, 1996.
23. Ning, X.; Ishida, H., Phenolic materials via ring-opening polymerization: Synthesis and characterization of bisphenol-A based benzoxazines and their polymers. *J. Polym. Sci., Part A: Polym. Chem.* **1994,** 32, (6), 1121-1129.
24. Brunovska, Z.; Liu, J. P.; Ishida, H., 1,3,5-Triphenylhexahydro-1,3,5-triazine – active intermediate and precursor in the novel synthesis of benzoxazine monomers and oligomers. *Macromol. Chem. Phys.* **1999,** 200, (7), 1745-1752.
25. Espinosa, M. A.; Cádiz, V.; Galià, M., Synthesis and characterization of benzoxazine-based phenolic resins: Crosslinking study. *J. Appl. Polym. Sci.* **2003,** 90, (2), 470-481.
26. Andreu, R.; Reina, J. A.; Ronda, J. C., Studies on the thermal polymerization of substituted benzoxazine monomers: Electronic effects. *J. Polym. Sci., Part A: Polym. Chem.* **2008,** 46, (10), 3353-3366.
27. Imran, M.; Kiskan, B.; Yagci, Y., Concise synthesis and characterization of unsymmetric 1,3-benzoxazines by tandem reactions. *Tetrahedron Lett.* **2013,** 54, (36), 4966-4969.
28. Liu, C.; Shen, D.; Sebastián, R. M.; Marquet, J.; Schönfeld, R., Catalyst effects on the ring-opening polymerization of 1,3-benzoxazine and on the polymer structure. *Polymer* **2013,** 54, (12), 2873-2878.
29. Dunkers, J.; Ishida, H., Reaction of benzoxazine-based phenolic resins with strong and weak carboxylic acids and phenols as catalysts. *J. Polym. Sci., Part A: Polym. Chem.* **1999,** 37, (13), 1913-1921.
30. Gorodisher, I.; DeVoe, R. J.; Webb, R. J., Catalytic Opening of Lateral Benzoxazine Rings by Thiols. In *Handbook of Benzoxazine Resins*, Hatsuo, I.; Tarek, A., Eds. Elsevier: Amsterdam, 2011; pp 211-234.
31. Beyazkiliç, Z.; Kahveci, M. U.; Aydoğan, B.; Kişkan, B.; Yağci, Y., Synthesis of polybenzoxazine precursors using thiols: Simultaneous thiol–ene and ring-opening reactions. *J. Polym. Sci., Part A: Polym. Chem.* **2012,** 50, (19), 4029-4036.
32. Kasapoglu, F.; Cianga, I.; Yagci, Y.; Takeichi, T., Photoinitiated cationic polymerization of monofunctional benzoxazine. *J. Polym. Sci., Part A: Polym. Chem.* **2003,** 41, (21), 3320-3328.
33. Wang, Y.-X.; Ishida, H., Synthesis and properties of new thermoplastic polymers from substituted 3,4-dihydro-2H-1,3-benzoxazines. *Macromolecules* **2000,** 33, (8), 2839-2847.
34. Sudo, A.; Kudoh, R.; Nakayama, H.; Arima, K.; Endo, T., Selective formation of poly(N,O-acetal) by polymerization of 1,3-benzoxazine and its main chain rearrangement. *Macromolecules* **2008,** 41, (23), 9030-9034.
35. Ran, Q.-C.; Zhang, D.-X.; Zhu, R.-Q.; Gu, Y., The structural transformation during polymerization of benzoxazine/$FeCl_3$ and the effect on the thermal stability. *Polymer* **2012,** 53, (19), 4119-4127.
36. Nair, C. P. R., Advances in addition-cure phenolic resins. *Prog. Polym. Sci.* **2004,** 29, (5), 401-498.
37. Tasdelen, M. A.; Kiskan, B.; Gacal, B.; Kasapoglu, F.; Cianga, L.; Yagci, Y., Light-Induced Reactions of Benzoxazines and Derivatives. In *Handbook of Benzoxazine Resins*, Hatsuo, I.; Tarek, A., Eds. Elsevier: Amsterdam, 2011; pp 183-191.
38. Calo, E.; Maffezzoli, A.; Mele, G.; Martina, F.; Mazzetto, S. E.; Tarzia, A.; Stifani, C., Synthesis of a novel cardanol-based benzoxazine monomer and environmentally sustainable production of polymers and bio-composites. *Green Chem.* **2007,** 9, (7), 754-759.
39. Campaner, P.; D'Amico, D.; Longo, L.; Stifani, C.; Tarzia, A.; Tiburzio, S., Study of a Cardanol-Based Benzoxazine as Reactive Diluent and Toughening Agent of Conventional Benzoxazines. In *Handbook of Benzoxazine Resins*, Hatsuo, I.; Tarek, A., Eds. Elsevier: Amsterdam, 2011; pp 365-375.
40. Lochab, B.; Varma, I.; Bijwe, J., Thermal behaviour of cardanol-based benzoxazines. *J. Therm. Anal. Calorim.* **2010,** 102, (2), 769-774.

41. Agag, T.; An, S. Y.; Ishida, H., 1,3-bis(benzoxazine) from cashew nut shell oil and diaminodiphenyl methane and its composites with wood flour. *J. Appl. Polym. Sci.* **2013,** 127, (4), 2710-2714.
42. Li, S.; Yan, S.; Yu, J.; Yu, B., Synthesis and characterization of new benzoxazine-based phenolic resins from renewable resources and the properties of their polymers. *J. Appl. Polym. Sci.* **2011,** 122, (5), 2843-2848.
43. Kimura, H.; Murata, Y.; Matsumoto, A.; Hasegawa, K.; Ohtsuka, K.; Fukuda, A., New thermosetting resin from terpenediphenol-based benzoxazine and epoxy resin. *J. Appl. Polym. Sci.* **1999,** 74, (9), 2266-2273.
44. Yildirim, C.; Erciyes, A. T.; Yagci, Y., Thermally curable benzoxazine-modified vegetable oil as a coating material. *J. Coat. Technol. Res.* **2013,** 10, (4), 559-569.
45. Li, S.; Zou, T.; Liu, X.; Tao, M., Synthesis and characterization of benzoxazine monomers from rosin and their thermal polymerization. *Des. Monomers Polym.* **2013**, 1-7.
46. Wang, C.; Sun, J.; Liu, X.; Sudo, A.; Endo, T., Synthesis and copolymerization of fully bio-based benzoxazines from guaiacol, furfurylamine and stearylamine. *Green Chem.* **2012,** 14, (10), 2799-2806.
47. Xu, H.; Lu, Z.; Zhang, G., Synthesis and properties of thermosetting resin based on urushiol. *RSC Advances* **2012,** 2, (7), 2768-2772.
48. Xu, H.; Zhang, W.; Lu, Z.; Zhang, G., Hybrid polybenzoxazine with tunable properties. *RSC Advances* **2013,** 3, (11), 3677-3682.
49. Comí, M.; Lligadas, G.; Ronda, J. C.; Galià, M.; Cádiz, V., Renewable benzoxazine monomers from "lignin-like" naturally occurring phenolic derivatives. *J. Polym. Sci., Part A: Polym. Chem.* **2013**, DOI:10.1002/pola.26918
50. Wilbon, P. A.; Chu, F.; Tang, C., Progress in renewable polymers from natural terpenes, terpenoids, and rosin. *Macromol. Rapid Commun.* **2013,** 34, (1), 8-37.
51. Williams, C. K.; Hillmyer, M. A., Polymers from renewable resources: A perspective for a special issue of polymer reviews. *Polym. Rev.* **2008,** 48, (1), 1-10.
52. Güner, S. F.; Yağcı, Y.; Erciyes, A. T., Polymers from triglyceride oils. *Prog. Polym. Sci.* **2006,** 31, (7), 633-670.
53. Gellerstedt, G.; Henriksson, G., Lignins: Major Sources, Structure and Properties. In *Monomers, Polymers and Composites from Renewable Resources*, Belgacem, M. N.; Gandini A., Eds. Elsevier: Amsterdam, 2008; pp 201-224.
54. Miller, S. A., Sustainable polymers: opportunities for the next decade. *ACS Macro Lett.* **2013,** 2, (6), 550-554.
55. Wang, C.; Zhao, C.; Sun, J.; Huang, S.; Liu, X.; Endo, T., Synthesis and thermal properties of a bio-based polybenzoxazine with curing promoter. *J. Polym. Sci., Part A: Polym. Chem.* **2013,** 51, (9), 2016-2023.
56. Yamauchi, Y.; Oshima, R.; Kumanotani, J., Configuration of the olefinic bonds in the heteroolefinic side-chains of japanese lacquer urushiol: separation and identification of components of dimethylurushiol by means of reductive ozonolysis and high- performance liquid chromatography. *J. Chromatogr. A* **1982,** 243, (1), 71-84.
57. Bozell, J. J.; Petersen, G. R., Technology development for the production of biobased products from biorefinery carbohydrates-the US Department of Energy's "Top 10" revisited. *Green Chem.* **2010,** 12, (4), 539-554.
58. Fitzpatrick, W. S. Production of levulinic acid from carbohydrate-containing materials. European Patent 0873294 A4, 1997.
59. Hayes, D. J.; Fitzpatrick, S.; Hayes, M. H. B.; Ross, J. R. H., The Biofine Process: Production of Levulinic Acid, Furfural, and Formic Acid from Lignocellulosic Feedstocks. In *Biorefineries-Industrial Processes and Products*, Wiley-VCH Verlag GmbH: 2008; pp 139-164.
60. Isoda, Y.; Azuma, M. Preparation of bis(hydroxyaryl)pentanoic acids. Japanese Patent 08053390, 1996.
61. Guo, Y.; Li, K.; Clark, J. H., The synthesis of diphenolic acid using the periodic mesoporous $H_3PW_{12}O_{40}$-silica composite catalysed reaction of levulinic acid. *Green Chem.* **2007,** 9, (8), 839-841.
62. Davis, M. E., New vistas in zeolite and molecular sieve catalysis. *Acc. Chem. Res.* **1993,** 26, (3), 111-115.

63. Yu, X.; Guo, Y.; Li, K.; Yang, X.; Xu, L.; Guo, Y.; Hu, J., Catalytic synthesis of diphenolic acid from levulinic acid over cesium partly substituted Wells–Dawson type heteropolyacid. *J. Mol. Catal. A: Chem.* **2008,** 290, (1–2), 44-53.
64. Van de Vyver, S.; Helsen, S.; Geboers, J.; Yu, F.; Thomas, J.; Smet, M.; Dehaen, W.; Román-Leshkov, Y.; Hermans, I.; Sels, B. F., Mechanistic insights into the kinetic and regiochemical control of the thiol-promoted catalytic synthesis of diphenolic acid. *ACS Catal.* **2012,** 2, (12), 2700-2704.
65. Van de Vyver, S.; Geboers, J.; Helsen, S.; Yu, F.; Thomas, J.; Smet, M.; Dehaen, W.; Sels, B. F., Thiol-promoted catalytic synthesis of diphenolic acid with sulfonated hyperbranched poly(arylene oxindole)s. *Chem. Commun.* **2012,** 48, (29), 3497-3499.
66. Bozell, J. J.; Moens, L.; Elliott, D. C.; Wang, Y.; Neuenscwander, G. G.; Fitzpatrick, S. W.; Bilski, R. J.; Jarnefeld, J. L., Production of levulinic acid and use as a platform chemical for derived products. *Resour. Conserv. Recy.* **2000,** 28, (3–4), 227-239.
67. Chafetz, H.; Kennedy, T. A.; Liu, C. S.; Papke, B. L. Lubricating oil composition containing the reaction product of an alkenylsuccinimide with a bis(hydroxyaromatic) substituted carboxylic acid. US Patent 5445750, 1995.
68. Holmen, R. E.; Olander, S. J. Paint composition for making paved surfaces. US Patent 4031048, 1977.
69. Blegen, J. R. Coating compositions based on polyester resins hardenable by vapor permeation, for flexible supports. Belgian Patent 891465, 1982.
70. Zhang, P.; Wu, L.; Bu, Z.; Li, B.-G., Interfacial polycondensation of diphenolic acid and isophthaloyl chloride. *J. Appl. Polym. Sci.* **2008,** 108, (6), 3586-3592.
71. Chu, F.; Hawker, C. J.; Pomery, P. J.; Hill, D. J. T., Intramolecular cyclization in hyperbranched polyesters. *J. Polym. Sci., Part A: Polym. Chem.* **1997,** 35, (9), 1627-1633.
72. Ping, Z.; Linbo, W.; Bo-Geng, L., Thermal stability of aromatic polyesters prepared from diphenolic acid and its esters. *Polym. Degrad. Stab.* **2009,** 94, (8), 1261-1266.
73. Wang, C.; Nakamura, S., Synthesis of aromatic polyesters having pendant carboxyl groups in the side chains and conversion of the carboxyl groups to other reactive groups. *J. Polym. Sci., Part A: Polym. Chem.* **1995,** 33, (13), 2157-2163.
74. Moore, J. A.; Tannahill, T., Homo- and co- polycarbonates and blends from diphenolic acid. *High Perform. Polym.* **2001,** 13, (2), S305-316.
75. Zhang, R.; Moore, J. A., Synthesis, characterization and properties of polycarbonate containing carboxyl side groups. *Macromol. Symp.* **2003,** 199, (1), 375-390.
76. Fischer, R. P.; Robert Hartranft, G.; Heckles, J. S., Diphenolic acid ester polycarbonates. *J. Appl. Polym. Sci.* **1966,** 10, (2), 245-252.
77. Greenlee, S. O. Novel diphenolic acid co-amides. US Patent 2933517, 1960.
78. Weber, M.; Heckmann, W., Compatibilization of polysulfone/polyamide-blends by reactive polysulfones – evidence for copolymer formation. *Polym. Bull.* **1998,** 40, (2-3), 227-234.
79. Esser, I. C. H. M.; Parsons, I. W., Modified poly(ether sulfone)/poly(ether ether sulfone) polymers: approaches to pendent carboxyl groups. *Polymer* **1993,** 34, (13), 2836-2844.
80. Tagle, L. H.; Diaz, F. R.; Cerda, G.; Oyarzo, M.; Peñafiel, G., Polymerization by phase transfer catalysis. *Polym. Bull.* **1997,** 39, (1), 9-14.
81. Yang, L.; Yan, Z.; Zhengping, F., Design, synthesis and application of novel flame retardants derived from biomass. *BioResources* **2012,** 7, (4), 4914-4925.
82. Zhang, Y.; Chen, X. L.; Fang, Z. P., Flame Retardant ABS with a Novel Polyphosphate Derived from Biomass. *Adv. Mat. Res.* **2011,** 284-286, 187-192.
83. Bergman, A.; Heindel, J. J.; Jobling, S.; Kidd, K. A.; Zoeller, R. T. *State of the science of endocrine disrupting chemicals 2012*; 2012; pp 1-29.
84. Takeuchi, T.; Tsutsumi, O.; Ikezuki, Y.; Takai, Y.; Taketani, Y., Positive relationship between androgen and the endocrine Disruptor, bisphenol A, in normal women and women with ovarian dysfunction. *Endocr. J.* **2004,** 51, (2), 165-169.

85. Talsness, C. E.; Andrade, A. J. M.; Kuriyama, S. N.; Taylor, J. A.; vom Saal, F. S., Components of plastic: experimental studies in animals and relevance for human health. *Phil. Trans. R. Soc. B* **2009,** 364, (1526), 2079-2096.
86. Lang, I. A.; et al., Association of urinary bisphenol a concentration with medical disorders and laboratory abnormalities in adults. *J. Am. Med. Assoc.* **2008,** 300, (11), 1303-1310.
87. Howdeshell, K. L.; Hotchkiss, A. K.; Thayer, K. A.; Vandenbergh, J. G.; vom Saal, F. S., Environmental toxins: Exposure to bisphenol A advances puberty. *Nature* **1999,** 401, (6755), 763-764.
88. Moriyama, K.; Tagami, T.; Akamizu, T.; Usui, T.; Saijo, M.; Kanamoto, N.; Hataya, Y.; Shimatsu, A.; Kuzuya, H.; Nakao, K., Thyroid hormone action is disrupted by bisphenol A as an antagonist. *J. Clin. Endocrinol. Metab.* **2002,** 87, (11), 5185-5190.
89. Luo, G.; Wei, R.; Niu, R.; Wang, C.; Wang, J., Pubertal exposure to Bisphenol A increases anxiety-like behavior and decreases acetylcholinesterase activity of hippocampus in adult male mice. *Food Chem. Toxicol.* **2013,** 60, (0), 177-180.
90. Nakamura, K.; Itoh, K.; Dai, H.; Han, L.; Wang, X.; Kato, S.; Sugimoto, T.; Fushiki, S., Prenatal and lactational exposure to low-doses of bisphenol A alters adult mice behavior. *Brain Dev.* **2012,** 34, (1), 57-63.

CHAPTER 2

DIPHENOLIC ACID AS PLATFORM CHEMICAL FOR THE SYNTHESIS OF POLYBENZOXAZINE MATERIALS

2.1. INTRODUCTION

The necessity to reduce the extensive dependence on fossil fuels suggests the development and commercialization of new bio-based products more environmentally-friendly that can enhance quality of life, security and the economy. This possibility is given, among others, by the production of polymers partially or totally derived from non-petrochemical feedstocks such as diphenolic acid (DPA).

As it has previously mentioned in the Chapter 1, DPA is emerging as an interesting compound capable to replace bisphenol A. Its origin and characteristics have already been discussed in that chapter. Most of the polymers are required to be fire-retardant for different applications mainly due to their high flammability and easy ignitability.

This chapter explores the use of DPA as starting diphenolic compound for the synthesis of benzoxazine monomers. Moreover, the preparation of high performance flame retardant thermosetting resins in DPA is described.

2.2. FLAME RETARDANCY IN POLYMERS

Plastic materials are present in our daily life, a quick look is enough to realize that we are surrounded by films, fibers, bottles and foams most of them made from polymers. These materials present a clear disadvantage relative to their high flammability, especially the commodity polymers. According to fire statistics[1], in Spain the total number of victims caused by fire in 2011 amounted to 2349 of which 2191 (93%) suffered injuries and 158 (7%) died, *i.e.,* 16 people pass away every week. The 76% of all deaths (131) has occurred in buildings. Within this category, 121 deaths happened in dwelling, representing 70% of all deaths, and 92% from the total deaths caused in buildings. Compared with 2010, the number of fire fatalities fell by 10% from 192 to 173. These results can be attributed, among others, to good fire behavior of materials used in construction and the contribution of improved Spanish legislation regarding to fire protection. The role of flame retardant polymeric materials is also probably other contributor.

Flame retardants (FRs) account for about 27% of the plastic additive market, a value that far exceeds other types of additives as heat stabilizers (15.6%), antioxidants (7.6%), lubricants (6%) and UV stabilizers (5%)[2]. In 2006 the total consumption of flame retardants in Europe was 465000 tones according to European Flame Retardants Association (EFRA)[3]. It is clear that FRs are an important part of polymer formulations for applications in which polymer have a significant chance of being exposed to an ignition source, where polymers are easy ignitable, or where fast spread of a fire may cause serious problems when evacuating people[4].

2.2.1. Polymer combustion

A flame retardant is a chemical compound able to retard a flame, or a polymer to shows ability to slow fire growth when ignited[5]. FRs reduce the chances of a fire starting by rendering increased resistance to ignition. They delay the spread of flame, providing extra time in the early stages when the fire can be extinguished or an escape can be made. To understand their mode of action is needed to know the mechanism of polymer combustion.

The process stars when an external source of heat comes into contact with the polymer surface (fuel) generating volatile degradation products which react with oxygen from the air (combustive) to produce a flame and heat. The combustion is an exothermic process that releases energy in form of heat. Part of this heat is transferred back to the polymer surface maintaining the flow of more volatile residues which continuously feed the combustion cycle **(Figure 1)**.

2.2.2. General flame retardant mechanisms

Although exist several types of flame retardant additives, they are usually classified according to their general mechanism of action as gas phase active or condensed phase active. Gas phase active flame retardants, or their degradation products, act interrupting the free-radical mechanism of the combustion process by a chemical reaction with reactive species that results in the formation of less reactive or even inert molecules. Other flame retardants present a physical action in the gas phase. They degrade endothermally cooling down the temperature of the reaction medium or release inert gases that dilute the fuel in the solid and gaseous phases limiting the possibility of ignition. In this category are included aluminum trihydroxide (ATH)[6] and magnesium hydroxide (MDH)[7].

Condensed phase flame retardants act commonly by charring either by a physical retention of the polymer or a chemical interaction of the flame retardant and the polymer. In this way, the formation of a protective layer between the gaseous and the solid phase has beneficial effects by reducing the heat transfer from the heat source to the material and also limiting the transfer of matter such as combustible volatile gases and oxygen that feeds the flame. Some examples include phosphorous additives, inorganic borates[8] and silicon compounds[9].

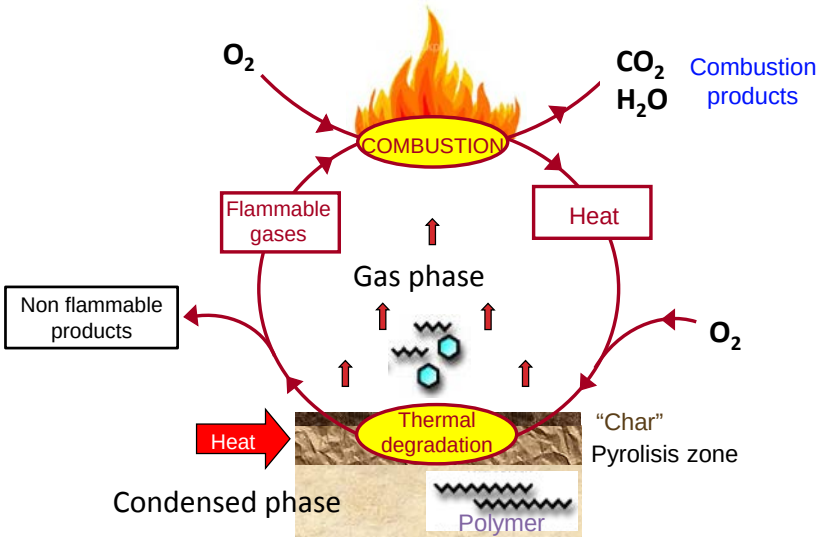

Figure 1. Combustion cycle of polymeric materials

Although some flame retardants operate by a single mode of action (MDH) their mechanisms should be considered as complex processes in which many individual stages occur simultaneously with one dominating. Combination of several mechanisms can often be synergistic[10].

2.2.3. Types of flame retardants

Two different methods for rendering fire retardant polymers include additive and reactive types. Additive flame retardants are easy to process since they are incorporated into the polymer matrix by physical means. Nonetheless, their incorporation presents several disadvantages. The additive is often required in high loadings to be effective (10-60 wt%) which may result in adverse changes to physical and mechanical properties. Other disadvantages include poor compatibility with polymer matrix and leaching from plastics. The reactive strategy may be achieved by copolymerization or by the introduction of suitable

chemical groups in the structure of the polymer. The relatively low amount required to achieve sufficient flame retardancy to a large extent can keep the original and mechanical properties of the polymer[11].

According to environment and health protection, flame retardants can also be classified in two groups: Halogenated-containing (HFRs) and non-halogenated-containing flame retardants. HFRs are most widely applied, being distinguished by their low price, versatility and exceptional efficiency. They include brominated, iodinated, fluorinated and chlorinated flame retardants. It is generally accepted that the main mechanism of flame retardant action of HFRs is in the gas phase. The reaction starts with the abstraction of halogen radical from the flame retardant which immediately abstracts hydrogen from either the flame retardant additive or the polymer[4]. Unfortunately, there are many concerns about their use, due to the potential release during combustion of corrosive, toxic and carcinogenic chemicals[12,13].

Due to increased most restrictive laws in the European Union in respect of environment and human health, phosphorus-based flame retardants (PFRs) have become as suitable candidates for replacing brominated flame retardants in traditional applications such as textile, fiber and electronic applications. PFRs can be inorganic (elemental red phosphorus, ammonium polyphosphate) or organic (*e.g.*, phosphonates, phosphinates). PFRs are considered environmentally-friendly flame retardants because they generated less toxic gas and smoke than HFRs[14-16]. PFRs are significantly more effective in oxygen or nitrogen based polymers, which could be either heterochain polymers or polymers with these elements in pendant groups.

The flame retarding mechanisms of PFRs can be active in the gas phase as radical scavenger or in the condensed phase by charring. It is reported[17] that the most abundant phosphorus radicals in the flame are $HPO_2^{\cdot}$, $PO^{\cdot}$, $PO_2^{\cdot}$ and $HPO^{\cdot}$. These radicals react with $^{\cdot}H$ and $^{\cdot}OH$ radicals in the gaseous phase intercepting the radical chain reactions in the flame and therefore reducing the heat production as can be observed in reactions [1] to [5]. In the condensed phase PFRs tend to react with the polymer or thermally decompose in phosphoric acid that later is transformed into polyphosphoric acid and water (Figure 2). Both compounds collaborate in the formation of a protecting layer and the dilution of oxidizing gas phase, respectively.

[1] $$HP\dot{O}_2 + \dot{H} \longrightarrow PO + H_2O$$

[2] $$HP\dot{O}_2 + \dot{H} \longrightarrow PO_2 + H_2$$

[3] $$HP\dot{O}_2 + O\dot{H} \longrightarrow PO_2 + H_2O$$

[4] $$P\dot{O} + \dot{H} + M \longrightarrow HPO + M$$

[5] $$P\dot{O} + O\dot{H} + M \longrightarrow HPO_2 + M$$

Within PFRs, phosphazene-based compounds have shown to be effective providing enhanced thermal and flame retardant properties to thermoplastic[18] and thermoset polymers[19]. Their retardancy mechanism could be categorized as intumescent (by the formation of a viscous swollen char on the surface of the polymer) although they can also act in the gaseous phase releasing non-flammable gases such as CO_2 that cut off the supply of oxygen.

Nanofillers are an alternative to the use of phosphorus compounds as environmentally-friendly flame retardants. Their first use as flame retardant additives was in 1950 when nanoclays where added to elastomers[20]. Nanofillers include the addition of nanoclays, nanoscale oxides, graphite, carbon nanotubes and graphene to polymers. Their contribution to flame retardancy in polymers hardly depend on their chemical structure, geometry, and morphology[21]. In comparison to well established flame retardants they are competitive owing to their beneficial effects that include: reinforcing organic char as a barrier layer, providing a catalytic surface to promote char-forming reactions, enhancing the structural rigidity of the polymer, changing the melt–flow properties of the polymer close to its ignition temperature, and providing intimate contact between a fire retardant and the host polymer[22].

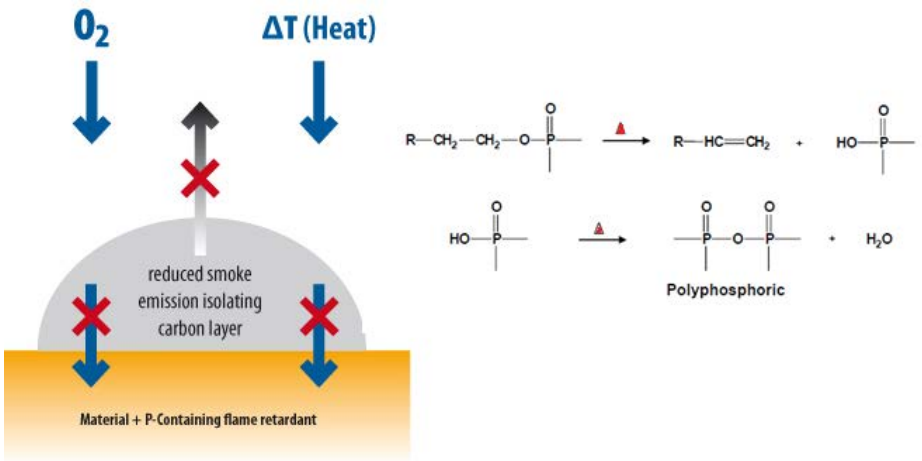

Figure 2. Condensed phase mechanisms of PFRs (adapted from[23])

Carbon nanotubes (CNT) are of interest for flame retardancy as they have shown an improvement in the flammability of various polymers at low concentrations[24,25]. They act through the formation of a continuous protective layer consisting of a network of nanoparticles. This layer serves as a heat shield and re-emits much of the incident radiation back decreasing the polymer degradation rate[26].Network structure can also enhance barrier character, suppressing evolution of combustible volatiles and inhibiting oxygen flow. Thereby, with better dispersion, higher loading and higher interface area of the CNT, the flame retardancy is found to improve[27].

2.2.4. Polymer flammability tests

Flammability of polymers is assessed through ignitability, flame spread and heat release[4]. The flame retardant ability of polymers is measured by some laboratory flammability tests which follow rigorous international standards being the American Society for Testing and Materials (ASTM), Underwriters Laboratories (UL) and the International Organization for Standardization (ISO) some of the most important. The most widespread small flame tests used in industrial laboratories or in the academic community are Underwriters' laboratory UL-94[28] and limiting oxygen index (LOI)[29].

The scope of the Underwriters' laboratory UL-94 test is assess the flammability of polymeric materials used for parts in devices and appliances in response to a small open flame or a radiant heat source under controlled laboratory conditions. The test measures ignitability and flame spread of polymeric materials exposed to a flame, for which the dripping characteristics, afterflame and afterglow times are recorded. There are three classifications **(Table 1)** according to the results obtained on vertical bar specimens[28].

Limiting oxygen index is the minimum concentration of oxygen in a mixture of oxygen and nitrogen that will just support flaming combustion of a material under the conditions of the test method that is, neither the extent of burning nor the period of burning after ignition could exceed 50 mm and 180 seconds, respectively. LOI test does not represent a real fire scenario but it is good as a screening tool considering that it is a sensitive measure to detect interactions between additives and flame retardant mechanisms[30]. Higher LOI values represent better flame retardancy. The method has been included in some international standards such as ASTM D2863 and ISO 4589.

Table 1. Materials classification according to the UL-94 test

Criteria conditions	V-0	V-1	V-2
Afterflame time for each individual specimen t_1 or t_2	≤10s	≤30s	≤30s
Total afterflame time for any condition set (t_1 plus t_2 for the 5 specimens)	≤50s	≤250s	≤250s
Afterflame plus afterglow time for each individual specimen after the second flame application (t_2+t_3)	≤30s	≤60s	≤60s
Afterflame or afterglow of any specimen up to the holding clamp	No	No	Yes
Cotton indicator ignited by flaming particles or drops	No	No	No

t_1: Time required for the flame extinguish after first ignition
t_2: Time required for the flame extinguish after second ignition
t_3: Time required for the fire glow to disappear

2.3. POLYBENZOXAZINE/ FIBERGLASS COMPOSITES

As above-commented one of the main drawback of polybenzoxazine resins is its brittleness. One way to address this problem is the development of composites. Benzoxazine resins are suitable materials for the preparation of fiber composites with high dimensional accuracy, largely due to the near-zero volume shrinkage and no volatile release during cure. Among many fillers and fibers, glass fiber (GF) is one of the most frequently used reinforcement in civilian applications. Moreover the benzoxazine composites can be used in the electrical insulation industry because of their good electrical insulation properties[31]. The composites can be fabricated by laminating or molding process procedures. Particularly, those benzoxazines with low melt viscosities can be used for liquid molding techniques such as resin transfer molding (RTM) technology[32].

The interface between matrix and fiber plays the most important role for improving the mechanical and physical properties of composites. Often due to the nature of the fibers or matrices the adhesion strength between them is not suitable. As a result of this, is necessary to modify the surface of the fiber by surface treatments (plasma) or chemical modification. Also, the use of silane coupling agents, coating and sizing of fiber can be chosen to get a desirable interface. For instance, Hatsuo Ishida et al[33] prepared GF/benzoxazine composites using a new silicon-containing benzoxazine and compared their mechanical properties with GF/novolac composites and GF/bisphenol A-based benzoxazine composites treated with two silane coupling agents. The fiber content of all composites was roughly 60 volume%. By means of the interlaminar

short-beam shear characterization technique (ILSS), they found that the ILSS strength of the glass-cloth reinforced polybenzoxazine composite is significantly higher than that of the novolac composite when no surface treatment of the glass fiber was applied. Furthermore, a wet strength retention of 100% was obtained with the silane treatment on the polybenzoxazine composite.

Another way to solve the above mentioned problem is the employ of two types of polymer matrices. One that provides mechanical and thermal properties while the other acts as wetting agent to promote infiltration and interface between fibers and polymeric matrices. Based on foregoing, Mingzhen Xu et al[34] prepared fiber-reinforced composite laminates using a cyano groups-containing benzoxazine and an epoxy resin to enhance the interfacial adhesions because of its excellent impregnation. The amount of glass fiber cloth used was 60 wt%. The results indicated that the ultimate performance of the composite laminates improve significantly as a result of the incorporation of epoxy.

For their part, Yi Gu and coworkers have extensively studied the use of glass fiber to develop high performance polybenzoxazine composites. Different benzoxazine monomers[35,36] as well as their mixture with epoxy resin[37] and/or phenolic resin have been utilized as matrices. As a result of their research, a GF/polybenzoxazine laminated was successfully used as rotor blade in a vacuum pump industry[31]. GF composites had excellent physical, mechanical, higher heat resistance and good dielectric properties as well as low water absorption.

Additionally, Hajime Kimura et al[38] prepared GF reinforced composites using the prepreg method with a silane treated glass cloth and a mixture of benzoxazine, bisoxazoline and latent curing agents as the matrix resin. The obtained composites showed good heat resistance, flame resistance, and mechanical properties compared with those of the conventional glass fiber-reinforced epoxy or flame-retardant epoxy composites. The reason was considered that the matrix resin from benzoxazine and bisoxazoline with the latent curing agent had a lot of benzene rigid structure components, high crosslink density, high char yield, and nitrogen-rich structures.

2.4. OBJECTIVES

The main objective of the work described in this chapter is to develop new polybenzoxazine resins using diphenolic acid as renewable resource. To fulfill this objective it is necessary to accomplish the following specific objectives:

1. To synthesize two novel benzoxazine monomers based on the renewable diphenolic acid and to compare their polymerization and properties with the bisphenol A-based benzoxazine.

2. To prepare benzoxazine mixtures of MDP-Bz and DPA with or without fiberglass and to evaluate the impact of DPA on the final resins properties.

3. To synthesize a DPA-phosphazene derivative and to study its performance as flame retardant additive.

2.5. EXPERIMENTAL PROCEDURES AND RESULTS

The following two studies including experimental procedures and results performed in this chapter have been published in scientific journals.

The first work described in section 2.5.1 has been published in the *Journal of Polymer Science Part A: Polymer Chemistry*. Vol. 49, (2011), pp. 1219-1227. This work contemplates the use of diphenolic acid, as a renewable resource in the synthesis and characterization of diphenolic acid based benzoxazine (DPA-Bz) and ester of diphenolic acid derivative benzoxazine (MDP-Bz). Their properties and polymerization were compared with the common bisphenol A-based benzoxazine (BPA).

The second work described in section 2.5.2 has been published in *Polymer*, Vol. 53, (2012), pp. 1617-1623. The first part of this work deals with the preparation of mixtures of renewable diphenolic acid and MDP-Bz with or without glass fiber, as well as the assessment of their thermal and mechanical properties. The second part is focused on the development of high performance flame retardant resins through the mixture of MDP-Bz and diphenolic acid-phosphazene

salt (DPA-PPZ).The impact of the additive is evaluated in terms of the dinamomechanical, thermal and flame retardant properties of the final materials.

REFERENCES

1. Cuena, J. L. Victimas de incendio en España 2011. http://www.semanadelaprevencion.com. (25-06-13).
2. Mouritz, A. P.; Gibson, A. G., Flame Retardant Composites. In *Fire Properties of Polymer Composite Materials*, Springer Netherlands: 2006; pp 237-286.
3. van der Veen, I.; de Boer, J., Phosphorus flame retardants: Properties, production, environmental occurrence, toxicity and analysis. *Chemosphere* **2012,** 88, (10), 1119-1153.
4. Levchik, S. V., Introduction to Flame Retardancy and Polymer Flammability. In *Flame Retardant Polymer Nanocomposites*, Morgan, A. B.; Wilkie, C. A., Eds. John Wiley & Sons, Inc.: 2006; pp 1-29.
5. Morgan, A. B.; Wilkie, C. A., An introduction to polymeric flame retardancy, Its role in materials science, and the current state of the field. In *Fire Retardancy of Polymeric Materials, Second Edition*, Morgan, A. B.; Wilkie, C. A., Eds. Taylor & Francis: 2010; pp 1-14.
6. Román-Lorza, S.; Rodriguez-Perez, M. A.; De Saja Sáez, J. A.; Zurro, J., Cellular structure of EVA/ATH halogen-free flame-retardant foams. *J. Cell. Plast.* **2010,** 46, (3), 259-279.
7. Hornsby, P. R., The application of magnesium hydroxide as a fire retardant and smoke-suppressing additive for polymers. *Fire Mater.* **1994,** 18, (5), 269-276.
8. Li, S.; Long, B.; Wang, Z.; Tian, Y.; Zheng, Y.; Zhang, Q., Synthesis of hydrophobic zinc borate nanoflakes and its effect on flame retardant properties of polyethylene. *J. Solid. State. Chem.* **2010,** 183, (4), 957-962.
9. Pape, P. G.; Romenesko, D. J., The role of silicone powders in reducing the heat release rate and evolution of smoke in flame retardant thermoplastics. *J. Vinyl. Addit. Techn.* **1997,** 3, (3), 225-232.
10. Bourbigot, S.; Duquesne, S., Fire retardant polymers: recent developments and opportunities. *J. Mater. Chem.* **2007,** 17, (22), 2283-2300.
11. Manias, E.; Polizos, G.; Nakajima, H.; Heidecker, M. J., Fundamentals of Polymer Nanocomposite Technology. In *Flame Retardant Polymer Nanocomposites*, John Wiley & Sons, Inc.: 2006; pp 31-66.
12. Camino, G.; Lomakin, S., Intumescent materials. In *Fire Retardant Materials*, Horrocks, A. R.; Price, D., Eds. Woodhead Publishing: Cambridge, 2001; pp 318-336.
13. Dumler, R.; Thoma, H.; Lenoir, D.; Hutzinger, O., Thermal formation of polybrominated dibenzodioxins (PBDD) and dibenzofurans (PBDF) from bromine containing flame retardants. *Chemosphere* **1989,** 19, (1–6), 305-308.
14. Chen, J.; Liu, S.; Zhao, J., Synthesis, application and flame retardancy mechanism of a novel flame retardant containing silicon and caged bicyclic phosphate for polyamide 6. *Polym. Degrad. Stab.* **2011,** 96, (8), 1508-1515.
15. Maiti, S.; Banerjee, S.; Palit, S. K., Phosphorus-containing polymers. *Prog. Polym. Sci.* **1993,** 18, (2), 227-261.
16. Shieh, J.-Y.; Wang, C.-S., Synthesis and properties of novel phosphorus-containing hardener for epoxy resins. *J. Appl. Polym. Sci.* **2000,** 78, (9), 1636-1644.
17. Hastie, J. W.; Bonell, D. W. *Molecular chemistry of inhibited combustion systems*; National bureau of standards: Gaithersburg MD, 1980; pp 1-39.
18. Kumar, D.; Khullar, M.; Gupta, A. D., Synthesis and characterization of novel cyclotriphosphazene-containing poly(ether imide)s. *Polymer* **1993,** 34, (14), 3025-3029.
19. El Gouri, M.; El Bachiri, A.; Hegazi, S. E.; Rafik, M.; El Harfi, A., Thermal degradation of a reactive flame retardant based on cyclotriphosphazene and its blend with DGEBA epoxy resin. *Polym. Degrad. Stab.* **2009,** 94, (11), 2101-2106.

20. Carter, L. W., Hendricks, John G., Bolley, Don S. Elastomer reinforced with a modified clay. US Patent 2531396, 1950.
21. Schartel, B., Considerations Regarding Specific Impacts of the Principal Fire Retardancy Mechanisms in Nanocomposites. In *Flame Retardant Polymer Nanocomposites*, John Wiley & Sons, Inc.: 2006; pp 107-129.
22. Hull, T. R.; Stec, A. A., Introduction Polymers and Fire. In *Fire Retardancy of Polymers: New Strategies and Mechanisms*, Hull, T. R.; Kandola, B. K., Eds. The Royal Society of Chemistry: 2009; pp 1-14.
23. CEFIC Flame retardants: Technologies/mode of action. www.cefric-efra.com. (29-06-13).
24. Peeterbroeck, S.; Laoutid, F.; Taulemesse, J. M.; Monteverde, F.; Lopez-Cuesta, J. M.; Nagy, J. B.; Alexandre, M.; Dubois, P., Mechanical properties and flame-retardant behavior of ethylene vinyl acetate/high-density polyethylene coated carbon nanotube nanocomposites. *Adv. Funct. Mater.* **2007,** 17, (15), 2787-2791.
25. Cai, Y.; Xu, X.; Gao, C.; Wang, L.; Wei, Q.; Song, L.; Hu, Y.; Qiao, H.; Zhao, Y.; Chen, Q.; Fong, H., Effects of carbon nanotubes on morphological structure, thermal and flammability properties of electrospun composite fibers consisting of lauric acid and polyamide 6 as thermal energy storage materials. *Fiber. Polym.* **2012,** 13, (7), 837-845.
26. Kashiwagi, T.; Grulke, E.; Hilding, J.; Groth, K.; Harris, R.; Butler, K.; Shields, J.; Kharchenko, S.; Douglas, J., Thermal and flammability properties of polypropylene/carbon nanotube nanocomposites. *Polymer* **2004,** 45, (12), 4227-4239.
27. Moniruzzaman, M.; Winey, K. I., Polymer nanocomposites containing carbon nanotubes. *Macromolecules* **2006,** 39, (16), 5194-5205.
28. Underwriters Laboratories Inc, Test for Flammability of Plastic Materials for Parts in Devices and Appliances UL 94 In *Fifth edition*, Underwriters Laboratories Inc: Northbrook, IL, United States, 2006.
29. ASTM, Standard Test Method for Measuring the Minimum Oxygen Concentration to Support Candle-Like Combustion of Plastics (Oxygen Index). In *D2863-10*, ASTM International: West Conshohocken, PA, United States, 2010.
30. Weil, E. D.; Patel, N. G.; Said, M. M.; Hirschler, M. M.; Shakir, S., Oxygen index: Correlations to other fire tests. *Fire Mater.* **1992,** 16, (4), 159-167.
31. Gu, Y.; Ran, Q.-C., Chapter 28 - Polybenzoxazine/Fiber Composites. In *Handbook of Benzoxazine Resins*, Hatsuo, I.; Tarek, A., Eds. Elsevier: Amsterdam, 2011; pp 481-494.
32. Xiang, H.; Ling, H.; Wang, J.; Song, L.; Gu, Y., A novel high performance RTM resin based on benzoxazine. *Polym. Compos.* **2005,** 26, (5), 563-571.
33. Ishida, H.; Low, H. Y., Synthesis of benzoxazine functional silane and adhesion properties of glass-fiber-reinforced polybenzoxazine composites. *J. Appl. Polym. Sci.* **1998,** 69, (13), 2559-2567.
34. Xu, M.; Yang, X.; Zhao, R.; Liu, X., Copolymerizing behavior and processability of benzoxazine/epoxy systems and their applications for glass fiber composite laminates. *J. Appl. Polym. Sci.* **2013,** 128, (2), 1176-1184.
35. Ling , H.; Gu, Y.; Xie, M., A new F grade insulating glass cloth laminate based on benzoxazine. *Insul. Mater.* **2001,** 34, (1), 20-23.
36. Xie, M.; Gu, Y.; Hu, Z., Study on properties of polybenzoxazine/GF laminates. *Insul. Matter. Commun.* **2004,** 5, 21-25.
37. Wang, J.; Gu, Y.; Xie, M., Study on glass laminate based on benzoxazine-epoxy resin. *China. Plast. Ind.* **2001,** 29, 6-8.
38. Kimura, H.; Matsumoto, A.; Ohtsuka, K., Glass fiber-reinforced composite based on benzoxazine resin. *J. Appl. Polym. Sci.* **2009,** 114, (2), 1256-1263.

2.5.1

POLYBENZOXAZINES FROM RENEWABLE DIPHENOLIC ACID

Polybenzoxazines from renewable diphenolic acid

C. Zúñiga, M. S. Larrechi, G. Lligadas, J. C. Ronda, M. Galià, V. Cádiz
Departament de Química Analítica i Química Orgànica. Universitat Rovira i Virgili. Campus Sescelades Marcel.lí Domingo s/n. 43007 Tarragona. Spain.

ABSTRACT: The novel benzoxazine monomers, DPA-Bz and MDP-Bz from renewable diphenolic acid (DPA), which mimics the structure of bisphenol A (BPA), were synthesized by traditional approaches. The structure and purity of the monomers was confirmed by FTIR, ^{1}H NMR and ^{13}C NMR spectra. The thermally activated polymerization of the MDP-Bz and DPA-Bz afforded thermosetting polybenzoxazines with higher T_g's, 270 ºC and 208 ºC respectively, and higher crosslinking density compared to BPA-Bz, due to the transesterification or esterification reactions occurred during curing process. These reactions are in accordance with the number of independent reactions determined analyzing by SVD the chemical rank of the IR spectra data matrices recorded along the homopolymerization reactions monitored at 200 ºC. Spectral and concentration profiles of the active chemical species involved in these processes were obtained by MCR-ALS.

KEYWORDS: benzoxazine; crosslinking; diphenolic acid; infrared spectroscopy; renewable resource

---

INTRODUCTION The development of environmentally compatible polymers is one of the current challenges in polymer chemistry. The scarcity of non renewable resources encouraged the scientific community to develop and commercialize new bio-based products that can alleviate the wide-spread dependence on fossil fuels and, enhance security, the environment and the economy.[1] Polymers from renewable resources will play an increasing role because of economical and environmental benefits and the new property profiles that renewable polymers can exhibit, such as biocompatibility and biodegradability.[2]

Polybenzoxazine as a novel phenolic type thermoset has been developed to overcome the short-comings associated with traditional phenolics resins such as releasing condensation by-products and using strong acids as catalysts, while retaining good thermal properties and flame retardancy of phenolic resins.[3] It

can be prepared from benzoxazines via thermally induced ring opening polymerisation.[4] Benzoxazines are readily synthesized either in solution or by a melt-state reaction using a combination of a phenolic derivative, formaldehyde, and a primary amine.[5] Polybenzoxazines have not only the advantageous properties of conventional phenolic resins but also other interesting advantages such as heat resistance, superior electronic properties, low water absorption, low surface energy and excellent dimensional stability.[6] Though, polybenzoxazines offer a variety of advantages, pure polybenzoxazine-based polymers also suffer number of disadvantages too. The disadvantages of the typical polybenzoxazines are the high temperature needed for complete curing and the brittleness of the cured materials that can sometimes limit their potential applications. To properly address these issues and overcome the associated disadvantages, several strategies such as: preparation of monomers with additional functionality, synthesis of novel polymeric precursors and blending with a high-performance polymer or filler and fiber, have been attempted.[7]

The synthesis of bisphenol A (BPA) based benzoxazine has been reported,[8] and its polymerization yields thermosets with high structural integrity and thus the materials would possess very good properties. In recent decade, it has attracted much attention from researchers to synthesize new polyesters and polycarbonates using diphenolic acid (DPA)[9-12] instead of BPA, because DPA has a structure similar to BPA. The research interest resulted from that DPA is commercially available and much cheaper than BPA and it can introduce functional carboxyl group into the polymer structure. Moreover, DPA is a condensation product of phenol and levulinic acid. Levulinic acid is believed to be a cheap platform chemical and can be commercially produced from cellulose-rich biomass (especially from waster biomass) in large scale.[13]

In this paper, we report the synthesis of DPA based benzoxazine (DPA-Bz) and the DPA ester derivative, MDP, based benzoxazine (MDP-Bz), (see Scheme 1), and compare the polymerization and properties of both DPA and MDP based benzoxazines with those of the standard BPA based benzoxazine (BPA-Bz). The presence of a carboxylic acid in DPA monomer should lower the high temperature needed to complete curing of these benzoxazines. We have previously found that the presence of carboxyl groups influences thermal curing and the processing

temperatures are lower.[14] The curing behaviour of these materials was studied by differential scanning calorimetry (DSC) and FTIR.

Conventional spectroscopy and chemometric analysis of the FTIR spectra data obtained in monitoring both benzoxazine homopolymerizations were carried out. The number of the independent reactions that take place in the processes were evaluated from the rank of the matrix data by singular value decomposition (SVD).[15] Spectra and concentration profiles of the representative chemical species involved in the reactions were obtained applying multivariate curve resolution-alternating least square (MCR-LS).[16]

Finally, the properties of the materials were evaluated by termogravimetric analysis (TGA) and dynamic mechanical analysis (DMTA).

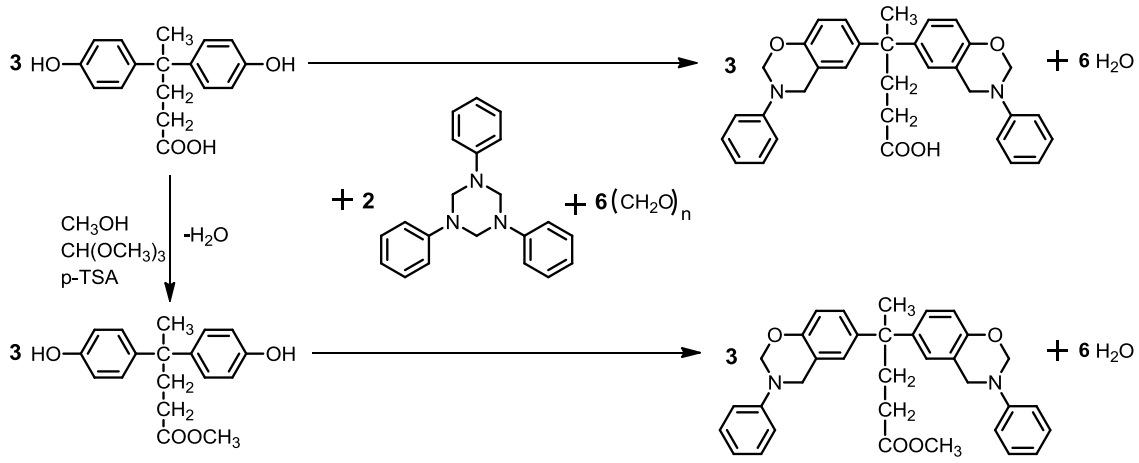

SCHEME 1 Synthesis of DPA-Bz and MDP-Bz.

EXPERIMENTAL

Materials

The following chemicals were obtained from the sources indicated and used as received: ammonium sulphate (Probus), paraformaldehyde (Probus), 4,4´-bis(4-hydroxyphenyl) pentanoic acid (Aldrich), trimethylorthoformate (Fluka), steraic acid (Aldrich), methylstearate (Aldrich), 2,4-dimethylphenol (Fluka), p-toluenesulfonic acid monohydrate (Panreac) and benzyldimethylamine (Fluka).

The 1,3,5-triphenylhexahydro-1,3,5 triazine and Bisphenol A based benzoxazine (BPA-Bz) were synthesized according to the reported procedure.[17,18] All solvents were purified by standard procedures.

Synthesis of 4,4´-bis-[6-(3-phenyl-3,4-dihydro-2*H*-1,3-benzoxazine)] pentanoic acid (DPA-Bz)

1,3,5-triphenylhexahydro-1,3,5-triazine (0.04 mol), paraformaldehyde (0.12 mol), 4,4´-bis(4-hydroxyphenyl) pentanoic acid (0.06 mol) and 240 mL of toluene were placed into 500 mL two-necked round bottom flask. The reaction mixture was heated at 110°C for 6 h. The resulting light orange solution was filtered and concentrated under vacuum to obtain a syrup that was subsequently dried under high vacuum giving a yellowish solid with a yield of 95% of DPA-Bz.

^{1}H NMR ($CDCl_3$/TMS, δ ppm): 7.30-6.70 (16H, Ar-H), 5.34 (4H, s, O-CH_2-N), 4.58 (4H, s, Ar-CH_2-N), 2.35 (2H, t), 2.13 (2H, t), 1.53 (3H, s).
^{13}C NMR ($CDCl_3$, δ ppm): 179.9 (s), 152.5 (s), 148.5 (s), 141.1 (s), 129.4 (d), 126.9 (d), 125.3 (d), 121.4 (d), 120.4 (s), 118.1 (d), 116.7 (d), 79.2 (t), 50.7 (t), 44.6 (s), 36.4 (t), 30.2 (t), 27.8 (q).
IR: ν (cm^{-1}) 1702 (C=O st)

Synthesis of methyl-4,4´-bis(4-hydroxyphenyl) pentanoate

A 500 mL round bottom flask equipped with a condenser was charged with 4,4´-bis(4-hydroxyphenyl) pentanoic acid (0.26 mol), *p*-toluenesulfonic acid monohydrate ($2.6x10^{-4}$ mol), trimethylorthoformate (0.38 mol) and 200 mL of methanol. The mixture was refluxed for 16 h, the methanol was removed under vacuum and the resulting syrup was dissolved in ethyl ether and washed several times with a $NaHCO_3$ saturated solution and with water. Finally, the ethyl ether was removed with a rotary evaporator and the product was dried under vacuum at room temperature. The resulting product was milled and used without further purification in the next step. A yield of 98% was obtained.

^{1}H NMR ($CDCl_3$/TMS, δ ppm): 7,05 (4H, d, J_o= 6.8 Hz), 6.73 (4H, d, J_o= 6.8), 4.68 (2H, s, OH) 3.62 (3H, s, OCH_3), 2.39 (2H, t), 2.10 (2H, t), 1.56 (3H, s).
^{13}C NMR ($CDCl_3$, δ ppm): 172.8 (s), 153.9 (s), 138.3 (s), 126.8 (d), 113.6 (d), 50.2 (q), 42.9 (s), 35.4 (t), 28.8 (t), 26.4 (q).
IR: ν (cm^{-1}) 1700 (C=O st)

Synthesis of methyl 4,4´-bis-[6-(3-phenyl-3,4-dihydro-2*H*-1,3-benzoxazine)] pentanoate (MDP-Bz)

A 1 L two-necked round bottom flask equipped with a magnetic stirrer and a condenser was charged with 1,3,5-triphenylhexahydro-1,3,5-triazine (0.08 mol), paraformaldehyde (0.24 mol), methyl 4,4´-bis(4-hydroxyphenyl)pentanoate (methyl diphenolate) (0.12 mol) and 480 mL of toluene. The mixture was refluxed at 110°C for 20 h. After cooling to room temperature the benzoxazine monomer was filtered, dissolved in ethyl ether and washed 5 times with a 3N NaOH aqueous solution and with water. After washing, the organic phase was dried over sodium sulfate and the solvent was evaporated under vacuum at room temperature. A pale yellowish solid was obtained with a yield of 93%.

^{1}H NMR ($CDCl_3$/TMS, δ ppm): 7.32-6.74 (16H, Ar-H), 5.37 (4H, s, O-CH_2-N), 4.62 (4H, s, Ar-CH_2-N), 3.63 (3H, s, OCH_3), 2.40 (2H, t), 2.14 (2H, t), 1.56 (3H, s).
^{13}C NMR ($CDCl_3$, δ ppm): 174.4 (s, C=O), 152.5 (s), 148.5 (s), 141.2 (s), 129.3 (d), 126.9 (d), 125.3 (d), 121.3 (s), 120.3 (s), 118.0 (d), 116.6 (d), 79.2 (t, O-CH_2-N), 51.7 (q, OCH_3), 50.7 (t, Ar-CH_2-N), 44.6 (s), 36.6 (t), 30.1 (t), 27.8 (q).
IR: ν(cm^{-1}) 1735 (C=O st)

Crosslinking reaction.

Polybenzoxazine samples were prepared with a manual hydraulic press 15-ton sample pressing (SPECAC) equipped with a water cooled heated platens. Previously, each monomer was degassed in a glass oven for 30 min at 140 °C. Samples were compressed in rectangular steel mold (80 mm x 51.5 mm x 3 mm) under a pressure of 9.2 MPa. Because of every monomer has different thermal polymerization behavior, the curing temperatures were adjusted according to each DSC thermogram. BPA-Bz and MDP-Bz were heated at 190 °C for 2h, 215 °C for 2h, 235 °C for 8 h and 260 °C for 2h, while DPA-Bz was heated at 140°C for 2h, 160°C for 2h, 180°C for 8 h and 190°C for 2h. (Table 1)

Instrumentation

The FTIR spectra were recorded on a JASCO 680 FTIR spectrophotometer with a resolution of 4 cm^{-1} in the absorbance and transmittance modes. An attenuated total reflection (ATR) accessory with thermal control and a diamond crystal (Golden Gate heated single-reflection diamond ATR, Specac Teknokroma) was

used to determine FTIR spectra. ^{1}H (400 MHz) and ^{13}C (100.5 MHz) NMR spectra were obtained using a Varian Gemini 400 spectrometer with Fourier transform and $CDCl_3$ as solvent.

TABLE 1 DSC data and curing conditions of the benzoxazine monomers

Sample	T_{onset} (°C)	T_{max} (°C)	ΔH_o (kJ/mol)	Curing conditions
BPA-Bz	210	256	122	190 °C (2h), 215 °C (2h), 235 °C (8h), 260 °C (2h)
DPA-Bz	150	192	154	140 °C (2h), 160 °C (2h), 180 °C (8h), 190 °C (2h)
MDP-Bz	210	261	129	190 °C (2h), 215 °C (2h), 235 °C (8h), 260 °C (2h)

Calorimetric studies were carried out on a Mettler DSC821e thermal analyzer using N_2 as a purge gas (100 ml/min) at scanning rate of 20 ºC/min. Thermal stability studies were carried out on a Mettler TGA/SDTA851e/LF/1100 with N_2 or air as a purge gas at scan rates of 10 ºC/min. Mechanical properties were measured using a dynamic mechanical thermal analysis (DMTA) apparatus (TA DMA 2928). Specimens (10 mm x 6 mm x 1.9 mm) were tested in a three point bending configuration. The thermal transitions were studied in the 35-320 ºC range at a heating rate of 3 ºC/min and at a fixed frequency of 1 Hz.

Data acquisition of FTIR spectra

The data obtained correspond to the FTIR/ATR spectra recorded between 600 and 2000 cm^{-1} every 0.482 cm^{-1} for DPA-Bz and MDP-Bz homopolymerizations. The reactions were monitored along 4.5h for DPA-Bz and 15h for MDP-Bz. The bands at 1490, 1230 and 940 cm^{-1} associated to the benzoxazine ring, were used to follow the progress of the reaction. In the DPA-Bz homopolymerization, 71 spectra were obtained. In the MDP-Bz homopolymerization, 180 spectra were obtained, and 70 spectra were selected for analysis, corresponding to the obtained each 5 min during the first hour, each 10 min during the second hour and the rest each 15 min. The spectra recorded in the FTIR/ATR were exported and converted into MATLAB binary files,[19] to carry out the chemometric analysis.

The recorded spectra were arranged in two matrices **M** (71 x 2905) and **N** (70 x 2905) whose rows were the number of recorded spectra and whose columns

were the wavelengths of DPA-Bz and MDP-Bz reactions, respectively.

RESULTS AND DISCUSSION

1,3,5-triphenylhexahydro-1,3,5-triazine is an active intermediate and precursor in the synthesis of aromatic amine-based benzoxazine structures.[17,18]It is therefore possible to obtain this triazine from aniline and paraformaldehyde, which reacts with bisphenol A and paraformaldehyde leading to the bis(3,4-dihydro-2*H*-3-phenyl-1,3-benzoxazinyl) isopropane (BPA-Bz) in high yield and purity. In a similar way, the synthetic route for DPA-Bz (Scheme 1) uses triazine and DPA to obtain methyl 4,4´-bis-[6-(3-phenyl-3,4-dihydro-2*H*-1,3-benzoxazine)] pentanoic acid (DPA-Bz) also with high yield. It is worth to note that the resulting benzoxazine was obtained in high purity, thus, no further purification procedure was necessary. Probably in this case, byproducts and oligomeric species form the insoluble fraction that was removed by filtration. Likewise, previous esterification of DPA with methanol, the resulting pentanoate reacts with triazine and paraformaldehyde leading to the methyl 4,4´-bis-[6-(3-phenyl-3,4-dihydro-2*H*-1,3-benzoxazine)] pentanoate (MDP-Bz).

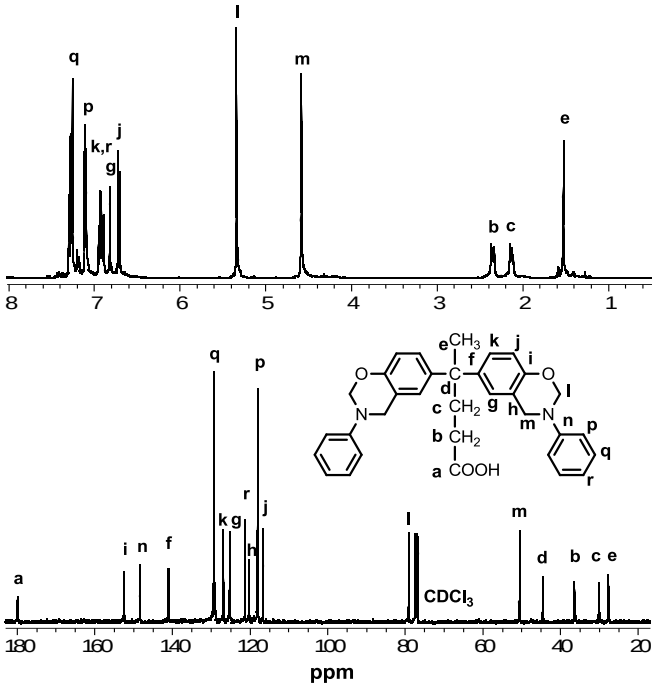

FIGURE 1^{1}H and ^{13}C NMR spectra of DPA-Bz.

The structure of the benzoxazine monomers was confirmed by spectral analysis. As can be seen from Figure 1 the nuclear magnetic resonance spectroscopy (^{1}H NMR) spectrum of the DPA-Bz exhibits not only the specific signals of the benzoxazine ring, but also chemical shifts that belong to the alkyl chain and the aromatic signals. Notably, while the two signals at 5.3 and 4.6 ppm correspond to –*CH_2* protons of benzoxazine ring, methyl protons of the pentanoic acid appears at 1.5 ppm (singlet, *3H*) and methyl protons of the pentanoate at 3.6 ppm (in the case of MDP-Bz). Alkyl protons of the propionic acid or propionate moiety resonate at 2.1 ppm (triplet, C-*CH_2*, 2H) and 2.3 ppm (triplet, -*CH_2*-COOH, *2H*) or 2.4 ppm (triplet, -*CH_2*-$COOCH_3$, *2H*). The COOH proton is not observed when $CDCl_3$ is used as solvent. The lack of any resonance around 3.7 ppm, typical frequency for ring opened oligomers due to the Mannich bridge protons of open oxazine rings: -CH_2-NPh-CH_2- structure, indicates that all the monomers are essentially free of ring-opened oligomers, and the purification procedure, when it was needed, was good enough to obtain samples with high purity. Moreover, integration analysis of the oxazine and aromatic proton peaks pointed out that the closed-ring structured monomer is about 99%. Specially, it is important to have high purity monomers free of phenolic impurities and ring-opened oligomeric species for the evaluation of the polymerization rate as these species lower the polymerization temperature of the monomers acting as acid cationic initiators. The corresponding ^{13}C NMR spectrum also supports the structure of these compounds. The two singlets at 79.2 ppm and 50.7 ppm are typical of the carbon resonances of –N-CH_2-O- and –N-CH_2-Ph of the oxazine ring, respectively. No detectable resonances due to impurities are seen in the spectrum.

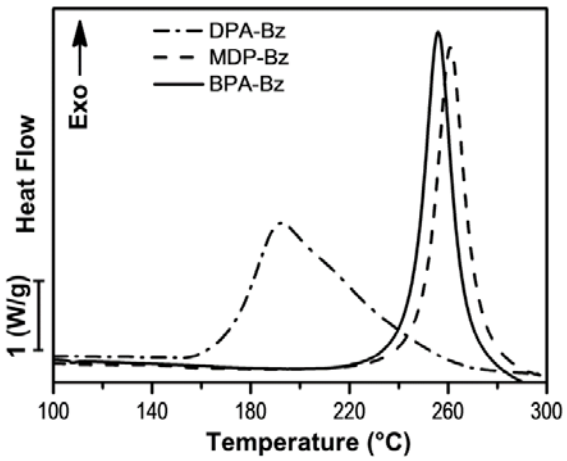

FIGURE 2 DSC plots of DPA-Bz, MDP-Bz and BPA-Bz.

Moreover, the expected structures of the monomers were further evidenced by FT-IR. For both monomers, the presence of cyclic ether of benzoxazine structure is confirmed by the absorbance peaks at about 1230 and 1035 cm^{-1} due to the C-O-C symmetric stretching and asymmetric stretching modes respectively. The characteristic band at 952-942 cm^{-1} due to the C-H out-of-plane deformation mode indicated the formation of oxazine rings.[20]

It is well known that 1,3-benzoxazines exhibit exothermic ring opening reaction around 200-250 ºC, which can be monitored by DSC. Figure 2 shows the DSC plots of the synthesized systems DPA-Bz, MDP-Bz and the BPA-Bz for comparison. In Table 1 are collected the onset and maximum temperatures of the crosslinking exotherms. As can be seen, the ring opening of benzoxazines of MDP-Bz and BPA-Bz occur at very similar temperature, about 260 ºC. However, the polymerization temperature observed for DPA-Bz was quite low compared to those of the ordinary benzoxazines. The thermogram reveals a broad exotherm with an onset at 150 ºC and a maximum at 190 ºC with 154 kJ/mol as the exothermic energy. As NMR data show high purity monomers free of oligomers, the low polymerization temperature of this monomer can directly be attributed to monomer characteristic, that is, to the presence of carboxylic group.

According to DSC data the curing benzoxazine resins were carried out in a mold with compression by heating samples at different temperatures and times collected in Table 1.

The dynamomechanical properties of the polybenzoxazines were investigated by DMTA. The dynamic mechanical behavior of the cured benzoxazine resins was obtained as a function of the temperature beginning in the glassy state of each composition to the rubbery plateau of each material (Figure 3a). For the thermoset polymerized from benzoxazine monomers, the storage modulus is maintained approximately the same value for a wide temperature range up to 150 ºC. The crosslinking density of a polymer can be estimated from the plateau of the elastic modulus in the rubbery state.[21] However, this theory is strictly valid only for lightly crosslinked materials, and was therefore used only to make qualitative comparisons of the level of crosslinking among the various polymers. BPA-Bz shows the lowest crosslinking density while DPA-Bz and MDP-Bz show higher crosslinking density.

DMTA enables T_g's of the crosslinked materials to be determined. It is detected as the maximum of the loss modulus (E"), which corresponds to the initial drop from the glassy state into the transition. Moreover, the α-relaxation peak of the loss factor, tan δ, is associated with T_g and corresponds to the transition midpoint of the log of the E' curve. As shown in Figure 3b, the T_g, determined as the peak temperature of tan δ curve is as high as 270 ºC and 208 ºC for MDP-Bz and DPA-Bz, respectively. The T_g values from both measurements are shown in Table 2. As expected, T_g as tan δ peak is higher than E" peak. In this table is also collected the T_g value, as $1/2\Delta Cp$, determined by DSC, which is in accordance with DMTA values. The analysis of the height of the tan δ peak values indicates a higher crosslinking density for MDP-Bz and DPA-Bz compared to BPA-Bz. This could be explained by the transesterification or esterification of the acidic group and the phenolic OH, which is resulted from ring opening of oxazine, respectively. Similar condensation was previously observed in the poly(amic acid)-phenolic OH condensation[22] and in benzoxazines with p-carboxyphenyl linkage.[23]

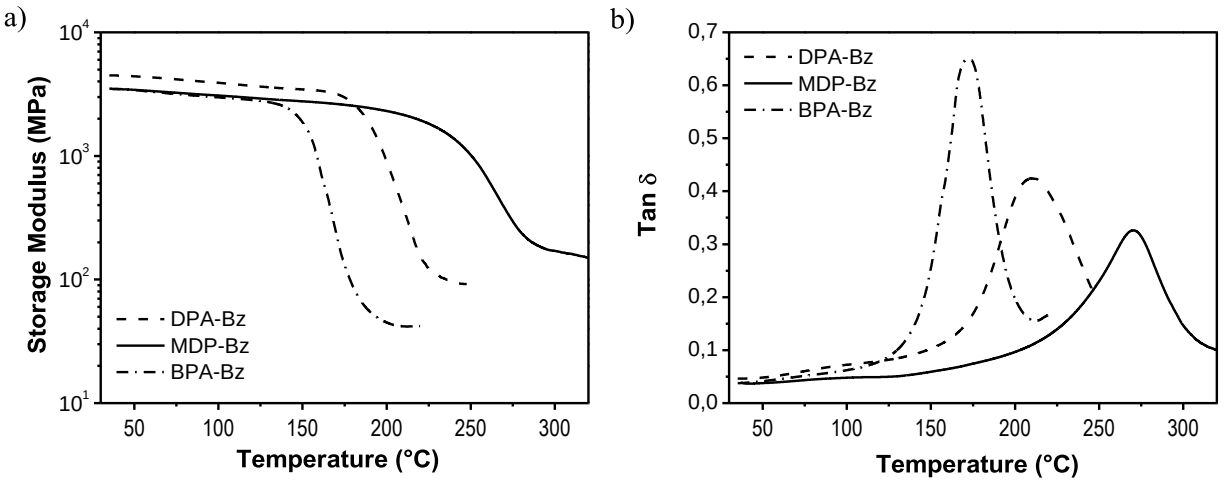

FIGURE 3a) Tan delta and b) Storage modulus versus temperature of DPA-Bz, MDP-Bz and BPA-Bz.

To gain more insight about the curing processes, the most common method used to monitor the benzoxazine ring opening, DSC, do not provide direct information about the mechanism of the reaction. The number of species involved in the curing reaction can be obtained by separation techniques such as high performance liquid chromatography.[24]This is essentially an offline technique and

it is often used for the kinetic investigation of reactions that do not evolve towards solid products. Spectroscopic techniques such as FTIR/ATR and chemometrics analysis of the recorded data through the reaction make it possible to monitor the process on line and provided useful information about the number of the chemical structures evolved in the curing reaction. We studied the behavior of DPA-Bz and MDP-Bz polymerizations by monitoring by FTIR/ATR spectroscopy in isothermal experiments at 200 ºC.

TABLE 2 Thermal and Thermogravimetric Properties of Cured Polybenzoxazines

	T_g (°C)			TGA (N_2)			TGA (O_2)		
Sample	½ΔC_p	E''_{max}	Tan δ_{max}	$T_{10\%}$ (°C)[a]	T_{max} (°C)[b]	Y_{800} (%)[c]	$T_{10\%}$ (°C)[a]	T_{max} (°C)[b]	Y_{800} (%)[c]
BPA-Bz	170	154	172	366	427	34	386	418	18
DPA-Bz	207	185	208	348	425	32	353	423	7
MDP-Bz	265	235	270	379	420	31	388	418	12

[a] Temperature of 10% weight loss
[b] Temperature of the maximum weight loss rate
[c] Char yield at 800 ºC

This technique allowed us to follow the evolution of the functional groups involved in the process by means of the variation in the corresponding absorptions. Figure 4 shows FTIR spectra of DPA-Bz and MDP-Bz polymerizations at different times. These spectra show the characteristics benzoxazine bands at about 1230 cm^{-1}, 1030 cm^{-1} and 940 cm^{-1} which follow a progressive diminution with time. However, as can be seen, the evolution of benzoxazine bands is different in both processes, being much faster in DPA-Bz. Moreover, the trisubstituted benzene ring bands in the benzoxazine structures at about 1490 cm^{-1}, 820 cm^{-1},and 690 cm^{-1}follow the same trend as crosslinking proceeded, decreasing as a tetrasubstituted benzene rings appear, and consequently much faster in DPA-Bz. Both figures show the different evolution in the bands corresponding to carbonyl groups, in the zone around 1700 cm^{-1}, of DPA-Bz and MDP-Bz. From the first stages of the reaction of DPA-Bz, two carbonyl bands can be distinguished corresponding to the phenolic ester (about 1728 cm^{-1}) and the free carboxylic group (about 1710 cm^{-1}), however at the beginning of the MDP-Bz homopolymerization, only a strong band at 1735 cm^{-1}attributable to initial methyl ester carbonyl group is observed which decreases with time at once other absorptions appear, as can be seen in Figure 5 where the expanded carbonylic zone is shown. So, at 135 min (spectrum 3), two different absorptions are clearly

zone is shown. So, at 135 min (spectrum 3), two different absorptions are clearly detected: one the above mentioned at about 1735 $cm^{-1}$and a second at about 1725 cm^{-1}attributable to phenolic ester carbonyl group as a consequence of the transesterification process that presumably has taken place. When the reaction makes progress up to 435 min (spectrum 4), a third absorption, at 1712 cm^{-1}, is detected that could be due to the carbonyl group of a carboxylic acid from a partial hydrolysis of the ester group.

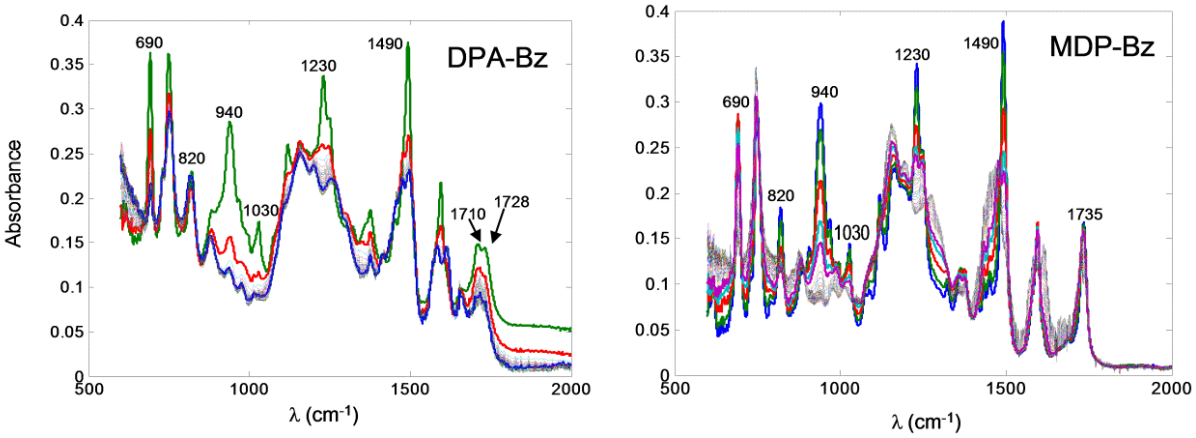

FIGURE 4 FTIR-ATR spectra of DPA-Bz and MDP-Bz homopolymerizations at 200 ºC.

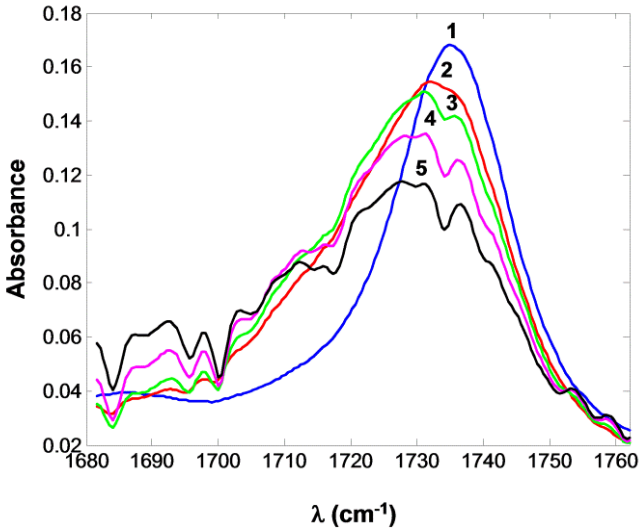

FIGURE 5 Expanded carbonylic zone of FTIR spectra of MDP-Bz polymerization at 5 min (1), 45 min (2), 135 min (3), 435 min (4), 885 min (5).

Additional information about the number of independent reactions involved in the homopolymerization processes can be obtained from the rank analysis of the spectra data matrices M and N evaluated by singular value decomposition (SVD).[15]As example in Table 3, the values of the 8 first singular values are showed. Considering as threshold the singular values associated to the noise (λ = 0.5) in both **M** (DPA-Bz) and **N** (MDP-Bz) matrices, four factors are significantly different from noise, thus, the chemical rank is four. Analysis of the rank associated with matrices of data obtained in the study of a chemical reaction has been widely discussed by Amrheim et al,[25] who showed that in this type of matrix data the rank is equal to minimum of (*r*+1, *c*) where *r* is the number of independent reactions in the chemical system and *c* is the number of absorbent species. This result allows us to propose that for the DPA-Bz and MDP-Bz thermal curing, three processes are involved: benzoxazine ring opening to form Mannich bridges, further crosslinking and esterification or transesterification processes in DPA-Bz or MDP-Bz respectively. Four chemical species representatives of the structures involved in these reactions are postulated: A, B, C and D (Scheme 2).

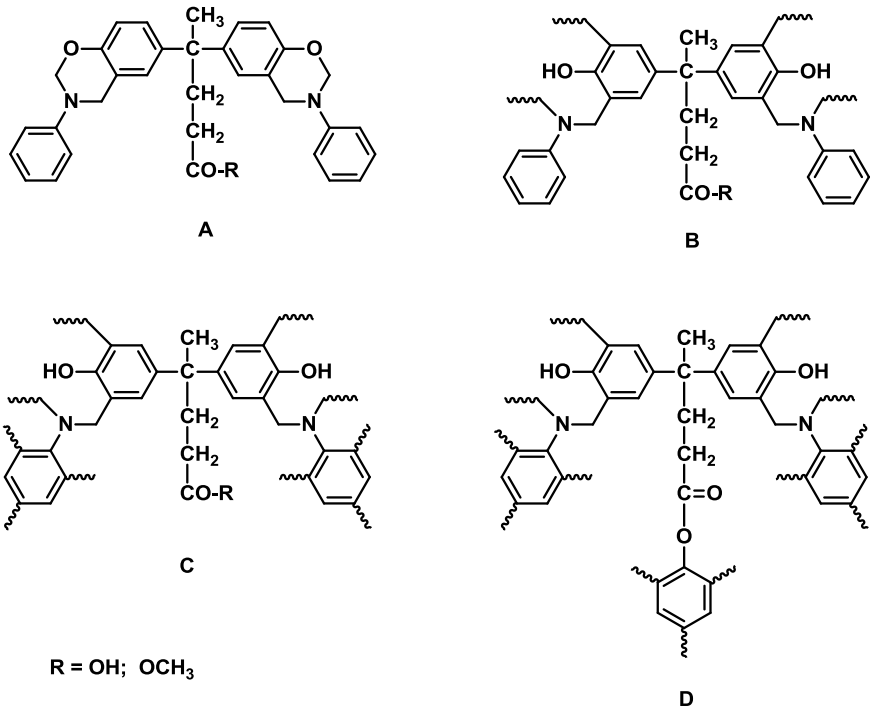

SCHEME 2 Postulated chemical structures involved in the crosslinking process.

Spectral and concentration profiles of their evolution along of the reaction can be obtained when the experimental spectra data matrix were fitted to the model *D*

$= C.S^T + E$ equation, where D represent the experimental spectra data matrix (M and N in our case), C contain the concentration profiles of the chemical species A, B, C and D, S their pure spectra and E accounts for the experimental error. This resolution was carried out by multivariate curve resolution-alternating least squares method (MCR-ALS).[16]This method analyzes the data based on very few fundamental restrictions, implicit in Beer-Lambert law.

TABLE 3 Rank Analysis of Matrices **M** and **N**

Eigen value(λ)	DPA-Bz	MDP-Bz
1	68.4914	57.1656
2	3.6771	4.9428
3	1.0860	1.6592
4	0.5678	0.3945
5	0.1816	0.2459
6	0.1431	0.1629
7	0.1160	0.1294
8	0.1108	0.1252

The variance associated with the solutions, found by MCR-LS for the DPA-Bz and MDP-Bz homopolymerizations was 99.99% and 99.98%, respectively.

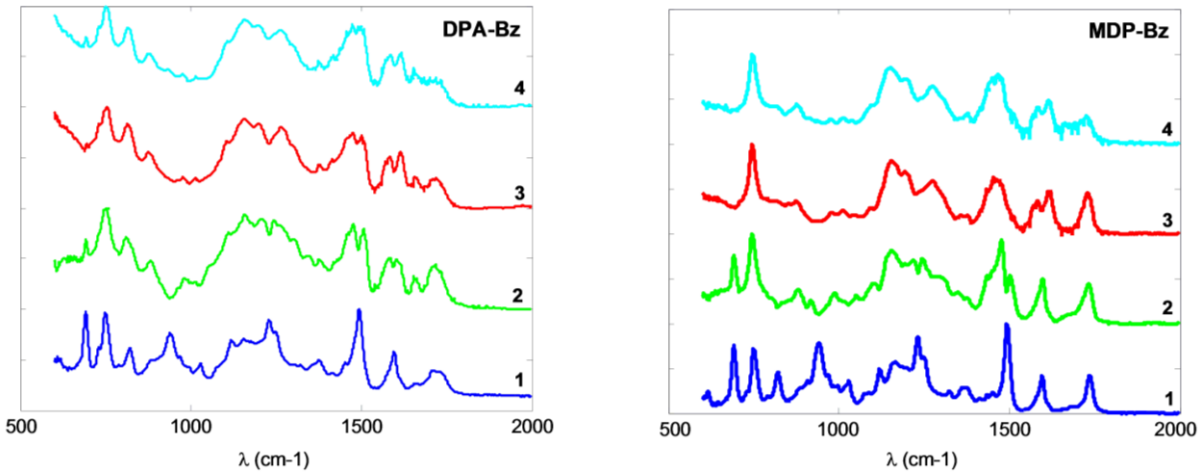

FIGURE 6 Spectra Profiles recovered by MCR-LS for DPA-Bz and MDP-Bz homopolymerizations.

Figure 6 shows the normalized spectra for each of the above postulated four chemical structures. In both cases, the spectrum (1) contains characteristic absorption bands of the initial benzoxazines (Figure 4). Their similarity with the experimental spectra was evaluated through the correlation coefficient, founding values of 0.9990 and 0.9999, respectively. The spectrum (2), is in agreement with the disappearance of characteristic bands at 1230 cm^{-1}, 1030 cm^{-1} and 940 cm^{-1}, of benzoxazine ring, thus, these spectra can be considered representative of Mannich bridge structures from ring opening. In the spectra 2, 3 and 4 in DPA-Bz and spectra 3 and 4 in MDP-Bz is possible to observe double absorption peaks around 1600 cm^{-1}, characteristic vibrations of C=C aromatic ring, which could be associated to a new crosslinked species (C and D in scheme 2). Moreover, differences in the carbonylic absorptions around 1700 cm^{-1}, can be observed in spectra 3 and 4, associated to the esterification processes (D in scheme 2). After this discussion it is worth to point out that spectra 2, 3 and 4 can not be considered as pure spectra of each species, but they are a good estimation of them.

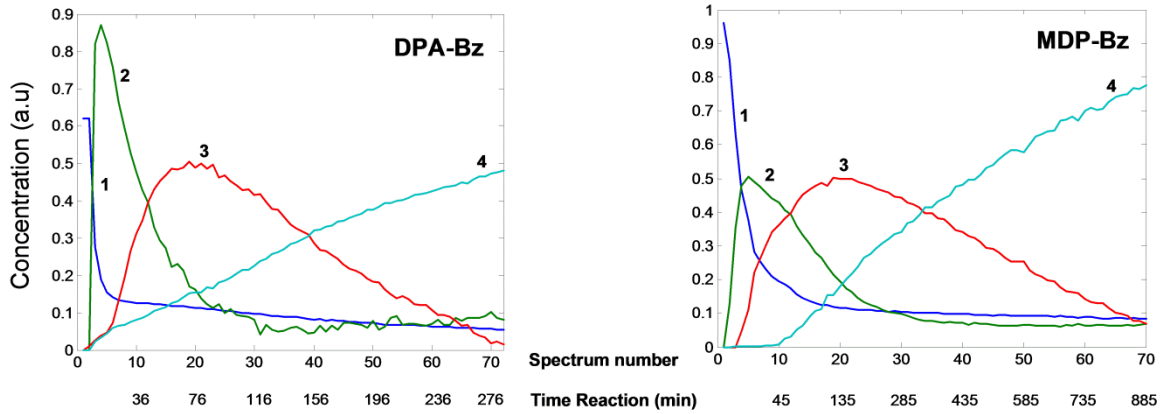

FIGURE 7 Concentration profiles recovered by MCR-LS for DPA-Bz and MDP-Bz homopolymerizations.

Information about the kinetic of these reactions can be obtained by analyzing the evolution of the concentration of each chemical species, A, B, C, and D along the homopolymerizations (Figure 7). Curves 1 that undergo a fast decrease from the beginning are associated with the starting benzoxazine monomers (spectra 1 in Figure 6 and A in Scheme 2) which rapidly suffer the ring opening. Curves 2,

associated to Mannich bridge structures (spectra 2 in Figure 6 and B in scheme 2), increase at the same rate as curves 1 decrease at the beginning of reaction and decrease progressively as the curing proceed and new crosslinked sites are formed including the reactive positions in the aniline ring (C in scheme 2). This new chemical situations should be depicted by curves 3. Finally, curves 4 would be associated to the esterification process (D in scheme 2) that in the DPA-Bz reaction is observed from the beginning of the reaction while in the MDP-Bz reaction needs an induction time of about 50 minutes before transesterification started. This fact could be related with the more acidic medium in the first reaction that facilitates the esterification. To unravel the transesterification process a model experiment in which methylestearate and 2,4-dimethylphenol were heated at 200 ºC, in presence of dimethylbenzylamine, was carried out. The reaction was followed by IR showing the disappearance of the absorption at 1739 cm^{-1} due to the carbonyl group of methylestearate and the appearance of a band at 1725 cm^{-1} of the corresponding carbonyl group of phenolic ester.

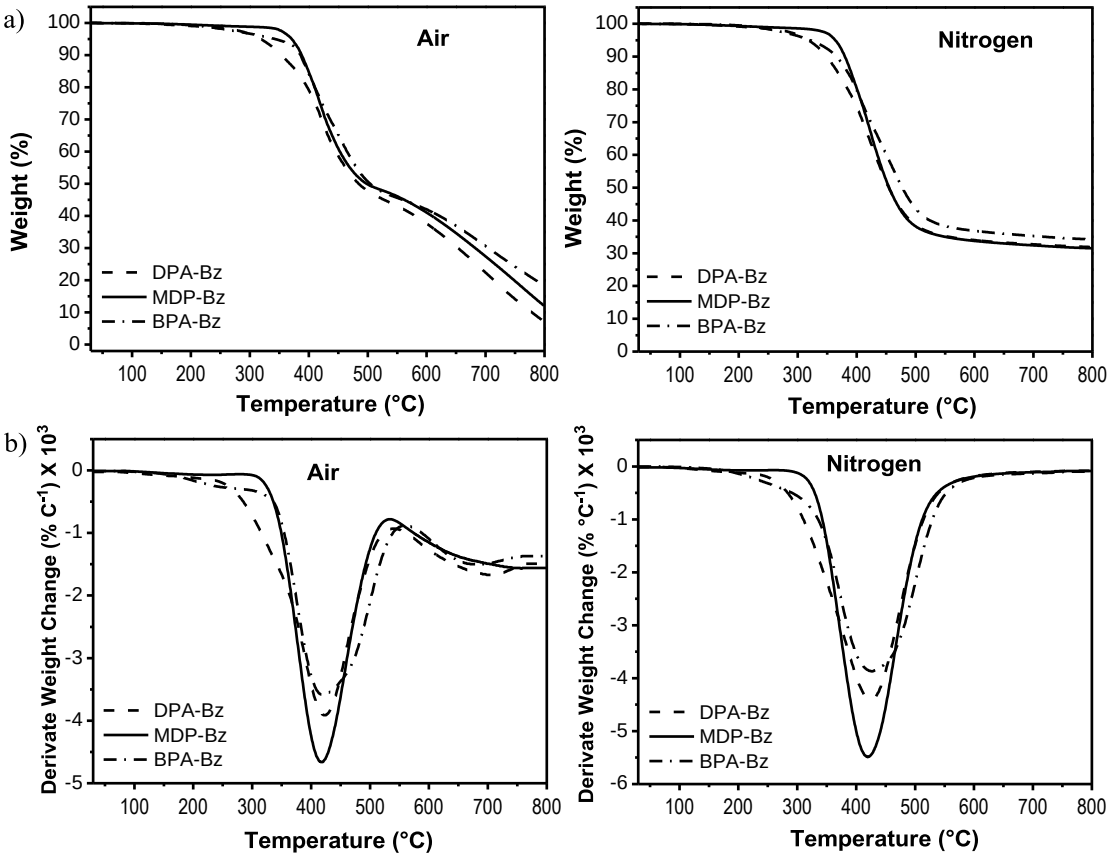

FIGURE 8 TGA plots in nitrogen and air of polybenzoxazines from DPA-Bz, MDP-Bz and BPA-Bz.

To determine the thermal stability and the decomposition behaviour, thermogravimetric analysis were carried out under nitrogen and air atmospheres. Figure 8 shows TGA curves and the first derivative curves and Table 2 summarizes TGA data. Under air or nitrogen atmosphere, samples were thermally stable below 250 ºC, and the degradation takes place in one step. However a higher temperature of 10% weight loss is observed for MDP-Bz derivative under nitrogen indicating a slightly higher resistance than DPA-Bz and BPA-Bz derivatives to degrade. No significant differences can be seen in temperature of the maximum weight loss rate and in char yields at 800 ºC indicating that all systems exhibit quite a similar thermal behavior.

CONCLUSIONS

We have synthesized two novel benzoxazine monomers, DPA-Bz and MDP-Bz from renewable diphenolic acid (DPA), with similar structure of bisphenol A (BPA), by traditional approaches. The thermally activated polymerization of the monomers afforded thermosetting polybenzoxazines, being the low polymerization temperature of DPA-Bz attributed to the presence of carboxylic group. Polybenzoxazines from MDP-Bz and DPA-Bzshowed higher T_g's, 270 ºC and 208 ºC respectively, and higher crosslinking density compared to BPA-Bz, due to the transesterification or esterification of the acidic groups and the phenolic OHs, formed during ring opening of oxazines. These reactions are in accordance with the number of independent reactions determined analyzing by SVD the chemical rank of the IR spectra data matrices recorded along the homopolymerization reactions monitored at 200 ºC. Spectral and concentration profiles of the active chemical species involved in these processes were obtained by MCR-ALS. DPA-Bz esterification is observed from the beginning of the reaction while the MDP-Bz transesterification needs an induction time of about 50 minutes under the studied conditions.

The authors express their thanks to CICYT (Comisión Interministerial de Ciencia y Tecnología) (MAT2008-01412) for financial support for this work.

REFERENCES AND NOTES

1. Feedstocks for the Future: Renewable for the Production of Chemicals and Materials; ACS Symposium Series 921; Bozell, J. J.; Patel, M., Eds.; American Chemical Society: Washington, DC, 2006

2. a) Belgacem M.N.; Gandini, A. Monomers, Polymers and Composites from Renewable Resources. Elsevier, Oxford 2008; b) Gandini A. Macromolecules 2008, 41, 9491-9504.

3. Ghosh, N. N.; Kiskan, B.; Yagci, Y. Prog Polym Sci 2007, 32, 1344-1391.

4. Endo, T.; Sudo, A. J Polym Sci Part A: Polym Chem 2009, 47, 4847-4858.

5. Ning, X.; Ishida, H. J Polym Sci Part A: Polym Chem Ed 1994, 32, 1121-1129.

6. Low, H.Y.; Ishida, H. Macromolecules 1997, 30, 1099-1106.

7. Yagci, Y.; Kiskan, B.; Ghosh, N.N. J Polym Sci Part A: Polym Chem 2009, 47, 5565-5576.

8. Ishida, H.; Rodríguez, Y. Polymer 1995, 36, 3151-3158.

9. Zhang, R. F.; Moore, J. A. Macromol Symp 2003, 199, 375-390.

10. Ping, Z.; Linbo, W.; Bo-Geng, L. Polym Degrad Stab 2009, 94, 1261-1266.

11. Moore, J. A.; Tannahill, T. High Perform Polym 2001, 13, S305-S316.

12. Chu, F. K.; Hawker, C. J.; Pomery, P. J.; Hill, D. J. T. J Polym Sci Part A Polym Chem 1997, 35, 1627-1633.

13. Bozell, J. J.; Moens, L.; Elliot D. C.; Wang, Y.; Neuenscwander, G. G.; Fitzpatrick, S. W.; Bilski, R. J.; Jarnefeld, J. Resources, Conservation Recycling 2000, 28, 227-239.

14. Andreu, R.; Reina, J. A.; Ronda, J. C. J Polym Sci Part A Polym Chem 2008, 46, 6091-6101.

15. Vandeginste, M. G.; Massart, D. L.; Buydens, L. M. C.; de Jong, S.; Lewi, P. J.; SmeyersVerbeke J. Handbook of Chemometrics and Qualimetrics: part B, Elsevier, Amsterdam, 1998.

16. De Juan, A.; Tauler, R. Anal Chim Acta 2003, 500, 195-210

17. Brunovska, Z.; Liu, J. P.; Ishida, H. Macromol Chem Phys 1999, 200, 1745-1752.

18. Espinosa, M. A.; Cádiz, V.; Galià, M. J Appl Polym Sci 2003, 90, 470-481.

19. The Mathworks, MATLAB Version 7.0, Natick, MA, 2004.

20. Dunkers, J.; Ishida, H. Spectrochim Acta Part A 1995, 51, 855-867.

21. Tobolsky, A. V.; Carlson, D.W.; Indictor, N. J. J Polym Sci 1961, 54, 175-192.

22. Takeichi, T.; Guo, Y.; Rimdusit, S. Polymer 2005, 46, 4909-4916

23. Lin, C. H.; Lin, H. T.; Chang, S. L.; Hwang, H. J.; Hu, Y. M.; Taso, Y. R.; Su, W. C. Polymer, 2009, 50, 2264-2272

24. Mijovic, J.; Fishbain, A.; Wijaya, J. Macromolecules 1992, 25, 979-985.

25. Amrhein, M.; Srinivasan, B.; Bonvin, D.; Schumacher, M. M. Chem Intell Lab Syst 1996, 33, 17-33.

2.5.2

RENEWABLE POLYBENZOXAZINES BASED IN DIPHENOLIC ACID

Renewable polybenzoxazines based in diphenolic acid

C. Zúñiga, G. Lligadas, J. C. Ronda,* M. Galià, V. Cádiz

Departament de Química Analítica i Química Orgànica. Universitat Rovira i Virgili. Campus Sescelades Marcel.lí Domingo s/n. 43007 Tarragona. (Spain).

ABSTRACT

The reaction of mixtures of renewable diphenolic acid (DPA) and its methylesterbenzoxazine derivative (MDP-Bz) has been studied. The DPA was introduced to lower the high temperature needed to complete the curing of the pure benzoxazine. In this way, samples with different DPA/MDP-Bz ratio (0, 2, 5, 10 and 25% of DPA) were investigated. Moreover, high performance flame retardant thermosetting resins with phosphorus were prepared through the mixture of MDP-Bz and a DPA-phosphazene derivative (DPA-PPZ). The curing behavior of these materials was studied by differential scanning calorimetry (DSC). Finally, the properties of the materials were evaluated by termogravimetric analysis (TGA), dynamic mechanical analysis (DMTA), tensile measurements, limiting oxygen index (LOI) and UL-94 Burn Test.

Keywords: renewable resources, diphenolic acid, polybenzoxazines

1. Introduction

Over the last decade, an interesting addition cure phenolic resin, namely benzoxazine, has attracted significant attention of the research community because of its unique advantages over most of the known polymers [1]. Polybenzoxazines have become one of a rare few new polymers commercialized in the past 30 years.

The chemistry of benzoxazines is responsible for a number of inherent processing advantages, including low melt viscosity, no harsh catalyst required, and no volatile release during cure and minimal cure shrinkage. They also have a good thermal stability that is demonstrated by their high glass transition temperatures, degradation temperatures, and char yields. A unique combination of intramolecular and intermolecular hydrogen bonding also contributes to the properties of polybenzoxazines.

Although, polybenzoxazines offer a variety of advantages, pure polybenzoxazine-based polymers suffer a number of disadvantages too. The disadvantages of the typical polybenzoxazines are the high temperature needed for complete curing and the brittleness of the cured materials that can sometimes limit their potential applications. The crosslinking densities of polybenzoxazine homopolymers are believed to be considerably lower than those of ordinary thermosetting resins. The tightening of the network structure has been achieved by introducing additional crosslinkable sites. To properly address these issues and overcome the associated disadvantages, the most successful strategies are the preparation of monomers with additional functionality, the synthesis of novel polymeric precursors and the blending with high-performance polymer, filler or fiber [2].

Until now, benzoxazine monomers are synthesized either in solution or by a melt-state reaction using a combination of petroleum-based phenolic derivatives, formaldehyde and primary amines. The scarcity of nonrenewable resources encouraged the scientific community to develop and commercialize new bio-based products that can alleviate the wide-spread dependence on fossil fuels and, enhance security, the environment and the economy. The literature reports only few examples of renewable resources-based benzoxazine materials. One of them is the low viscosity cardanol-based benzoxazine that has been described as possible alternative to the standard petroleum-based ones [3]. Cardanol is a well known phenol obtained as a renewable organic resource and harmful by-product of the cashew industry. Cardanol-based benzoxazines and their potential applications were studied as a matrix for natural fiber-reinforced composites [4] and as reactive diluents in the synthesis process of bisphenol A (BPA) based benzoxazines [5].

We have recently focused our attention on the synthesis of new diphenolic acid (DPA) based benzoxazines and its methylesterbenzoxazine derivative (MDP-Bz) pursuing the strategies to minimize the environmental impact of new materials [6]. DPA has a structure similar to BPA but incorporates an additional carboxylic functionality. It must be pointed out that BPA has recently shown estrogenic properties and endocrine modulating activity [7], so the replacement of BPA by DPA offers additional advantages due to these safety concerns. The research interest resulted enhanced as DPA is commercially available and much cheaper than BPA and it can introduce functional carboxyl group into the polymer structure. Moreover, DPA is a condensation product of phenol and levulinic acid.

Levulinic acid is believed to be a cheap platform chemical and can be commercially produced from cellulose-rich biomass (especially from waster biomass) in large scale [8].With regard to phenol, which is currently produced exclusively from petrochemical resources, its bioproduction from glucose has been described [9,10] and so DPA could be considered as a fully renewable component.

As mentioned, we have recently developed the benzoxazine monomer derived from the DPA methylester (MDP-Bz). This benzoxazine, in addition to its renewable origin, offers a number of advantages over other conventional benzoxazine monomers due to the presence of the methyl ester moieties. Upon curing, extensive transesterification reactions between the ester and phenolic groups resulting from the benzoxazine ring opening, take place. This curing process leads to resins with a superior crosslinking degree which results in materials with much better thermal and mechanical performance when compared to similar BPA-based polybenzoxazine materials [6]. The main drawback of this benzoxazine is the high temperature needed for the uncatalyzed curing process (260 ºC).

In this work, we studied the thermal behavior of mixtures of renewable DPA and MDP-Bz. The presence of a carboxylic group in DPA monomer is expected to catalyze the benzoxazine ring opening lowering the temperature needed to complete the curing of these benzoxazines [11]. Moreover, the DPA phenolic aromatic rings react with the benzoxazine affording the complete incorporation of DPA in the polymeric network and avoiding the problems originated by the use of non reactive catalysts.

Moreover, this paper focuses on developing high performance flame retardant thermosetting resins through the mixture of MDP-Bz and DPA-PPZ. As is well known these new phosphorus-containing polybenzoxazines impacted the properties of the final material and improved the flame resistance [12].

The curing behavior of these materials was studied by differential scanning calorimetry (DSC). Finally, the properties of the materials were evaluated by termogravimetric analysis (TGA), dynamic mechanical analysis (DMTA), tensile measurements, limiting oxygen index (LOI) and UL-94 Burn Test.

2. Experimental Part

2.1. Materials

The following chemicals were obtained from the sources indicated and used as received: ammonium sulphate (Probus), paraformaldehyde (Probus), 4,4´-bis(4-hydroxyphenyl) pentanoic acid (Aldrich), trimethylorthoformate (Fluka), p-toluenesulfonic acid monohydrate (Panreac), 1-*terc*-butyl-4,4,4-tris(dimethylamino) 2,2[tris(dimethylamino)phosphoranylideneamino]-2λ^5,4λ^5-catenadi(phosphazene) (P_4-t-Bu) solution 1 M in hexane (Aldrich). 1,3,5-Triphenylhexahydro-1,3,5 triazine, methyl 4,4´-bis(4-hydroxyphenyl) pentanoate (MDP) and methyl 4,4´-bis-[6-(3-phenyl-3,4-dihydro-2*H*-1,3-benzoxazine)] pentanoate (MDP-Bz) were synthesized according to our reported procedures (Scheme 1) [6]. Tetrahydrofuran (THF) was distilled over sodium/benzophenone. Other solvents were purified by standard procedures. Chopped Strand Fiberglass Mat (CSM) (E-glass, 73 g/m^2, thickness: 0.5 mm) was kindly supplied by Aismalibar S.A.

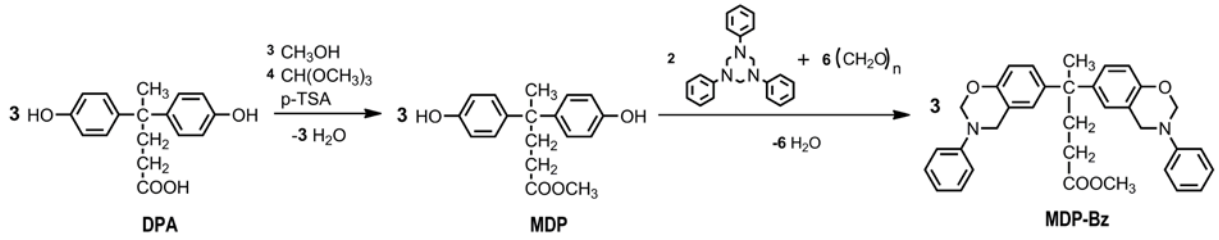

Scheme 1. Synthesis of MDP and MDP-Bz

2.2. Synthesis of DPA-phosphazene salt (DPA-PPZ) (Scheme 2)

In a 100 mL round bottom flask equipped with a pressure-equalized addition funnel and under inert atmosphere 0.53 g (0.83 mmol) of P_4-t-Bu were dissolved in 20 mL anhydrous THF. A solution of 0.24 g (0.83 mmol) of DPA in 20 mL anhydrous THF were added dropwise at room temperature with stirring. The reaction was further carried out for 12 h at room temperature. The excess of THF was removed under vacuum to obtain DPA-PPZ as a white solid with 95% yield.

^{1}H NMR (DMSO-d_6, δ ppm): 9.73 (2H, OH), 6.89 (4H, d, Ar-H), 6.60 (4H, d, Ar-H), 2.62 (54H, d), 2.11 (2H, t), 2.56 (2H, t), 1.40 (3H, s), 1.26 (9H, s).

^{31}P NMR (DMSO-d_6, δ ppm, H_3PO_4): -23.5 ppm (q, 1P, $^{2}J_{PP}$: 48.7 Hz), 12.6 ppm (d, 3P, $^{2}J_{PP}$ 48.7 Hz)

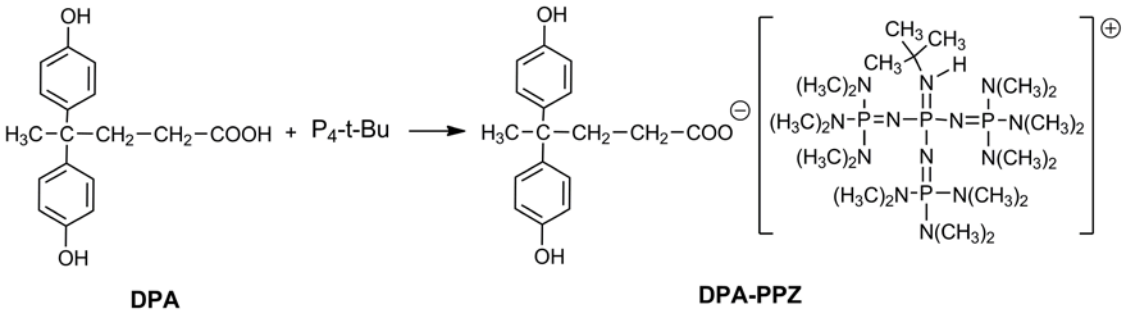

Scheme 2. Synthesis of DPA-phosphazene derivative (DPA-PPZ)

2.3. Crosslinking reaction

MDP-Bz was degassed in a glass oven for 30 min at 140 °C. After this, the appropriate amount of melted (190 °C) DPA was mixed by hand for 5 min with the MDP-Bz. The used amounts of DPA were 0, 2, 5, 10 and 25 wt.% of the total weight mixture. Polymerization of the mixtures was carried out into a manual hydraulic press 15-ton sample pressing (SPECAC) equipped with water cooled heated platens. Samples were compressed in a rectangular Teflon mold (80 mm x 60 mm x 0.5 mm) under a pressure of 2.3 MPa to obtain films. Samples of 30 mm x 7 mm x 0.5 mm were taken for measurements. As every mixture has different thermal polymerization behavior, the curing temperatures were adjusted according to DSC thermogram of the corresponding formulations.

Fiberglass reinforced polybenzoxazines were also prepared. An appropriate amount of degassed MDP-Bz and DPA were melted at 190 °C and mixed by hand for 5 min. Subsequently, this mixture at 140°C was manually spread with a brush of each of the sides of a fiberglass sheet, which was previously cut to desired dimensions. The resultant materials were placed into a Teflon mold (cavity dimension: 50 mm x 50 mm x 0.5 mm) and compressed at 2.3 MPa using a manual hydraulic press (SPECAC). The used amounts of DPA and curing temperatures were as above mentioned for nonreinforced samples. The fiberglass content was ca. 15 wt.% in all mixtures.

Flame retardant polybenzoxazines were prepared by dissolving appropriate amounts of DPA, MDP-Bz and DPA-PPZ in acetone/methanol and subsequently evaporating the solvents at 45 °C for 60 h and finally under vacuum at 140 °C. The weight ratios of MDP-Bz, DPA and DPA-PPZ were 82.5/10/7.5 (1.7% P) and 80/10/10 (2.3% P). Resin bars were obtained by placing the compounds into a steel mold (cavity dimension: 70 mm x 6 mm x 3 mm) and compressing (SPECAC equipment) at 9.2 MPa. The curing temperatures were adjusted according to each DSC thermogram.

2.4. Extraction and pyrolysis experiments

About 200 mg of each MDP-Bz/DPA resin were extracted with boiling THF during 12 h. The soluble fractions were negligible in all cases except for MDP-Bz-25wt.% DPA in which 13 mg (6.3 %) were obtained starting from 210 mg of sample. This fraction was analyzed by ^{1}H and ^{13}C NMR.

240 mg of 80 wt.% MDP-Bz /10 % DPA/10 wt.% DPA-PPZ were pyrolized in a quartz tube at 350 °C under vacuum for 30 min. The condensates, 57.6 mg (24%) were collected in a frozen trap and analyzed by ^{1}H and ^{31}P NMR.

2.5. Instrumentation

^{1}H (400 MHz), ^{13}C (100.5 MHz) and^{31}P (161.9 MHz) NMR spectra were obtained using a Varian Gemini 400 spectrometer with Fourier transform and DMSO-d_6 as solvent.

Calorimetric studies were carried out on a Mettler DSC821e thermal analyzer using N_2 as a purge gas (100 ml/min) at scanning rate of 20 ºC/min. Thermal stability studies were carried out on a Mettler TGA/SDTA851e/LF/1100 with N_2 or air as a purge gas at scan rates of 10 ºC/min.

Mechanical properties were measured by triplicate using a dynamic mechanical thermal analysis (DMTA) apparatus (TA DMA 2928). Reinforced and non reinforced specimens (10 mm x 7 mm x 0.45 mm) were tested in a three point bending configuration. In the case of phosphorus-containing samples, the dimensions of the bars were 10 mm x 6 mm x 2.5 mm. The thermal transitions were studied in the 30-350 ºC range at a heating rate of 3 ºC/min and at a fixed frequency of 1 Hz. Tensile testing was performed using an Instron machine 3366 with a 100 N load cell at crosshead speed of 5 mm/min and at 25 °C. The

dimensions of the test specimens were 50 mm x 4 mm x 0.35 mm. The tensile properties were determined from the average of at least five samples.

LOI measurements were performed on a Stanton Redcroft FTA flammability unit provided with an Oxygen Analyzer. Samples (70 mm x 6 mm x 3 mm) were prepared by compression molding at 9.2 MPa and tested by triplicate.

2.6. General Procedure for Modified UL-94 Burn Test

Three sample bars (0.5 mm x 10 mm x40 mm) were used for this test. The Bunsen burner flame height was 25 mm and the height from the top of the Bunsen burner to the bottom of the test bar was 10 mm. The sample was subjected to two 10 s ignitions with a calibrated methane-fueled flame in a controlled-size unit that was free of passing air currents. After the first ignition, the flame was removed and the time the polymer took to self-extinguish was recorded. The second ignition was then performed on the same sample and the self-extinguishing time/dripping characteristics were recorded. If the sample self-extinguished in less than 10 s with no dripping, we considered it to be a V-0 material, which is an industry standard for flame retardancy.

3. Results and discussion

In our previous work, we reported a facile synthesis of methyldiphenolic acid-based benzoxazine (MDP-Bz) by the reaction of diphenolic acid methyl ester (MDP), 1,3,5-triphenylhexahydro-1,3,5-triazine and formaldehyde [6]. DPA is a commercially available condensation product of phenol and levulinic acid, containing the functional carboxyl group (Scheme 1).

It is well known that 1,3-benzoxazines exhibit exotherm ring opening reaction around 200-250 ºC, which can be monitored by DSC. MDP-Bz showed an exothermic peak with an onset at 220 °C, a maximum temperature at 261 °C and 129 kJ as exothermic energy (Fig. 1a). As it has been mentioned, these high temperatures required for curing is one of the main drawbacks of polybenzoxazines preparation and can be addressed by using acidic catalyst, such as carboxylic acids, to catalyze the thermal ring opening of the benzoxazine group.

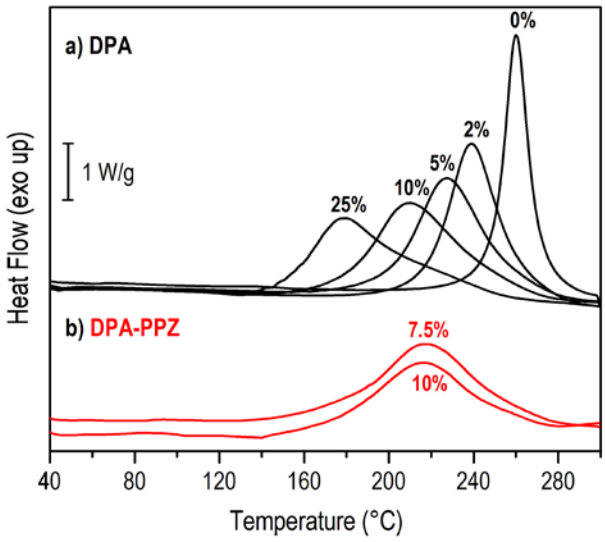

Fig. 1. DSC plots of MDP-Bz with different a) DPA and b) DPA-PPZ contents.

In this work we used DPA to low the MDP-Bz curing temperature. In this way, we studied the thermal behavior of mixtures of MDP-Bz with different amounts of DPA. Fig. 1a shows the DSC thermograms of the mixtures of MDP-Bz and 2, 5, 10, and 25 wt.% of DPA. A shifting of the polymerization exotherm to lower temperatures can be seen as DPA amount increases. A similar behavior was observed in the onset temperatures of the exothermic peaks. Table 1 summarizes all these values. As can be seen, when 2 wt.% DPA is added to MDP-Bz the enthalpy value undergoes an increase, suggesting a more complex polymerization mechanism in which carboxylic and phenolic groups are involved. For higher DPA amounts enthalpy values decrease progressively due to the lower content of the benzoxazine monomer in the mixture. As it has been reported previously, phenolic hydroxyl compounds produce an outstanding decrease in the benzoxazines polymerization temperature, acting hydroxyl groups as acid cationic initiators in the ring opening polymerization [13,14]. As DPA contains both phenolic hydroxyl and carboxyl groups a test was carried out with MDP that only contains hydroxyl groups, to prove the higher catalytic effect of carboxylic acid group in DPA. So, mixtures of 2, 5, 10, and 25 wt.% of MDP-Bz/MDP were prepared and their thermal behavior was analyzed by DSC. Data were summarized in Table 1. A notable difference in the maximum temperatures of curing was observed. The MDP-Bz/25 wt.% DPA compared to MDP-Bz/25 wt.% MDP shows a decrease of 40 ºC, due to the presence of catalytic carboxylic acid.

Table 1
DSC data and curing conditions of mixtures of MDP-Bz with DPA, MDP and DPA-PPZ.

Composition	T_{onset} (°C)	T_{max} (°C)	ΔH_o (kJ/mol)	Curing conditions
MDP-Bz	220	260	122	190 °C (2 h), 215 °C (2 h), 235 °C (8 h), 260 °C (2 h)
MDP-Bz + 2% DPA	180	239	147	170 °C (2 h), 190 °C (2 h), 225 °C (8 h), 240 ºC (2 h)
MDP-Bz + 2% MDP	173	246	145	
MDP-Bz + 5% DPA	165	228	142	160 °C (2 h), 180 °C (2 h), 210 °C (8 h), 230 ºC (2 h)
MDP-Bz + 5% MDP	158	240	143	
MDP-Bz + 10% DPA	150	209	134	150 °C (2 h), 165 °C (2 h), 195 °C (8 h), 210 ºC (2 h)
MDP-Bz + 10% MDP	163	234	139	
MDP-Bz + 25% DPA	135	179	108	135 °C (2 h), 150 °C (2 h), 170 °C (8 h), 180 ºC (2 h)
MDP-Bz + 25% MDP	150	220	115	
MDP-Bz +10% DPA +7.5% DPA-PPZ	140	217	142	140 °C (2 h), 160 °C (2 h), 200 °C (8 h), 215 °C (2 h)
MDP-Bz +10% DPA +10% DPA-PPZ	140	216	117	140 °C (2 h), 150 °C (2 h), 195 °C (8 h), 215 °C (2 h)

The curing conditions, collected in Table 1, were selected according the DSC traces. Temperature cycles starting just below the onset temperature of the exotherm (T_{onset}) and up to the maximum temperature of the exotherm (T_{max}) were used. In all cases DSC measurements were carried out showing the completeness of the curing process. To evaluate the crosslinked fraction, samples were extracted with THF showing no noticeable soluble materials with the exception of the MDP-Bz/25 wt.% DPA which contained a 6.3% of soluble fraction.

The dynamo-mechanical, mechanical and thermogravimetric properties of the polybenzoxazines were investigated. According to DSC data, the curing of the benzoxazine resins was carried out in a mold under compression by heating samples at different temperatures and times collected in Table 1. Due to the brittleness of some samples fiberglass reinforced polybenzoxazines were also prepared to improve their mechanical properties. The dynamic mechanical behavior of the cured benzoxazine resins was obtained as a function of the temperature beginning in the glassy state of each composition to the rubbery plateau of each material. The plots are shown in Fig. 2.

Polymer, 2012, 53, 1617-1623

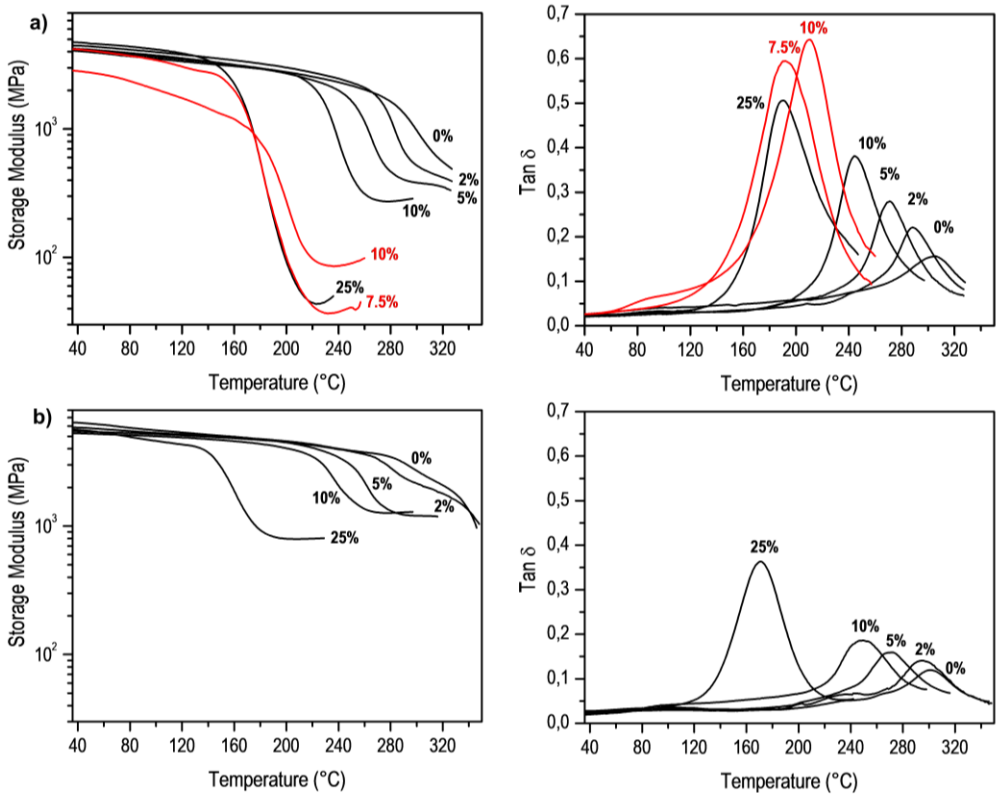

Fig. 2. Storage modulus and tan δ of a) polybenzoxazines with different DPA and DPA-PPZ content and b) reinforced polybenzoxazines with different DPA content.

There are a number of important material parameters that can be derived from the dynamic mechanical data. The storage modulus, E', of a solid sample at room temperature provides a measure of material stiffness under shear deformation, and is plotted for the mixtures as a function of temperature. For all the thermosets polymerized from MDP-Bz and DPA (Fig. 2a), the storage modulus maintains approximately the same value for a wide temperature range up to 220 ºC with the exception of the sample with 25 wt.% DPA. A same behavior is observed in those reinforced with fiberglass (Fig. 2b). Moreover, as expected, it is also observed that when samples are reinforced the storage modulus is greater. The glass transition temperatures (Tg's) of the crosslinked materials can be detected as the maximum of the loss modulus (E''), which corresponds to the initial drop from the glassy state into the transition, or as the α relaxation peak of the loss factor, tan δ, which corresponds to the transition midpoint of the log of the E' curve. Table 2 shows the Tg values of both measurements.

Table 2
Thermal and mechanical properties of polybenzoxazines.

Composition	Tg (°C)			Mechanical Properties	
	½ ΔC_p	E''_{max}	tan δ_{max}	Young Modulus (MPa)	Tensile Strength[b] (MPa)
MDP-Bz	301	282	303	-	-
MDP-Bz[a]	298	296	301	1484.6±58	41.6±2.4
MDP-Bz + 2% DPA	272	274	288	-	-
MDP-Bz + 2% DPA[a]	274	279	293	1146.6±28	25.2±3.2
MDP-Bz + 5% DPA	249	260	269	-	-
MDP-Bz + 5% DPA[a]	255	256	271	1074.8±88	23.8±4.7
MDP-Bz + 10% DPA	224	232	244	-	-
MDP-Bz + 10% DPA[a]	223	234	247	967.3±98	17.2±3.5
MDP-Bz + 25% DPA	159	166	190	-	-
MDP-Bz + 25% DPA[a]	163	152	171	996.0±85	21.5±4.3
MDP-Bz +10% DPA +7.5% DPA-PPZ	196	163	191	-	-
MDP-Bz +10% DPA + 10% DPA-PPZ	208	176	210	-	-

[a] Fiberglass reinforced benzoxazine mixtures (15 wt.%).
[b] Tensile strength at yield elongation.

As expected, Tg as tan δ peak is higher than E'' peak. In this Table is also collected the Tg value, as the half-height of the heat capacity increase (½ΔCp), determined by DSC, which is in good accordance with DMTA values. The analysis of the height of the tan δ peak values indicates in general a lower crosslinking density for the mixtures compared to MDP-Bz. The height of tan δ peak increases with the content of DPA in the mixtures, indicating that the crosslinking density decreases due to the decrease of the MDP-Bz in the mixture. Polybenzoxazines reinforced with fiberglass show a different behavior being the height of tan δ peaks lower than nonreinforced ones. Moreover, the higher the DPA content the lower the Tg's. This could be explained again by the lower percentage of MDP-Bz and consequently a decrease in the crosslinking density which takes place through transesterification reactions between the ester groups and the phenolic OHs, either resulted from ring opening of benzoxazine or from DPA [6]. The tan δ peak width at half height is quite narrow and similar for all samples suggesting a similar homogeneity.

TGA data under nitrogen and air atmospheres of these materials were determined and analyzed. Fig. 3a and b show the weight loss with the

Polymer, 2012, 53, 1617-1623

temperature for the different compositions without and with fiberglass respectively, and Table 3 summarizes the thermogravimetric data.

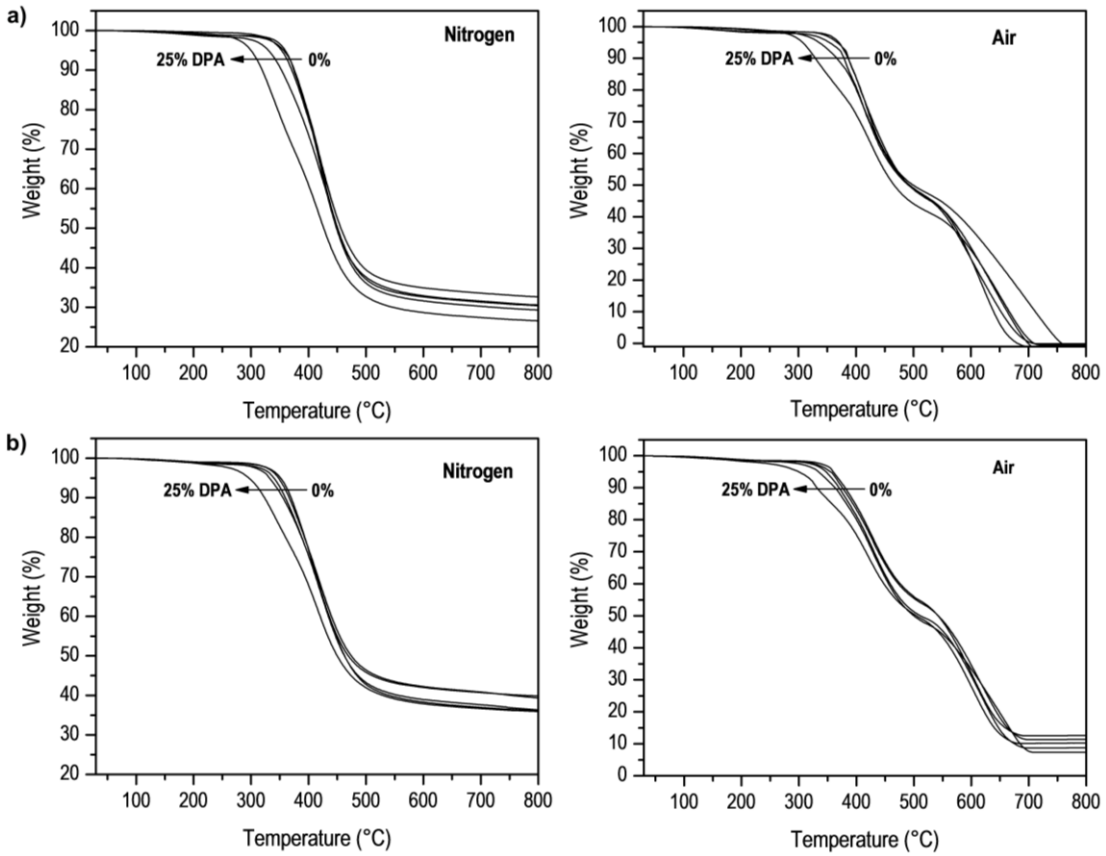

Fig. 3. TGA plots of a) polybenzoxazines with different DPA content and b) reinforced polybenzoxazines with different DPA content in nitrogen and air.

Both in nitrogen and air the decomposition temperature decrease with DPA content. In nitrogen, a maximum weight loss rate, at approximately 420 ºC appears in all the samples except when 25 wt.% DPA is added. This behavior indicates that there is a single decomposition mechanism which is similar for all resins. However, for the resin from MDP-Bz/25 wt.% DPA, two maximum weight loss rates appear at 344 ºC and 417 ºC. The first one could be related to DPA polyester decomposition. The analysis of the soluble extract by ^{1}H and ^{13}C NMR indicates as main component the hyperbranched polyester produced by self condensation of DPA molecules that seems to occur when a large excess of DPA is used [15]. No significant differences of behavior are observed with the reinforced samples. In air two stages of weight loss appear in all the samples except when 25 wt.% DPA is added that another stage, at lower temperature, is

also observed as explained above. Temperatures of 10% weight loss decrease with the DPA content being especially significant the decrease for the MDP-Bz/25 wt.% DPA. Char yields at 800 ºC are quite similar for all the resins, although as expected the reinforced counterparts showed higher values of char yield.

Table 3

Thermogravimetric and LOI values of polybenzoxazines.

Composition	TGA (O_2)			TGA (N_2)			LOI
	$T_{10\%}$ (°C)[b]	T_{max} (°C)[c]	Y_{800} (%)[d]	$T_{10\%}$ (°C)[b]	T_{max} (°C)[c]	Y_{800} (%)[d]	
MDP-Bz	386	418, 693	0	375	417	32	27.6
MDP-Bz[a]	380	427, 603	12	369	409	40	-
MDP-Bz +2%DPA	379	409, 620	0	374	421	29	-
MDP-Bz +2%DPA[a]	375	427, 618	11	366	416	39	-
MDP-Bz +5%DPA	379	410, 641	0	371	426	30	-
MDP-Bz +5%DPA[a]	369	428, 616	11	359	421	36	-
MDP-Bz +10%DPA	366	416, 600	0	352	439	30	25.8
MDP-Bz +10%DPA[a]	362	427, 660	8	355	426	36	-
MDP-Bz +25%DPA	329	332, 425, 651	0	319	344, 417	26	-
MDP-Bz +25%DPA[a]	331	330, 419, 603	11	323	346, 415	35	-
MDP-Bz +10%DPA + 7.5%DPA-PPZ	356	369, 625	1	348	377	36	27.5
MDP-Bz +10%DPA + 10%DPA-PPZ	348	368, 643	1	342	377	36	28.4

[a] Fiberglass reinforced benzoxazine mixtures [b] Temperature of 10 % weight loss
[c] Temperatures of maximum weight loss rate [d] Char yield at 800 °C

The preparation of reinforced benzoxazines with fiberglass was necessary for the mechanical characterization of these resins. Fig. 4 shows the stress-strain curves for the different reinforced polybenzoxazines and Table 2 summarizes their mechanical properties. Young´s modulus and tensile strength at yield elongation decrease as the DPA increases. As it is known, molecular flexibility, intermolecular packing, molecular architecture and molecular weight between crosslinks affect the tensile strength and elongation at break [16]. As above noted an increase in DPA percentage in MDP-Bz mixtures decreases crosslinking density, thus generating a fall of the tensile strength and Young´s modulus.

One of the main concerns about the use of polymeric materials is their flammability. For this reason fire retardants such as phosphorus or silicon are

usually introduced into polybenzoxazines to enhance their flame retardancy [12]. Thus, we studied the possibility of inferring flame retardancy to MDP-Bz by mixing with a phosphazene diphenolic acid derivative (DPA-PPZ). The synthesis of this compound was carried out by mixing DPA and P_4-t-Bu in THF. Its ^{31}P NMR spectrum was consistent with the protonated form of P_4-t-Bu with chemical shifts at -23.5 ppm (q, 1P, $^2J_{PP}$: 48,7 Hz) and 12.6 ppm (d, 3P, $^2J_{PP}$ 48.7 Hz) [17].

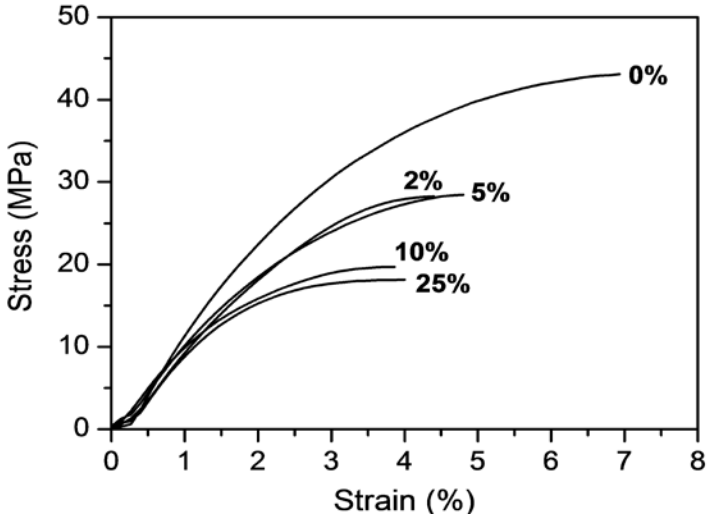

Fig. 4. Stress-strain plots of reinforced polybenzoxazines with different DPA content.

Two mixtures of DPA-PPZ/DPA/MDP-Bz with weight ratios of 7.5/10/82.5 and 10/10/80 were prepared to give resins with 1.7% and 2.3% of phosphorus content respectively. The DSC plots of MDP-Bz with DPA-PPZ are shown in Fig. 1b. A similar behavior in both the onset temperatures and the enthalpies of the exothermic peaks was observed in both exotherms and that corresponding to MDP-Bz/10 wt.% DPA (Fig. 1a). The presence of DPA-PPZ does not seem to have any significant influence.

To examine the effect of phosphorus content on thermal stability and the decomposition behavior, TGA data, under nitrogen and air atmospheres, of phosphazene-based polymers were determined and analyzed. MDP-Bz/10 wt.% DPA was also considered for comparison. Fig. 5 shows the weight loss with the temperature and the similar decomposition behavior either in nitrogen or in air, for all resins.

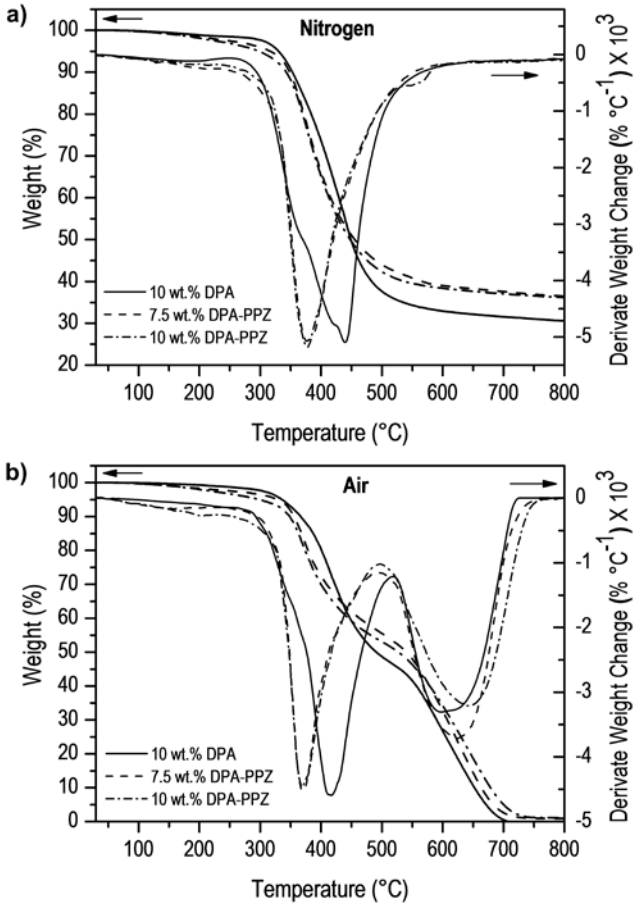

Fig. 5. TGA and DTG plots of DPA and DPA-PPZ based polybenzoxazines in a) nitrogen and b) air.

Table 3 summarizes the thermogravimetric data. Decomposition temperatures ($T_{10\%}$) for the phosphorus-containing resins are lower than for the phosphorus free-resin due to the decomposition of P-N bonds which have lower thermal stability than C-C bonds. Because of its lower atomic bond energy (279.7 kJ/mol) [18], the P-N bond will be destroyed before the C-C bond (347 kJ/mol) in the main macromolecular chain. In nitrogen (Fig. 5a) the three samples exhibit a single major break in their decomposition while in air two step break in the decomposition curves suggest a more complex decomposition pathway. The decomposition process observed at temperatures above 600 ºC came from the oxidation of the formed char. In nitrogen, it is also noticed that the char yields of the phosphorus-containing resins are slightly higher than that of the free-phosphorus one. This result indicates that the incorporation of phosphazene into the resins can increase the char yield because of the formation of phosphorus-rich char during the decomposition of the phosphazene moiety. However, in air the char yield is near 0% for all resins indicating that the flame

retardant mechanism of the phosphazene-based polymers must be also a gas phase mechanism [19]. The phosphazene moieties can release non-flammable gases such as CO_2, NH_3 and N_2 during burning to dilute the hot atmosphere and cool the pyrolysis zone at the combustion surface. These non flammable gases can cut off the supply of oxygen. To unravel whether if phosphorus compounds are released to gas phase during the early stage in the decomposition process, we performed a pyrolysis experiment at 350 °C. The ^{31}P NMR analysis of the collected volatile products showed the total absence of phosphorus species. ^{1}H NMR analysis shows that the degradation products are mainly aromatic compounds with methyl amino moieties.

The LOI values, which can be taken as an indicator to evaluate the polymer's flame retardancy of the resins were measured and shown in Table 3. As can be seen the presence of phosphorus slightly increases the LOI values even when the phosphorus content is low (1.7% and 2.3%) according to the expected behavior for fire-retarded phosphorus-containing materials.

We also tested the flame retardancy of the synthesized material with the UL-94 flame test, in which the sample was suspended above cotton [20]. According to the UL-94 test, the samples with a phosphorus content produced a V-0 material, as can is to be expected. These materials, therefore, have outstanding fire-retardancy properties.

4. Conclusions

We have synthesized renewable thermosetting polybenzoxazines from mixtures of renewable diphenolic acid (DPA) and its methylesterbenzoxazine derivative (MDP-Bz) with low polymerization temperatures. A shifting of the polymerization exotherm to lower temperatures can be seen as DPA amounts increase being this low temperature attributable to the presence of carboxylic acid. Fiberglass reinforced samples had to be prepared to achieve good tensile properties. High performance flame retardant thermosetting resins through the mixture of MDP-Bz and DPA-PPZ were obtained. These phosphorus-containing materials increased their LOI values and showed a V-0 grade according to the UL-94 test, even with low phosphorus content, corresponding to their excellent flame retardant properties.

Acknowledgements

The authors express their thanks to CICYT (Comisión Interministerial de Ciencia y Tecnología) (MAT2008-01412) for financial support for this work and to Dr. Miguel Angel López-Manchado for his help in the mechanical properties measurements.

References

[1] Ishida H. In: Ishida H, Agag T, editors. Handbook of benzoxazine resins. Amsterdam: Elsevier; 2011. p. 3-81 [chapter 1]
[2] Yagci Y, Kiskan B, Ghosh NN. J Polym Sci Part A: Polym Chem 2009;47:5565-76.
[3] Minigher A, Benedetti E, De Giocomo O, Campaner P, Aroulmoji V. Nat Prod Comm 2009;4:521-8.
[4] Calò E, Maffezzoli G, Mele F, Martina SE, Mazetto A, Tarzia A, Stifani C, Green Chem 2007;9:754-759.
[5] Lochab B, Varma IK, Bijwe JJ. Therm Calorim 2010;102:769-4.
[6] Zúñiga C, Larrechi MS, Lligadas G, Ronda JC, Galià M, Cádiz V. J Polym Sci Part A Polym Chem 2011;49:1219-27.
[7] Chen M-Y, Ike M, Fujita M. Environmental Toxicology 2002;17:80-6.
[8] Bozell JJ, Moens L, Elliot DC, Wang Y, Neuenscwander GG, Fitzpatrick SW, Bilski RJ, Jarnefeld J, Resources, Conservation and Recycling 2000;28:227-39.
[9] Gibson JM, Thomas PS, Thomas JD, Barker JL, Chandran SS, Harrup MK, Draths KM, Frost JW, Angew Chem Int Ed 2001;40:1945-48.
[10] Wierckx NJP, Ballerstedt H, Bont JAM, Wery J Appl Environ Microbiol 2005; 71:8221-27.
[11] Andreu R, Reina JA, Ronda JC. J Polym Sci Part A Polym Chem 2008;46: 6091-6101.
[12] Cádiz V, Ronda JC, Lligadas G, Galià M. In: Ishida H, Agag T, editors. Handbook of benzoxazine resins. Amsterdam: Elsevier; 2011. p. 557-77 [chapter 32]
[13] Espinosa MA, Cádiz V, Galià M. J Appl Polym Sci 2003;90:470-81.
[14] Ishida H, Rodriguez Y. J Appl Polym Sci 2005;58:1751-60.
[15] Chu F, Hawker CJ, Pomery PJ, Hill DJT. J Polym Sci Part A Polym Chem 1997;35:1627-33.
[16] Xiang H, Ling H, Wang J, Song L, Gu Y, Polym Compos 2005;563-71.
[17] Memeger W Jr, Campbell GC, Davidson F. Macromolecules 1996;29:6475-6480.
[18] Mortimer CT. Pure Appl Chem 1961;2:71-6.
[19] Liu R, Wang X. Polym Deg Stab 2009;94:617-24.
[20] Underwriters Laboratories. UL94: standard for tests for flammability of plastic materials for parts in devices and appliances. 4th ed. Research Triangle Park, NY: Underwriters Laboratories, Inc; 1991.

CHAPTER 3

POLYBENZOXAZINE FOAMS

3.1. INTRODUCTION

In our day to day most people encounter with many polymeric materials much of them in the form of foams. Among the most palpable examples is the foamed polyurethane seat cushion of the sofa or the chair, the flexible foam in the mattress, the polyurethane sponge for washing the dishes, and the foamed polystyrene cups, take-out boxes or trays. Foams also can be found applied in sports, military applications, vehicles, aircraft, train, and in the home.

The mechanical properties dictate the potential application of a polymeric foam. Foams are mainly influenced by the solid phase which in turn depends on the polymeric matrix, and the geometry of the foam. So, it is a challenge to model them in function of the variables involved in the foaming process.

Besides, flame retardant properties have also been increasingly required in polymeric foams. The industries dealing with construction and transportation are the two of greatest importance. Despite their great efficiency, halogen-containing flame retardants are rejected by the majority of end users and materials industries because they can produce a large amount of smoke and toxic hydrogen chloride and bromine gases during combustion. This fact, has led to the development of phosphorus-based flame retardant compounds as alternative to halogen counterparts in order to obtain safer and environmentally-friendly polymeric materials.

This chapter describes a novel kind of polybenzoxazine foams obtained through a self-induced foaming process of the diphenolic acid based benzoxazine described in Chapter 2. Neat rigid and flame retardant foams were prepared and characterized.

3.2. GENERAL ASPECTS OF FOAMS

Until 2011 the world's lightest material (0.9 kg/m^3), based on periodic hollow-tub microlattices, was created by a team of engineers for the University of California[1]. Less than two years, a new graphene aerogel[2] developed by Chinese researchers has dethroned the metallic micro-lattice with a density of 0.16 kg/m^3 that is lower than the density of helium (0.18 kg/m^3) and twice as much as

hydrogen (0.089 kg/m^3) (**Figure 1**). These efforts exemplify the hard work of getting increasingly lighter materials. Other examples of ultralight materials include silica aerogels (ρ ≥ 1 mg/cm^3), carbon nanotube aerogels (ρ ≥ 4 mg/cm^3), metallic foams (ρ ≥ 10 mg/cm^3) and polymer foams (ρ ≥ 8 mg/cm^3). These materials have a wide range of applications, such as thermal insulation, shock or vibration damping, acoustic absorption, and current collectors in battery electrodes and catalyst supports.

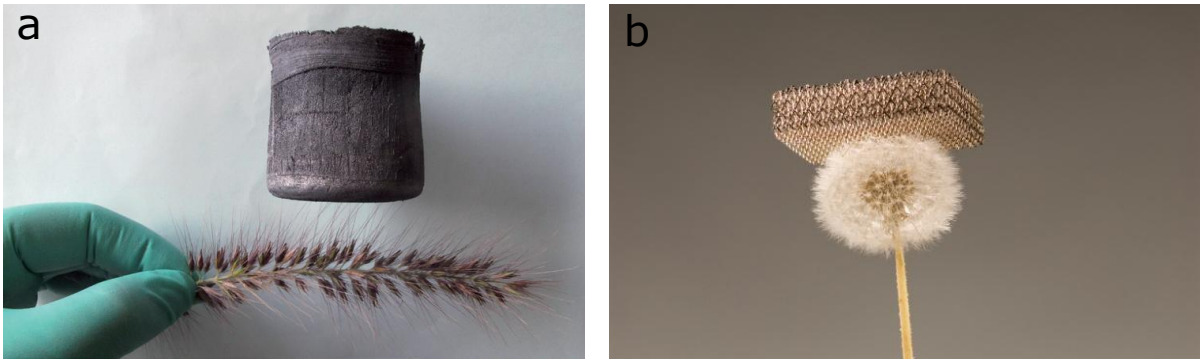

Figure 1. a) Graphene aerogel cylinder standing on a delicate plant[2] and b) metallic microlattice over a dandelion[3]

Polymeric foams consist of a minimum of two phases, a solid polymer matrix and a gaseous phase derived from a blowing agent. Foams could be classified according to the physical state as flexible or rigid, which in turn depends on their glass transition temperature. Moreover, the microstructure classification divides the foams into open cell or closed cell **(Figure 2)**. In open cell foams the air could pass freely between the interior of cells making them suitable for car seating, furniture, bedding and acoustical insulation. In closed cell foams, each cell is surrounded by connected faces being isolated from each others. They are best for thermal insulation although sometimes are utilized for packing or impact protection[4].

In many polymeric foams the formation of the gas phase is achieved by adding external blowing agents that depending on their nature could be classified as chemicals blowing agents (CBA) or physical blowing agents (PBA).

CBA are compounds that decompose and generate gases *via* reactions and/or thermally decomposition at the desired polymer processing temperature. A common CBA is the azodicarbonamide (ADC) which combine most of the

requirements for a successful foaming agent. It decomposes around 210 ºC, the majority gas evolutions are nitrogen (65%) and carbon monoxide (32%) and it has a very high yield of 220 mL/g[5]. ADC is widely used in polyurethane, polystyrene, and crosslinked-polyethylene foam industry.

PBA are compounds that produce gases as a result of a physical process (change of state) at low pressure or high temperature. In general, PBA are volatile organic chemicals (VOC) including hydrocarbons, chlorofluorocarbons, hydrochlorofluorocarbons, and hydrofluorocarbons. Inorganic gases, such as carbon dioxide (in a supercritical or nonsupercritical state), nitrogen, and argon, have been tempted as alone blowing agents and blends with other VOC. For instance, PBA are usually added as auxiliary blowing agents to enhance PU foam expansion.

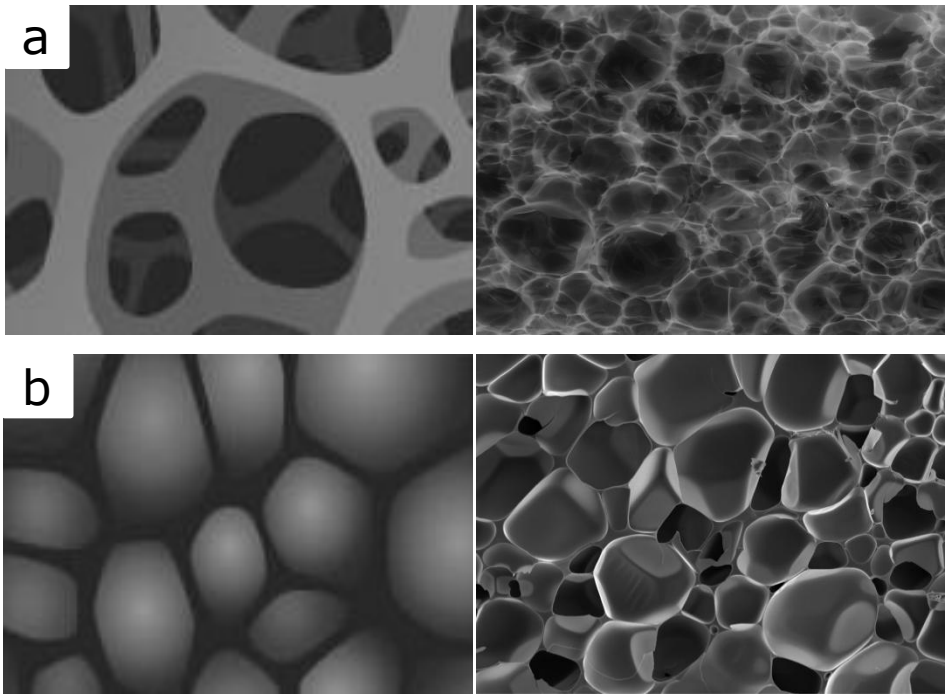

Figure 2. Types cellular structure of foams. a) Open cell and b) closed cell

Reactive foaming is also a chemical process in which a chemical reaction involves the formation of a certain amount of gases that suffuses the newly polymerized matrix, ultimately creating a polymeric foam. In other words, blowing and polymerization occur simultaneously until stabilization. It is typical for thermoset polyurethanes, silicon and polyisocyanurate foams[5].

A less common manner to achieve the porous structure in foams is the self-induced foaming process. It lays in the generation of the blowing agent *in situ* as a result of the degradation of thermolabile groups present in the polymer structure. By varying foaming time and/or foaming temperature is possible to control the extent of decarboxylation and therefore the morphology of the materials[6-8].

Specific examples of uses of polymeric foams include films, cups, food trays, containers, flooring, decorative items (ribbons, etc.), insulation boards, sound dampening, transportation, bedding, carpet padding, furniture parts, chair cushions, toys, fibers, automobile parts (*e.g.,* seats and back-rests, bumpers, headliners), sporting goods (*e.g.,* helmets and clothing), flotation (*e.g.,* boat parts, surf boards, life vests), footwear parts (*e.g.,* soles and inserts), insulation for appliances, and in packaging of just about all types of non-food items as well[9].

3.3. PROPERTIES OF FOAMS

A polymeric foam has unique physical, mechanical, thermal and flame retardant properties, which are governed by the polymer matrix, the cellular structure and the gas composition. Among the structural parameters are the cell density, expansion ratio, cell size distribution, open-cell content and cell integrity. These parameters are governed by the foaming technology used in processing and therefore, on the type of polymer to be foamed.

3.3.1 Mechanical properties

In general, the mechanical properties of foams are dependent on the kind of solid polymeric matrix from which the foam is made, cellular structure and the enclosed gas pressure. The first two factors are of great importance for the properties of any foam while the third one is negligible for open cell foams owing to their interconnected cell structure. Among the most important mechanical parameters, the solid polymer determines intrinsic properties such as the density, the Young's modulus, the plastic yield strength, and the fracture

strength. Meanwhile, the remarkable features of foams are the relative density, open/closed cell content and anisotropy ratio, cell size and cell wall thickness[10].

3.3.2 *Thermal properties*

Thermal properties of a foam largely determine its final application since most foamed materials are utilized as thermal insulators in areas including building and construction, transportation, and appliances. Thermal conductivity is one of the main properties of polymeric foams. It depends on the conductivity of the cell gas mixture, the conductivity of the solid polymer and the radiation between cells. The conduction through the gas generally is the major contributor, while the radiation and conduction through the solid together amounting only to about 1/3 of the gas conduction. Other important thermal properties of foams include the melting point, specific heat, and thermal expansion coefficient[11].

3.4. TYPES OF POLYMERIC FOAMS

Since it is virtually possible to transform any polymeric matrix into a foamed material, because many of the basic principles governing this technology and its processes are applicable to most resins, nowadays there are a wide range of polymeric foams. Roughly, there are two major classes of polymeric foams: thermoplastic and thermoset foams.

Thermoplastic foams are based on linear or slightly branched polymers. They have characteristics associated with thermoplastics so they can be reprocessed and recycled. They exhibit a definite melting range and are generally susceptible to be attacked by organic solvents. With thermoplastic foam systems the polymerization of the base resin is first completed, and then the polymer is compounded, melted and foamed. The market for commodity thermoplastic foams (polystyrene, polyolefin and PVC) is dominated by polystyrene which has applications mainly in building, construction and packaging[11]. For their part, engineering thermoplastic foams include acetal, acrylonitrile butadiene styrene, nylon, polycarbonate, polyester and polyetherimide, plus various glass- or carbon-reinforced resins[12].

Thermosetting foams can be defined as foams having no thermoplastic properties. Consequently, thermosetting foams include not only cross-linked

foams, but also some linear polymeric ones having no thermoplastic properties, e.g., carbodiimide and polyimide foams. These foams are intractable and turn to char by heating. During their preparation, the polymer formation and gas generation take place concurrently. Polyurethane foams are the most extended example of this kind of foams, becoming one of the most versatile polymeric materials due to their formulation could meet specific requirements and, hence, are used in diverse applications[13].

Phenolic foams are categorized as thermosetting foams. They are usually divided into novolac and resol. For their preparation are utilized a great variety of phenols, aldehydes, surfactants, blowing agents, modifiers and additives. Phenolic foams exhibit low thermal conductivity, exceptional fire-resistant properties, high thermal stability over a broad range of temperatures, self-adhesive properties, highly effective energy absorption characteristics and low cost. These advantageous features become this type of foam suitable for applications as structural (sandwich panels), decorative (floral foams) and thermal insulating (continuous laminated boards) materials where fire resistance is critical[13].

3.5. FLAME RETARDANT FOAMS

Polymeric foam is a cellular material formed of solid walls, struts and filled with a gaseous phase. The cellular structure, the nature of the foam (open or closed cell) and the low heat capacity are responsible of their high flammability[14]. In fact, polymeric foam tends to burn quickly in comparison to their solid counterpart as a consequence of these factors. Fire involving polymeric cellular materials develops in extremely rapid way when compared with solid polymer, giving rise to high temperatures and producing large amount of smoke in a short period of time[15]. This difference is mainly caused by the cellular structure of foams since they have a high surface area per unit mass resulting in a complete pyrolysis of combustible matter nearby the radiation and flame. Furthermore, there exist some differences between open and closed cells. In open cell foams the pyrolysis and burning processes are accelerated due to the transport of combustible gases is promoted through the open channels and because the oxygen feeds the fire. Contrary, in closed cell foams the isolated cells act as

thermal insulators contributing to delay the heat transfer and therefore decreasing the time for reaching the ignition temperature.

Foam density, mean cell size, surface area and open cell content influence the flammability and thermal stability of foams. For example, reported studies by Xiang-Chen Bian et al[16] and Richard Horrocks et al[17] have shown that the fire behavior of polyurethane foams (PUF) is better at higher densities due to a more compact burned layer, that is, low density foams give lower LOI (limiting oxygen index) value, whilst the high density foams render higher ones. On their behalf, Silvia Román-Lorza et al[18] found bigger differences in the LOI measurements of EVA foams at different open cell contents proving that a closed-cell cellular structure presents a better fire behavior. Also, Martha Williams et al[19] reported that in the case of polyimide foams with the same density but different surface areas the peak heat release rate (PHRR) measured by cone calorimeter, showed great variation.

Burning behavior differs according to the nature and the chemical structure of the polymeric matrix. In the case of thermoplastic foams, when they are exposed to heat they soft and melt without forming char, *i.e.,* burning with flaming droplets. Polyurethane foams are an example of the latter. During burning the produced melt promotes severe dripping that increases the fire hazard[15]. On the contrary, thermosetting foams present a 3D crosslinked structure that does not allow withdrawing from the flames. They tend to form a protecting layer of char that avoid further attack by flames and also causes extinction[20]. For example, when phenolic foams are exposed to an open flame, they still maintain their high flame retardance and non-ignition properties because of their low flammability and low smoke density[15].

Many compounds have been used in polymeric foams to improve their flame retardance. The way as they are introduced could be classified in three main categories: additives, reactives and coatings[21]. The first ones are usually incorporated to the formulation by simple mechanical mixing. Their easy processability is sometimes overshadowed by a reduction in the physical and mechanical properties, especially when are used above 15 wt%. Other disadvantages include the tendency to migrate to the surface, the (discoloration) and the shrinkage scorching of the foams. Some examples have been widely reviewed in the literature[22-24] and include the use of organophosphorus (phosphonates, phosphates, phosphites and phosphoramidites), phosphorus-halogen, organohalides, inorganic fire retardants (alumina trihydrate, borates,

silicon based compounds) and intumescent systems. Reactive compounds have generally a better performance than the additives because they form part of the foam structure through chemical bounds between the functional groups of the fire retardant compounds and the polymer chain[21]. Examples include the use of brominated[25,26], phosphorus and nitrogen containing polyols[27-29], the addition of polyphosphazene[30] into polyurethane foams as well as brominated epoxy[31] into phenolic foams. In the third one a coated layer is applied on the top surface of the flammable foam[32,33]. This approach is useful when low water vapor permeability and good weather protection are desired[34].

Most recently, the use of nanofillers has become an attractive alternative in the preparation of nanocomposite foams since they have exhibited some improvements in terms of flame retardancy and thermal stability[35]. One of the main advantages of nanofillers in contrast to traditional flame retardants additives is their positive impact on the mechanical properties. Furthermore, because they are eco-friendly, they may be categorized as a halogen-free alternative[36]. The way as the nanofillers modifies the foam morphology influences the final foam properties. Thus, nanofillers act as heterogeneous nucleation sites decreasing cell size and reinforcing the polymeric matrix. Other advantages of them include the possibility to provide multifunctionality to the foam, change the rheological properties and low the energy barrier for bubble nucleation[35]. Diverse nanoparticles have been assessed as flame retardant additives such as graphene[37] nanoclays[38,39] and carbon nanotubes[40]. In some cases they have demonstrated a positive synergistic effect when they have been used along with traditional flame retardant additives[41,42].

3.6. BENZOXAZINE DERIVED FOAMS

To date, the study on the preparation and characterization of polybenzoxazine foams have been addressed by a couple of researchers. K.S. Santosh and coworkers[43,44] reported the preparation and characterization of polybenzoxazine-syntactic foams[a] **(Figure 3b)**. The first work consisted in the preparation of polybenzoxazine containing silica fiber (19.8-9.1 vol%) and glass microballons

[a] Syntactic foams are lightweight materials made of hollow microspheres dispersed in a resin.

(36.5-68.9 vol%) using a solvent-based method followed by compression and thermal curing. The foam densities ranged from 879 to 507 kg/m^3. The authors assessed the variation of mechanical (tensile, compressive and flexural), dynamomechanical and thermal properties of the foams in relation to the change in composition. Thus, the incorporation of microballons showed a significantly decrease in the strength of silica filler materials, an improvement in the damping property and the thermal and thermo-oxidative stability of the foams. In the second work, they prepared polybenzoxazine foams of lower densities (512 to 293 kg/m^3), similarly to the first work using a higher volume percentage of microballons (61.4 to 78.0). The foams were deeply characterized in terms of flexural, tensile and compressive strengths and correlated with the void fraction and the interfacial bonding between the matrix and microballons.

Parkpoom Lorjai et al[45] prepared polybenzoxazine foams using bisphenol A-based benzoxazine as matrix and azodicarbonamide (AZD) as foaming agent at different weight ratios (1, 3, 5, 7 and 10 wt%). These authors obtained a series of foam densities ranging from 273 to 407 kg/m^3 by heating Bz-BPA/AZD mixtures from 30 ºC to 210 ºC **(Figure 3a)**. The mechanical properties were measured in terms of the compressive strength and the compressive modulus with values in the range of 5.2-12.4 MPa and 268-681 MPa, respectively. Additionally, they studied the transformation of the lowest density polybenzoxazine foam into carbon foam by carbonization under nitrogen at 800 ºC. They observed an increase in the foam density as well as the compressive properties after carbonization.

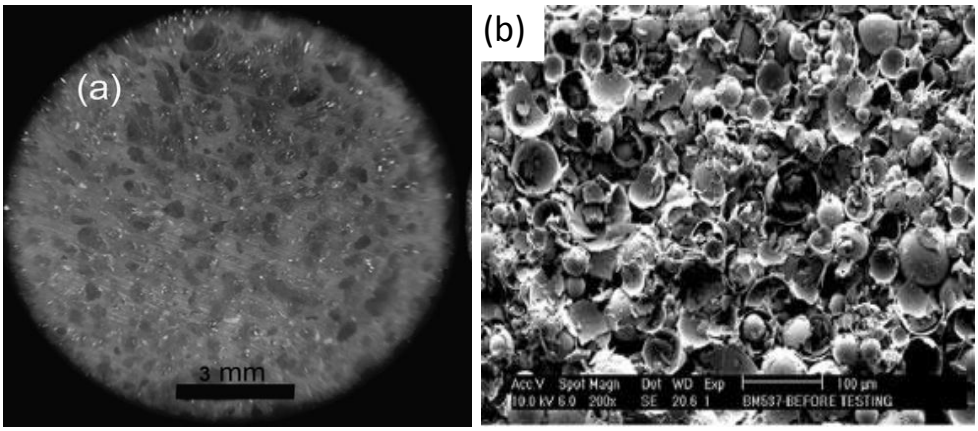

Figure 3. a) Microscope image of a polybenzoxazine foam[45] and b) SEM image of a syntactic polybenzoxazine foam[43]

Finally, Mònica Ardanuy et al[46] prepared polybenzoxazine foams using Bz-BPA and 5 wt % of AZD by heating a mixture of Bz-BPA/AZD from 150 ºC to 200 ºC for 80 min in a closed mold. They performed a detailed characterization of the cellular structure of the foams. The results indicated that the obtained foams exhibited an isotropic cellular structure with densities in the range 414-720 kg/m^3 and an average cell size between 499 and 119 μm. Moreover, the foams showed compressive modulus ranging from 400 to 1100 MPa, compressive strengths in the range of 10-70 MPa, and thermal conductivities between 0.06 and 0.12 W/mK. According to the authors, the obtained foams could be suitable for structural applications.

3.7. OBJECTIVES

The main objective of the work described in this chapter is to prepare and characterize different polybenzoxazine foam materials using the diphenolic acid-based benzoxazine monomer. To fulfill this objective, it is necessary to accomplish the following specific objectives:

1. To prepare polybenzoxazine foams by a self-induced foaming process and to investigate the influence of the foaming temperature on the cellular structure of the materials.
2. To improve the flame retardancy of the diphenolic acid based polybenzoxazine foams by incorporating a phosphorus-containing compound.
3. To determine the influence of the foaming time and temperature on the physical, mechanical and flame retardant properties using statistical models.

3.8. EXPERIMENTAL PROCEDURES AND RESULTS

The following three studies including experimental procedures and results performed in this chapter have been published or submitted to scientific journals.

The first work described in section 3.8.1 has been published in *Polymer* Vol. 53, (2012), pp. 3089-3095. This work contemplates the use of the diphenolic acid-based benzoxazine (DPA-Bz) for obtaining rigid foams through a self-foaming process. The foaming agent (CO_2) is generated *in situ* owing to a decarboxylation reaction of the carboxylic acid pendant groups present in the structure of DPA-Bz. The influence of the foaming temperature on the cellular structure and therefore on the final mechanical properties was also investigated.

The second work described in section 3.8.2 has been accepted for publication in *Polymer Degradation and Stability* DOI:10.1016/j.polymdegradstab.2013.09.023. This work concerns the investigation of flame retardant polybenzoxazine foams based on diphenolic acid (DPA), capable of generate *in situ* CO_2 as foaming agent, with 9,10-dihydro-9-oxa-methylphosphaphenanthrene-10-oxide (DOPO) or 9,10-dihydro-9-oxa-10-(1-hydroxy-1-methylethyl)phosphaphenanthrene-10-oxide (DOPO-2Me) as additives. The physical, thermal and flame retardancy properties as well as the cellular structure of the resulting foams were investigated.

The third work described in section 3.8.3 has been submitted to *Polymer Testing*. The first part of this work deals with the modeling of the density, compressive modulus and the compressive strength of the flame retardant polybenzoxazine foams in terms of the foaming time and temperature. The second part is focused on the discussion about the relationship between the compressive properties and the crosslinking degree of the foams and the evaluation of their flammability properties.

REFERENCES

1. Schaedler, T. A.; Jacobsen, A. J.; Torrents, A.; Sorensen, A. E.; Lian, J.; Greer, J. R.; Valdevit, L.; Carter, W. B., Ultralight metallic microlattices. *Science* **2011,** 334, (6058), 962-965.
2. Sun, H.; Xu, Z.; Gao, C., Multifunctional, ultra-flyweight, synergistically assembled carbon aerogels. *Adv. Mater.* **2013,** 25, (18), 2554-2560.
3. HRL Laboratories. HRL Researchers Develop World's Lightest Material. www.hrl.com. (15-07-2013).
4. Klempner, D.; Sendijarevic, V., *Handbook of polymeric foams and foam technology. 2nd edition*. Carl Hanser Verlag: Munich, 2004; pp 1.
5. Lee, S. T.; Park, C. B.; Ramesh, N. S., *Polymeric Foams: Science and Technology*. Taylor & Francis: Boca raton, 2006; pp 19, 30.
6. Merlet, S.; Marestin, C.; Schiets, F.; Romeyer, O.; Mercier, R., Preparation and characterization of nanocellular poly(phenylquinoxaline) foams. A new approach to nanoporous high-performance polymers. *Macromolecules* **2007,** 40, (6), 2070-2078.

7. Merlet, S.; Marestin, C.; Romeyer, O.; Mercier, R. g., "Self-Foaming" poly(phenylquinoxaline)s for the designing of macro and nanoporous materials. *Macromolecules* **2008,** 41, (12), 4205-4215.
8. Doğan, E.; Küsefoğlu, S., Synthesis and in situ foaming of biodegradable malonic acid ESO polymers. *J. Appl. Polym. Sci.* **2008,** 110, (2), 1129-1135.
9. Khemani Kishan, C., Polymeric Foams: An Overview. In *Polymeric Foams*, American Chemical Society: 1997; Vol. 669, pp 1-7.
10. Gibson, L. J.; Ashby, M. F., *Cellular Solids: Structure and Properties. 2nd edition*. Cambridge University Press: 1997; pp 175-176.
11. Eaves, D., *Handbook of Polymer Foams*. Rapra Technology Limited: Shawbury, 2004; pp 6,7,202.
12. Landrock, A. H., 3 - Thermoplastic foams. In *Handbook of Plastic Foams*, Arthur, H. L., Ed. William Andrew Publishing: Park Ridge, NJ, 1995; pp 221-245.
13. Ashida, K.; Iwasaki, K., 2 - Thermosetting foams. In *Handbook of Plastic Foams*, Arthur, H. L., Ed. William Andrew Publishing: Park Ridge, NJ, 1995; pp 11-220.
14. Stone, H.; Pcolinsky, M.; Parrish, D. B.; Beal, G. E., The effect of foam density on combustion characteristics of flexible polyurethane foam. *J. Cell. Plast.* **1991,** 27, (1), 78-79.
15. Michele, M.; Alessandra, L., FR Design for Foam Materials. In *Fire Retardancy of Polymeric Materials, Second Edition*, CRC Press: 2009; pp 763-781.
16. Bian, X.-C.; Tang, J.-H.; Li, Z.-M.; Lu, Z.-Y.; Lu, A., Dependence of flame-retardant properties on density of expandable graphite filled rigid polyurethane foam. *J. Appl. Polym. Sci.* **2007,** 104, (5), 3347-3355.
17. Horrocks, A. R.; Price, D.; Edwards, N. L. C., The burning behaviour of combustion modified high resilience polyurethane foams. *J. Fire Sci.* **1992,** 10, (1), 28-39.
18. Román-Lorza, S.; Rodriguez-Perez, M. A.; De Saja Sáez, J. A.; Zurro, J., Cellular structure of EVA/ATH halogen-free flame-retardant foams. *J. Cell. Plast.* **2010,** 46, (3), 259-279.
19. Williams, M. K.; Holland, D. B.; Melendez, O.; Weiser, E. S.; Brenner, J. R.; Nelson, G. L., Aromatic polyimide foams: factors that lead to high fire performance. *Polym. Degrad. Stab.* **2005,** 88, (1), 20-27.
20. Troitzsch, J. H., How Do Foams Perform Under Fire Conditions? In *Fire and Cellular Polymers*, Buist, J. M.; Grayson, S. J.; Woolley, W. D., Eds. Springer Netherlands: 1987; pp 77-91.
21. Singh, H.; Jain, A. K., Ignition, combustion, toxicity, and fire retardancy of polyurethane foams: A comprehensive review. *J. Appl. Polym. Sci.* **2009,** 111, (2), 1115-1143.
22. Wang, J. Q.; Chow, W. K., A brief review on fire retardants for polymeric foams. *J. Appl. Polym. Sci.* **2005,** 97, (1), 366-376.
23. Papa, A. J., Flame retardation of polyurethane foams in practice. *Ind. Eng. Chem. Prod. Res. Develop.* **1972,** 11, (4), 379-389.
24. Levchik, S. V.; Weil, E. D., Thermal decomposition, combustion and fire-retardancy of polyurethanes—a review of the recent literature. *Polym. Int.* **2004,** 53, (11), 1585-1610.
25. Moss, E. K.; Skinner, D. L., Modified isocyanurate foams-Part III *J. Cell. Plast.* **1977,** 13, (6), 399-403.
26. Walch, P., Halogenated Polyetherpolyol IXOL® for Rigid Cellular PUR Materials with Improved Flame Retardancy. In *Fire and Cellular Polymers*, Buist, J. M.; Grayson, S. J.; Woolley, W. D., Eds. Springer Netherlands: 1987; pp 251-263.
27. Sivriev, C.; Żabski, L., Flame retarded rigid polyurethane foams by chemical modification with phosphorus- and nitrogen-containing polyols. *Eur. Polym. J.* **1994,** 30, (4), 509-514.
28. Sivriev, H.; Kaleva, V.; Borissov, G.; Zabski, L.; Jedlinski, Z., Rigid polyurethane foams with reduced flammability, modified with phosphorus- and nitrogen-containing polyol, obtained from tetrakis(hydroxymethyl)phosphonium chloride. *Eur. Polym. J.* **1988,** 24, (4), 365-370.
29. Papa, A. J., Reactive flame retardants for polyurethane foams. *Ind. Eng. Chem. Prod. Res. Develop.* **1970,** 9, (4), 478-496.

30. Modesti, M.; Zanella, L.; Lorenzetti, A.; Bertani, R.; Gleria, M., Thermally stable hybrid foams based on cyclophosphazenes and polyurethanes. *Polym. Degrad. Stab.* **2005,** 87, (2), 287-292.
31. Auad, M. L.; Zhao, L.; Shen, H.; Nutt, S. R.; Sorathia, U., Flammability properties and mechanical performance of epoxy modified phenolic foams. *J. Appl. Polym. Sci.* **2007,** 104, (3), 1399-1407.
32. Zhang, X.-G.; Ge, L.-L.; Zhang, W.-Q.; Tang, J.-H.; Ye, L.; Li, Z.-M., Expandable graphite-methyl methacrylate-acrylic acid copolymer composite particles as a flame retardant of rigid polyurethane foam. *J. Appl. Polym. Sci.* **2011,** 122, (2), 932-941.
33. Kim, Y. S.; Davis, R.; Cain, A. A.; Grunlan, J. C., Development of layer-by-layer assembled carbon nanofiber-filled coatings to reduce polyurethane foam flammability. *Polymer* **2011,** 52, (13), 2847-2855.
34. Szycher, M., *Szycher's Handbook of Polyurethanes Second Edition*. CRC Press INC: Boca Raton, 1999; pp 291.
35. Chen, L.; Rende, D.; Schadler, L. S.; Ozisik, R., Polymer nanocomposite foams. *J. Mater. Chem. A* **2013,** 1, (12), 3837-3850.
36. Schartel, B., Considerations Regarding Specific Impacts of the Principal Fire Retardancy Mechanisms in Nanocomposites. In *Flame Retardant Polymer Nanocomposites*, John Wiley & Sons, Inc.: 2006; pp 107-129.
37. Gedler, G.; Antunes, M.; Realinho, V.; Velasco, J. I., Thermal stability of polycarbonate-graphene nanocomposite foams. *Polym. Degrad. Stab.* **2012,** 97, (8), 1297-1304.
38. Semenzato, S.; Lorenzetti, A.; Modesti, M.; Ugel, E.; Hrelja, D.; Besco, S.; Michelin, R. A.; Sassi, A.; Facchin, G.; Zorzi, F.; Bertani, R., A novel phosphorus polyurethane FOAM/montmorillonite nanocomposite: Preparation, characterization and thermal behaviour. *Appl. Clay Sci.* **2009,** 44, (1–2), 35-42.
39. Han, X.; Zeng, C.; Lee, L. J.; Koelling, K. W.; Tomasko, D. L., Extrusion of polystyrene nanocomposite foams with supercritical CO_2. *Polym. Eng. Sci.* **2003,** 43, (6), 1261-1275.
40. Verdejo, R.; Barroso-Bujans, F.; Rodriguez-Perez, M. A.; Antonio de Saja, J.; Arroyo, M.; Lopez-Manchado, M. A., Carbon nanotubes provide self-extinguishing grade to silicone-based foams. *J. Mater. Chem.* **2008,** 18, (33), 3933-3939.
41. Wai, S. K.; Sahrim, A. H.; Zubir, S. A., Synergism between flame retardant and phosphonium salt modified layered silicate on properties of rigid polyurethane foam nanocomposite *Adv. Mat. Res.* **2012,** 501, 8-12.
42. Modesti, M.; Lorenzetti, A.; Besco, S.; Hrelja, D.; Semenzato, S.; Bertani, R.; Michelin, R. A., Synergism between flame retardant and modified layered silicate on thermal stability and fire behaviour of polyurethane nanocomposite foams. *Polym. Degrad. Stab.* **2008,** 93, (12), 2166-2171.
43. Santhosh Kumar, K. S.; Reghunadhan Nair, C. P.; Ninan, K. N., Mechanical properties of polybenzoxazine syntactic foams. *J. Appl. Polym. Sci.* **2008,** 108, (2), 1021-1028.
44. Santhosh Kumar, K. S.; Reghunadhan Nair, C. P.; Ninan, K. N., Silica fiber–polybenzoxazine–syntactic foams; Processing and properties. *J. Appl. Polym. Sci.* **2008,** 107, (2), 1091-1099.
45. Lorjai, P.; Wongkasemjit, S.; Chaisuwan, T., Preparation of polybenzoxazine foam and its transformation to carbon foam. *Mater. Sci. Eng., A* **2009,** 527, (1–2), 77-84.
46. Ardanuy, M.; Rodríguez-Pérez, M. A.; de Saja, J. A.; Velasco, J. I., Foaming behavior, cellular structure and physical properties of polybenzoxazine foams. *Polym. Adv. Technol.* **2012,** 23, (5), 841-849.

3.8.1

SELF-FOAMING DIPHENOLIC ACID BENZOXAZINE

Self-Foaming Diphenolic Acid Benzoxazine

Camilo Zúñiga, Gerard Lligadas, Juan Carlos Ronda, Marina Galià, Virginia Cádiz*

Departament de Química Analítica i Química Orgànica. Universitat Rovira i Virgili. Campus Sescelades. Marcel.lí Domingo s/n. 43007 Tarragona. Spain.

ABSTRACT

This work concerns the investigation of porous polybenzoxazines based on the non-toxic renewable diphenolic acid. The approach described relies on the *in situ* generation of foaming agent (CO_2) during the thermal curing. For this purpose, the previously synthesized benzoxazine monomer from diphenolic acid was thermally polymerized at different temperatures. As the beginning of decarboxylation is about 200 ºC, we selected five foaming temperatures (T_f) ranging from 190 to 230 ºC. The influence of the foaming temperature on the cellular structure and its dependency on final properties is discussed.

Keywords: Polybenzoxazine foam, self-foaming, diphenolic acid

1. Introduction

Polymeric foam is a two-phase material consisting of gas dispersed in a continuous polymer matrix. This material is important and useful due to its strength-to-weight ratio. Furthermore the chemical resistance, cushioning performance, shock absorption, and thermal insulation are also prominent characteristics of this type of material [1]. Polyurethane (PU), polyethylene (PE) and polystyrene (PS) foams are the most popular polymeric foams because they have low thermal conductivity and good mechanical strength. Phenolic foams are another inexpensive commercial thermosetting material used when fire resistance is desired [2,3].

Polybenzoxazine is a newly developed class of phenolic resins derived from ring opening polymerization. Polybenzoxazine can overcome the drawbacks of conventional phenolic resin synthesis by eliminating the release of byproducts during the curing reactions, the need of strong acid as catalyst and for toxic materials. Furthermore, polybenzoxazine has many advantageous characteristics compared with the traditional phenolic resin, such as high thermal stability,

excellent mechanical properties, easy processability, and low water absorption and near zero shrinkage after polymerization [4,5].

The cellular structure of polymer foam is generally produced by introducing a blowing agent in the polymer matrix. Depending on their nature, the foaming agents can be classified as chemical and physical. The chemical blowing agents (CBA) provide gases from a chemical reaction and the physical ones (PBA) generate gases via a physical process. This CBA, usually an organic compound with a low molecular weight, is mixed with a polymeric matrix. There is a temperature above which the nucleation agent is decomposed, a gas is produced and bubbles appear. This simple operation does not give good control of porosity and products often exhibit non-uniform cellular structures. This also implies the presence of residues in the final product and the need for an additional stage to eliminate them.

PBAs can also be used. Upon their vaporisation due to a change in pressure and/or temperature, these agents create porosity in the final product. Currently, the focus is on CO_2 due to its relative ease of handle and more favourable interaction with polymers compared to other inert gases [6]. Moreover, traditional PBAs like chlorofluorocarbons (CFCs) and hydrochlorofluorocarbons (HCFCs) are known for their contribution to the depletion of the ozone layer. Further, hydrofluorocarbons aggravate the greenhouse effect and hydrocarbons pose hazard due to their high flammability [7].

Moreover, a self-foaming process has been reported that takes place in some cases. Thus, an original strategy has been used to develop self-foaming poly(phenylquinoxaline)s (PPQs) which consists in grafting thermolabile groups [tert-butoxycarbonyl-(Boc-)] on a PPQ chain. Then, this modified PPQ in the dense thin film form is submitted to a fitted thermal treatment to induce the degradation of the Boc groups into CO_2 and isobutene, leading to the formation of a porous structure [8]. Biodegradable cellular materials were synthesized and *in situ* foamed from the reaction of malonic acid with epoxidized soybean oil. This reaction provides not only polymerization but also blowing of synthesized polymer due to the decarboxylation capability of malonic acid monoester [9].

Limited work has been done regarding to the study of polybenzoxazine foams [10-13]. In all cases a bisphenol A based benzoxazine was used. In the first case, the work was focused on the preparation and investigation on the mechanical properties of the hollow glass microspheres-filled polybenzoxazine

syntactic foams. The other works used bisphenol A based benzoxazine and azodicarbonamide (ADC), as blowing agent.

This study deals with a new type of rigid phenolic foams derived from a polybenzoxazine obtained from the non-toxic renewable diphenolic acid (DPA) [14], which contains a carboxylic group capable to thermal decarboxylation. The influence of the foaming temperature on the cellular structure and its dependency on final properties is discussed.

2. Experimental

2.1. Materials

The following chemicals were obtained from the sources indicated and used as received: ammonium sulphate (Scharlau), paraformaldehyde (Probus) and 4,4´-bis(4-hydroxyphenyl)pentanoic acid (DPA) (Aldrich). 1,3,5-triphenylhexahydro-1,3,5-triazine and 4,4´-bis-[6-(3-phenyl-3,4-dihydro-2*H*-1,3-benzoxazine)]pentanoic acid (DPA-Bz) were synthesized according to our reported procedure [14].

2.2. Crosslinking reaction

DPA-Bz was degassed in a glass oven for 30 min at 140 °C and then was compressed in a rectangular steel mould (cavity dimension: 70 mm x 6 mm x 3 mm) under a pressure of 9.2 MPa using a manual hydraulic press 15-ton sample pressing (SPECAC) equipped with water cooled/heated platens. Further, DPA-Bz was heated at 140 °C for 6 h and at 160 °C for 2 h in order to obtain a rigid polymer sample.

2.3. Foaming process

The above polymerized DPA-Bz was placed in a conventional glass oven (Büchi B-585) and heated from 30 °C up to selected foaming temperature (190, 200, 210, 220 and 230 °C) at a heating rate of 3.5 °C/min for 4 h. After the foaming process, samples were cooled to room temperature and the surface was peeled before analysing.

Polymer 2012, 53, 3089-3095

2.4. Measurements

The FTIR spectra were recorded on a JASCO 680 FTIR spectrophotometer with a resolution of 4 cm^{-1} in the absorbance or transmittance mode. An attenuated total reflection (ATR) accessory with thermal control and a diamond crystal (Golden Gate heated single-reflection diamond ATR, Specac Teknokroma) was used to determine FTIR spectra.

Calorimetric studies were carried out on a Mettler DSC821e thermal analyzer using N_2 as a purge gas (100 ml/min) at scanning rate of 20 ºC/min.

Thermal stability study was performed on a Mettler TGA/SDTA851e/LF/1100 usingN_2 as a purge gas at a heating rate of 10 ºC/min. Isothermal studies were performed under N_2 as a purge gas for 4 h at temperatures of 190, 200, 210, 220 and 230 °C.

Thermogravimetric Mass Spectroscopy Analysis (TGA-MS) was carried out on a Q600 TA Instruments coupled to a quadrupolar mass spectrometer (Thermostar QMS200 M3) at a heating rate of 10 °C/min under nitrogen atmosphere.

Dynamic mechanical thermal analysis (DMTA) of crosslinked polymer before foaming was tested on a TA DMA 2928 in a three point bending configuration. Sample was compressed in a rectangular steel mould (10 mm x 7 mm x 2.7 mm) and further heated from 40 to 220 ºC using a heating rate of 3 ºC/min and a fixed frequency of 1 Hz. Mechanical properties were determined on an Instron machine 3366 at 25 °C with a 5 kN load cell. Rectangular specimens with an average thickness of 6 mm and a cross-section area of ca. 117 mm^2 were compressed between two parallel steel plates using a crosshead speed of 1 mm/min. The compressive properties were determined from stress-strain curves of the average of at least five different samples.

Polymer matrix density was determined indirectly by the flotation method. A 5M solution of $(NH_4)_2SO_4$ was mixed with distilled water to get different aqueous solutions with densities lower or higher than the sample. Finally, the density of the solution in which the sample remained suspended was measured by the standard pycnometer method. The polymer foam density was calculated by dividing the weight by the measured volume of rectangular shaped samples. The density value was determined from the average of at least three samples.

The cellular structure of the polymer foams was observed on a JEOL JSM-6400 scanning electron microscopy (SEM) operated at an accelerating potential of 15 kV. Cross-section of the foams was fractured in liquid nitrogen and sputter-coating with gold at 30 mA for 3 min. The images were analyzed using ImageJ (1.43u) taking Fereter´s diameter as a measure of average cell size and cell size distribution. The cell density N_o (number of cells per unit volume) was calculated from the micrographs using the following equation [15]:

$$N_o = \left[\frac{nM^2}{A}\right]^{\frac{3}{2}}$$

where n is the number of cells in the micrographs, M the magnification of the micrograph and A the area of the micrograph in cm^2. At minimum of 200 pores per foam were manually traced and used in the image analysis.

3. Results and discussion

3.1. Curing and foaming process of the DPA-Bz

DPA-Bz was synthesized using 1,3,5-triphenylhexahydro-1,3,5 triazine which reacts with DPA and paraformaldehyde, in high yield and purity (Scheme 1).

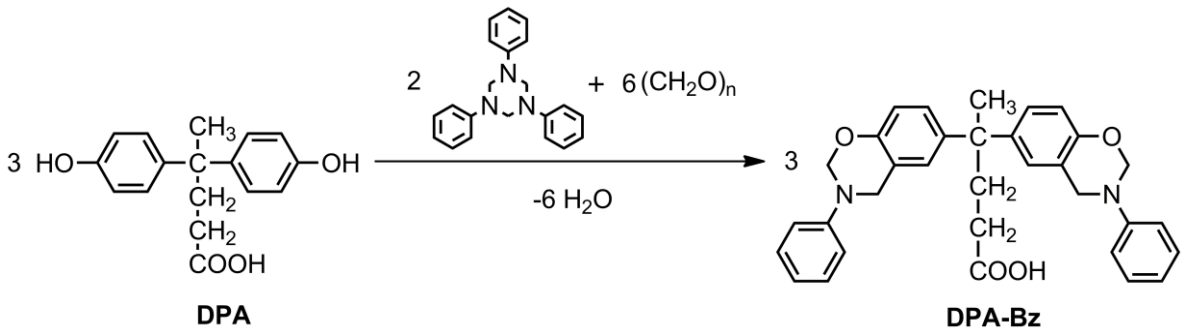

Scheme 1. Synthesis of DPA-Bz.

Curing of this DPA-Bz under pressure (2h/140 ºC, 2h/160 ºC, 8h/180 ºC and 2h/190 ºC) leads to a fully crosslinked system with Tg of 207 ºC. The analysis of this material by FTIR-ATR spectroscopy showed the existence of esterification reaction between the carboxylic groups and the phenolic OHs,

Polymer 2012, 53, 3089-3095

formed during the ring opening of oxazines, which could be related to the high crosslinking degree [14]. Interestingly, curing studies by DSC showed that when the curing was carried out without pressure an extensive foaming process occurred, probably due to the partial decarboxylation of the sample. To study this foaming process, DPA-Bz was partially cured under pressure following two curing cycles: 6 h at 140 ºC and 2 h at 160 ºC. These curing conditions were selected after several tests at different temperatures and times measuring the foam formation ability.

The resulting material showed by DSC a Tg at 145 ºC followed by an endothermic peak at 211 ºC that could be attributed to the decarboxylation reaction (Fig. 1).

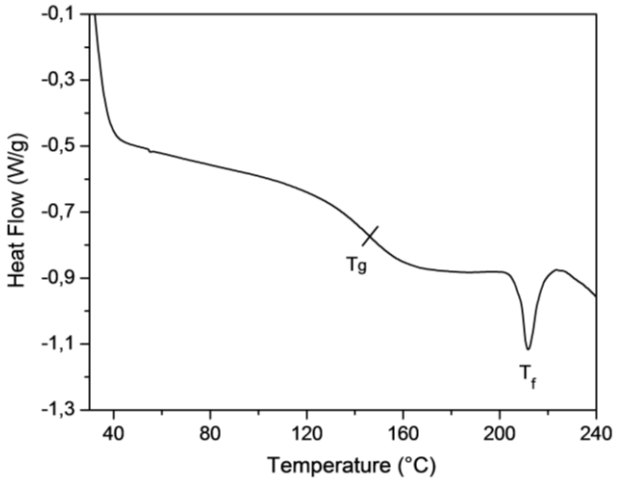

Fig. 1. DSC thermogram of partially cured polybenzoxazine.

Both thermal processes were also detected by DMTA, as two different slopes in the loss of storage modulus plot versus temperature. In the Tan δ plot, a positive peak at 178 ºC corresponding to the Tg and a negative peak at 207 ºC corresponding to the foaming process were also observed (Fig. 2).

It must be noted that a slight increase in the storage modulus can be observed at 130-150 ºC which can be attributed to the residual curing. This phenomenon is not detected by DSC probably due to its low associated enthalpy.

When this partially cured sample was further heated from 30 ºC to 220 ºC, without pressure, rigid foam was formed with a notable volume increase. According to DSC measurements, the Tg of the resulting polybenzoxazine foam

was similar (198 ºC) to the completely cured DPA-Bz under pressure (207 ºC) [14] indicating a similar final crosslinking degree for both polybenzoxazines. However the density of the compact material was 1221 ± 0.6 kg/m^3 whereas the density of the foamed material was 48.6 ± 0.9 kg/m^3. The decreasing of the density corresponds to the resulting gases evolved during the foaming process which increase the volume of the original sample around 25 times under the studied conditions (Fig. 3).

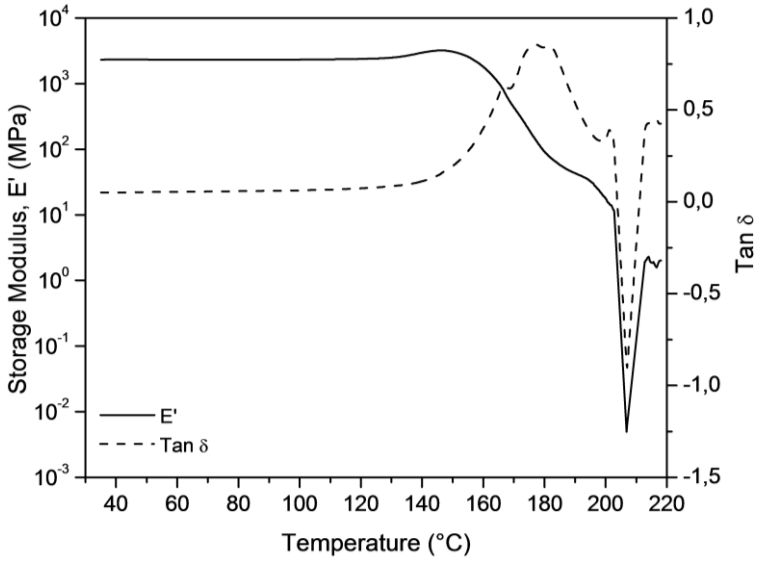

Fig. 2. Storage modulus and tan δ of partially cured polybenzoxazine.

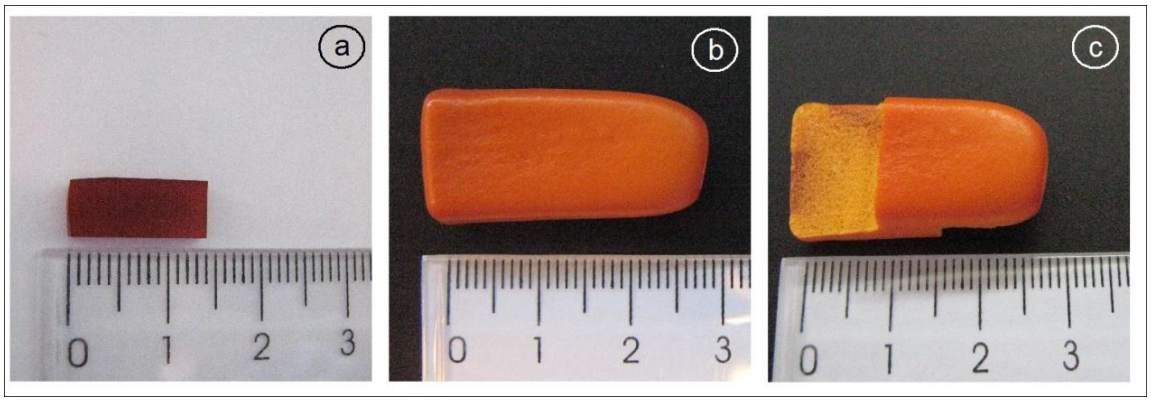

Fig. 3. Photographs of a) partially cured polybenzoxazine, b) polybenzoxazine foam at T_f 220 ºC, c) cross-section of this polybenzoxazine foam.

Polymer 2012, 53, 3089-3095

3.2. Foaming process characterization

To unravel the origin of the self-foaming process the partially cured polybenzoxazine was studied by TGA and the evolved gases were analyzed by mass spectrometry (TGA-MS). As can be seen in Fig. 4, about 200 ºC the sample starts to degrade and this decomposition practically coincides with the beginning of the CO_2 evolving. Decomposition gases analysis revealed that CO_2 is the main component and the formation of water remains negligible, thus demonstrating that the foaming is due to the decarboxylation reaction. We assume that radical species are formed when CO_2 is released. These species can further undergo radical recombination giving aliphatic chains which would increase the crosslinking density.

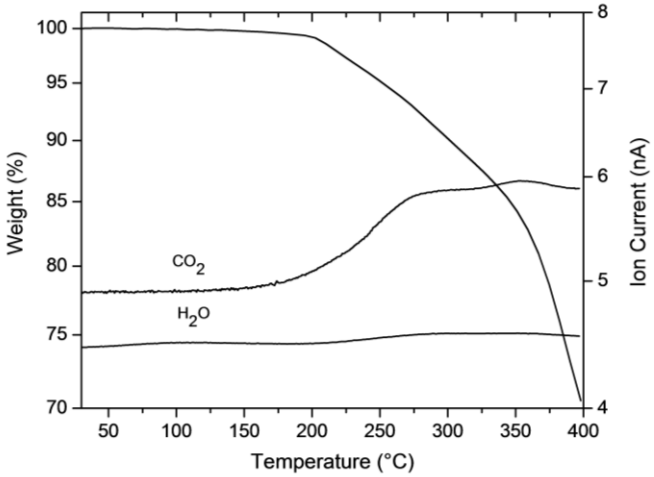

Fig. 4. TGA-MS analysis of partially cured polybenzoxazine.

To gain more insight about this assumption the foaming process was followed by FTIR at 200 ºC. Fig. 5 shows the decrease of the C=O vibration of carboxylic acid group at 1715 cm^{-1} and the progressive increase of the asymmetric stretching of O=C=O at 2350 cm^{-1}, corresponding to the CO_2 trapped in the porous structure, when the sample is heated during 4 h. Unfortunately, the FTIR spectra do not show significant changes in the intensity of absorptions at 1380 cm^{-1} ($-CH_3$ symmetric bending) and 730 cm^{-1} [$(-CH_2-)_n$ rocking] that would confirm the formation of these moieties.

It is well known that heat and mass transport phenomena are expected to affect the foaming process. In our case the temperature and heating time are significant parameters to control the foam morphology and the final properties.

As above mentioned the TGA analysis shows that the beginning of degradation is about 200 ºC, thus we selected five foaming temperatures (T_f) ranging from 190 to 230 ºC. An isothermal TGA analysis of samples at these selected foaming temperatures was carried out for 4 h (Fig. 6 a).

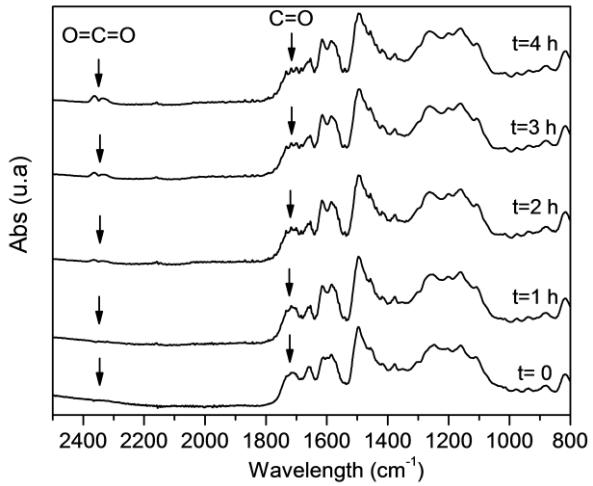

Fig. 5. FTIR spectra of partially cured polybenzoxazine at different time.

The TGA plots indicate that decarboxylation proceeds in a fast way, almost reaching a plateau. For foamed samples at above 190 ºC the weight loss corresponds practically to the theoretical CO_2 loss (8.5%) indicating the complete decarboxylation. For the foamed sample at 190 ºC the plateau is reached for a weight loss of 6.8% indicating that in this case the decarboxylation extent is 80%. To assure the completion of the foaming and crosslinking processes we selected a heating time of 240 min in the macroscopic samples. By FTIR-ATR spectroscopy (Fig. 6 b) could be also proved the complete decarboxylation for all the samples except for foamed sample at 190 ºC, which shows a remaining carbonyl band at 1710 cm^{-1}. Moreover the absence of absorbance peaks associated to the benzoxazine ring at 1230, 1035 and 952-942 cm^{-1} confirms the complete ring opening polymerization has taken place [14]. The absence of cell collapse was visually assessed throughout the foaming process. Also no

significant colour changes were observed with the exception of samples foamed at 230 ºC, which strengths its orange colour.

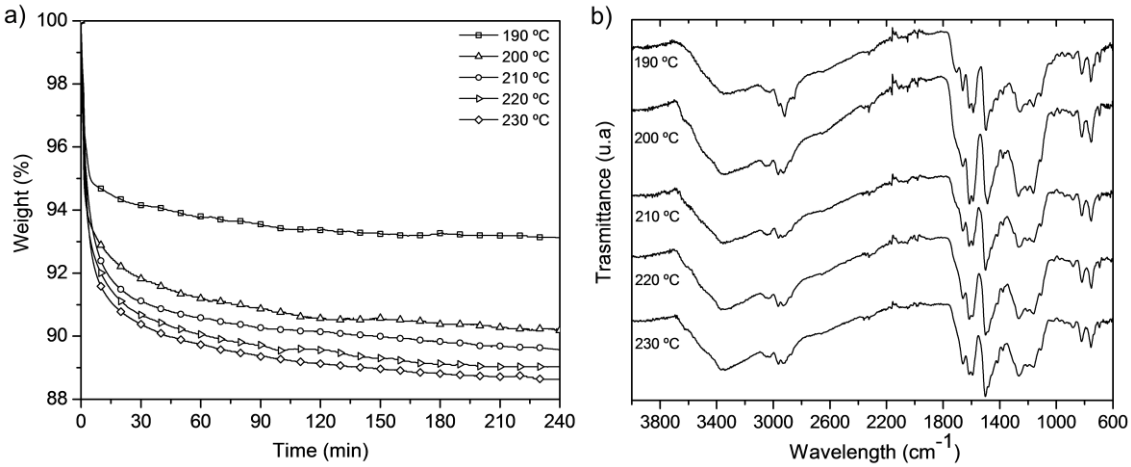

Fig. 6. a) Isothermal TGA plots of partially cured polybenzoxazine at different temperatures and b) FTIR-ATR spectra of the formed polybenzoxazine foams after 4 h.

3.3. Foam characterization

3.3.1. Foam density

Most of the physical characteristics of polymer foam are related to the density. The foam density values are collected in Table 1. The density has a great dependence of the T_f and as a general trend the higher the T_f the lower the foam density. In our case we obtained density values ranging 38-98 kg/m^3. According to cellular plastic classification [16] we can consider that two classes of materials were obtained: light materials for T_f ranging 190-210 ºC and very light materials for T_f of 220 ºC and 230 ºC.

3.3.2. Foam Tg's

In the same Table, Tg values are also collected as ½ ΔC_p, determined by DSC. Although all the values are very close it is observed a slight increase of Tg's with the T_f becoming apparent a high crosslinking of foamed samples at 220 ºC. Interestingly, these values are higher than that of highly crosslinked unfoamed polymer (207 ºC) what confirms that the decarboxylation process also contributes to increase the crosslinking degree.

3.3.3. Foam compressive properties.

Rigid polymer foams are used most often in compression than in tension. Compressive properties of cellular materials are related to the density which also depends on the cell size. With decreasing density, the number of cells and the average volume of cells increase, and the cell walls become thinner, therefore compressive modulus decreases [17]. The compressive modulus and compressive strength were calculated from the stress-strain curves (Fig. 7) and their values are collected in Table 1.

Table 1. Properties of the polybenzoxazine foams.

T_f(°C)	Density (kg/m^3)	Tg (°C)	CM[a] (MPa)	CS[b] (MPa)	SpCM[c] ($MPa/g/cm^3$)	SpCS[d] ($MPa/g/cm^3$)	Cell size (μm)	N_o [e] ($cells/cm^3$)
190	98.2±2.0	228	22.2±1.1	1.50±0.13	226.1±6.4	15.3±1.5	69.0	2.1×10^{12}
200	76.8±1.3	238	12.4±0.9	0.78±0.06	161.5±9.2	10.2±0.7	69.0	8.2×10^{11}
210	64.3±1.5	238	7.8±1.0	0.47±0.07	121.3±12.4	7.3±0.9	118.7	6.7×10^{11}
220	48.6±0.9	239	5.9±0.5	0.31±0.04	121.4±7.9	6.4±0.7	136.5	3.6×10^{11}
230	38.4±2.7	244	5.0±0.2	0.24±0.03	130.2±3.7	6.3±0.3	146.1	3.1×10^{11}

[a] Compressive Modulus [b] Compressive Strength [c] Specific Compressive Modulus
[d] Specific Compressive Strength [e] Cell density

Values of the compressive modulus between 5.0-22.2 MPa and 0.24-1.50 MPa for the compressive strength were measured. As expected, the compressive properties values clearly increase when the density increases, following the same trend as previous studies [12,13]. Different response of the foams at different T_f is found. Foamed sample at 190 °C shows higher mechanical properties values in comparison to those of the foamed samples at higher T_f. This is possibly due to the cellular morphology of the foam. It is well known, that the compressive modulus of the cellular material depends not only of the polymer matrix and density but also on the cell structure [17]. As shown below the foam obtained at 190 ºC, shows the narrowest cell size distribution and the highest content of small cells.

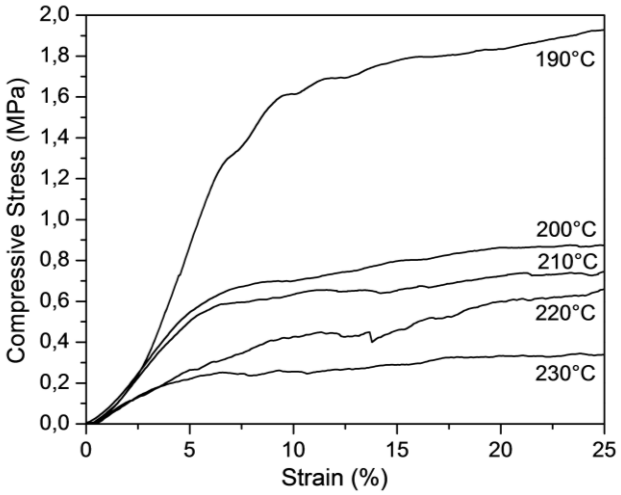

Fig. 7. Compressive stress-strain curves of polybenzoxazine foams at different T_f.

According to the theory, a compression stress-strain curve of foams exhibits three regions [18]. To compare the foam samples, the first two regions are plotted in Fig. 7. As expected, the samples exhibit the typical compressive behaviour of foams. The linear elastic region is followed by a plateau without having a drop of the compressive strength, indicating a flexible deformation manner, that is, the foams not completely lose their integrity after breakage, in a similar way as previously described for similar foams [12].

Specific compressive properties are defined as the ratio between compressive strength (SpCS) or compressive modulus of the material and its density. Usually their values are used to compare different materials. Santhosh

et al. [11] prepared polybenzoxazine syntactic foams from bisphenol-A using different contents of glass microspheres with SpCS values ranging from 6.1 to 16.6 MPa/g/cm^3. Similar results were obtained for our polybenzoxazine foams (SpCS = 6.3-15.3 MPa/g/cm^3) but it must be noticed that in this case no external chemical agent or filler had been added. Additionally, we compare the polybenzoxazine foams with some common commercial foams [17]. Rigid epoxy and phenolic foams show lower SpCS, with values of 3.6-4.3 MPa/g/cm^3 and 4.3-9.7 MPa/g/cm^3 respectively, while rigid polyurethane-ether and polyvinylchloride foams have values of SpCS 7.5-14.8 and 10.8-16.1 MPa/g/cm^3, similar than that of polybenzoxazine foam.

3.3.4. Foam cellular structure characterization.

The porosity in most polymer foams is related to its foaming process, that is, the traditional mechanism of bubble nucleation, bubble growth and stabilization. In a previous study on self-foaming polymer it has been reported that there are two main factors which affect the foaming process: the T_f and the polymer/gas mixture Tg [19]. Polymers are known to be plasticized by the presence of gases, particularly CO_2 [20]. In our case the thermolabile carboxylic groups present in the partially polymerized structure are able to generate a bubble nuclei through heating, that later grow into a final cell. When the T_f is set above the partially cured polybenzoxazine Tg (145 °C) the polymer/gas mixture viscosity is low enough to afford that the blowing reaction starts by the generation of CO_2, which produces the bubble growth. As T_f increases the CO_2 pressure inside the bubble becomes higher than the outside surrounding media resulting in larger cells. With time and temperature the crosslinking reaction continues as well as the cells stabilization. As above mentioned, decarboxylation process occurs at the beginning of the foaming process, nevertheless an additional curing time is necessary to complete crosslinking reaction and stabilize the foam. In other words, the foam porosity is conditioned by T_f and polybenzoxazine/gas mixture Tg. Both variables are inter-related between themselves determining that an increase in T_f produces a decreasing in the polybenzoxazine/gas mixture Tg, as above mentioned, and thus generating higher cells growth and therefore higher porosity.

The visual examination of a cross-section of the foams obtained at different temperatures was carried out using SEM. Fig. 8 shows typical SEM micrographs of the cellular structure of polybenzoxazine foams as a function of their T_f. A

global examination of the foams revealed well-foamed structure. The foams show a fine heterogeneous structure of relatively open cell roundness with interconnected pores. The cell morphology shows changes with T_f. At 190-200 ºC, anisotropic cells are mainly observed while at 210 ºC the cells become slightly rounded. However, at 220-230 °C as the bubbles grow enough to produce low-density foams, most of the cells present a typical polyhedral geometry.

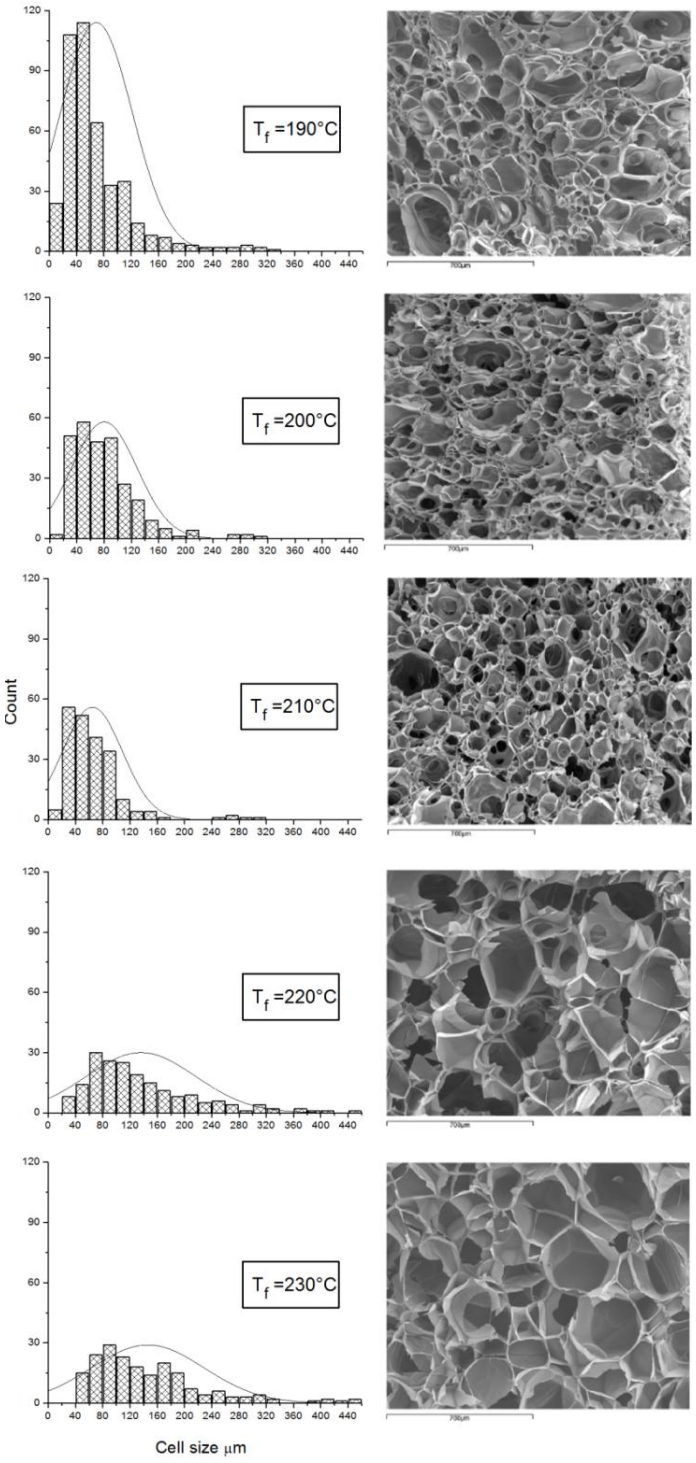

Fig. 8. Cell size distribution and SEM images at different T_f.

In the same Fig. 8 can be seen also the cell size distribution. The numerical data of the morphology characterization are collected in Table 1.

Cell size and cell size distribution depend not only on the polymer grade but also on the process conditions for foaming [16]. The cell size could be related to the viscosity of the system, so the high viscosity at lower T_f prevents an extensive cell growth. When T_f ranging from 190-210 °C is used, a narrow cell size distribution could be observed, however as T_f was risen (220 and 230 °C) the distribution becomes wider. The average cell size for the polybenzoxazine foams varies from 69.0 to 146.1 μm and therefore a decrease in the foam density is observed. Although, theoretically the relation between the density and the average cell size follows a hyperbolic function [16] a linear trend is observed in our case. Similar behaviour was observed in the characterization of nanocellular *in situ* poly(phenylquinoxaline) foams [19]. The cell density (number of cells per unit volume) can be related to the effectiveness of the bubble nucleation mechanism. As is expected, an increase in polymer foam density occurs when cell size decreases and so cell density increases.

4. Conclusions

In this work new polybenzoxazine rigid foams based on the non-toxic renewable diphenolic acid were prepared. Thermal reaction provides not only polymerization but also blowing of synthesized polymer due to the decarboxylation capability of diphenolic acid based benzoxazine. Therefore, the proposed polybenzoxazine foam synthesis has the elegance of using the same chemical as crosslinking monomer and the blowing agent. We can control the relative decarboxylation reaction by varying the temperature, which gives an excellent and simple method for controlling foam properties. The obtained low-density foams exhibit high glass transition temperatures with heterogeneous open-cell morphology. Cell size, cell size distribution, cell density and compressive properties are dependent of the foaming temperature.

Acknowledgement

The authors express their thanks to CICYT (Comisión Interministerial de Ciencia y Tecnología) (MAT2008-01412 and MAT2011-24823) for financial support for this work and to Dr. Raquel Verdejo for mechanical measurements.

References

[1] Rodríguez-Pérez MA. Adv Polym Sci 2005;184:97-126.

[2] Shen H, Nutt S. Composites Part A, 2003;34:899-906.

[3] Tseng C, Kuo KT. J Quant Spectrosc Radiat Transfer 2002;72:349-59.

[4] Ishida H. In: Ishida H, Agag T, editors. Handbook of benzoxazine resins. Amsterdam: Elsevier; 2011. p. 3-81 [chapter 1]

[5] Yagci Y, Kiskan B, Ghosh NN. J Polym Sci Part A: Polym Chem 2009;47:5565-76.

[6] Sauceau M, Fages J, Common A, Nikitine C, Rodier E. Prog Polym Sci 2011;36: 749-66.

[7] Tomasko DL, Burley A, Feng L, Yeh SK, Miyazono K, Nirmal-Kumar S, Kusaka I, Koelling K. J Supercrit Fluids 2009;47:493-99.

[8] Merlet S, Marestin C, Romeyer O, Mercier R. Macromolecules 2008;41:4205-15.

[9] Dogan E, Küsefoglu S. J Appl Polym Sci 2008;110:1129-35.

[10] Santhosh KS, Reghunadhan CP, Ninan KN. J Appl Polym Sci 2008;107:1091-9.

[11] Santhosh KS, Reghunadhan CP, Ninan KN. J Appl Polym Sci 2008;108:1021-8.

[12] Lorjai P, Wongkasemjit S, Chaisuwan T. Mat SciEng A 2009;527:77-84.

[13] Ardanuy M, Rodriguez-Pérez MA, De Saja JA, Velasco JI. Polym Adv Technol 2011; doi: 10.1002/pat.1978.

[14] Zúñiga C, Larrechi MS, Lligadas G, Ronda JC, Galià M, Cádiz V. J Polym Sci Part A: Polym Chem 2011;49:1219-27.

[15] Zeng C, Hossieny N, Zang C, Wang B. Polymer 2010;51:655-64.

[16] Klempner D, Sendijarevic V. Polymeric foams and foam technology, Munich: Hanser Gardner Pub; 2004. p. 24-25, 34.

[17] Suh KW, Web DD. Encyclopedia of Polymer Science and Engineering; vol. 3. New York: John Wiley; 1985. p. 1-5.

[18] Eaves D, editor. Handbook of polymer foams, Shawbury: Rapra Technology Limited; 2004. pp. 3-4.

[19] Merlet S, Marestin C, Schiets F, Romeyer O, Mercier R. Macromolecules 2007;40: 2070-8.

[20] Cooper AI. J Mater Chem 2000;10:207-34.

3.8.2

PHOSPHORUS FLAME RETARDANT POLYBENZOXAZINE FOAMS BASED ON RENEWABLE DIPHENOLIC ACID

Phosphorus Flame Retardant Polybenzoxazine Foams Based on Renewable Diphenolic Acid

C. Zúñiga, M. S. Larrechi, G. Lligadas, J.C. Ronda*, M. Galià, V. Cádiz

Departament de Química Analítica i Química Orgànica. Universitat Rovira i Virgili. Campus Sescelades. Marcel.lí Domingo s/n. 43007 Tarragona. Spain.

ABSTRACT

Flame retardant polybenzoxazine foams were prepared in a two step process, by heating mixtures of the benzoxazine derived from renewable diphenolic acid (DPA-Bz) with 9,10-dihydro-9-oxa-10-phosphaphenanthrene-10-oxide (DOPO) or 9,10-dihydro-9-oxa-10-(1-hydroxy-1-methylethyl) phos-phaphenanthrene-10-oxide (DOPO-2Me) as additives. In the first step partial curing was achieved at different times and temperatures. In the second step, these materials underwent self foaming when heated at 220 ºC. By means of a factorial design 2^3 the effect of curing conditions and type of additive on the foam density were evaluated. DOPO-2Me additive was found to partially react with the DPA-Bz leading to a decrease in the glass transition temperature of the materials. The cellular structure of the foams was characterized by scanning electron microscope in terms of cell size, cell size distribution, closed-cell content and anisotropy ratio. The presence of DOPO-2Me into the solid precursors and foams greatly influenced the thermal degradation and the flame retardancy properties as evaluated by TGA, LOI and UL-94 respectively.

Keywords: self-foaming; phosphorus-compound; polybenzoxazine; foam; flame retardancy; renewable resources.

1. Introduction

One very desirable property for sustainable polymers is flame retardancy. The use of flame retardants to reduce combustibility of the polymers, and smoke or toxic fume production, therefore becomes a pivotal part of the development and applications of new materials. The application of reactive flame retardants involves either the design of new, intrinsically flame retardant polymers or

modification of existing polymers. Halogenated flame retardants have been the most common systems used up to date. However many of them, specially brominated flame retardants, are nowadays restricted in many countries due to their migration to the environment, toxicity and the formation of hydrogen halides and dioxins during combustion [1]. These drawbacks have increased the amount of research into the development of innovative and environmentally friendly halogen-free flame retardant polymers [2]. The development of high performance halogen-free "green" polymeric materials for electronics, electrical, aerospace, and transportation continue demanding high performance flame retardants. Phosphorus-containing polymers are well recognized for their flame retardant properties, and they are increasingly becoming more popular than their halogen counterparts, as they generally give off non toxic combustion products.

A new approach to environmentally friendly flame retardants not only involves the design of halogen-free systems but also the use of renewable resources. The growing demand for petroleum-based products and the resulting negative impact on the environment, plus the scarcity of non-renewable resources, are some of the many factors that have recently focused interest on the field of polymers derived from non-petrochemical feedstock [3].

Phenolic foams are inexpensive commercial thermosetting materials used when fire resistance is desired [4,5]. Recently, a new type of rigid phenolic foams [6] derived from a polybenzoxazine obtained from renewable diphenolic acid (DPA) was reported [7]. DPA is emerging as a potential "green" candidate to displace bisphenol A because of its similar chemical structure, its lower price and because it has an extra functionality (carboxylic acid) which may be utilized for polymer synthesis.

With the aim of improving in the flame retardance of these foams, this work deals with the incorporation of a phosphorus-containing compound. Among organophosphorus flame retardants, 9,10-dihydro-9-oxa-10-phosphaphenanthrene-10-oxide (DOPO) and its derivatives have been shown to induce excellent flame retardant properties. Since 1972, this cyclic organophosphorus compound, and its derivatives have been used to make many synthetic flame retardant resins [8]. Few examples of the use of these organophosphorus compounds as flame retardant additives in foams have been reported. In flexible polyurethane foams, the addition of methyl ester of DOPO [9,10] and amino substituted DOPO [11] showed very high flame retardant efficiency and good thermal stability. Another recent approach was based in the

use of maleated DOPO in rigid bio-foams. The resulting materials exhibited high mechanical properties, flame resistance and an improvement in biodegradability [12].

This study was focused on obtaining halogen-free flame retardant renewable polybenzoxazine foams by mixing the previously synthesized DPA-based benzoxazine (DPA-Bz) with DOPO or with 9,10-dihydro-9-oxa-10-(1-hydroxy-1-methylethyl)phosphaphenanthrene-10-oxide (DOPO-2Me). After a partial polymerization at different temperatures and times, the resulting resins led to a series of rigid foams by decarboxylation at higher temperatures (Scheme 1).

To explore how the experimental conditions affect the preparation of rigid foams, a factorial design 2^3 was used to analyze the influence of the process variables (temperature, time and type of additive) on the foam density value.

Thermal stability of the foams was studied by TGA and flame retardancy was evaluated using UL-94 burn and LOI tests.

2. Experimental

2.1. Materials

The following chemicals were obtained from the sources indicated and used as received: ammonium sulphate (Scharlau), potassium bromide (Panreac), paraformaldehyde (Probus) and 4,4´-bis(4-hydroxyphenyl)pentanoic acid (DPA) (Aldrich). 9,10-Dihydro-9-oxa-10-phosphaphenanthrene-10-oxide (DOPO) (Aismalibar S.A) was previously dehydrated at reduced pressure for 3h/130 °C, 1h/145 °C and 1h/160 °C. 1,3,5-Triphenylhexahydro-1,3,5-triazine, [7] 4,4´-bis-[6-(3-phenyl-3,4-dihydro-2*H*-1,3-benzoxazine)]pentanoic acid (DPA-Bz) [7] and 6,8-dimethyl-3-phenyl-2H,4H-benzo[e]1,3-oxazine (2,4-Me-Bz) [13] were synthesized according to reported procedures.

2.2. *Synthesis of 9,10-dihydro-9-oxa-10-(1-hydroxy-1-methylethyl)phosphaphenanthrene-10-oxide (DOPO-2Me) (Scheme 1)*

For the synthesis of DOPO-2Me a reported procedure [14] was modified as follows: to a 100 mL round-bottomed flask equipped with a condenser and a magnetic stirrer, 5 g (0.023 mol) of DOPO and 14 mL (0.190 mol) of acetone

were added. The mixture was heated at 55 °C for 14 h and then was kept in the refrigerator overnight. The precipitate which formed was collected by filtration, washed with cold acetonitrile (20 mL) and subsequently was crystallized from chloroform (4 mL/g) and dried overnight at 60 °C. The desired product was obtained as white crystals in a yield of 60%.

^{1}H NMR (DMSO-d_6, δ ppm): 8.24-8.15 (1H, Ar-H), 8.14-8.13 (1H, Ar-H), 7.97-7.92 (1H, Ar-H), 7.81-7.87 (1H, Ar-H), 7.62-7.56 (1H, Ar-H), 7.43-7.39 (1H, Ar-H), 7.26-7.22 (2H, Ar-H), 5.5-5.49 (1H, -OH, J_{PH}: 6.8 Hz), 1.41-1.37 (3H, CH_3, , J_{PH}: 14.8 Hz), 1.27-1.23 (3H, CH_3, , J_{PH}: 14.8 Hz)

^{31}P NMR (DMSO-d_6, δ ppm, H_3PO_4): 36.6

FTIR (cm^{-1}): 3276 (-OH); 1594, 1477, 1430, 1117, 1006 (P-C_{Ar}); 1203 (P=O); 1225, 916 (P-O-C_{Ar}); 783 (P-C); 1134 (C-O), 746 (C_{Ar}-H)

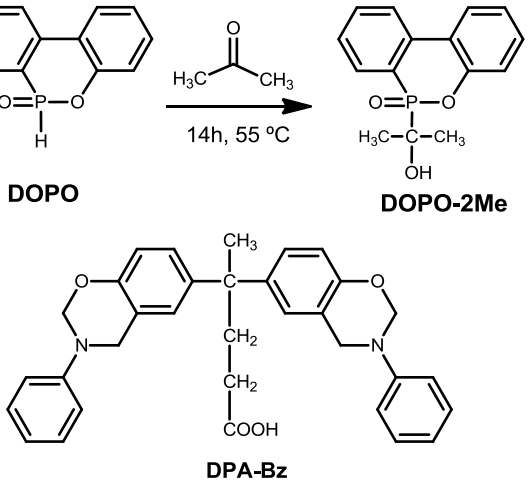

Scheme 1. Chemical structures of DOPO, DOPO-2Me and DPA-Bz

2.3. Crosslinking reaction

Appropriate amounts of DPA-Bz and DOPO or DOPO-2Me were dissolved in dichloromethane. Solvent was removed from the solution by evaporation at 45°C for 60 h and then at 140 °C for 10 min at reduced pressure. The amount of DOPO-2Me and DOPO used was 15.6 wt.% and 15.3 wt.% of the total weight of the mixture which corresponds in both cases to a 1 wt.% P. Resin bars were obtained by transferring the mixture to a Teflon mold (cavity dimension: 1 cm x 1.5 cm x 0.3 cm) and compressing under a pressure of 9.1 MPa using a manual

hydraulic press (15-ton sample press SPECAC equipped with water cooled heated platens). Ten samples were prepared by varying the type of phosphorus compound, polymerization time and temperature. The curing conditions are shown in Table 1. A neat polybenzoxazine sample was also prepared in the same way for the sake of comparison. Unfoamed materials are denoted with a P in the text and in forthcoming tables and figures.

2.4. Foaming process

A sample of previously synthesized polymer was placed in a conventional oven and heated from 30°C to 220 °C at a heating rate of 2.8 °C/min for 2 h. After foaming, the sample was allowed to cool slowly to room temperature. The surface was peeled off before analysis. A neat polybenzoxazine foam was also prepared in the same way for the sake of comparison. Foamed materials are denoted with a F in the text and in forthcoming tables and figures.

2.5. Instrumentation

^{1}H (400 MHz) and ^{31}P (161.9 MHz) NMR spectra were obtained using a Varian Gemini 400 spectrometer with Fourier transform and DMSO-d_6 or $CDCl_3$ as solvent.

The FTIR spectra were recorded using a JASCO 680 FTIR spectrophotometer with a resolution of 4 cm^{-1} in the transmittance and absorbance modes. An attenuated total reflection (ATR) accessory with thermal control and a diamond crystal (Golden Gate heated single-reflection diamond ATR, Specac Teknokroma) was used.

Calorimetric studies were carried out at a scanning rate of 20 ºC/min using a Mettler DSC821e thermal analyzer using N_2 as a purge gas (100 ml/min).

Thermal stability study was evaluated at a heating rate of 10 ºC/min using a Mettler TGA/SDTA851e/LF/1100 and N_2 as a purge gas.

Polymer matrix density was determined indirectly by the flotation method. A solution of KBr (40 wt.%) was mixed with distilled water to get different aqueous solutions with densities lower or higher than the sample. Finally, the density of the solution in which the sample remained suspended was measured by a standard pycnometer method. The polymer foam density was

calculated by dividing the weight by the measured volume of rectangular shaped speciman. The density value was determined from the average of at least three measurements using different specimen.

The closed-cell volume percentage was determined with a Micromeritics AccuPyc 1330 Gas Pycnometer thermostatized at 40 ºC, using argon as gas according to a modification of ASTM D6226-10. At least three specimen were measured and their volume was at least 15% of the volume of the speciman chamber. The specimen characterized did not present outward skin on any of their faces.

The closed-cell volume percentage (C_v) was calculated according to ASTM standard using the following equation:

$$C_v(\%) = 100 - \left(\frac{V_s - V_p}{V_s}\right) x\ 100 - \left(\frac{m}{\rho_s - V_s}\right) x\ 100$$

where V_s is the geometric volume of the speciman in cm^3, V_p is the volume measured with the pycnometer in cm^3, m is mass of the specimen and ρ_s is the specific density of the polymer matrix in g/cm^3.

The cellular structure of the polymer foams was observed using a JEOL JSM-6400 scanning electron microscope (SEM) operated at an accelerating potential of 15 kV. Cross-sections of the foams were fractured in liquid nitrogen and sputter-coating with gold at 30 mA for 3 min. The atomic mapping was measured using an ESEM (Environmental Scanning Electron Microscope) FEI Quanta 600 coupled to an Oxford INCA Energy Dispersive X-Ray Micro. Images were analyzed using ImageJ (1.43u) taking Fereter´s diameter as a measure of average cell size and cell size distribution. A minimum of 150 pores per foam were manually traced and used in the image analysis. An anisotropy ratio was determined by dividing the cell size in the horizontal direction by that in the vertical direction.

The UL-94 burn test was subject to some modifications related to speciman dimensions. Three unfoamed specimen (6 mm x 3 mm x50 mm) and three foamed specimen (11 mm x 6 mm x 50 mm) were used for this test. The speciman was clamped vertically so that the lower end was ca. 300 mm above a horizontal layer of cotton. The Bunsen burner flame height was ca. 20 mm and the height from the top of the Bunsen burner to the bottom of the speciman was ca. 10 mm. All test specimen were subjected to two 10 s ignitions. After the first

one the flame was withdrawn and the afterflame time was recorded. The second ignition was carried out immediately after the flame has ceased. Dripping characteristics as well as afterflame and afterglow times were recorded.

LOI measurements were performed using a Stanton Redcroft FTA flammability unit provided with an oxygen analyzer. Solid specimen used for the test were70 mm x 6 mm x 3 mm and were prepared by compression molding at 9.2 MPa. In the case of the foamed specimen the dimensions were 6 mm x 10 mm x 70 mm.

2.6. Experimental Design 2^3

2.6.1. Experiments.

A total of 16 experiments (8 by duplicate) were carried out following a 2^3 full factorial experimental design. The experimental plan is depicted in Table 1. The chosen variables and their high or low levels were: temperature (140 ºC and 150 ºC), time (4 h and 8 h) and DOPO (additive A) and DOPO-2Me (additive B). In addition, to evaluate the experimental error, two triplicate experiments were prepared with the experimental conditions corresponding to the central point (CP) of the experimental domain defined for each additive. The density value was considered as a response variable to evaluate the effect of the temperature, time and type of additive in the quality of the prepolymer.

2.6.2. Analysis of variance.

The effect of each variable in the density of the obtained prepolymer was evaluated as average of the value detected in the eight experiments. The significance of this effect was tested using an ANOVA test.

3. Results and discussion

The diphenolic acid benzoxazine monomer (DPA-Bz) was prepared as previously described [7]. The flame retardant additive DOPO-2Me (Scheme 1) was synthesized *via* a modification of a reported method using DOPO instead of the hydrated DOPO. It is well known that the P-(O)-H group reacts with the carbonyl group of acetone forming a P-C bound *via* nucleophilic addition [15,16]. The chemical structure of the phosphorus compound was confirmed by FT-IR, ^{1}H NMR and ^{31}P NMR. The FT-IR spectrum of DOPO-2Me showed the lack of any

absorption peak at 2438 cm^{-1} (P-H from DOPO) and 1710 cm^{-1} (C=O from the acetone) demonstrating the occurrence of the nucleophilic reaction. Similarly, the observance of the absorption peaks at around 3276 cm^{-1} (-OH), 1203 cm^{-1} (P=O) and 783 cm^{-1} (P-C) is evidence of the presence of DOPO ring in the compound. Likewise, no ^{1}H NMR signal was observed corresponding to P-H bond (8.8 ppm) and as expected, the appearance of new absorption peaks was in accordance with the chemical structure of the compound (see experimental section). Moreover, a peak at 36.6 ppm in the ^{31}P NMR spectrum, indicates the presence of a single phosphorus compound.

3.1. Influence of the experimental conditions in the foaming process

According to previous results, diphenolic acid based polybenzoxazine can undergo a self-foaming process due to the release of CO_2 during decarboxylation of the pendant carboxylic acid group present in its structure [6]. These polybenzoxazine foams present significant advantages such as the use of a non-toxic renewable reagent for the preparation of the monomer, the use of the *in situ* generated CO_2 as blowing agent and the control of the relative decarboxylation reaction by varying time or temperature [6]. To take advantage of the good performance displayed by these rigid foams, two different phosphorus compounds, DOPO or DOPO-2Me were added to the DPA-Bz for studying the influence as flame retardant additives in the final properties of the polybenzoxazine foams.

For this purpose, a prepolymer material was first prepared by curing DPA-Bz with DOPO (additive A) or DOPO-2Me (additive B) at 150 ºC for 8 h under pressure. The amount of both additives was adjusted to give 1 wt% P. A further heating of the prepolymers at 220 ºC for 2 h was performed in order to foam the samples. Fig. 1, shows the SEM images of the cellular structure of both polybenzoxazine foams. Notable differences could be seen according to the additive type. The sample that contains DOPO-2Me presents a fine heterogeneous structure of relative closed-cell at approximately spheroid geometry. In contrast, an irregular structure with mostly open cells and bigger cell size is observed when DOPO was used.

An experimental design was carried out to study in depth the prepolymer foamability in terms of the influence of the experimental conditions: addition of both phosphorus additives and polymerization time and temperature.

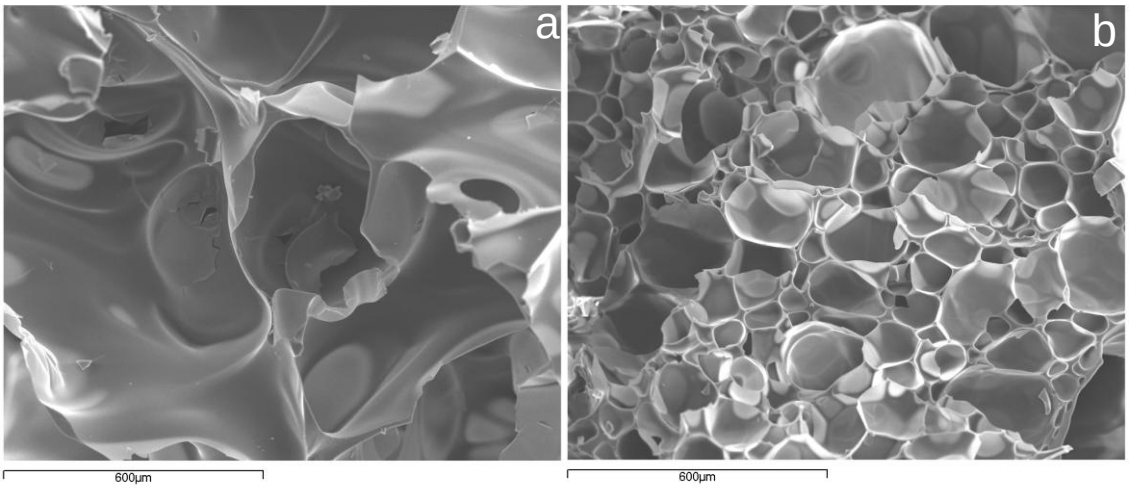

Fig. 1. Comparative SEM images of polybenzoxazine foams using a) DOPO and b) DOPO-2Me as additives (scale bar = 600 μm).

The average results of the density values for the obtained foams, when the experiments were carried out in each one of the experimental conditions are included in the Table 1.

Table 1
Experimental plan of a 2^3 design and results for foam density property

Samples	Analyzed factor			Response
	Temperature (ºC)	Time (h)	Additive[a]	Density (kg/m^3)
F1	140	4	A	131.3
F2	150	4	A	186.2
F3	140	8	A	198.2
F4	150	8	A	210.1
F5	145	6	A	161.2
F6	140	4	B	151.2
F7	150	4	B	171.3
F8	140	8	B	196.5
F9	150	8	B	228.2
F10	145	6	B	142.3

[a] A: DOPO; B: DOPO-2Me

The column (a) in Table 2 shows the coefficient values associated with the effect of the individual variables on the density (b1, b2, b3) and their interactions (b12, b13, b23). The results of the ANOVA test are included in column (b) of this table. The variance (MSS_R) related to the experimental error

was calculated from the repetitions of the density value of the obtained foams under the conditions shown in Table 1. It was assumed that the random error is constant in all the performed experiences. From the calculated F-ratios, it could be inferred that for an $\alpha = 0.05$ the associated variance to the effects of all variables: temperature (b1), time (b2) and additive (b3) significantly differs from the experimental error. According to the F value (b13 and b23), it is possible to conclude that the effect of the temperature on the density value significantly varies as a function of the type of additive used and the effect of the additive on the density value varies as a function of time.

The coefficients of the estimated effects and the results of the ANOVA test are summarized in Table 2.

Table 2
a) Coefficients of the estimated effects and b) results of ANOVA test.

(a)		(b)		
b0: average	182.97	Sum square	Mean Square	F ratio
b1: temperature (T)	42.95	3689.40	3689.40	125.57
b2: time (t)	61.55	7576.80	7576.80	257.89
b3: additive (A)	-17.38	755.16	755.16	25.70
b12: T x t	5.45	59.41	59.41	2.02
b13: T x A	-26.10	1362.42	1362.42	46.37
b23: t x A	-19.50	760.50	760.50	25.89

Degrees of freedom were 1 in all cases
Mean square of experimental error (MSS_R) = 29.38 Fcritic (1,2,α=0.05) = 18.5

A global analysis of the coefficient values helps to detect the influence of the variables considered in the foam density. A negative value of the coefficient indicates that the response decreases in response to a change in the experimental conditions for each variable, from their low to their high level. The influence of a variable is proportional to its absolute value. So, from the values in column (a) of Table 2, it can be concluded that the most influential variables are time and temperature. However, when the interaction effect between variables is significant, as in this case, the interpretation of the variable influence requires a deeper analysis.

In Fig. 2 the density of the foams obtained in the experiments numbered in the corner of each square is indicated in the centre of the square. Also in the same figure, the interaction between temperature and type of additive may be

analyzed by evaluating the increase or decrease of the density value when the experiments were carried out at low temperature (140 ºC) or at high temperature (150 ºC). These differences (d) are also included in Fig. 2. It is possible to observe that although the foam density is higher if the experiment is done at 150 ºC (experiment 2 and 6 in Fig. 2a, 4 and 8 in Fig. 2b) the temperature influence is lower when the additive B is used (d = 20.1 in Fig. 2a and d = 13.6 in Fig. 2b *vs*. d = 54.9 in Fig. 2a and d = 83.2 in Fig. 2b (additive A)), independent of the time value employed, 4 h for experiments shown in Fig. 2a and 8 h for experiments shown in Fig. 2b.

Similarly, the interaction between time and type of additive can be observed (Fig. 2 c and d). The time influence on the foam density is less significant when the additive B is employed, d = 45.3 and d = 38.8 *vs*. d = 66.9 and d = 95.2 for additive A.

This detailed analysis suggests that although the type of additive used is not a significant variable in the process, it plays an important role in the impact that other variables (T and t) have on the density values for the foams. When DOPO was used non-homogeneous prepolymers were obtained which upon foaming gave irregular cellular structure. On the contrary when DOPO-2Me was used more homogeneous prepolymers and foams were obtained and therefore only foams with this additive (F6 to F10) were characterized.

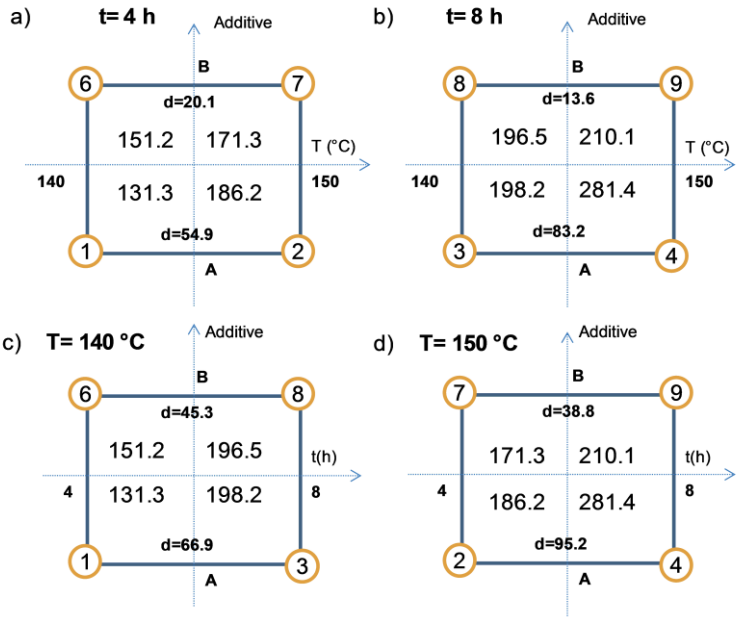

Fig. 2. Density of the foams at different curing conditions

3.2. Structural characterization of the foams

Foam density and relative density values are collected in Table 3. Most of the physical characteristics of polymer foams are related to its density. As it is known, polymeric foam is a two-phase material consisting of a gas dispersed in a continuous polymer matrix and its density may be calculated using the relationship between weight and volume of both phases. At medium and high expansion the gas weight and the polymer volume become negligible, being functions of polymer weight and gas volume [17]. In this case the volume of the foaming gas (CO_2) is a function of polymer weight in the mixture. For the neat DPA-Bz foam the theoretical maximum weight of CO_2 released during the foaming process is 8.5% (42.7 mL/g) [6]. As a consequence, a reduction in the mass of DPA-Bz reduces the theoretical volume of gas generated (36.0 mL/g) resulting in higher density of the flame retardant foams compared to neat foam. In the same way, it was found that the density values for the flame retardant foams exhibited dependence on the curing conditions and the crosslinking degree of the solid precursors as the amount of CO_2 released was the same in all cases. Thus, the higher the prepolymer crosslinking degree, the higher the foam density. From the values of the relative density in Table 3, it can be calculated the volume increase upon foaming. In the case of the neat sample a 20-fold volume increase was observed whereas for the flame retardant samples the increase was lower (6 to 9 times depending on the crosslinking degree).

Table 3
Main cellular characteristics of polybenzoxazine foams

Sample	Density (kg/m^3)	Relative density (ρ_f/ρ_s)	Cell size (μm)	Closed cell content (%)	Average anisotropy ratio
F6	153.7±3.5	0.12	155.6	53.7	0.89
F7	200.6±5.8	0.16	141.1	58.4	0.88
F8	169.8±2.2	0.14	148.3	55.4	0.83
F9	210.1±3.7	0.17	117.2	61.0	0.96
F10	140.0±3.6	0.11	163.3	51.2	0.92
Neat F7	54.2±3.4	0.05	218.7	18.8	0.87

The Structural parameters such as cell density, expansion ratio, cell size distribution, open/closed-cell content, and cell integrity are governed by the

foaming technology used in processing and play an important role in determining the properties, which, in turn, dictate the foam's possible applications [17]. Fig. 3 shows the visual examination of a cross-section of some foam samples by SEM. The numerical data for the main cellular characteristics are collected in Table 3. In general, it has been observed that the foams contain a well-cellular structure. The flame retardant foams showed closed-cell morphology of relatively spherical cells with some interconnected pores. The neat foam F7 presented by majority open-cell morphology with a typical polyhedral geometry of cells that seems to be connected to each other. Although the foams were free-expanded, it was possible to observe a certain degree of anisotropy in the cellular structure in both types of foams.

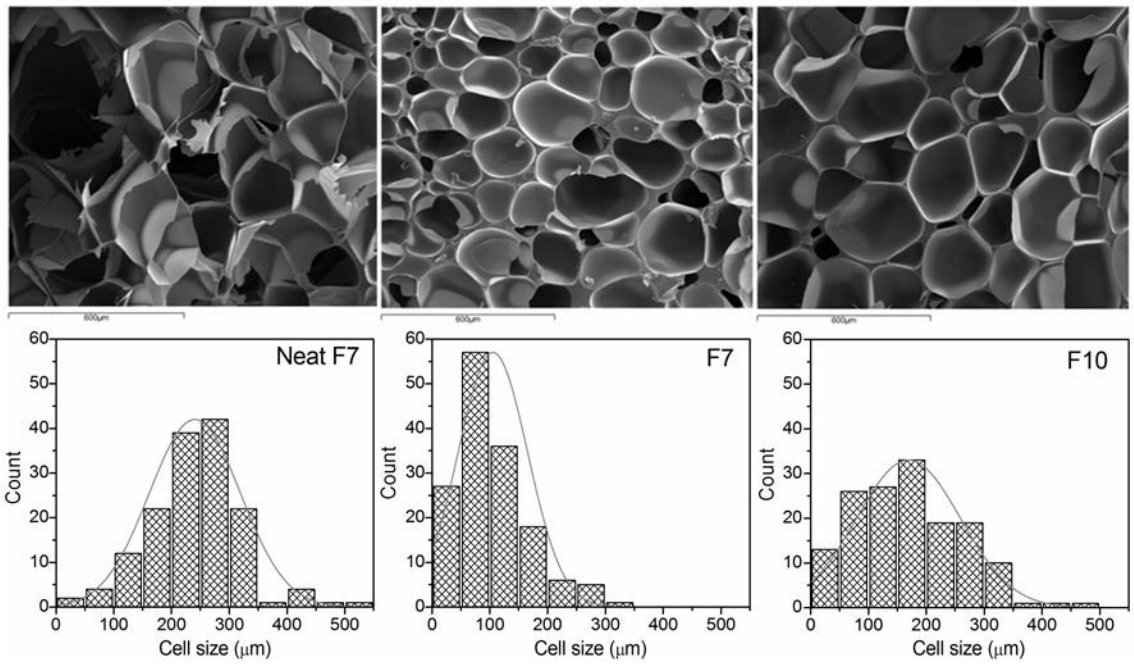

Fig. 3. SEM images and cell size distribution of neat F7, F7 and F10 (scale bar size: 600 μm)

The closed-cell content of the foams was influenced by the addition of DOPO-2Me. It was found that the amount of closed-cells increases as the cell size decreases. As result of a higher quantity of evolved gas during foaming, the neat F7 had a lower amount of closed-cell of 18.8%. No significant differences were found in the closed-cell content between the flame retardant foams. Such differences may be related to the polymerization conditions of the prepolymers

before the foaming process. Thus, for example, the closed-cell content varied from 51.2% to 61.0 % for foam F10 and F9, respectively.

Cell size distribution of the flame retardant foams is also shown in Fig. 3. It is well known, that cell size and cell size distribution depend on the cell nucleation and cell growth mechanism. In a previous study on polybenzoxazine foams [6], it was established that the cell formation and cell growth were conditioned by the foaming temperature and the Tg of the polybenzoxazine/CO_2 mixture. In this case, the effect of the foaming temperature is negligible, since the samples were foamed at the same temperature, therefore must be function of the amount of CO_2 and the Tg of the polybenzoxazine/CO_2 mixture. The average cell size for the polybenzoxazine foams varied from 117.2 to 218.7 μm. A reduction in cell size for the flame retardant foams was observed and could be related to a decrease in the amount of CO_2 generated during the foaming process that prevents an extensive cell growth. Neat F7 presented a wide cell size distribution feature of homogeneous nucleating mechanism. When DOPO-2Me was added, the cell size distribution of the foams became narrower and the cell size smaller. Hence, DOPO-2Me induced heterogeneous nucleation, provided an extra number of nucleation sites, and rendered a smaller cell size.

To further confirm the distribution of DOPO-2Me within the flame retardant foams, ESEM and element mapping with energy-dispersive X-ray spectroscopy analysis (EDX) were performed on the foam F8 surface. Fig. 4 shows a homogeneous distribution of phosphorus (2.04 keV) in the sample (white points denote P rich zones).

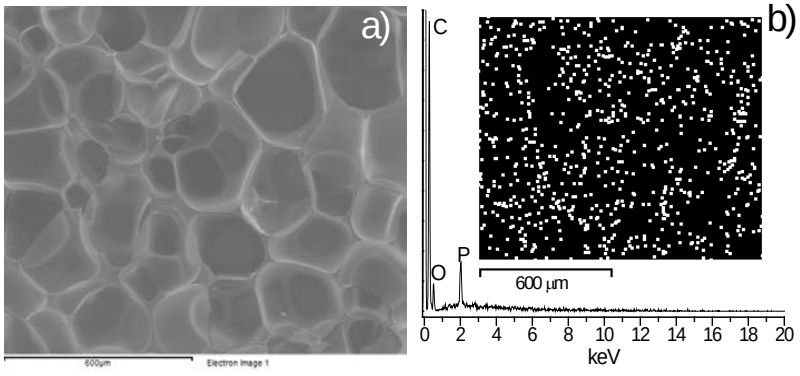

Fig. 4. a) ESEM image and b) ESEM-EDX P-mapping and EDX spectra of image of foam F8

3.3. Glass transition behavior

Glass transition temperatures (Tgs) of polybenzoxazine precursors and polybenzoxazine foams, measured using DSC as ½Δ C_p, are shown in the Table 4. Solid precursor samples present similar Tg values, ranging from 113 ºC to 117 ºC. With increasing time or temperature, Tgs slightly increase. For example, the sample P7 (curing for 8 h at 140 ºC) showed a Tg of 114 ºC while the sample P9 (curing for 8 h at 150 ºC) showed a Tg of 117 ºC. On polybenzoxazine foams a slight increase of the Tg value (between 199 ºC and 203 ºC) is observed which could be related with the higher croslinking density of the prepolymer precursors. In addition, the unfoamed and foamed samples with DOPO-2Me, present lower Tg values in comparison to neat samples. Similar results were previously observed on flame retardant epoxy systems with reactive DOPO-based compounds [18,19]. In these studies, Tg decrease was attributed to the reaction of the DOPO additive with epoxy groups, so lowering the crosslinking degree.

To gain more insight about the effect of DOPO-2Me on the chemical structure of the materials and the crosslinking process, a model reaction was proposed using DOPO-2Me and 2,4-Me-Bz (scheme 2). This benzoxazine contains two methyl groups in both *ortho* and *para* position of the benzene ring, which prevent its polymerization. For this purpose a mixture of DOPO-2Me/2,4-Me-Bz (1:1 w/w) was heated for 4 h at 150 ºC. At selected time intervals, samples were taken and analyzed using ^{1}H NMR and ^{31}P NMR. In the same way, FT-IR measurements were performed *in situ* at 150 ºC for 1h. The proposed resulting chemical reactions are shown in scheme 2.

After 45 min of reaction, the intensity of the characteristic ^{1}H NMR signals corresponding to the methylene protons of the oxazine ring at 4.5 and 5.2 ppm decreased in relation to the pure monomer. The appearance of some signals at about 3.8 ppm associated with both methylene protons of the Mannich bridge structure resulting from the oxazine ring opening was also observed. Additionally, a peak at about 8.6 ppm, associated to an imine proton, was detected. This peak was also observed when pure 2,4-Me-Bz was heated at 150 ºC. Spectrum of the mixture after 2.5 h showed that: 1) proton signals of the oxazine ring completely disappeared, 2) the peak intensity of methylene protons at 3.8 ppm significantly increased, 3) a new signal at 8.8 ppm, standing for the P-H proton in DOPO (due to the degradation of DOPO-2Me) appeared and 4) the signal of imine proton disappeared and two low intensity signals, at 4.8 ppm and

5.2 ppm, associated to the P-CH of structure b) in scheme 2, appeared. It is worth noting that when pure benzoxazine 2,4-Me-Bz was heated after 2.5 h, the above mentioned imine proton signal and the methylene protons of the oxazine ring were observed. These results indicate that during the first stage of the reaction, DOPO-2Me partially decomposes to DOPO which produces the opening of the oxazine ring. At high temperature benzoxazine ring is in equilibrium with its imine form and therefore DOPO can react with both species rendering the structures a) and b) in scheme 2. The DOPO-2Me degradation [14] was confirmed by TGA. Three loss stages were observed, the first one, at about 198 ºC and 23.3 wt.% weight loss, corresponding to the loss of acetone.

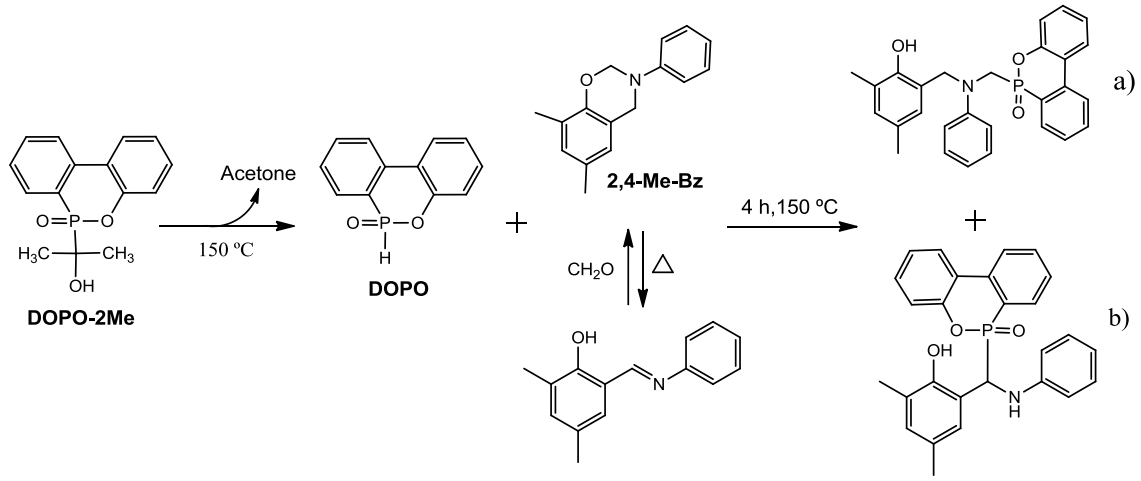

Scheme 2. Proposed chemical reactions on heating DOPO-2Me and 2,4-Me-Bz.

The reaction was also monitored using ^{31}P NMR. As the reaction progressed, the signal intensity of DOPO-2Me (36.6 ppm) decreased and three new signals at 14.8, 31.6 and 39.1, corresponding to DOPO and structures a) and b) respectively, appeared.

Fig. 5 shows the FT-IR spectra of the model reaction between the 2,4-Me-Bz and DOPO-2Me at different times. As can be seen, the benzoxazine monomer presents the oxazine ring absorption at 960 cm^{-1}, 1031 cm^{-1} and 1222 cm^{-1} characteristic of the C-H out of plane and the C_{ar}-O-C asymmetric and symmetric stretching modes. As the reaction progresses, the oxazine ring absorptions disappear indicating the ring opening. After 10 min (Fig. 5c), the peaks at 1430 cm^{-1}, 1117 cm^{-1} and 1006 cm^{-1}, associated to P-C_{ar} begin to increase their intensity as result of the linkage of DOPO to the benzoxazine (structure a in

Scheme 2). Likewise, bands at 1200 cm^{-1} and 1234 cm^{-1}, standing for the absorption of P=O and P-O-C_{Ar}, respectively, gradually appear and remain until 60 min. The absence of absorptions at 820 cm^{-1} and 1500 cm^{-1} (trisubstituted benzene ring) suggests that the ring opening takes place through a Mannich type structure.

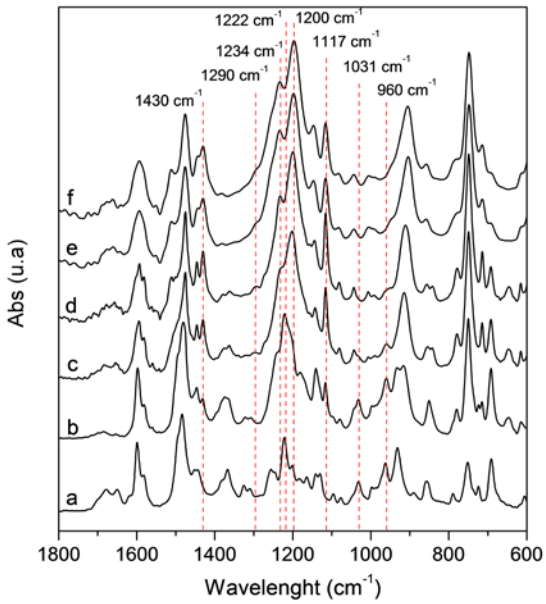

Fig. 5. FTIR spectra of 2,4-Me-Bz/DOPO-2Me mixture at different reaction times. a) pure 2,4-Me-Bz, b) 2,4-Me-Bz/DOPO-2Me initial mixture, c) 10 min, d) 20 min, e) 40 min and f) 60 min.

These changes confirm the results obtained using NMR and are in agreement with those previously reported [20,21]. The appearance of the O=P-C and Ar-OH absorptions in its FT-IR spectrum was observed when DOPO was reacted with bisphenol F-based benzoxazine. Benzoxazine ring opening mechanism has been described *via* the formation of iminium ions [22-24]. It is possible to synthesize DOPO-derivative benzoxazines and other compounds by reacting imines with the active hydrogen of DOPO [25-27]. Based on this assumption, structure b) in Scheme 2 was proposed. Fig. 5 shows the increase of the absorption at 1290 cm^{-1}, attributable to the C-N stretching, as a result of the addition of DOPO on the imine linkage [26].

Findings by FT-IR and NMR evidence the reaction of DOPO with the oxazine ring during the polymerization process, thus leading to a reduction of available

benzoxazine groups for crosslinking (Scheme 3). In this way, the lower Tg value of the phosphorus prepolymer is a consequence of its lower crosslinking degree. Moreover, part of the DOPO-2Me seems not to decompose into DOPO acting as non-reactive additive and contributing also to the reduction of the Tg value.

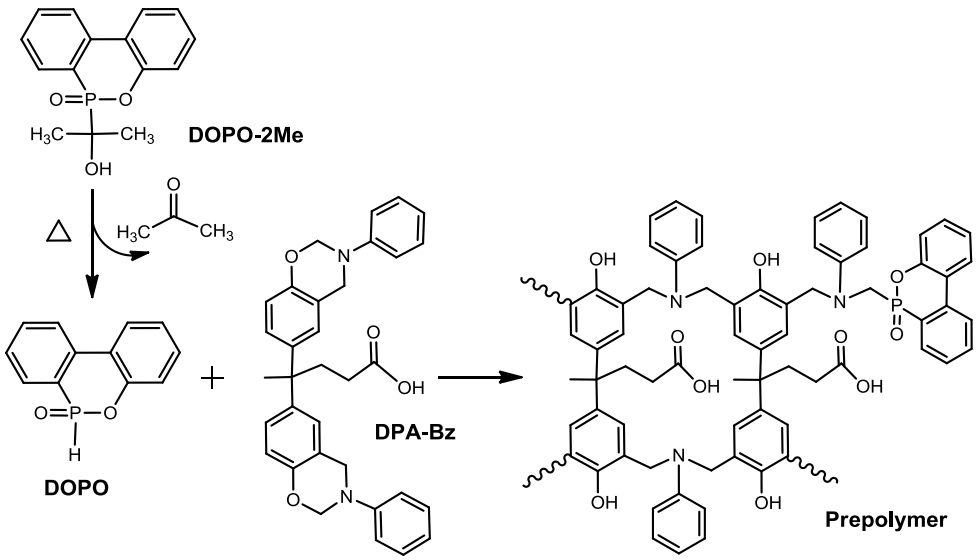

Scheme 3. Representative chemical structures involved during the reaction of DOPO-2Me and DPA-Bz

A comparable behavior was also observed in polybenzoxazine foams. Fig. 6 shows the FT-IR spectra of neat F7 and F7. The appearance of P-C_{ar} bonds with absorptions at 1476 cm^{-1}, 1446 cm^{-1}, and 1116 cm^{-1}, P=O at 1195 cm^{-1}, P-O-C_{ar} at 921 cm^{-1} [28] and the presence of the band at 752 cm^{-1} (1,2 disubstituted benzene) denote that the cyclic DOPO structure remains after the foaming process. The appearance of a new absorption band at 718 cm^{-1} associated with the aliphatic P-C bond, confirms the linkage of the phosphorus compound to the polybenzoxazine foam network.

3.4. Thermal stability

The Prepolymers and foamed polybenzoxazines were characterized by TGA under nitrogen and air atmospheres to determine the effect of DOPO-2Me on the thermal stability of the materials. The thermogravimetric data for all the polymers are summarized in Table 4. As an example in Fig. 7, the comparative

thermograms and derivative thermogravimetric (DTG) curves of the neat P7 and F7 as well as the corresponding flame retardant materials, are shown. Under nitrogen atmosphere the flame retardant prepolymers present an initial degradation step in the temperature range of 135-165 ºC (1% weight loss) which corresponds to the loss of acetone of the unreacted DOPO-2Me. At about 200 ºC a degradation step takes place due to the release of CO_2 [6]. In the third stage, a maximum weight loss rate (T_{max}) for the neat P7 appears at 427 ºC while the phosphorus-containing P7 presents two maximums at 402 ºC and 459 ºC. The first T_{max} value, attributed to benzoxazine degradation, is lower than on neat P7 due to its lower crosslinking degree. The second T_{max} can be attributed to the decomposition of the DOPO moiety, as DOPO shows a weight loss at the same temperature in TGA. The char yield of the prepolymer P7 increased about 7 wt.% in comparison to the neat P7 as result of the phosphorus promoted char protective layer on the polymer surface preventing further decomposition [2]. A similar trend in the thermal stability of the rest of the prepolymer samples was observed.

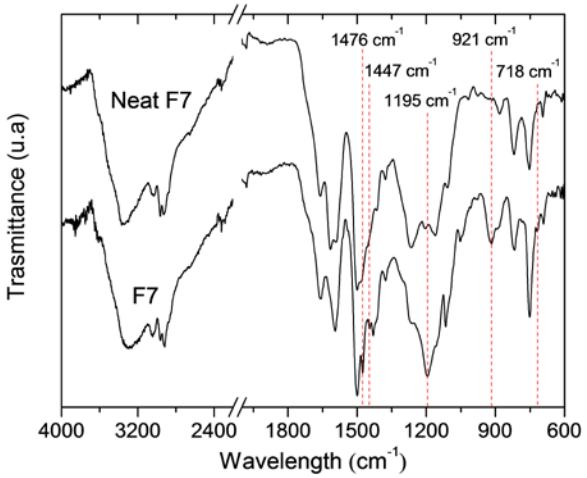

Fig. 6. FTIR spectra of F7 and neat F7

Foamed samples under nitrogen atmosphere presented the reported three-stages of weight loss for aniline and diphenolic based polybenzoxazines (Fig. 7c) [29]. Differences were found in the initial decomposition temperature and the temperatures of 10% of weight loss ($T_{10\%}$) of the materials. In the case of the neat foam F7 the decomposition took place 40 ºC above of the foam F7. As above-mentioned, DOPO group is linked to the polymer network through a P-C

linkage, which has a low bond energy (260 kJ/mol) in comparison to the C-C bond (349 kJ/mol), generating a lower thermal stability of the resin. Foams that came from more crosslinked prepolymers presented slightly higher $T_{10\%}$ although similar T_{max}. The same tendency of charring of 7 wt.% for foam F7 was again observed. The flame retardant effect of DOPO was specially observed above 400 ºC in both materials (solid and foamed). According to literature, during the decomposition of DOPO radical species such as PO, PO_2 and $POCH_3$ (which reaches its maximum at about 400-450 ºC) are formed. These radicals react with H and OH radicals in the gaseous phase intercepting the radical chain reactions in the flame and therefore reducing the heat production [9,30,31].

Table 4
Thermal and flame retardant properties of the prepolymers and the foams

Sample	Tg (°C)[b]	TGA (N_2)			TGA (O_2)			UL-94 Grade	LOI
		$T_{10\%}$ (°C)[c]	T_{max} (°C)[d]	Y_{800} (%)[e]	$T_{10\%}$ (°C)[c]	T_{max} (°C)[d]	Y_{800} (%)[e]		
P6	114	313	282,404	34.7	327	385,455,600	1.6	V-0	-
F6	199	329	406	33.7	368	385, 590	1.8	V-0	34.9
P7	114	317	287,402	35.2	329	392,470,595	1.4	V-0	31.6
F7	202	337	405	36.9	368	374, 582	2.2	V-0	35.2
P8	117	314	287,401	33.0	331	392,455,595	3.0	V-0	-
F8	203	340	404	35.7	363	348, 609	2.2	V-0	35.0
P9	117	324	291,397	33.8	335	392,455,602	2.7	V-0	33.2
F9	202	333	407	34.9	368	373, 574	3.1	V-0	35.4
P10	113	316	284,400	35.2	333	394,455,582	2.7	V-0	-
F10	201	335	404	34.7	362	351, 613	1.8	V-0	33.7
Neat P7[a]	146	308	276,427	28.6	312	431, 602	0.0	V-1	22.8
Neat F7[a]	248	365	404	30.0	392	416, 554	0.0	V-1	23.6

P: Denotes that is a solid sample
F: Denotes that is a foamed sample
[a] Sample without additive
[b] Measured by DSC
[c] Temperature of 10% of weight loss
[d] Temperature of the maximum weight loss rate
[e] Char Yield at 800°C

In air, prepolymer polybenzoxazines presented multiple stages of weight loss as a result of a complex degradation pathway (Fig. 7b and 7d). The thermal degradation processes identified in nitrogen and associated with the loss of the aliphatic moiety of the unreacted DOPO-2Me, decarboxylation reaction and the degradation of the char, were also detected. As can be observed in Fig. 7d the foamed samples presented two degradation stages. As in nitrogen, the degradation onset of the flame retardant foams begins at a lower temperature than the neat foam. This behavior was also observed in similar DOPO containing polymers [12,20,32]. In general, the flame retardant foams present high thermal

stability in comparison to the neat foam as well as a slight increase in the char yield. For instance, the T_{max} of the second degradation stage of the F7, related to thermo-oxidative decomposition of the char, was shifted almost 30 ºC. Again the foam F9 that came from the more crosslinked prepolymer showed the similar trend found in nitrogen.

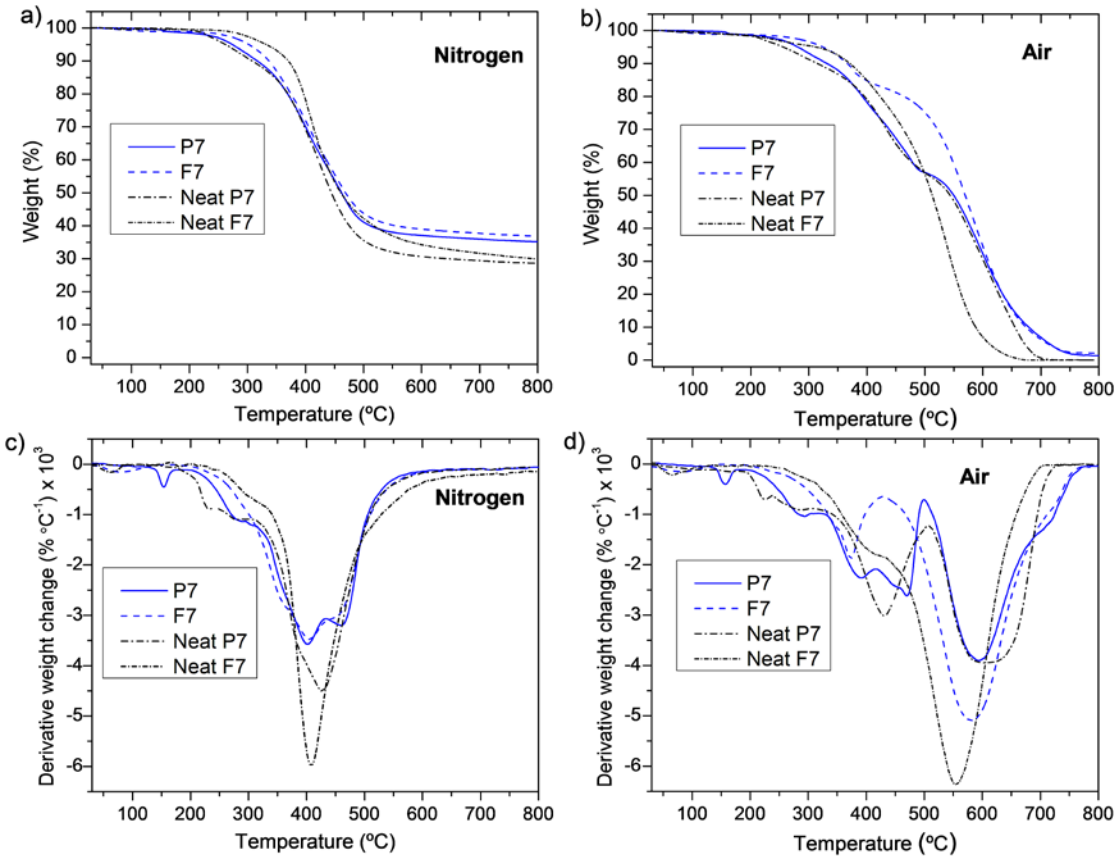

Fig. 7. TGA plots (a and c) and DTG plots (b and d) of neat P7, P7, neat F7 and F7 in nitrogen and air.

Differences in thermal stability of solid prepolymers and foamed samples were observed. Under nitrogen and air, the solid prepolymer P7 presented a premature degradation due to the above-explained decarboxylation reaction. From that point on, the foam F7 showed a higher thermal stability regarding the solid P7. These results could be explained according to two reasons: the transformation of the prepolymer into a foam which results in a more crosslinked structure and the cellular structure of the foam (mainly closed-cell) which acts as thermal insulator reducing the heat and mass transfer.

3.5. Flame retardancy

Flame retardant properties of solid precursors and foams were measured by UL-94 test and limiting oxygen index (LOI). Numerical data are collected in Table 4. According to results of UL-94 test, neat solid precursors and foams were rated as V-1 while those that contained DOPO-2Me were rated as V-0. During the test no burning drops were observed. Phosphorus containing samples showed significant higher LOI values (up to 35) than those neat ones (23) as result of the strong flame retardant effect of the phosphorus compound. Moreover, it has been found that LOI values for foamed samples are higher than those of the solid ones for both neat and phosphorus-containing samples. This difference could be caused by the closed-cell cellular structure in foamed samples, which prevents the transport of heat and combustible gases inside the sample. It is worth mentioning that foam density also affects the LOI values, as previously reported [33]. Thus, the higher the density, the higher the LOI value.

4. Conclusions

Mixtures of DPA-Bz and DOPO rendered non homogeneous cellular structures. In contrast, homogeneous foams with close cell cellular structure and spherical shape were obtained when DOPO-2Me was added. DOPO-2Me has been found to lose acetone between 135 and 165 ºC giving DOPO, which partially reacted with the benzoxazine rings. Prepolymer curing conditions, temperature and time, strongly affected structure, shape and density on the final foams. Prepolymers and foams containing DOPO-2Me showed lower Tg values than the neat counterparts. All phosphorus-containing foams were rated as V-0 according to the UL-94 test. Both, phosphorus-containing solid precursors and foams, had higher LOI values than the neat counterparts showing the beneficial effect of phosphorus on the flame retardant properties. Notably, foamed materials presented higher LOI values than unfoamed precursors.

Acknowledgements

The authors express their thanks to CICYT (Comisión Interministerial de Ciencia y Tecnología) (MAT2011-24823) for financial support.

References

[1] Stevens GC, Mann AH. Risks and Benefits in the Use of Flame Retardants in Consumer Products: A Report for the Department of Trade and Industry. Surrey: University of Surrey, Polymer Research Centre; 1999.

[2] Lu S-Y, Hamerton I. Recent developments in the chemistry of halogen-free flame retardant polymers. Prog Polym Sci. 2002;27:1661-712.

[3] Belgacem MN, Gandini A. Monomers, Polymers and Composites from Renewable Resources. Amsterdam: Elsevier; 2008.

[4] Shen H, Nutt S. Mechanical characterization of short fiber reinforced phenolic foam. Composites Part A. 2003;34:899-906.

[5] Tseng C-J, Kuo K-T. Thermal radiative properties of phenolic foam insulation. J Quant Spectrosc Radiat Transfer. 2002;72:349-59.

[6] Zúñiga C, Lligadas G, Ronda JC, Galià M, Cádiz V. Self-foaming diphenolic acid benzoxazine. Polymer. 2012;53:3089-95.

[7] Zúñiga C, Larrechi MS, Lligadas G, Ronda JC, Galià M, Cádiz V. Polybenzoxazines from renewable diphenolic acid. J Polym Sci, Part A: Polym Chem. 2011;49:1219-27.

[8] Saito T. Cyclic organophosphorus compounds and process for making same. U.S. Patent 3702878. 1972.

[9] König A, Kroke E. Flame retardancy working mechanism of methyl-DOPO and MPPP in flexible polyurethane foam. Fire Mater. 2012;36:1-15.

[10] König A, Kroke E. Methyl-DOPO—a new flame retardant for flexible polyurethane foam. Polym Adv Technol. 2011;22:5-13.

[11] Mispreuve H, Näscher R, Gaan S, Neisius M, Mercoli P, Liang S. Novel phosphonamidates - synthesis and flame retardant applications.Eur. Patent 2557085 A1, 2013

[12] Qiu JF, Zhang MQ, Rong MZ, Wu SP, Karger-Kocsis J. Rigid bio-foam plastics with intrinsic flame retardancy derived from soybean oil. J Mater Chem A. 2013;1:2533-42.

[13] Chutayothin P, Ishida H. Cationic Ring-Opening Polymerization of 1,3-Benzoxazines: Mechanistic Study Using Model Compounds. Macromolecules. 2010;43:4562-72.

[14] Yamada Y, Yasuda H, Saito T. A Novel synthesis of 6-hydroxyalkyl-and 6-hydroxy-aralkyl-6H-dibenz[c,e][1,2]oxaphosphorin 6-Oxides. J Heterocycl Chem. 1990;27:845–50.

[15] Wu CS, Liu YL, Chiu Y-S. Synthesis and characterization of new organosoluble polyaspartimides containing phosphorus. Polymer. 2002;43:1773-9.

[16] Lin CH, Chang SL, Wei TP, Ding SH, Su WC. Facile, one-pot synthesis of phosphinate-substituted bisphenol A and its alkaline-stable diglycidyl ether derivative. Polym Degrad Stab. 2010;95:1167-76.

[17] Lee ST, Park CB, Ramesh NS. Polymeric Foams: Science and Technology: Taylor & Francis; 2006.

[18] Liu YL. Flame-retardant epoxy resins from novel phosphorus-containing novolac. Polymer. 2001;42:3445-54.

[19] Perez RM, Sandler JKW, Altstädt V, Hoffmann T, Pospiech D, Ciesielski M, et al. Effect of DOP-based compounds on fire retardancy, thermal stability, and mechanical properties of DGEBA cured with 4,4'-DDS. J Mater Sci. 2006;41:341-53.

[20] Chang HC, Lin HT, Lin CH. Benzoxazine-based phosphinated bisphenols and their application in preparing flame-retardant, low dielectric cyanate ester thermosets. Polym Chem. 2012;3:970-8.

[21] Lin CH, Cai SX, Leu TS, Hwang TY, Lee HH. Synthesis and properties of flame-retardant benzoxazines by three approaches. J Polym Sci, Part A: Polym Chem. 2006;44:3454-68.

[22] Andreu R, Reina JA, Ronda JC. Studies on the thermal polymerization of substituted benzoxazine monomers: Electronic effects. J Polym Sci, Part A: Polym Chem. 2008;46:3353-66.

[23] Dunkers J, Ishida H. Reaction of benzoxazine-based phenolic resins with strong and weak carboxylic acids and phenols as catalysts. J Polym Sci, Part A: Polym Chem. 1999;37:1913-21.

[24] Kudoh R, Sudo A, Endo T. A Highly Reactive Benzoxazine Monomer, 1-(2-Hydroxyethyl)-1,3-Benzoxazine: Activation of Benzoxazine by Neighboring Group Participation of Hydroxyl Group. Macromolecules. 2010;43:1185-7.

[25] Spontón M, Lligadas G, Ronda JC, Galià M, Cádiz V. Development of a DOPO-containing benzoxazine and its high-performance flame retardant copolybenzoxazines. Polym Degrad Stab. 2009;94:1693-9.

[26] Sun D, Yao Y. Synthesis of three novel phosphorus-containing flame retardants and their application in epoxy resins. Polym Degrad Stab. 2011;96:1720-4.

[27] Su H, Liu Z. The structure and thermal properties of novel DOPO-containing 1,3-benzoxazines. J Therm Anal Calorim. 2013:1-9.

[28] Daasch L, Smith D. Infrared Spectra of Phosphorus Compounds. Anal Chem. 1951;23:853-68.

[29] Yee Low H, Ishida H. Structural effects of phenols on the thermal and thermo-oxidative degradation of polybenzoxazines. Polymer. 1999;40:4365-76.

[30] Schäfer A, Seibold S, Lohstroh W, Walter O, Döring M. Synthesis and properties of flame-retardant epoxy resins based on DOPO and one of its analog DPPO. J Appl Polym Sci. 2007;105:685-96.

[31] Granzow A. Flame retardation by phosphorus compounds. Acc Chem Res. 1978;11:177-83.

[32] Lin CH, Wang CS. Novel phosphorus containing epoxy resins Part I. Synthesis and properties. Polymer. 2001;42:1869-78.

[33] Horrocks AR, Price D, Edwards NLC. The Burning Behaviour of Combustion Modified High Resilience Polyurethane Foams. J Fire Sci. 1992;10:28-39.

3.8.3

MODELING OF THE FOAMING PROCESS OF A PHOSPHORUS FLAME RETARDANT POLYBENZOXAZINE

Modeling of the foaming process of a phosphorus retardant polybenzoxazine

Camilo Zúñiga, Maria Soledad Larrechi, Gerard Lligadas, Juan Carlos Ronda, Marina Galià, Virginia Cádiz*

Departament de Química Analítica i Química Orgànica. Universitat Rovira i Virgili. Campus Sescelades. Marcel.lí Domingo s/n. 43007 Tarragona. Spain.

ABSTRACT

Flame retardant polybenzoxazine foams containing 1% P were prepared from diphenolic acid-based benzoxazine (DPA-Bz) and 9,10-dihydro-9-oxa-10-(1-hydroxy-1-methylethyl)phosphaphenanthrene-10-oxide (DOPO-2Me). Statistical predictive models were developed to determine the influence of the foaming time (t_f) and foaming temperature (T_f) on the density, compressive modulus and compressive strength of the foams. Results showed that the density of the foams exhibited great dependence on t_f, whereas both compressive properties were more dependent on T_f and t_f. Additionally, the flammability of the foams was also characterized by the limiting oxygen index (LOI). The presence of DOPO-2Me greatly improved the flame retardancy of the resulting foams.

Keyword: Modeling and simulation, mechanical properties, polybenzoxazines, self-foaming, statistical analysis.

1. Introduction

Conventional phenolics are crosslinked products of low molecular weight precursors, typically formed through a condensation reaction between phenols and aldehydes. They are widely produced industrially due to the versatility of their structures and the fact that they display desirable properties. However, there are some drawbacks associated with these materials such as poor toughness properties, poor shelf life, and production of byproducts during their process of polymerization that requires, in many cases, the use of a strong acid or base catalyst to cure [1]. In the search for higher performance replacements

for phenolic resins many materials have received attention, and published reports of the preparation of aromatic oxazines, or benzoxazines, date back some 60 years [2]. Although commercial exploitation of the corresponding polymers has only come about relatively recently, they are now receiving a great deal of academic and industrial interest [3]. Polybenzoxazines have many advantageous characteristics compared with the traditional phenolic resins, such as high thermal stability, excellent mechanical properties and easy processability.

Over the last years, rigid polymer foams are gaining interest as core materials for sandwich structures in aerospace, naval and automotive and other commercial applications due to their higher energy absorption capabilities, especially in the event of impact loading. Among them, phenolic foams exhibit low thermal conductivity, exceptional fire-resistant properties, high thermal stability over a broad range of temperatures and low cost [4]. However, structural applications of phenolic foams have been limited due to the friable and brittle nature of these foams. Regarding to the study of polybenzoxazine foams, limited work has been done, most referred to bisphenol A-based benzoxazine [5-8]. It is recently reported a rigid phenolic foam from a renewable diphenolic acid-based benzoxazine [9], and also their phosphorus-containing flame retardant counterparts [10]. In this last work, it was studied the effect of curing conditions and type of phosphorus additive on density, cellular structure, thermal stability and flammability of the foams.

The structural response of polymeric foams strongly depends on the foam density, microstructure, such as cell size, shape, type (open or closed) and solid polymer properties [11]. So, it is a challenge to model the foam properties in function of the variables involved in the foaming process.

Different analytical tools have been employed to predict the elastic behavior of foams as a function of cell irregularity and relative density. An alternative approach to the mechanical modeling of foams involves the use of statistical methods. Statistical approaches greatly reduce the number of experimental iterations required when comparing to other modeling approaches while simultaneously yielding a wealth of information about multiple, interacting variables which influence the system. Some works have reported the use of statistical approaches to analyze the influence of material or formulation variables on the mechanical properties of reinforced epoxy foams [12] or phenolic foams [13-15].

The aim of the present work is to develop a statistical model describing the density (ρ), compressive modulus (E) and compressive strength (σ) of the previously reported phosphorus flame retardant polybenzoxazine foam [10], in terms of the foaming process variables: temperature and time. Glass transition temperature (Tg) and limiting oxygen index (LOI) values of the foam samples have also been considered.

An experimental design has been used to establish the simplest model that fit to the experimental data, following the response surface methodology (RSM) [16].

2. Experimental

2.1. Materials

The following chemicals were obtained from the sources indicated and used as received: paraformaldehyde (Probus) and 4,4´-bis(4-hydroxyphenyl)pentanoic acid (DPA) (Aldrich). 9,10-Dihydro-9-oxa-10-phosphaphenanthrene-10-oxide (DOPO) (Aismalibar S.A) was previously dehydrated at reduced pressure for 3 h/130 °C, 1 h/145 °C and 1h/160 °C. 1,3,5-Triphenylhexahydro-1,3,5-triazine, 9,10-dihydro-9-oxa-10-(1-hydroxy-1-methylethyl) phosphaphenanthrene-10-oxide (DOPO-2Me) and 4,4´-bis-[6-(3-phenyl-3,4-dihydro-2H-1,3-benzoxazine)]pentanoic acid (DPA-Bz) (Sceme 1) were synthesized according to reported procedures [10,17].

2.2. Crosslinking reaction

Appropriate amounts of DPA-Bz and DOPO-2Me were dissolved in dichloromethane. Solvent was removed from the solution by evaporation at 45 °C for 60 h and then at 140 °C for 10 min at reduced pressure. The amount of DOPO-2Me used was 15.6 wt.% of the total weight of the mixture which corresponds to a 1% P. Resin bars were obtained by transferring the mixture to a stainless steel mold (cavities dimensions: 1.5 cm x 1.5 cm x 7 cm) and compressing under a pressure of 135 bar using a hot press for 4 h at 140 ºC.

2.3. Foaming process

A sample of previously synthesized polymer was placed in a conventional oven and heated until selected foaming temperatures and times. The foaming conditions are shown in Table 1. In all the cases the initial foaming temperature (T_f) was 30 ºC and the heating rate was 2 °C/min. After the foaming process, the sample was allowed to cool slowly to room temperature. The surface was peeled off before analysis.

2.4. Instrumentation

Calorimetric studies were carried out at a scanning rate of 20 ºC/min using a Mettler DSC821e thermal analyzer and N_2 as a purge gas (100 ml/min). Thermal stability study was performed on a Mettler TGA/SDTA851e/LF/1100 using N_2 as a purge gas at a heating rate of 10 ºC/min

Polymer foam density was calculated by dividing the weight by the measured volume of rectangular shaped specimens of 1 cm x 2 cm x 2 cm. The density value was determined from the average of at least three measurements using different samples.

Mechanical properties were determined at 25 ºC using an Instron machine 3366 with a 100 N load cell. Rectangular samples with an average thickness of 1 cm and a cross-section area of ca. 4 cm^2 were compressed between two parallel steel plates using a crosshead speed of 1 cm/min. The compressive properties were determined from stress-strain curves of the average of at least three measurements using different samples.

LOI measurements were performed using a Stanton Redcroft FTA flammability unit provided with an Oxygen Analyzer. Three foamed samples of 1 cm x 1 cm x 10 cm were tested.

2.5. Model experimental set-up and procedure

The foaming process was studied in the experimental domain defined by the following ranges: from 170 ºC to 210 ºC for temperature, and from 1.5 h to 2.5 h for time. In terms of the experimental design, the highest and lowest values of each variable are respectively codified as (+1) and (-1).

The response surface methodology (RSM) was used to find the simplest model that allows predicting the response (y): density (ρ), compressive modulus (E) and compressive strength (σ), in function of temperature and time.

The first model postulate was given by Equation (1):

$$y = b_0 + b_1 x_1 + b_2 x_2 + b_{12} x_1 x_2 \quad (1)$$

where, b_i are the linear coefficients which describe the sensitivity of y response to the variations in the process variables (x_1 and x_2 refer to codified variables: temperature and time, respectively), and b_{12} is the crossproduct coefficient which enable to establish the first-order response surface.

Four experiments (1-4) in the conditions associated to a 2^2 factorial design were performed to calculate the coefficients. Also, three additional experiments (5-7) were carried out, in the conditions of midpoint of the range studied (Table 1), to evaluate the significance of the coefficients in the model, employing an ANOVA test [18].

To evaluate if this model fits to the experimental data, the sum of squares for pure quadratic curvature ($SS_{pure\ quadratic}$) are calculated as follows: (Equation 2)

$$SS_{purequadratic} = \frac{n_F n_C (\overline{y_F} - \overline{y_C})^2}{n_F + n_C} \quad (2)$$

where $\overline{y_F}$ is the average of the response of the experiments 1-4 and $\overline{y_C}$ is the average of the responses of the experiments 5-7, $n_F=4$ is the number of points in the factorial design and $n_C=3$ is the number of replicates at the midpoint.

The sum of squares for pure quadratic curvature ($SS_{pure\ quadratic}$) was compared with the $SS_{residual}$ obtained with the replicates of the midpoint by means of an F-test [16]. There is no quadratic curvature when both values are statistically comparable. If this does not occur, a second-order model was postulated by means of Equation 3:

$$y = b_0 + b_1 \cdot x_1 + b_2 \cdot x_2 + b_{12} \cdot x_1 x_2 + b_{11} \cdot x_1^2 + b_{22} \cdot x_2^2 \quad (3)$$

where b_{11} and b_{22} are the new coefficients that correspond to the quadratic terms that describe the curvature.

A common strategy for obtaining second-order response surfaces is to use a central composite design (CCD). This design locates the axial points on the centers of the faces of the previous full factorial design 2^2. In this work, four CCD (11 runs: 2^2 + 3 centre points + 4 star points) were performed to calculate the coefficients between a foam property and temperature and time. The experimental conditions that correspond to the CCD are collected in Table 2. Data processing was performed using statistical software/statgraphics.

3. Results and discussion

3.1. Preparation of the flame retardant foams

DPA-Bz and DOPO-2Me (Scheme 1) were prepared as previously described from renewable diphenolic acid (DPA) and DOPO respectively. DOPO-2Me has been proved as an effective phosphorus additive of DPA-Bz producing homogeneous mixtures and foams with relatively uniform closed cell structure and spheroid geometry [10]. Density, cell size and cell size distribution were found to strongly depend on the prepolymer preparation and the foaming process conditions. These structural parameters are governed by the foaming technology in processing and play an important role in determining the properties, which, in turn, dictate de foam's possible application [19]. As the most applications of rigid polymer foams are structural, the mechanical properties are a crucial parameter. So, establishing statistical models which allow accurately predict the final mechanical properties as a function of the foaming conditions is still a challenge nowadays.

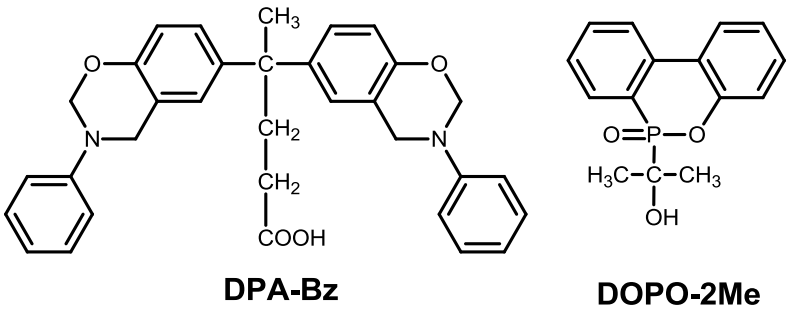

DPA-Bz **DOPO-2Me**

Scheme 1. Chemical structures of DPA-Bz and DOPO-2Me

Prepolymer was prepared by mixing appropriate amounts of DPA-Bz and DOPO-2Me to yield mixtures with 1% phosphorus content, and heating at 140 ºC for 4 h using a hot press. In this way, a rigid material with a Tg of 100 ºC was obtained. Samples of this prepolymer were self-foamed, by heating at different preset temperatures (170 ºC, 190 ºC and 210 ºC) and times (1.5, 2.0 and 2.5 h) following the conditions associated to a 2^2 factorial design. Temperature and time ranges were selected according to previous studies, [9] as well as to the results of dynamic and isothermal TGA experiments of the prepolymer material.

3.2. Foam density model

Table 1 shows the measured density values for the four foamed samples (runs 1-4) obtained in the conditions designed according to the 2^2 experimental design. As can be observed the foam density decreases as the temperature increases, independently of the considered time. Moreover, a slight diminution occurs when time is increased. These variations are similar to those observed for the three replicates, done in the conditions of the midpoint of the experimental domain (runs 5-7), which can be considered representative of the experimental error. So, it appears to be that time, as foaming variable, does not influence on the foam density. However, a deeper analysis of the results allows detecting that the time has some effect, as the difference in the foam density of experiences 1 and 2 (d = -22) is higher than the one in experiences 3 and 4 (d = -13). Taking into account this fact, both foaming process variables were considered. The density values of the four foamed samples were linearly correlated with temperature and time values according to the Equation 1.

Table 1

Foaming conditions and characteristics of resulting foams

run	Temperature (ºC)	Time (h)	Density (kg/m^3)	*E* (kPa)
1	170	1.5	79	602
2	210	1.5	57	1553
3	170	2.5	74	1634
4	210	2.5	59	2059
Midpoint				
5	190	2	65	1496
6	190	2	70	1519
7	190	2	63	1389

The model for the foam density (ρ) is given by the following Equation 4:

$$\rho = 67.3 - 18.5 \cdot x_1 - 1.5 \cdot x_2 + 3.5 \cdot x_1 x_2 \quad (4)$$

As expected, coefficient (x_1) associated with temperature is higher than coefficient (x_2) associated with time, and the interaction coefficient of both variables ($x_1 x_2$) is slightly higher than time coefficient.

The difference between the density value predicted by this model for a sample obtained in the conditions of the midpoint of the experimental domain ($\rho_{predicted}$ = 67.3 kg/m^3) and the average of the density values of the experiments (5-7) (ρ = 66.5 kg/m^3), was statistically assessed by a F-test (see Equation 2). The calculated F was 0.05 and the $F_{(7,\ 2,\ 0.05,\ 2\ tails)}$ tabulated was 19.35. So, it could be concluded that quadratic curvature does not exist and therefore a first order model fits to foam density in the considered range.

The model for the density value in function of the temperature (T) and the time (t) is given by the Equation 5:

$$\rho = 224.63 - 0.81 \cdot T - 34.75 \cdot t + 0.18 \cdot T \cdot t \quad (5)$$

Fig. 1 shows the contour map of the foam densities predicted by the model. Foaming temperature had a greater influence on density of the flame retardant foams than foaming time, being specifically over 200 ºC. As above mentioned, foams with higher densities should be obtained at lower temperatures. This behavior is in accordance to our previous study on neat polybenzoxazine foams [9].

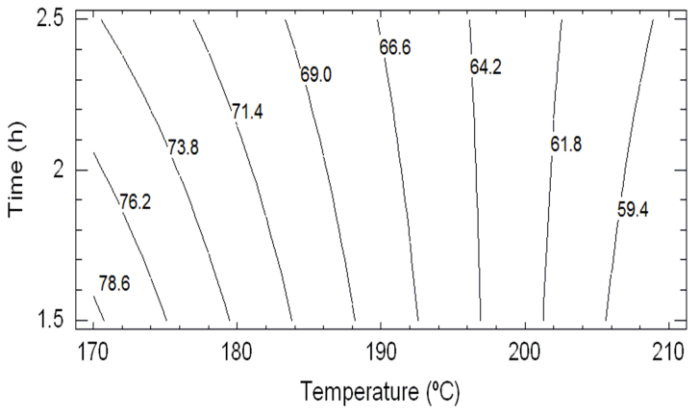

Fig. 1. Contour map for foam density (kg/m^3)

It was found that density showed a great dependence on the foaming temperature (T_f), decreasing as the temperature increases. In addition, dependence of polybenzoxazine/gas mixture Tg and T_f was observed on the foam porosity. Both variables were inter-related between themselves determining that an increase in foaming temperature produces a decreasing in the polybenzoxazine/gas mixture Tg which leads to higher cells growth and therefore lower density. In reference to foaming time (t_f), our results indicated that most of the CO_2 releases during the first 90 min. From that point on foaming proceeds in a slower way and therefore longer times not significantly affect foam density.

3.3. Foam compressive modulus model

The column 5 of Table 1 shows the measured values of the foam compressive modulus obtained in the experiments 1-7. Following the same strategy discussed for the density, the relation between the compressive modulus and the temperature and time is verified to fit also to a first order model.

Both variables exhibit a *P*-values <0.05 in the ANOVA analysis (results not shown) indicating that temperature and time have significant influence on the compressive modulus of the foams.

The model for the compressive modulus (E) is given by the following Equation 6:

$$E = -8338.43 + 43.5 \cdot T + 3267.5 \cdot t - 13.15 \cdot T \cdot t \quad (6)$$

Fig. 2 shows the contour map for compressive modulus of the foams. Both T_f and t_f exhibit similar influence on the compressive modulus of the polybenzoxazine foams. It is possible to observe that higher values of E should be obtained when the foaming process takes place at higher temperatures and times. The optimum value predicted by the model for E is 2061.6 kPa at 210 ºC and 2.5 h.

The mechanical properties of foams depend on their structure, the properties of the solid material of which the cells are made and the factors related to the test. The solid material mainly determines the Young's modulus, the yield strength and the fracture strength [11]. To relate and evaluate the relation between morphology and properties of the foams is important to

consider some cellular structure parameters such as the size and shape of the cells, apparent density, type of cells (open or closed cells), isotropic or anisotropic structure, cell distribution and cell wall thickness [20]. In turn, foam properties are also affected by the test characteristics *i.e.,* rate of strain, rate of deformation, temperature, sample conditioning, among the most important. Regarding to solid material factors, foam theory states that the compressive properties are directly proportional to their relative density, that is, *E* and σ increase with the relative density fitting a mathematical equation in which the fitting constants vary according to the type of foam and the cellular structure [11].

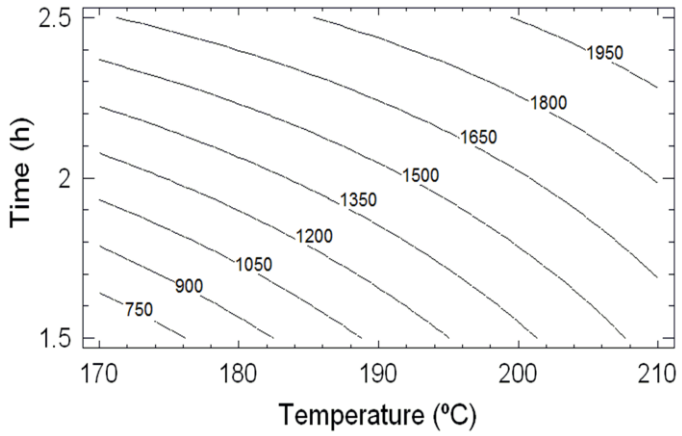

Fig. 2. Contour map for foam compressive modulus (kPa)

In this case, the polybenzoxazine foams followed a completely different trend, given that the compressive modulus increases as the foam density decreases. As also determined in the previous reported neat foams, T_f and t_f are significant parameters that control the foam morphology and the final foam properties because the foaming and crosslinking processes occur simultaneously. At the beginning, the CO_2 formation and ring-opening of the oxazine groups start at the same time and proceed in a fast way. Once all the CO_2 is released, the formed resin continues curing until the selected t_f. At this point, the network reaches a certain degree of crosslinking that is clearly dependent on t_f. Hence, an increase in the T_f and t_f, results in a higher crosslinking degree of the resin and consequently in higher compressive properties.

Surprisingly, the crosslinking degree of the base polymer had a greater influence on the compressive modulus than the cellular structure of the foam. As observed in Fig. 2, the compressive modulus continually increases with time and temperature. Thus, the main effect that influences the modulus of the foam is the degree of crosslinking, and the variation in T_f and t_f are the main causes. To gain more insight about the crosslinking degree of the foams, their glass transition temperature (Tg) were determined by DSC and their resulting values are summarized in Table 2. In general, the Tg of the foams increases as T_f and t_f increases too, and the difference of Tg values becomes more significant at higher temperatures. For instance, at 210 ºC the Tg of the sample foamed (run 2) at 1.5 h is 187 ºC while the Tg of the sample foamed (run 4) at 2.5 h is 213 ºC. These results indicate that at lower T_f and t_f the obtained foams are not totally crosslinked or the achieved crosslinking degree is lower. For higher T_f and t_f the crosslinking gradually rises up to reach almost fully crosslinked materials.

Table 2

Tg and LOI values of polybenzoxazine foams

Run	Tg (ºC)	LOI (% O_2)
1	150	28.1
2	187	31.2
3	159	28.4
4	213	31.4
5	179	29.1
8	140	29.4
9	248	31.9
10	166	28.5
11	184	29.8

3.4. Foam compressive strength model

In this case, to correlate the compressive strength of the foams (σ) with the foaming temperature and time it was necessary to postulate a model of second order as the indicated in Equation 3. To evaluate the coefficients, four additional experiments were carried out to complete the central composite design (2^2 + 3 center point + 4 star points). The results of the compressive strength of the foams and the experimental design are included in the Table 3.

Table 3

Central composite design, along with the compressive strength values for the foams

Run	Temperature (ºC)	Time (h)	σ (kPa)
1	170	1.5	95.9
2	210	1.5	186.1
3	170	2.5	187.7
4	210	2.5	210.2
5	190	2	199.5
6	190	2	193.0
7	190	2	203.4
8	150	2	210.6
9	230	2	246.9
10	190	1	115.1
11	190	3	206.5

The model for the foam compressive strength with all significant effects is given by the Equation 7:

$$\sigma = -553.95 + 1.03 \cdot T + 504.84 \cdot t - 110.89 \cdot t^2 \quad (7)$$

The temperature quadratic term (T^2) and the interaction temperature·time term ($T \cdot t$) were rejected because they presented P-values > 0.05 in the ANOVA analysis. Fig. 3 shows the contour map for compressive strength of the foams. It is possible to observe that higher values of the compressive strength (σ) should be obtained when the foaming process has place at higher temperatures and times. Both T_f and t_f had similar influence on the σ until *ca.* 2.1 h. From that, the variations on σ values seem to be somewhat affected by t_f. The optimum value predicted by the model for the σ is 244.4 kPa at 219 ºC and 2.3 h. Implementing this statistical approach with ANOVA revealed the influence of foaming parameters on the foam properties.

Again, it was detected a similar trend for the compressive strength to that presented by the compressive modulus of the foams. The highest values of compressive strength correspond with the highest crosslinking degrees, but not with the highest densities. As already discussed, the influence of the crosslinking degree was more meaningful in establishing the compressive strength of the foams than a variation in cellular structure.

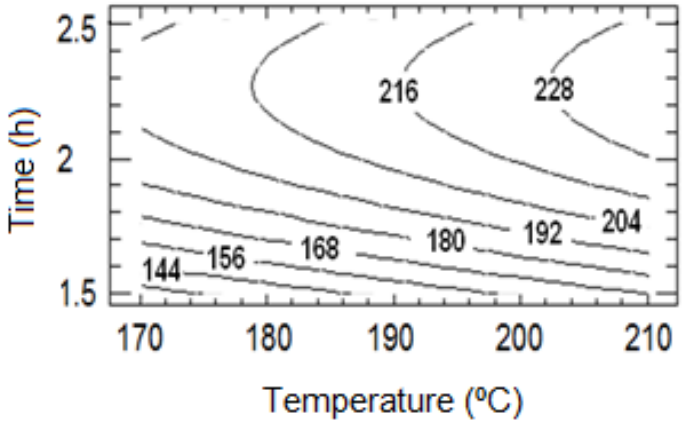

Fig. 3. Contour map for foam compressive strength (kPa)

3.5. Flame retardant properties

Flammability of polybenzoxazine foams with the same phosphorus content of 1% P, was assessed by the limiting oxygen index (LOI) test. The results have been collected in Table 2. The addition of DOPO-2Me to polybenzoxazine foams had a positive impact on their flammability since the LOI values were found to be ranging from 28.1 to 31.9. These values are higher than those for similar neat polybenzoxazine foams previously reported of 23.6 [10]. Such flammability improvement is result of the excellent flame retardant effect of the phosphorus compound that on burning forms a glass like polyphosphoric layer that promotes the formation a protecting char during combustion [21]. As the LOI values did not undergo significant differences, the statistical model is not worth considering.

Usually the LOI is a characteristic of the polymeric material, however it has been reported that for foamed materials the determination of the LOI not only depends on the test characteristics and the environment factors but also on sample density and structure [22]. In this way, LOI value increases with the density. In our case the LOI values of the polybenzoxazine foams were found to be more dependent on a change in the degree of crosslinking than on density, with the exception of the foam sample with the highest density (88.9 kg/m^3). Thus the highest recorded LOI values correspond to the highest foaming times and temperatures, which in turn are related to the highest degrees of crosslinking of the foams.

4. Conclusions

Polybenzoxazine foams based on the renewable diphenolic acid and an organophosphorus compound were prepared. Thermal polymerization provided not only crosslinking but also the *in-situ* generation of the blowing agent. A statistical design approach was employed to establish the influence of the foaming parameters on the density, compressive strength and compressive modulus of the foams. The density and the compressive modulus were well fitted to a simple linear model, while the compressive strength required a model of second order. Moreover, it was found that the crosslinking degree of the base polymer exerted a greater influence on the mechanical performance of the foams than the cellular structure.

Tg of the foams was significant influenced by the crosslinking degree of the polybenzoxazines, which in turn especially varied with the foaming temperature. The addition of the organophosphorus compound conferred flame retardancy to all the materials.

The obtained results demonstrate the possibility of producing and simulating flame retardant polybenzoxazine foams with good mechanical properties.

Acknowledgements

The authors express their thanks to CICYT (Comisión Interministerial de Ciencia y Tecnología) (MAT2011-24823) for financial support for this work and to Dr. Miguel Ángel López Manchado for mechanical measurements.

References

[1] M.A Espinosa, M. Galià, V. Cádiz. Novel phosphorilated flame retardant thermosets: epoxy–benzoxazine–novolac systems. Polymer 2004;45(18):6103.

[2] F.W Holly, A.C Cope. Condensation products of aldehydes and ketones with o-aminobenzyl alcohol and o-hydroxybenzylamine. J Am Chem Soc 1944;66(11):1875.

[3] H. Ishida, T. Agag. Handbook of benzoxazine Resins. Elsevier. 2011.

[4] P.T Kelly. Phenolic foams. In: Klempner D, Sendijarevic V, editors. Handbook of polymeric foams and foam technology. 2nd ed. Carl Hanser Verlag. Munich, 2004. p. 447-56.

[5] M. Ardanuy, M.Á Rodríguez-Pérez, J.A de Saja, J.I Velasco. Foaming behavior, cellular structure and physical properties of polybenzoxazine foams. Polym Adv Technol 2012;23(5):841.

[6] P. Lorjai, S. Wongkasemjit, T. Chaisuwan. Preparation of polybenzoxazine foam and its transformation to carbon foam. Mater Sci Eng, A 2009;527(1-2):77.

[7] K.S Santhosh Kumar, C.P Reghunadhan Nair, K.N Ninan. Silica fiber–polybenzoxazine–syntactic foams; Processing and properties. J Appl Polym Sci 2008;107(2):1091.

[8] K.S Santhosh Kumar, C.P Reghunadhan Nair, K.N Ninan. Mechanical properties of polybenzoxazine syntactic foams. J Appl Polym Sci 2008;108(2):1021.

[9] C. Zúñiga, G. Lligadas, J.C Ronda, M. Galià, V. Cádiz. Self-foaming diphenolic acid benzoxazine. Polymer 2012;53(15):3089.

[10] C. Zúñiga, G. Lligadas, J.C Ronda, M. Galià, V. Cádiz. Phosphorus flame retardant polybenzoxazine foams based on renewable diphenolic acid. Polym Degrad Stab 2013. In press. DOI:10.1016/j.polymdegradstab.2013.09.023

[11] L.J Gibson, M.F Ashby. Cellular solids: structure and properties. 2nd ed. Cambridge University Press. 1997.

[12] M.V Alonso, M.L Auad, S.R Nutt. Modeling the compressive properties of glass fiber reinforced epoxy foam using the analysis of variance approach. Compos Sci Technol. 2006;66(13):2126.

[13] B. Del Saz-Orozco, M. Oliet, M.V Alonso, E. Rojo, F. Rodríguez. Formulation optimization of unreinforced and lignin nanoparticle-reinforced phenolic foams using an analysis of variance approach. Compos Sci Technol 2012;72(6):667.

[14] A. Desai, S.R Nutt, M.V Alonso. Modeling of Fiber-reinforced Phenolic Foam. J Cell Plast 2008;44(5):391.

[15] A. Desai, S.R Nutt, M.V Alonso. Modeling of Hybrid Composite Foams. J Cell Plast 2010;46(2):113.

[16] D.C Montgomery. Design and analysis of experiments. John Wiley & Sons. 1997.

[17] C. Zúñiga, M.S Larrechi, G. Lligadas, J.C Ronda, M. Galià, V. Cádiz. Polybenzoxazines from renewable diphenolic acid. J Polym Sci, Part A: Polym Chem 2011;49(5):1219.

[18] D.L Massart, B.G M Vandeginste, L.M C Buydens, S.D Jong, P.J Lewi, J. Smeyers-Verbeke. Handbook of chemometrics and qualimetrics: Part A. Elsevier. 1997.

[19] S.T Lee, C.B Park, N.S Ramesh. Polymeric foams: Science and technology. Taylor & Francis. 2007.

[20] F. Shutov. Foamed polymers. Cellular structure and properties. In: Industrial Developments. Springer Berlin Heidelberg. Berlin, 1983. p. 155-218.

[21] S.Y Lu, I. Hamerton. Recent developments in the chemistry of halogen-free flame retardant polymers. Prog Polym Sci 2002;27(8):1661.

[22] A.R Horrocks, D. Price, N.L Edwards. The burning behaviour of combustion modified high resilience polyurethane foams. J Fire Sci 1992;10(1):28.

CHAPTER 4

MULTI WALLED CARBON NANOTUBES/ POLYBENZOXAZINE NANOCOMPOSITES

4.1. INTRODUCTION

In recent years, carbon nanotubes (CNT) have attracted a great interest in the field of polymer nanocomposites owing to they have clearly demonstrated their capability as reinforced fillers thanks to their exceptional mechanical, electrical and thermal properties. A large amount of work has been carried out worldwide to try solving the problems immersed in the development of the truly perfect nanotube/polymer composite that is theorized. Nonetheless, it is clear that some materials already developed have shown promising performance for applications including supercapacitors, actuators and lightweight electromagnetic shields.

This chapter explores the use of multi walled carbon nanotubes as nanoadditives in two different polybenzoxazines. The effect of the nanotubes on rheological, electrical, thermal, dynamo-mechanical and flammability properties of the resulting material has been assessed.

4.2. CARBON NANOTUBES

Graphite and diamond are two typical allotropic forms[a] of carbon; nonetheless, today is necessary to recognize two new forms, fullerenes (C_{60}) and carbon nanotubes (CNT). Discovered in 1985 by Harold Kroto et al[1] fullerenes have set off a wave of numerous studies by chemists, physicists and materials scientists around the world. Six years later Sumio Iijima[2] reported for its first time microtubular carbon structures that later were better known as carbon nanotubes.

CNT can be visualized as a hollow cylinder formed exclusively of covalently bonded carbon atoms that may or may not be capped by pentagonal carbon rings (**Figure 1**). Their length ranges from few nanometers to thousands of micrometers and their diameter between 0.8 and 100 nm.

There exist two main types of CNT depending on the number of walls that they possess. Single walled carbon nanotubes (SWNT) consist of a hollow cylinder of a graphite sheet. They are often seen as straight or elastic bending structures individually or in ropes[3]. Multi walled carbon nanotubes (MWNT)

[a] Structures with different physical properties, but constituted of the same element.

comprise a group of coaxial SWNT arranged around a central hollow core with an interlayer spacing of 0.34 nm (close to the distance between graphene layers in graphite)[4].

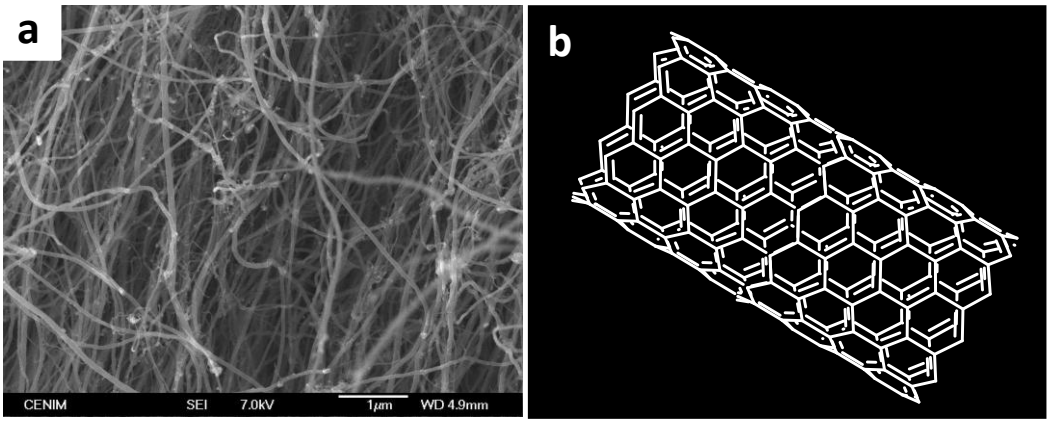

Figure 1. Types of CNT. a) Scanning electron microscope image of MWNT grown by chemical vapor deposition and b) schematic image of a SWNT with zigzag chirality

CNT can be produced using a wide variety of processes such as arc-discharge, pyrolysis of hydrocarbons over metal particles, laser vaporization of graphite targets, solar carbon vaporization, and electrolysis of carbon electrodes in molten ionic salts[5]. Within them, chemical vapor deposition (CVD) is the dominant mode of high-volume CNT production and typically uses fluidized bed reactors that enable uniform gas diffusion and heat transfer to metal catalyst nanoparticles. Currently, bulk purified MWNTs are sold for less than $100 per kg, which is 1- to 10-fold greater than commercially available carbon fiber[6].

CNT are characterized by having extraordinary properties that vary according to their type. As regards the mechanical properties, theoretical and experimental studies have reported Young`s modulus values between 1.0 TPa and 1.1-1.3 TPa for SWNT and MWNT[3] respectively, when considering the cross-sectional area of the CNT walls only. Their electrical properties strongly depend on their structure. For SWNT, they are determined by their diameter and chirality[b] and can be classified either metallic or semiconducting[7]. MWNT can also behave as metallic or semiconducting as the outermost tube is the dominant in their structure. Their thermal properties are determined by atomic vibrations of phonons along the CNT axis. Measurements of thermal conductivity have shown

[b] The manner in which the single sheet of hexagonally arrayed carbon atoms is wound

a strong dependence on the sample quality and alignment and have reported values above 200 W/mK for aligned SWNT[8], 3500 W/mK for individual SWNT[9] and >3000 W/mK for individual MWNT[10].

Many companies[11-13] are investing in diverse applications of CNT such as transparent conductors, thermal interfaces, antiballistic vests and wind turbine blades. Likewise, their use has also been spreading in coating paints[14], thin-film transistors[15], lithium ion batteries for notebook computers and mobile phones[16], fuel cells[17], water purification systems[18] and toxin detection sensors[19] among many others[6].

4.3. POLYMER NANOCOMPOSITES

In a confusing manner the term "nanocomposite" has been used extensively in the literature. A better and far more restrictive definition would require that a true nanocomposite should be a fundamentally new material in which the nanometer-scale component or structure gives rise to intrinsically new properties, which are not present in the respective macroscopic composites or the pure components[20].

The above-mentioned properties make CNT potential filling materials in polymer composites because the properties of the resulting composites are frequently tuned and altered by a synergistic effect. The properties of the nanotube/polymer nanocomposites vary significantly depending on the distribution of the type, diameter, aspect ratio, alignment and length of the CNT[21].

Besides the poor dispersion of CNT, because of their tendency to form agglomerates, the lack of interfacial adhesion between CNT and polymeric matrices is also a key factor to render an effective reinforcement in high performance polymer nanocomposites. The chemical functionalization of CNT[22,23] has been contemplated as a possible solution of the above-mentioned obstacles due to it permits to improve the dispersions of CNT and also enhance the compatibility between matrix and filler. On occasions, this modification entails some constraints such as the deterioration of the CNT walls and therefore the foreseen properties are affected. Another additional drawback is that their synthesis may require several steps.

4.3.1. Fabrication methods of carbon nanotube/polymer nanocomposites

There are mainly three methods used in the preparation of CNT/polymer nanocomposites applicable to thermoplastic and thermosetting polymer matrices, which are: solution mixing, melt blending and *in situ* polymerization.

Solution mixing is the most common and the simplest method because it is manageable to small sizes and also effective. This method involves the dispersion of CNT in a solvent (suitable and common for the polymer), mixing the solution of the polymer with the CNT dispersion, and then evaporating the solvent in a controlled way[24]. These three major steps are used in order to minimize the rupture of CNT.

Melt blending lies in disperse CNT in a polymer matrix at high temperature and high shear forces using traditional melt processing techniques. In comparison with the solution mixing method is: i) generally less effective at dispersing nanotubes in polymers, ii) limited to lower concentrations, iii) environmentally-friendly (due to the absence of solvents) and iv) the most compatible with industrial practices[21]. Most of the reported examples deal with thermoplastic polymers[25,26].

In situ polymerization is a very versatile method that uses the monomer rather than the polymer as a starting material. In this method a covalent bonding between the functionalized CNT and the polymer matrix is generated through diverse reactions. Usually, the nanoadditives are dispersed in the monomer (pure or dissolved) prior to the polymerization step. As the polymerization progresses the viscosity of the reaction medium increases, and the extent of *in situ* polymerizations might be limited[21]. Some examples include the use of MWNT in epoxy resins[27] and poly(methyl methacrylate)[28].

4.3.2. Properties of carbon nanotube/polymer nanocomposites

Most of the studies on the preparation of CNT/polymer nanocomposites have been centered on the study on mechanical and electric properties of the materials, whereas others have evaluated their flammability, thermal conductivity, thermal stability and rheological properties.

The incorporation of CNT into a matrix has presented a number of special challenges in the mechanical properties. One important requisite for achieving good results is the enhancement of the interface between filler and matrix to possibility the transfer external tensile loads to the CNT. Thus, for example

SWNT/PVA fibers have reached Young's modulus of up to 80 MPa and tensile strengths of 1.8 GPa suggesting applications such as bullet-proof vests[29]. Other study reported excellent results for SWNT/nylon composites. The incorporation of 2 wt% SWNT notably improved the elastic modulus in 214% and the yield strength in 162%[30].

Electrical properties of carbon nanotube/polymer composites have been studied from two distinct approaches. The first involves the addition of CNT to conducting polymers[31,32] while the second lies in conferring conductivity of non-conducting polymers[33,34]. The later have found applications as static electrical discharge, electromagnetic-radio frequency interference protection and static electrical dissipation for some aircraft component, computer housings and exterior automotive parts[24].

4.4. CARBON-BASED/POLYBENZOXAZINE NANOCOMPOSITES

To date, various studies on the preparation and characterization of polybenzoxazine carbon-based nanocomposites have been carried out using several benzoxazine monomers[35-39] together with epoxy[40-42] or epoxy-phenolic copolymers[43] (**Figure 2**). As carbon-based nanofillers, pure[39,44], functionalized[37-39,42,43,45] and surfactant treated MWNT[40] as well as modified graphene[35,36] have been used as carbon-based nanofillers.

The majority of the carbon-based/polybenzoxazine nanocomposites were prepared using a solvent-based method in which prior to the polymerization step the nanofillers were dispersed in an organic solvent with the aim to improve their dispersion into the monomer. Other environmentally-friendly approaches have been dealt with the dispersion of the nanofillers directly in the melt monomer or by using a liquid epoxy before the polymerization step.

These works have been centered on the study of the thermal (curing behavior), thermal mechanical (coefficient of thermal expansion, CTE), dynamomechanical, morphological, mechanical (flexural strength and impact fracture toughness) and electrical properties. Most remarkable results of the polybenzoxazine nanocomposites include: i) the preparation of superhydrophobic materials[44]; ii) fabrication of electrically-conductive resins (7×10^{-5} S/cm with 2.5% MWNT-FBz)[37]; iii) enhancement on the thermal stability (increment of degradation temperature at 10% and 50% weight loss by 33 ºC and 75 ºC) and

a reduction of CTE up to 48%[36]; iv) improvements in toughness and flexural strength by 160% and 30% respectively[43]; v) decrease in the polymerization temperature due to a catalytic effect of the functionalized nanofillers[35, 45] and vi) an improvement on the storage modulus in 285% and the glass transition temperature in 12 ºC[45].

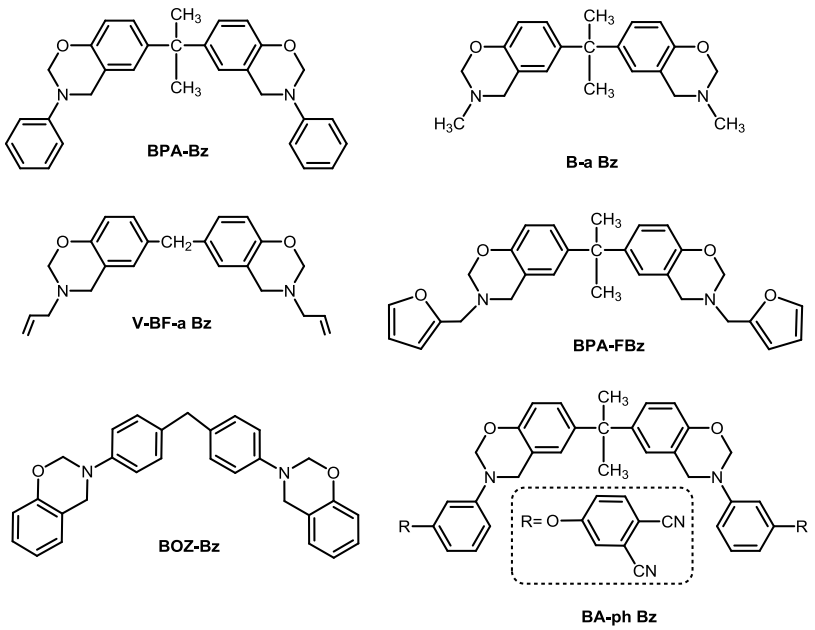

Figure 2. Chemical structure of different benzoxazine monomers used as matrices in the preparation of polybenzoxazine nanocomposites

These composite materials are expected to find potential applications like molding compounds, adhesives in microelectronics[40],metal-like electrically conductive materials[37], superhydrophobic coatings[44] where improvements in thermal stability, hydrophobicity and electrical conductivity are required and expected.

4.5. OBJECTIVES

The main objective of the work described in this chapter is to develop novel polybenzoxazine nanocomposites with high value added from two benzoxazines: bisphenol A-based benzoxazine, ester of diphenolic acid derivative benzoxazine and carbon nanotubes. To fulfill this objective it is necessary to evaluate the

properties of the polybenzoxazine composites in relation to the amount of nanotubes and the characteristics of matrices.

4.6. EXPERIMENTAL PROCEDURES AND RESULTS

The work described in section 4.6.1 has been submitted to *Journal of Materials Chemistry A*. It contemplates the use of MWNT as nanoadditives in two different polybenzoxazines. The nanocomposites were prepared by a solventless method varying the MWNT amount from 0.1 wt% to 1.0 wt%. The characterization of the resulting materials was performed in terms of the rheological, electrical, thermo-mechanical and thermal properties. Moreover the distribution of the fillers within both polybenzoxazines was observed using a transmission electron microscope.

REFERENCES

1. Kroto, H. W.; Heath, J. R.; O'Brien, S. C.; Curl, R. F.; Smalley, R. E., C60: Buckminsterfullerene. *Nature* **1985,** 318, (6042), 162-163.
2. Iijima, S., Helical microtubules of graphitic carbon. *Nature* **1991,** 354, (6348), 56-58.
3. Han, J., Structures and Properties of Carbon Nanotubes. In *Carbon Nanotubes: Science and Applications*, Meyyappan, M., Ed. CRC Press: Boca Raton, 2004; pp 1-24.
4. Awasthi, K.; Srivastava, A.; Srivastava, O. N., Synthesis of carbon nanotubes. *J. Nanosci. Nanotechnol.* **2005,** 5, (10), 1616-1636.
5. Terrones, M., SCIENCE AND TECHNOLOGY OF THE TWENTY-FIRST CENTURY: Synthesis, properties, and applications of carbon nanotubes. *Annu. Rev. Mater. Res.* **2003,** 33, (1), 419-501.
6. De Volder, M. F. L.; Tawfick, S. H.; Baughman, R. H.; Hart, A. J., Carbon nanotubes: present and future commercial applications. *Science* **2013,** 339, (6119), 535-539.
7. Subramoney, S., Carbon Nanotubes. In *Encyclopedia of Materials: Science and Technology (Second Edition)*, Editors-in-Chief: , K. H. J. B.; Robert, W. C.; Merton, C. F.; Bernard, I.; Edward, J. K.; Subhash, M.; Patrick, V., Eds. Elsevier: Oxford, 2006; pp 1-8.
8. Hone, J.; Llaguno, M. C.; Nemes, N. M.; Johnson, A. T.; Fischer, J. E.; Walters, D. A.; Casavant, M. J.; Schmidt, J.; Smalley, R. E., Electrical and thermal transport properties of magnetically aligned single wall carbon nanotube films. *Appl. Phys. Lett.* **2000,** 77, (5), 666-668.
9. Pop, E.; Mann, D.; Wang, Q.; Goodson, K.; Dai, H., Thermal conductance of an individual single-wall carbon nanotube above room temperature. *Nano Lett.* **2005,** 6, (1), 96-100.
10. Small, J. P.; Shi, L.; Kim, P., Mesoscopic thermal and thermoelectric measurements of individual carbon nanotubes. *Solid State Commun.* **2003,** 127, (2), 181-186.
11. ANS Carbon Nanostructure Fibers Boost NASA Spacecraft. http://www.appliednanostructuredsolutions.com/archives/4. (10/07/2013).
12. BASF Keeping sparks at bay. www.basf.com. (10/07/2013).
13. Seldon-Technologies Products: built on nanomesh. http://seldontechnologies.com/products/ (10/07/2013).

14. Beigbeder, A.; Degee, P.; Conlan, S. L.; Mutton, R. J.; Clare, A. S.; Pettitt, M. E.; Callow, M. E.; Callow, J. A.; Dubois, P., Preparation and characterisation of silicone-based coatings filled with carbon nanotubes and natural sepiolite and their application as marine fouling-release coatings. *Biofouling* **2008,** 24, (4), 291-302.
15. Sun, D.-m.; Timmermans, M. Y.; Tian, Y.; Nasibulin, A. G.; Kauppinen, E. I.; Kishimoto, S.; Mizutani, T.; Ohno, Y., Flexible high-performance carbon nanotube integrated circuits. *Nat Nano* **2011,** 6, (3), 156-161.
16. Dai, L.; Chang, D. W.; Baek, J.-B.; Lu, W., Carbon Nanomaterials for Advanced Energy Conversion and Storage. *Small* **2012,** 8, (8), 1130-1166.
17. Le Goff, A.; Artero, V.; Jousselme, B.; Tran, P. D.; Guillet, N.; Métayé, R.; Fihri, A.; Palacin, S.; Fontecave, M., From hydrogenases to noble metal–free catalytic nanomaterials for H_2 production and uptake. *Science* **2009,** 326, (5958), 1384-1387.
18. Holt, J. K.; Park, H. G.; Wang, Y.; Stadermann, M.; Artyukhin, A. B.; Grigoropoulos, C. P.; Noy, A.; Bakajin, O., Fast mass transport through sub-2-nanometer carbon nanotubes. *Science* **2006,** 312, (5776), 1034-1037.
19. Esser, B.; Schnorr, J. M.; Swager, T. M., Selective detection of ethylene gas using carbon nanotube-based devices: Utility in determination of fruit ripeness. *Angew. Chem. Int. Ed.* **2012,** 51, (23), 5752-5756.
20. Manias, E.; Polizos, G.; Nakajima, H.; Heidecker, M. J., Fundamentals of Polymer Nanocomposite Technology. In *Flame Retardant Polymer Nanocomposites*, John Wiley & Sons, Inc.: 2006; pp 31-66.
21. Moniruzzaman, M.; Winey, K. I., Polymer nanocomposites containing carbon nanotubes. *Macromolecules* **2006,** 39, (16), 5194-5205.
22. Balasubramanian, K.; Burghard, M., Chemically functionalized carbon nanotubes. *Small* **2005,** 1, (2), 180-192.
23. Tasis, D.; Tagmatarchis, N.; Bianco, A.; Prato, M., Chemistry of carbon nanotubes. *Chem. Rev.* **2006,** 106, (3), 1105-1136.
24. Harris, P. J. F., *Carbon Nanotube Science Synthesis, Properties and Applications*. Cambridge University press: New York, 2009; pp 227-246.
25. Manchado, M. A. L.; Valentini, L.; Biagiotti, J.; Kenny, J. M., Thermal and mechanical properties of single-walled carbon nanotubes–polypropylene composites prepared by melt processing. *Carbon* **2005,** 43, (7), 1499-1505.
26. Haggenmueller, R.; Gommans, H. H.; Rinzler, A. G.; Fischer, J. E.; Winey, K. I., Aligned single-wall carbon nanotubes in composites by melt processing methods. *Chem. Phys. Lett.* **2000,** 330, (3–4), 219-225.
27. Abdalla, M.; Dean, D.; Robinson, P.; Nyairo, E., Cure behavior of epoxy/MWCNT nanocomposites: The effect of nanotube surface modification. *Polymer* **2008,** 49, (15), 3310-3317.
28. Jia, Z.; Wang, Z.; Xu, C.; Liang, J.; Wei, B.; Wu, D.; Zhu, S., Study on poly(methyl methacrylate)/carbon nanotube composites. *Mater. Sci. Eng., A* **1999,** 271, (1–2), 395-400.
29. Dalton, A. B.; Collins, S.; Muñoz, E.; Razal, J. M.; Ebron, V. H.; Ferraris, J. P.; Coleman, J. N.; Kim, B. G.; Baughman, R. H., Super-tough carbon-nanotube fibres. *Nature* **2003,** 423, (6941), 703-703.
30. Moniruzzaman, M.; Chattopadhyay, J.; Billups, W. E.; Winey, K. I., Tuning the mechanical properties of SWNT/Nylon 6,10 composites with flexible spacers at the interface. *Nano Lett.* **2007,** 7, (5), 1178–1185.
31. Cochet, M.; Maser, W. K.; Benito, A. M.; Callejas, M. A.; Martinez, M. T.; Benoit, J.-M.; Schreiber, J.; Chauvet, O., Synthesis of a new polyaniline/nanotube composite: *"in situ"* polymerisation and charge transfer through site-selective interaction. *Chem. Commun.* **2001**, (16), 1450-1451.
32. Ginic-Markovic, M.; Matisons, J. G.; Cervini, R.; Simon, G. P.; Fredericks, P. M., Synthesis of new polyaniline/nanotube composites using ultrasonically initiated emulsion polymerization. *Chem. Mater.* **2006,** 18, (26), 6258-6265.
33. Grunlan, J. C.; Mehrabi, A. R.; Bannon, M. V.; Bahr, J. L., Water-based single-walled-nanotube-filled polymer composite with an exceptionally low percolation threshold. *Adv. Mater.* **2004,** 16, (2), 150-153.

34. Maiti, S.; Suin, S.; Shrivastava, N. K.; Khatua, B. B., Low percolation threshold and high electrical conductivity in melt-blended polycarbonate/multiwall carbon nanotube nanocomposites in the presence of poly(ε-caprolactone). *Polym. Eng. Sci.* **2013,** doi: 10.1002/pen.23600.
35. Zeng, M.; Wang, J.; Li, R.; Liu, J.; Chen, W.; Xu, Q.; Gu, Y., The curing behavior and thermal property of graphene oxide/benzoxazine nanocomposites. *Polymer* **2013,** 54, (12), 3107-3116.
36. Ho, K.-K.; Hsiao, M.-C.; Chou, T.-Y.; Ma, C.-C. M.; Xie, X.-F.; Chiang, J.-C.; Yang, S.-h.; Chang, L.-H., Preparation and characterization of covalently functionalized graphene using vinyl-terminated benzoxazine monomer and associated nanocomposites with low coefficient of thermal expansion. *Polym. Int.* **2013,** 62, (6), 966-973.
37. Wang, Y.-H.; Chang, C.-M.; Liu, Y.-L., Benzoxazine-functionalized multi-walled carbon nanotubes for preparation of electrically-conductive polybenzoxazines. *Polymer* **2012,** 53, (1), 106-112.
38. Huang, J.-M.; Tsai, M.-F.; Yang, S.-J.; Chiu, W.-M., Preparation and thermal properties of multiwalled carbon nanotube/polybenzoxazine nanocomposites. *J. Appl. Polym. Sci.* **2011,** 122, (3), 1898-1904.
39. Liu, Y.; Wang, B.; Jing, X., Thermal properties of hyperbranched polyborate functionalized multiwall carbon nanotube/polybenzoxazine composites. *Polym. Compos.* **2011,** 32, (9), 1352-1361.
40. Kaleemullah, M.; Khan, S. U.; Kim, J.-K., Effect of surfactant treatment on thermal stability and mechanical properties of CNT/polybenzoxazine nanocomposites. *Compos. Sci. Technol.* **2012,** 72, (16), 1968-1976.
41. Chapartegui, M.; Barcena, J.; Irastorza, X.; Elizetxea, C.; Fiamegkou, E.; Kostopoulos, V.; Santamaria, A., Manufacturing, characterization and thermal conductivity of epoxy and benzoxazine multi-walled carbon nanotube buckypaper composites. *J. Compos. Mater.* **2012,** 47, (14), 1705-1715.
42. Xu, M.; Hu, J.; Zou, X.; Liu, M.; Dong, S.; zou, Y.; Liu, X., Mechanical and thermal enhancements of benzoxazine-based GF composite laminated by in situ reaction with carboxyl functionalized CNTs. *J. Appl. Polym. Sci.* **2013,** 129, (5), 2629-2637.
43. Yang, L.; Zhang, C.; Pilla, S.; Gong, S., Polybenzoxazine-core shell rubber–carbon nanotube nanocomposites. *Composites Part A* **2008,** 39, (10), 1653-1659.
44. Wang, C.-F.; Chen, H.-Y.; Kuo, S.-W.; Lai, Y.-S.; Yang, P.-F., Rapid, low temperature microwave synthesis of durable, superhydrophobic carbon nanotube-polybenzoxazine nanocomposites. *RSC Advances* **2013,** 3, (25), 9764-9769.
45. Chen, Q.; Xu, R.; Yu, D., Multiwalled carbon nanotube/polybenzoxazine nanocomposites: Preparation, characterization and properties. *Polymer* **2006,** 47, (22), 7711-7719.

4.6.1

CONVENIENT AND SOLVENTLESS PREPARATION OF NEAT CARBON NANOTUBES/POLYBENZOXAZINE NANOCOMPOSITES WITH LOW PERCOLATION THRESHOLD AND IMPROVED THERMAL AND FIRE PROPERTIES

Convenient and solventless preparation of neat carbon nanotubes/polybenzoxazine nanocomposites with low percolation threshold and improved thermal and fire properties

Camilo Zúñiga[a], Gerard Lligadas[a], Juan Carlos Ronda[a], Marina Galià[a], Virginia Cádiz[a], Leïla Bonnaud[b] and Philippe Dubois[b*]

[a] Departament de Química Analítica i Química Orgànica. Universitat Rovira i Virgili. Campus Sescelades. Marcel.lí Domingo s/n, 43007 Tarragona, Spain.
[b] Laboratory of Polymeric and Composite Materials, Center of Innovation and Research in Materials and Polymers (CIRMAP), Materia Nova Research Center & University of Mons, 23 Place du Parc, B-7000, Mons, Belgium.

Keywords: Benzoxazine, carbon nanotubes, nanocomposite, percolation threshold, electrical and thermal, fire properties

Abstract

This work contemplates the use of pristine multi walled carbon nanotubes (MWNTs) as nanofillers in the bisphenol A-based polybenzoxazine and a diphenolic acid derived polybenzoxazine. The materials were prepared by a solventless method varying the MWNTs amount from 0.1 to 1.0 wt%. MWNTs were found to disperse well within both benzoxazine monomers and their dispersion was preserved during the polymerization process. Rheological and electrical percolation thresholds were obtained for MWNTs concentrations lower than 0.1 wt% indicating the existence of good affinity between MWNTs and polybenzoxazine matrices. The incorporation of MWNTs became electrically conductive both materials. The characterization of the resulting nanocomposites revealed that MWNTs affected differently the polybenzoxazines. The limiting oxygen index of the nanocomposites increased as a function of the nanotube content, in 3.5% and 6.2% for BPA-PBz and MDP-PBz, respectively. Moreover, MWNTs positively influenced the thermo-mechanical, thermal and mechanical properties of the nanocomposites. The resulting attractive properties have been attributed to the good interactions between the polybenzoxazines and the finely dispersed nanofillers.

1 Introduction

Carbon nanotubes (CNTs) are considered of high interest for polymeric matrices not only for their excellent mechanical, thermal and electrical properties but also for their low density and high aspect ratio.[1] However, to exploit their maximum potential as reinforcing agents it is necessary to clear up some issues related to their poor dispersion, due to their tendency to form agglomerates, and a possible lack of interfacial adhesion between them and polymeric matrices. To solve these obstacles, chemical functionalization of CNTs has often been considered.[2, 3] On occasions, this modification entails some constraints such as the deterioration of the CNTs walls and therefore the foreseen properties are affected. Another additional drawback is that their synthesis may require several steps. One valuable tool to assess the dispersion quality of nanoparticle-filled polymers is rheology. By measuring the rheological parameters such as storage modulus, loss modulus and complex viscosity, it is possible to correlate with the filler dispersion, the inter-particle interaction and the polymer-filler interaction.[4]

CNTs have been used to improve the electrical properties of non-conducting polymers as an alternative to common fillers such as carbon blacks and carbon fibers.[5,6] According to the range of electrical conductivity exhibited by these nanocomposites, some applications include their use as electromagnetic interference (EMI)-shielding packages and wafer carriers for the microelectronics industry, electrostatic-assisted painting, fuel lines and filters that dissipate electrostatic charge in the automotive industry.[7]

Among the many polymeric materials, polybenzoxazines have attracted significant attention of both industry and research community because of their unique advantages[8] becoming one of a rare few new polymers commercialized in the past 30 years. Polybenzoxazines can overcome the drawbacks of conventional phenolic resin synthesis by eliminating the release of byproducts during the curing reactions, the need of strong acid as catalyst and for toxic raw materials while retaining good thermal properties and flame retardancy of phenolic resins.[9]

Polybenzoxazines with high flame retardant properties have gained attention owing to the increased demand for electronic materials.[10] Previous works on enhancement of the flammability properties of polybenzoxazines have been focused on the use mainly of phosphorus-,[11-13] silicon-,[14] and nitrogen-based[15] flame retardants. Most of them have been incorporated directly by

chemical grafting onto the monomer through chemical modification of the amine or phenol precursors involved in the polybenzoxazine synthesis. Few studies have explored the dispersion of flame retardant additives[16-18] and to our knowledge none has used carbon-based nanostructures.

The synthesis of bisphenol A-based benzoxazine (BPA-Bz) has been reported, and its polymerization yields thermosets with high structural integrity and thus the materials possess good properties. Unfortunately, bisphenol A (BPA) has shown to contribute significantly to an array of diseases and other health problems.[19] As a possible competitive alternative for BPA-Bz, it was proposed the synthesis of methyl 4,4´-bis-[6-(3-phenyl-3,4-dihydro-2H-1,3-benzoxazine)]pentanoate (MDP-Bz), actually a monomer based on the ester derivative (MDP) of the renewable diphenolic acid (DPA).[20] DPA is emerging as a potential "green" candidate to displace BPA because of its similar chemical structure, its lower price and because it has an extra functionality that can be involved for the polymer synthesis. In comparison with BPA-Bz, MDP-Bz has a higher glass transition temperature, a higher degradation temperature at 10% weight loss and superior thermo-mechanical properties.

Studies on the preparation and characterization of carbon-based/polybenzoxazine nanocomposites have been carried out using several benzoxazine monomers[21-25] and epoxy copolymers,[26-28] all of them, derived from non-renewable resources. As carbon-based nanofillers, pristine,[25,29] functionalized[23-25,27,28,30] and surfactant treated multi walled carbon nanotubes(MWNTs)[26] as well as grapheme[21,22] have been used. The majority of these nanocomposites have been prepared using a solvent-based method, except when epoxy-benzoxazine mixtures were used[26,28] and the carbon nanotubes were chemically grafted to the monomer.[27] CNT/polybenzoxazine nanocomposites are expected to find potential applications like molding compounds, adhesives in microelectronics,[26] metal-like electrically conductive materials,[23] superhydrophobic coatings[29] where improvements in thermal stability, hydrophobicity and electrical conductivity are required and expected.

In this study, the use of pristine MWNTs as nanofillers in BPA-Bz and MDP-Bz is explored. Nanocomposites were prepared by a convenient solventless method varying the MWNTs amount from 0.1 to 1.0 wt%. Moreover, the dispersion of the MWNTs within both benzoxazines was evaluated using rheological measurements and transmission electron microscopy. Finally, the

characterization of the resulting materials was performed in terms of thermal, electrical, thermo-mechanical and fire properties.

2 Experimental Section

2.1 Materials

The following chemicals were obtained from Aldrich and used as received: ammonium sulphate, paraformaldehyde, 4,4´-bis(4-hydroxyphenyl) pentanoic acid, trimethylorthoformate, p-toluenesulfonic acid monohydrate, toluene and methanol. 1,3,5-Triphenylhexahydro-1,3,5-triazine, methyl 4,4´-bis(4-hydroxyphenyl) pentanoate (MDP) and methyl 4,4´-bis-[6-(3-phenyl-3,4-dihydro-2*H*-1,3-benzoxazine)]pentanoate (MDP-Bz) were synthesized as previously reported.[20] Bisphenol A-based benzoxazine (BPA-Bz) was supplied by Huntsman (Araldite MT 35600). Multi walled carbon nanotubes (MWNTs) were provided by Nanocyl (NC7000) and were used without any further purification. According to the supplier, the MWNTs have an average diameter of 9.5 nm, mean length of 1.5 μm, surface area ranging from 250 to 300 m^2/g and purity of ca. 90%.

2.2 Instrumentation

Rheological measurements were performed on an ARES rheometer LS2 using a geometry of parallel plates (40 mm diameter) at a fixed gap of 0.5 mm. Frequency sweeps were carried out between 0.05 and 1000 rad/s at 120 ºC. The selected strain amplitude of 1% was checked to be in the linear viscoelastic range. The measurements were done on one representative sample.

Calorimetric studies were carried out at scanning rate of 20 ºC/min using a Mettler DSC821e thermal analyzer using N_2 as a purge gas (100 ml/min). Thermal stability study evaluated at a heating rate of 20 ºC/min using a TGA Q50 (TA instruments) with N_2 or air as a purge gas (60 mL/min) from 40 to 800 ºC. The reported thermograms were obtained with one representative sample.

Mechanical properties were measured using a dynamic mechanical thermal analysis (DMTA) apparatus DMA Q800. Specimens (10 mm x 5.4 mm x 2.6 mm) were tested in a three point bending configuration. The thermal transitions were studied in the 30-330ºC range at a heating rate of 3 ºC/min and at a fixed frequency of 1 Hz. One representative sample was used for the measurements.

Limiting Oxygen Index (LOI) measurements were performed using a Stanton Redcroft FTA flammability unit provided with an Oxygen Analyzer. A minimum of 4 samples (70 mm x 6 mm x 3 mm) were tested to evaluate LOI values. Samples were prepared by compression molding using an AGILA PE20 hydraulic press.

TEM images were obtained with a Philips CM200 instrument using an accelerating voltage of 120kV. Samples of about 80 nm thick were prepared with a microtome (Leica Ultracut UCT) at room temperature. The micrographs reported are representative morphologies observed at least at 3 different places.

Electrical measurements were performed on a Keithley multimeter 2700 measuring the resistance of the materials. Three different samples (6.0 mm x 12.2 mm x 2.7 mm) were previously coated with a silver paint for decreasing the contact resistance and then tested at room temperature.

2.3 Preparation of polybenzoxazine/MWNT nanocomposites

The nanocomposites were prepared by a solventless method using two different benzoxazine monomers: the commercial BPA-Bz and the synthesized MDP-Bz. A general method of preparation consisted of mixing an appropriate amount of MWNTs with benzoxazine followed by a melting at 120 ºC using a silicon oil bath. The mixture was then manually stirred and subsequently dispersed using an ultrasonic probe (Branson S-50D equipment, 200 W, 20 kHz, 13 mm diameter) for 1 min. After, the mixture was degassed in a vacuum oven at 140 ºC for 10 min and transferred to a stainless steel mold (cavity dimensions: 13 x 3 x 70 mm) for curing. The used amounts of MWNTs were 0.1, 0.3, 0.5 and 1.0 wt% of the total mixture weight. Polymerization of the mixtures was carried out using an AGILA PE20 hydraulic press at 135 bar according to the following curing conditions: 200 ºC for 2h, 220 ºC for 2h, 235 ºC for 3h and 250 ºC for 3h. A post-curing step was done at 250 ºC for 2h in a conventional oven. A neat polybenzoxazine (without any MWNTs) was also prepared for the sake of comparison.

3 Results and discussion

3.1 Monomer synthesis

MDP-Bz is synthesized by the reaction of 1,3,5-triphenylhexahydro-1,3,5-triazine,methyl 4,4´-bis(4-hydroxyphenyl) pentanoate (MDP) and

paraformaldehyde in high yield and purity.[20] The bisphenol A-based benzoxazine (BPA-Bz) used in this study is the commercial counterpart shown in Scheme 1.

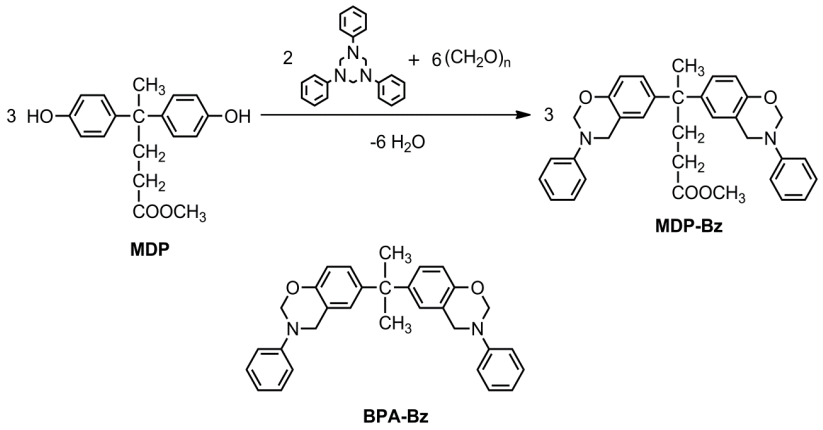

Scheme 1 Chemical structures of MDP, MDP-Bz and BPA-Bz

3.2 Rheological properties

The main factors known to affect the performances of polymer/MWNT nanocomposites are the degree of dispersion of the MWNTs within the polymer matrix and the extent of interfacial adhesion between the MWNTs and the matrix.[31] In order to examine the dispersion state of MWNTs within both benzoxazine resins (*i.e.,* BPA-Bz and MDP-Bz), a rheological approach was applied to the systems prior curing (see Figure 1). The viscosity sweep frequency curves of both benzoxazine pre-polymers reveal that their flow behavior is significantly modified in the presence of MWNTs. Indeed, neat BPA-Bz and MDP-Bz pre-polymers exhibit a Newtonian behavior whereas when MWNTs are incorporated in the benzoxazine monomers, a shear thinning behavior is observed. Storage modulus G' corresponding to the elastic properties and loss modulus G'' corresponding to viscous properties of the systems were also studied *versus* frequency. It appears that both neat benzoxazine monomers, similarly to epoxy uncured resins, follow the typical linear viscoelastic behavior of liquid whereas in both benzoxazine pre-polymers/MWNT suspensions, G' and G'' are found to increase significantly with MWNTs content and frequency. More specifically, at low frequency, a plateau is noticed and a solid-like behavior is observed as G' values are found to be higher than G'' values even at a very low amount of MWNTs (*i.e.,* 0.1 wt%). It is well known that MWNTs can organize

themselves and generate an interconnecting network similar to a gel within liquid or molten polymers. This structural network is responsible for the enhancement and the almost frequency independence of G' and G'' at low frequency range (plateau apparition). Moreover, the length of the plateau is found to be longer for G' when compared to G'' revealing that G' is more sensitive to MWNTs dispersion quality than G''. In addition, the increase of G' plateau value observed with increasing MWNTs loading can be explained by the improvement of the network connectivity mainly brought by the MWNTs particle interactions. It is worth noting that the transition from liquid-like to solid-like behavior occurs at a very low concentration of MWNTs (<0.1 wt%) suggesting that MWNTs exhibit very good interactions with both benzoxazines and disperse well within them.

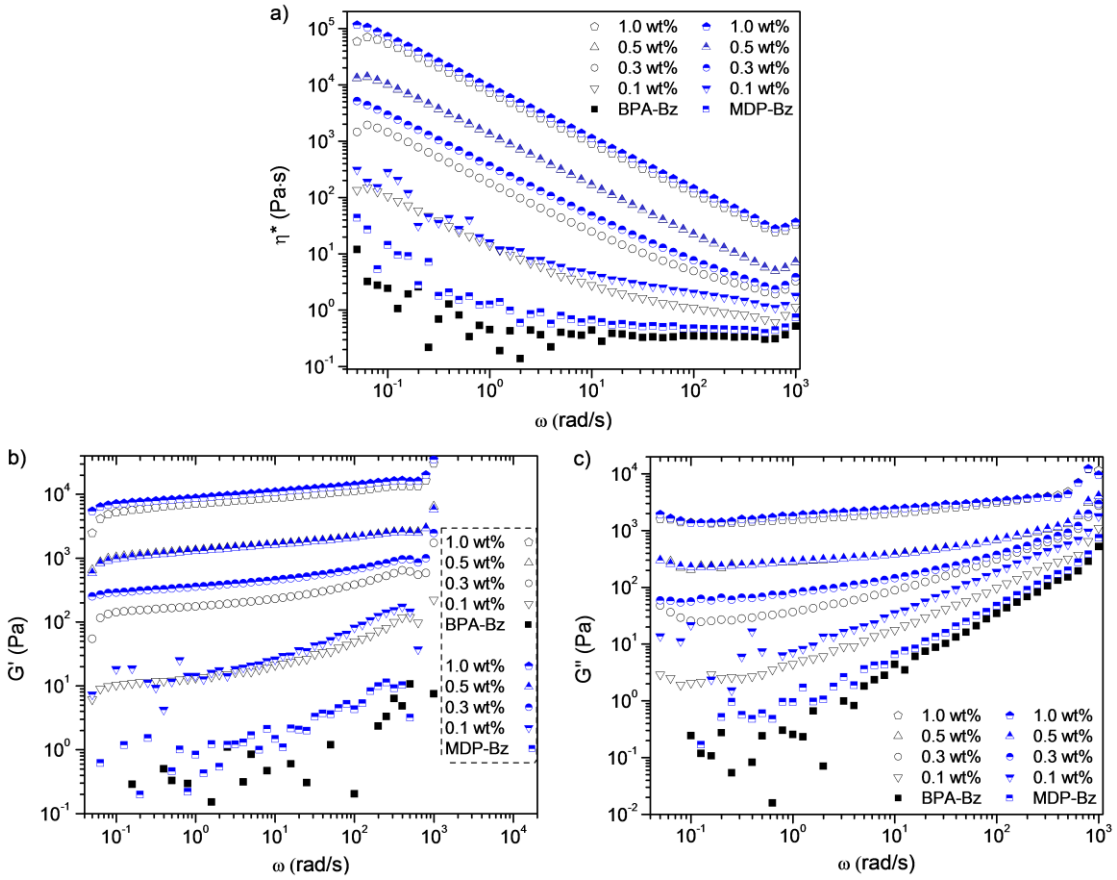

Fig. 1 Frequency dependence of complex viscosity, storage modulus (G'), loss modulus (G'') of Bz-BPA/MWNT and Bz-MDP/MWNT suspensions for different concentrations of MWNTs at 120°C

3.3 Curing behavior of MWNT/Bz mixtures

It is reported in the literature that percolation threshold does not depend only on nanoparticle content but it is also very sensitive to the curing conditions of the nanocomposite.[32,33] In order to identify the possible action of MWNTs on benzoxazine polymerization, DSC testing was performed for both benzoxazines in the presence of different concentrations of MWNTs. Figure 2 represents the DSC thermograms of the unfilled monomers and MWNT/Bz mixtures at different MWNTs contents. It appears that in both monomer mixtures (MDP-Bz/MWNT and BPA-Bz/MWNT) there is a single exothermic peak associated with a single chemical process, *i.e.,* the thermal ring-opening and crosslink reaction of benzoxazine functional groups. For both monomers (BPA-Bz and MDP-Bz), the addition of MWNTs does not cause a significant shifting of neither the onset nor the maximum of the polymerization exotherms. The polymerization enthalpy of the mixtures progressively decreases as consequence of the lower amount of the monomer but the enthalpy of thermal curing of benzoxazine groups is not significantly modified by the presence of MWNTs.

The curing conditions of the mixtures of benzoxazines and MWNTs were selected according to the DSC data. As no significant change in the curing process of the mixtures was observed and for the sake of comparison, the curing conditions were kept the same for all the systems.

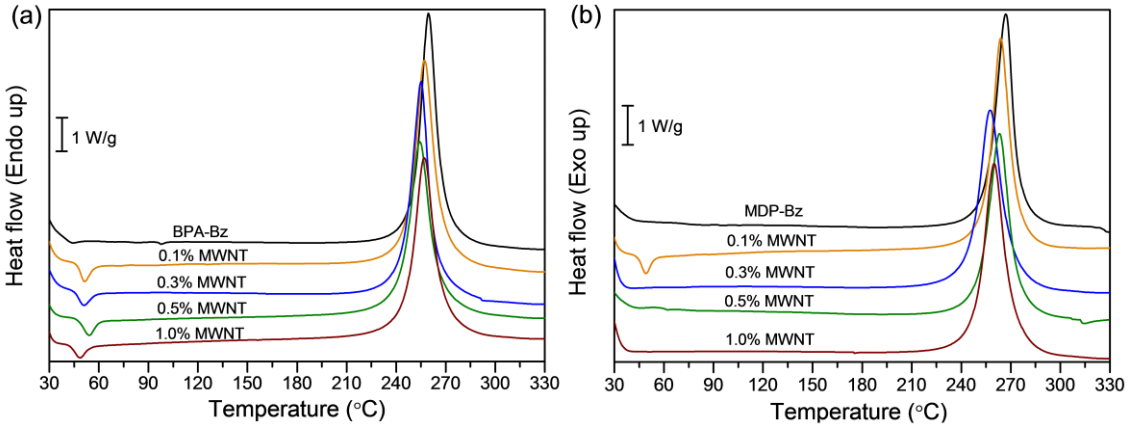

Fig. 2 DSC thermograms of a) BPA-B-z and b) MDP-Bz nanocomposites

3.4 Dispersion of the MWNTs within the nanocomposites

The distribution and the dispersion of pristine MWNTs within both polymer nanocomposites (MDP-PBz and BPA-PBz) after curing were examined by TEM.

The corresponding images for 1.0 wt% MWNTs are shown in Figure 3. As can be seen, MWNTs are well distributed and dispersed within both polybenzoxazines highlighting there is no need for MWNTs surface functionalization to achieve their good dispersion within benzoxazine matrices. Indeed, the good dispersion of MWNTs obtained initially within the monomers appears to be preserved during the curing of the benzoxazine matrices.

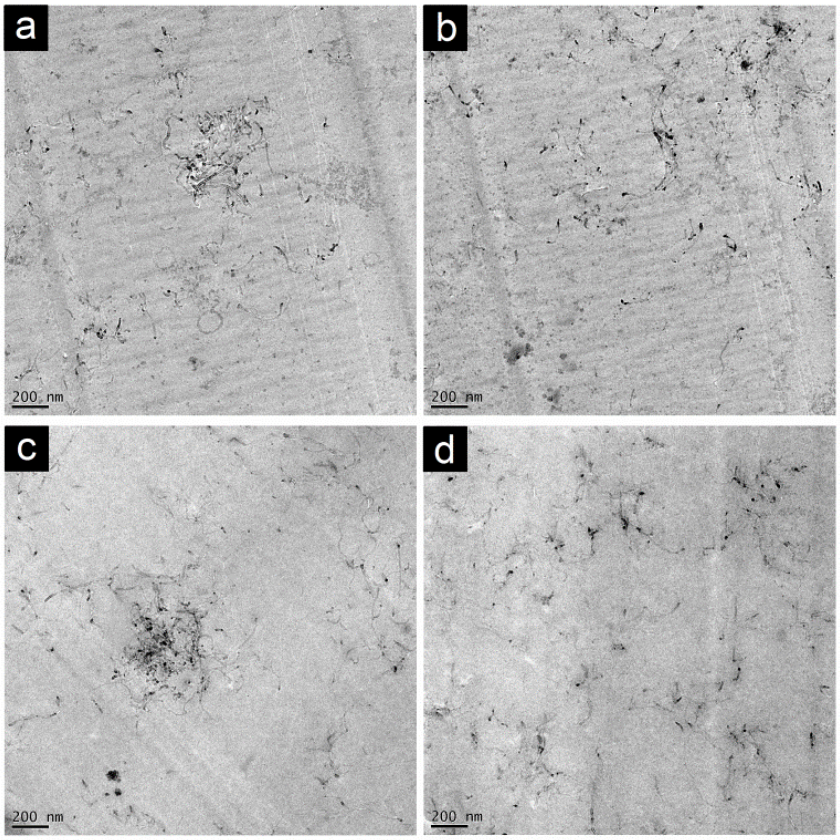

Fig. 3 TEM images of a) and c) 1.0 wt % MWNT/BPA-PBz nanocomposites, b) and d) 1.0 wt% MWNT/MDP-PBz nanocomposites

3.5 Electrical resistivity

The high aspect ratio of MWNTs, their fine dispersion and the formation of a "network-like" structure within the polymer matrix are key-parameters to endow polymers with improved electro-conductive properties. It was shown earlier in this paper that rheological percolation which requires contact between particles takes place at a very low concentration of MWNTs (<0.1 wt%) for both BPA-Bz and MDP-Bz matrices. In addition, TEM analyses further highlighted the good dispersion of MWNTs within the matrices. Electrical measurements of MWNT-

filled polybenzoxazine matrices gathered in Figure 4 are in good agreement with these results. Indeed, significant enhancement of electrical conductivity is obtained at a content in MWNTs as low as 0.1 wt%. Any further addition of MWNTs only increases slightly the electrical conductivity confirming the existence of a percolation threshold at a smaller concentration of MWNTs lower than 0.1 wt%.

There is only a previous study that reports an electrical conductivity of 6.8 $x10^{-5}$ S/cm (1.5 x 10^4 Ω.cm) using 2.5 wt% of functionalized MWNTs with benzoxazine groups.[23] In this case, higher values were found at lower concentrations using pristine CNT dispersed without the addition of a solvent.

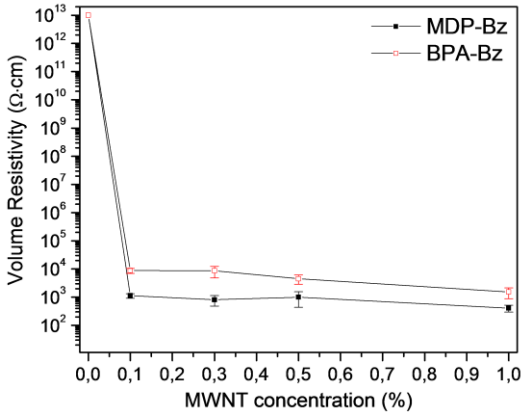

Fig. 4 Electrical volume resistivity of BPA-PBz and MDP-PBz nanocomposites

3.6 Thermo-mechanical properties

The effect of MWNTs content on the glass transition temperature (Tg) of polybenzoxazine nanocomposites was determined using DMTA (as the maximum peak of tan δ) and DSC (as the half-height of the change in specific heat capacity, ½ Δ Cp). The Tg values from both measurements are shown in Table 1. Two different behaviors were observed according to the type of polybenzoxazine matrix (Fig. 5). Tg values for MDP-PBz nanocomposites, as expected, are found to be higher than BPA-PBz ones due to the transesterification reaction taking place between the ester group present onto each MDP-Bz monomer, and the hydroxyl group resulting from the opening of the oxazine ring.[20]

For MWNT/BPA-PBz nanocomposites, Tg values of the materials do not seem to be significantly affected by the amount of MWNTs within the matrix. In addition, no marked change is observed in the height of tan δ peak suggesting the MWNTs content does not alter the crosslinking density of BPA-PBz.

For MWNT/MDP-PBz nanocomposites, the trend is different. More precisely, the presence of MWNTs triggers some important modifications of the Tg of the resulting materials. Quite interestingly, up to 0.5 wt% MWNTs, the recorded Tg values proved to increase, possible indication that interactions between the MWNTs and MDP-PBz are maintained after the crosslinking process, leading to a restriction of motion of the network in the nanocomposites. Moreover, the height of Tan δ peak significantly decreased and becomes broader confirming the restriction of mobility of the crosslinked system in presence of MWNTs (<0.5 wt%).[24] On the contrary, above 0.5 wt% MWNTs, Tg is observed to decrease to values lower than the Tg of neat MDP-PBz matrix. This phenomenon can be attributed to the volume saturation of the resin generating steric hindrance and preventing ester functional groups of the MDP-Bz matrix from reacting *via* transesterification leading to a decrease of the crosslinking density. In addition, it is to note that for MWNTs concentration higher than 0.5 wt%, the height of tan δ peak of MWNT/MDP-PBz systems is found to logically increase confirming the lower crosslinking density within the network allowing an increase of the network segment mobility.

Table 1 Tg values of the nanocomposites from DSC and DMTA

Sample	Tg (°C)	
	½ ΔC_p	tan δ_{max}
BPA-PBz	150	166
0.1 wt% MWNT	151	173
0.3 wt% MWNT	147	169
0.5 wt% MWNT	150	163
1.0 wt% MWNT	147	165
MDP-PBz	229	266
0.1 wt% MWNT	284	290
0.3 wt% MWNT	283	290
0.5 wt% MWNT	227	249
1.0 wt% MWNT	223	241

In addition to the thermo-mechanical transition which can be associated to the Tg of the materials, DMTA also allows to determining the temperature dependence of the storage modulus (E') for a material under shear deformation. For MWNT/BPA-PBz nanocomposites, in its glassy state, E' is observed to increase with the MWNTs content. The same trend is obtained for E' in the

rubbery state. These improvements of E' are again indicative of good interactions between MWNTs and BPA-PBz leading to some restriction of chain mobility.

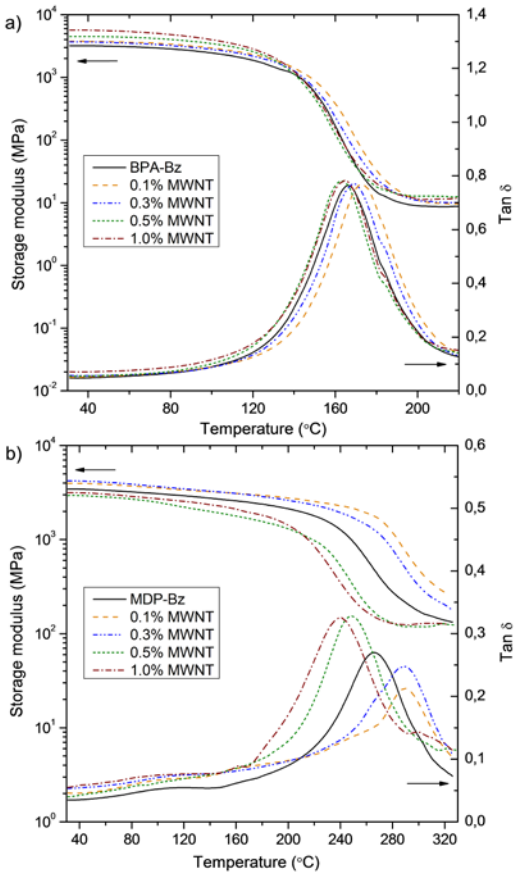

Fig. 5 Effect of MWNTs content on storage modulus and tan δ plots of a) BPA-PBz nanocomposites and b) MDP-PBz nanocomposites

As far as MWNT/MDP-Bz nanocomposites are concerned, the presence of MWNTs leads to more radical change of E' in the glassy and rubbery states with respect to of the related MWNT/BPA-PBz nanocomposites. Indeed, the addition of 0.1 wt% and 0.3 wt% of nanotubes results in an increase of E' whereas 0.5 wt% and 1.0% decreases E'. During the initial dispersion process of MWNTs within MDP-Bz, for low concentration of MWNTs (<0.5 wt%) interactions are tying down the MWNTs and the MDP-Bz chains leading to an increase of the crosslinking density and an increase of E' whereas for concentration of MWNTs higher than 0.5 wt%, the volume occupied by MWNTs becomes not neglectable and generates some steric hindrance preventing in some extent, esterification reactions to take place and hence the total curing of the forming network, resulting in a decrease of E'.

3.6 Thermal stability

To examine the effect of MWNTs on the thermal stability and the decomposition behavior of the polybenzoxazines, thermogravimetric analysis (TGA) was carried out under nitrogen and air atmospheres. Figure 6 shows TGA and derivative thermogravimetric (DTG) curves and Table 2 summarizes TGA data for all the polymers. Polybenzoxazines based on diphenolic compounds, *e.g.,* BPA-PBz and MDP-PBz, usually present three stages of weight loss under (inert) nitrogen atmosphere. The first two weight loss stages are assigned to the volatilization of aniline (up to 300 ºC) and phenolic moieties (300-400 ºC), respectively, and the third one is related to the degradation of the char (above 400 ºC).[34] Usually, the MDP-PBz exhibit higher thermal stability than the BPA-PBz as a consequence of a higher crosslinking density. It could be observed that the thermal properties of BPA-PBz and MDP-PBz were improved by incorporating MWNTs. Indeed, the addition of MWNTs induces a positive shift to higher temperatures in the decomposition temperatures of 1% ($T_{1\%}$) and 10% ($T_{10\%}$) weight loss. Similar results were reported in functionalized graphene/polybenzoxazine nanocomposites.[22] The main degradation temperature (T_{max}) of MWNT/MDP-PBz nanocomposites is slightly increased in comparison with the neat MDP-PBz. Moreover, it was observed that MWNTs promote the formation of char of the nanocomposites in comparison to neat polybenzoxazines, and more specifically the charring amount proved more important in the case of MWNT/MDP-PBz resins.

Table 2 Thermal properties and LOI values of polybenzoxazine nanocomposites

Sample	TGA (N_2)				TGA (Air)				LOI
	$T_{1\%}$ (°C)[a]	$T_{10\%}$ (°C)[b]	T_{max} (°C)[c]	Y_{800} (%)[d]	$T_{1\%}$ (°C)[a]	$T_{10\%}$ (°C)[b]	T_{max} (°C)[c]	Y_{800} (%)[d]	
BPA-PBz	241.2	387.5	437.9	32.8	254.1	409.4	416.4,643.6	0.12	35.2
0.1 wt%	263.1	398.2	431.4	33.8	293.2	410.0	426.3,657.8	0.13	36.4
0.3 wt%	282.9	398.5	432.9	34.5	297.0	407.3	424.4,656.5	0.44	38.0
0.5 wt%	282.7	404.7	433.3	34.5	289.7	407.6	423.6,667.3	0.15	38.5
1.0 wt%	280.7	401.4	432.8	34.5	289.3	410.0	426.5,669.0	0.19	38.7
MDP-PBz	325.7	413.7	440.5	32.8	312.8	419.5	440.3,608.2	0.16	31.2
0.1 wt%	358.7	413.7	448.0	32.9	372.7	417.2	444.7,624.8	0.22	35.1
0.3 wt%	359.1	413.5	444.1	34.1	371.4	417.2	451.3,623.1	0.32	36.4
0.5 wt%	334.4	420.1	448.0	36.2	343.5	424.0	444.4,635.5	0.23	36.8
1.0 wt%	324.4	420.1	447.5	36.0	344.5	420.8	445.3,638.2	0.20	37.4

[a] Temperature of 1% weight loss
[b] Temperature of 10% weight loss
[c] Temperatures of maximum weight loss rate
[d] Char yield at 800 °C

Under oxidative atmosphere, polybenzoxazines present two main processes related to the fragmentation of shift bases and the formation of char above 600 ºC. It was also observed a noticeable increase of ($T_{1\%}$) when 0.1 wt% and 0.3 wt% MWNTs were added to MDP-PBz, shifting from 312.8 ºC to 372.7 ºC and 371.4 ºC, respectively. The shift to higher temperatures in the first and most remarkable in the second peak of the degradation (T_{max}) of the polymers, attests for the increase in thermal stability triggered by the addition of MWNTs. This delay was more evident for MDP-PBz at a concentration of 1.0 wt% MWNTs. However, it was not possible to observe any important influence in the char yield.

Usually, the above mentioned improvements in the thermal stability of the polymer nanocomposites are attributed to: 1) the good dispersion of MWNTs which might hinder the flux of degradation products from the polymer into the gas phase delaying the onset of degradation; 2) the strong interfacial interactions between the polybenzoxazines and MWNTs restrict the mobility of the polymer chains near the nanotubes causing a delay in their degradation and therefore shifting T_{max} to higher temperatures and 3) the higher thermal conductivity in the polymer/nanotube nanocomposites that could ease heat dissipation within the materials.[35]

3.7 Flame retardant properties

Limiting Oxygen Index (LOI) defined as the minimum fraction of oxygen in a gas mixture of oxygen and nitrogen that can bear flaming combustion is a useful indicator to evaluate the flammability of the materials. The LOI values of the polybenzoxazine-based systems are collected in Table 2. They are found to increase with the content of MWNTs. The enhancement is slightly better in the case of MDP-PBz nanocomposites when compared to BPA-PBz counterparts and it is worth noting that low amounts of MWNTs (0.1 wt% and 0.3 wt%) already allow for achieving significant improvement of flame retardancy of both nanocomposites. It has been evidenced in the literature that the degree of dispersion affects the extent of the results and in presence of finely dispersed MWNTs, polymeric nanocomposites exhibit a greater flame retardancy behavior,[36,37] which is in agreement with our results. Moreover, LOI values are found to follow a similar trend with the char yield obtained by TGA. The LOI values obtained for both polybenzoxazine systems stress the beneficial effect of MWNTs to impart flame retardancy. It has been demonstrated that carbon

nanotubes can reduce the flammability of materials through the formation of a continuous protective layer consisting of a network of nanoparticles that serves as a heat shield and re-emits much of the incident radiation back decreasing the polymer degradation rate and hinders the attack of the matrix by oxygen radicals.[38,39]

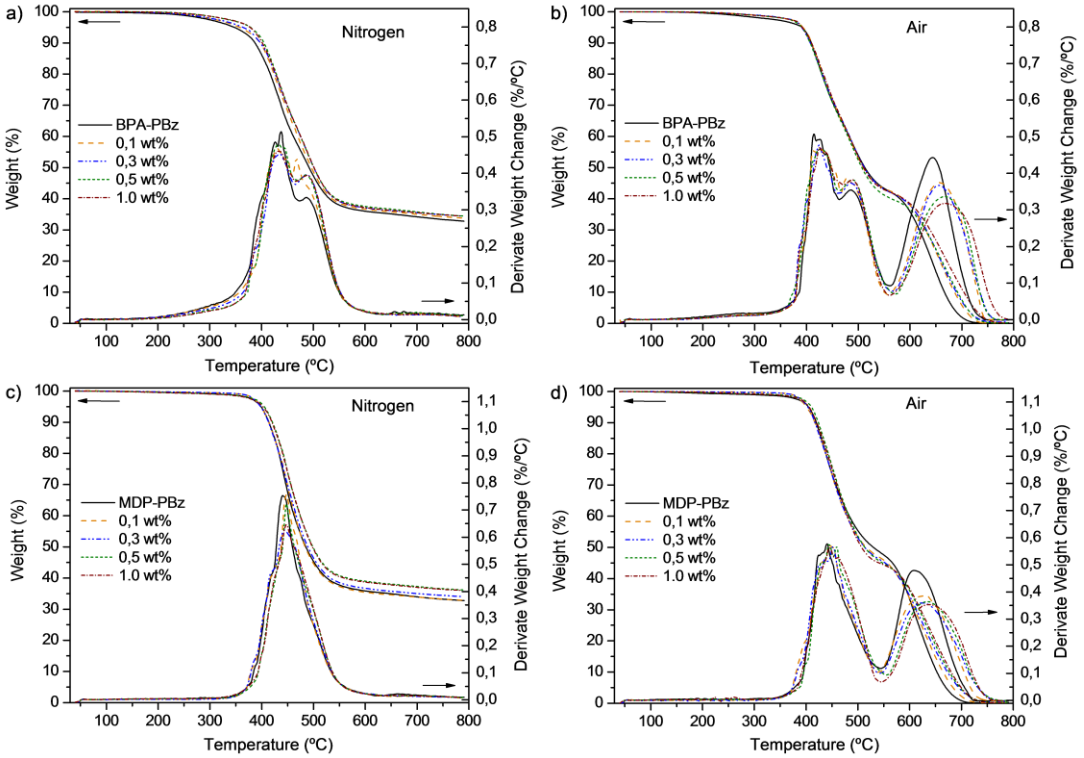

Fig 6. TGA and DTG plots of MWNT/BPA-PBz and MWNT/PBz-MDP nanocomposites in nitrogen (a and c) and air atmospheres (b and d), respectively.

4 Conclusions

Polybenzoxazine nanocomposites containing MWNTs were successfully prepared following a convenient and solventless process. The addition of MWNTs to both monomers did not interfere with the ring opening of the benzoxazines. Rheological measurements showed that benzoxazine/MNWT mixtures presented a low percolation threshold (<0.1 wt%) indicating a well dispersion state derived from the strong interactions between nanofillers and both monomers. TEM and electrical properties of the crosslinked polybenzoxazine nanocomposites confirmed the preservation of the good dispersion state after their curing. The electrical percolation threshold was in agreement with rheological results and it

was found to take place at a concentration lower than 0.1 wt% for both polybenzoxazine resins. The thermal stability of both nanocomposites was significantly affected by the amount of MWNTs, especially in the initial degradation step. The Tg of the MWNT/BPA-PBz nanocomposites was not affected by the MWNTs content whereas for MWNT/MDP-PBz counterparts, concentrations lower than 0.5 wt% significantly increased the Tg values. The good dispersion state of MWNTs and their good affinity with both resins induced a meaningful effect that was reflected in an increase of the storage modulus E' in both glassy and rubbery states and an enhancement in the char yield and fire behaviour (LOI) of the polybenzoxazine nanocomposites. It is worth noting that these promising results were obtained with pristine MWNTs and they did not require any surface treatment or functionalization to promote their dispersion within the benzoxazine matrices.

Acknowledgments

The authors wish to thank the "RégionWallonne" for the financial support in the framework of ECOTAC project from the "Pôle de compétitivité SKYWIN" and the Interuniversity Attraction Poles Programme initiated by the Belgian Science Policy Office. MATERIA NOVA and CIRMAP thank the European Community for general support in the frame of the 7th Framework research project "IASS", the ''Belgian Federal Government Office Policy of Science (SSTC)'' for its support in the frame of the PAI-6/27 and the ''RégionWallonne'' in the framework of the ''Programmed'Excellence: OPTI²MAT''. We thank Yoann Paint for the help on TEM. Authors also thank Nanocyl S. A. (Belgium) for kindly providing MWNTs and Huntsman Advanced Materials (Europe) for kindly supplying the BPA-Bz resin. The authors also express their thanks to CICYT (Comisión Interministerial de Ciencia y Tecnología) (MAT2011-24823 Spain) for financial support.

Notes and References

1. M. Terrones, *Annu. Rev. Mater. Res.*, 2003, **33**, 419-501.
2. K. Balasubramanian and M. Burghard, *Small*, 2005, **1**, 180-192.
3. D. Tasis, N. Tagmatarchis, A. Bianco and M. Prato, *Chem. Rev.*, 2006, **106**, 1105-1136.
4. Q. Zhang, F. Fang, X. Zhao, Y. Li, M. Zhu and D. Chen, *J. Phys. Chem. B*, 2008, **112**, 12606-12611.
5. M. H. Al-Saleh, W. H. Saadeh and U. Sundararaj, *Carbon*, 2013, **60**, 146-156.
6. L. Bonnaud, O. Murariu, N. De Souza Basso and P. Dubois, *Polym. Bull.*, 2013, **70**, 895-904.

7. M. F. L. De Volder, S. H. Tawfick, R. H. Baughman and A. J. Hart, *Science*, 2013, **339**, 535-539.
8. H. Ishida, in *Handbook of Benzoxazine Resins*, eds. I. Hatsuo and A. Tarek, Elsevier, Amsterdam, 2011, pp. 3-81.
9. N. N. Ghosh, B. Kiskan and Y. Yagci, *Prog. Polym. Sci.*, 2007, **32**, 1344-1391.
10. V. Cádiz, J. C. Ronda, G. Lligadas and M. Galià, in *Handbook of Benzoxazine Resins*, eds. I. Hatsuo and A. Tarek, Elsevier, Amsterdam, 2011, pp. 556-576.
11. H. Ling and Y. Gu, *J. Macromol. Sci., Phys.*, 2011, **50**, 2393-2404.
12. M. Spontón, J. C. Ronda, M. Galià and V. Cádiz, *Polym. Degrad. Stab.*, 2008, **93**, 2158-2165.
13. L.-K. Lin, C.-S. Wu, W.-C. Su and Y.-L. Liu, *J. Polym. Sci., Part A: Polym. Chem.*, 2013, **51**, 3523-3530.
14. M. Spontón, D. Estenoz, G. Lligadas, J. C. Ronda, M. Galià and V. Cádiz, *J. Appl. Polym. Sci.*, 2012, **126**, 1369-1376.
15. D. Wang, B. Li, Y. Zhang and Z. Lu, *J. Appl. Polym. Sci.*, 2013, **127**, 516-522.
16. C. Zúñiga, G. Lligadas, J. C. Ronda, M. Galià and V. Cádiz, *Polymer*, 2012, **53**, 1617-1623.
17. S. Rimdusit, N. Thamprasom, N. Suppakarn, C. Jubsilp, T. Takeichi and S. Tiptipakorn, *J. Appl. Polym. Sci.*, 2013, **130**, 1074-1083.
18. C. H. Lin, S. X. Cai, T. S. Leu, T. Y. Hwang and H. H. Lee, *J. Polym. Sci., Part A: Polym. Chem.*, 2006, **44**, 3454-3468.
19. C. E. Talsness, A. J. M. Andrade, S. N. Kuriyama, J. A. Taylor and F. S. vom Saal, *Phil. Trans. R. Soc. B*, 2009, **364**, 2079-2096.
20. C. Zúñiga, M. S. Larrechi, G. Lligadas, J. C. Ronda, M. Galià and V. Cádiz, *J. Polym. Sci., Part A: Polym. Chem.*, 2011, **49**, 1219-1227.
21. M. Zeng, J. Wang, R. Li, J. Liu, W. Chen, Q. Xu and Y. Gu, *Polymer*, 2013, **54**, 3107-3116.
22. K.-K. Ho, M.-C. Hsiao, T.-Y. Chou, C.-C. M. Ma, X.-F. Xie, J.-C. Chiang, S.-h. Yang and L.-H. Chang, *Polym. Int.*, 2013, **62**, 966-973.
23. Y.-H. Wang, C.-M. Chang and Y.-L. Liu, *Polymer*, 2012, **53**, 106-112.
24. J.-M. Huang, M.-F. Tsai, S.-J. Yang and W.-M. Chiu, *J. Appl. Polym. Sci.*, 2011, **122**, 1898-1904.
25. Y. Liu, B. Wang and X. Jing, *Polym. Compos.*, 2011, **32**, 1352-1361.
26. M. Kaleemullah, S. U. Khan and J.-K. Kim, *Compos. Sci. Technol.*, 2012, **72**, 1968-1976.
27. M. Xu, J. Hu, X. Zou, M. Liu, S. Dong, Y. zou and X. Liu, *J. Appl. Polym. Sci.*, 2013, **129**, 2629-2637.
28. L. Yang, C. Zhang, S. Pilla and S. Gong, *Composites Part A*, 2008, **39**, 1653-1659.
29. C.-F. Wang, H.-Y. Chen, S.-W. Kuo, Y.-S. Lai and P.-F. Yang, *RSC Advances*, 2013, **3**, 9764-9769.
30. Q. Chen, R. Xu and D. Yu, *Polymer*, 2006, **47**, 7711-7719.
31. M. Chapartegui, N. Markaide, S. Florez, C. Elizetxea, M. Fernandez and A. Santamaría, *Compos. Sci. Technol.*, 2010, **70**, 879-884.
32. G. Faiella, V. Antonucci, S. T. Buschhorn, L. A. S. A. Prado, K. Schulte and M. Giordano, *Composites Part A*, 2012, **43**, 1441-1447.
33. G. Olowojoba, S. Sathyanarayana, B. Caglar, B. Kiss-Pataki, I. Mikonsaari, C. Hübner and P. Elsner, *Polymer*, 2013, **54**, 188-198.
34. H. Yee Low and H. Ishida, *Polymer*, 1999, **40**, 4365-4376.
35. M. Moniruzzaman and K. I. Winey, *Macromolecules*, 2006, **39**, 5194-5205.
36. T. Kashiwagi, F. Du, K. I. Winey, K. M. Groth, J. R. Shields, S. P. Bellayer, H. Kim and J. F. Douglas, *Polymer*, 2005, **46**, 471-481.
37. S. Bourbigot, S. Duquesne and C. Jama, *Macromol. Symp.*, 2006, **233**, 180-190.
38. T. Kashiwagi, E. Grulke, J. Hilding, K. Groth, R. Harris, K. Butler, J. Shields, S. Kharchenko and J. Douglas, *Polymer*, 2004, **45**, 4227-4239.
39. S. Bocchini, A. Frache, G. Camino and M. Claes, *Eur. Polym. J.*, 2007, **43**, 3222-3235.

Conclusions

GENERAL CONCLUSIONS

1. Using renewable diphenolic acid (DPA) two benzoxazine monomers have been synthesized and characterized. During polymerization, these benzoxazines showed intramolecular transesterification or esterification reactions reaching high crosslinking degree. In comparison to structurally similar bisphenol A-based polybenzoxazines (BPA-Bz), the diphenolic acid based-polybenzoxazines exhibited superior thermal and thermomechanical properties.

2. Renewable thermosetting polybenzoxazines were obtained by mixing DPA with the methylester of DPA-based benzoxazine (MDP-Bz) with low polymerization temperatures. Fiberglass reinforced samples with good tensile properties were achieved. High performance flame retardant thermosetting resins were obtained by mixing MDP-Bz and phosphazene-DPA derivative.

3. Polybenzoxazine rigid foams from diphenolic acid-based benzoxazine (DPA-Bz) were obtained by a self-foaming induced process. The blowing agent (CO_2) was generated *in situ* as a result of decarboxylation of DPA-Bz. It was possible to control the relative decarboxylation reaction by varying the temperature and hence, the morphology of the materials and their corresponding properties.

4. Phosphorus-containing polybenzoxazine foams were prepared in order to enhance the flame retardancy of neat polybenzoxazine foams. Prepolymer curing conditions, temperature and time, strongly affect the structure, shape and density of the final foams. The incorporation of the phosphorus additive showed a beneficial effect on the flame retardant properties of both prepolymers and foams materials, as well as a decrease in their glass transition temperatures.

5. Analytical tools allowed establishing the influence of foaming time and temperature on the final properties of the phosphorus-containing polybenzoxazine foams. Mathematical models fitted to the experimental data. The mechanical properties of the foams were found to be more

dependent on the crosslinking degree of the solid phase than on the cellular structure features.

6. Polybenzoxazine nanocomposites containing pristine multi walled carbon nanotubes were successfully prepared following a convenient and solventless process. Carbon nanotubes were well dispersed within both matrices without any surface treatment or functionalization. Low amounts of carbon nanotubes were needed to positively enhance thermal, flame retardant and electrical properties of the nanocomposites.

APPENDICES

APPENDIX A LIST OF ABBREVIATIONS

½ ΔCp	Half-height of the change in specific heat capacity
^{1}H, ^{13}C, ^{31}P NMR	Proton, carbon and phosphorus nuclear magnetic resonance
2,4-Me-Bz	6,8-dimethyl-3-phenyl-2H,4H-benzo[e]1,3-oxazine
ANOVA	Analysis of variance
ATR	Attenuated total reflection
BPA	Bisphenol A
BPA-Bz	Bisphenol A based benzoxazine
Bz	Benzoxazine
CCD	Central composite design
$CDCl_3$	Deuterated chloroform
CNT	Carbon nanotubes
CSM	Chopped strand fiberglass mat
DMSO-d_6	Deuterated dimethylsulfoxide
DMA	Dinamycmechanical analysis
DOPO	9,10-dihydro-9-oxa-10-phosphaphenanthrene-10-oxide
DOPO-2Me	9,10-dihydro-9-oxa-10-(1-hydroxy-1-methylethyl) phosphaphenanthrene-10-oxide
DPA	Diphenolic acid
DPA-Bz	Diphenolic acid based benzoxazine
DPA-PPZ	Diphenolic acid phosphazene salt
DSC	Differential scanning calorimetry
DTG	Derivative thermogravimetric curves
E	Compressive modulus
E′	Storage modulus
E″	Loss modulus
EDX	Energy-dispersive X-ray spectroscopy
E-glass	Electrical grade glass fiber
ESEM	Environmental scanning electron microscopy
FT-IR	Fourier transform infrared spectrometry
G′	Storage modulus
G″	Loss modulus
LOI	Limiting oxygen index
MCR-ALS	Multivariate curve resolution alternating least square
MDP	Diphenolic acid methylester derivative
MDP-Bz	Methylester of diphenolic acid based benzoxazine
MWNT	Multi walled carbon nanotubes
NMR	Nuclear magnetic resonance spectroscopy
P_4-t-Bu	1-*terc*-butyl-4,4,4-tris(dimethylamino)-2,2-[tris(dimethylamino) phosphoranylideneamino]-2λ^5,4λ^5-catenadi (phosphazene)
PBz	Polybenzoxazine

RSM	Response surface methodology
SEM	Scanning electron microscopy
SpCM	Specific compressive modulus
SpCS	Specific compressive strength
SS	Sum of squares
SVD	Singular value decomposition
TEM	Transmission electron microscopy
T_f	Foaming temperature
T_g	Glass transition temperature
TGA	Thermogravimetric analysis
TGA-MS	Thermogravimetric mass spectroscopy analysis
THF	Tetrahydrofuran
TMS	Tetramethylsilane
UL-94	Underwriters' laboratory test #94
η*	Complex viscosity
ρ	Density
σ	Compressive strength

APPENDIX B LIST OF PUBLICATIONS

1. Zúñiga, C.; Larrechi, M. S.; Lligadas, G.; Ronda, J. C.; Galià, M.; Cádiz, V., Polybenzoxazines from renewable diphenolic acid. *J. Polym. Sci., Part A: Polym. Chem.* 2011, 49, (5), 1219-1227.

2. Zúñiga, C.; Lligadas, G.; Ronda, J. C.; Galià, M.; Cádiz, V., Renewable polybenzoxazines based in diphenolic acid. *Polymer* 2012, 53, (8), 1617-1623.

3. Zúñiga, C.; Lligadas, G.; Ronda, J. C.; Galià, M.; Cádiz, V., Self-foaming diphenolic acid benzoxazine. *Polymer* 2012, 53, (15), 3089-3095.

4. Zúñiga, C.; Larrechi, M. S.; Lligadas, G.; Ronda, J. C.; Galià, M.; Cádiz, V., Phosphorus flame retardant polybenzoxazine foams based on renewable diphenolic acid. *Polym. Degrad. Stab.* 2013. ***Accepted.*** DOI:10.1016/j.polymdegradstab.2013.09.023

5. Zúñiga, C.; Larrechi, M. S.; Lligadas, G.; Ronda, J. C.; Galià, M.; Cádiz, V., Modeling of the foaming process of a phosphorus flame retardant polybenzoxazine*. Polymer Testing*. 2013. ***Submitted***

6. Zúñiga, C.; Lligadas, G.; Ronda, J. C.; Galià, M.; Cádiz, V.; Bonnaud, L.; Dubois, P., Convenient and solventless preparation of neat carbon nanotubes/polybenzoxazine nanocomposites with low percolation threshold and improved thermal and fire properties. *J. Mater. Chem. A* 2013. ***Submitted***

APPENDIX C MEETING CONTRIBUTIONSAND STAGE

Meeting contributions

1. **Authors**: Camilo Zúñiga, Gerard Lligadas, Joan C. Ronda, Marina Galià, Virginia Cádiz
   Title: Benzoxazine Thermosets from Diphenolic Acid as Renewable Resource.
   Type: Poster
   Congress: 43rd IUPAC World Polymer Congress. Macro 2010
   Place of meeting: Glasgow, UK **Date of meeting:** July 2010

2. **Authors:** Camilo Zúñiga, Gerard Lligadas, Joan C. Ronda, Marina Galià, Virginia Cádiz
   Title: Polybenzoxazine foams from renewable diphenolic acid
   Type: Poster
   Congress: European Polymer Congress 2011
   Place of meeting: Granada, Spain **Date of meeting:** June 2011

3. **Authors:** Camilo Zúñiga, Gerard Lligadas, Joan C. Ronda, Marina Galià, Virginia Cádiz
   Title: Thermosets from methyldiphenolic acid-based benzoxazine and diphenolic acid mixtures
   Type: Poster
   Congress: European Polymer Congress 2011
   Place of meeting: Granada, Spain **Date of meeting:** June 2011

4. **Authors:** Camilo Zúñiga, Gerard Lligadas, Joan C. Ronda, Marina Galià, Virginia Cádiz
   Title: Preparación de espumas rígidas de polibenzoxazinas derivadas del ácido difenólico
   Type: Oral presentation
   Congress: VI Congreso nacional de jóvenes investigadores en polímeros (JIP 2012)
   Place of meeting: Huelva, Spain **Date of meeting:** April 2012

5. **Authors:** Camilo Zúñiga
   Title: Polybenzoxazines from renewable resources
   Type: Oral presentation and poster
   Congress: CEICS-Nobel Campus –Chemistry for life
   Place of meeting: Tarragona, Spain **Date of meeting:** July 2012

6. **Authors:** Camilo Zúñiga, Gerard Lligadas, Joan C. Ronda, Marina Galià, Virginia Cádiz
   Title: Flame retardant polybenzoxazine foams based on renewable diphenolic acid
   Type: Poster
   Conference: 10th International Conference on Foam Materials & Technology FOAMS 2012
   Place of meeting: Barcelona, Spain **Date of meeting:** September 2012

7. **Authors:** Camilo Zúñiga, Gerard Lligadas, Joan C. Ronda, Marina Galià, Virginia Cádiz
   Title: Flame retardant polybenzoxazine foams based on renewable diphenolic acid and phosphorus compounds
   Type: Poster
   Symposium: The Third International Symposium Frontiers in Polymer Science
   Place of meeting: Sitges, Spain **Date of meeting:** May 2013

Stay abroad

Organization: Université de Mons-Materia Nova
Department: Laboratory of Polymeric and Composite Materials
City: Mons **Country**: Belgium
Length: 4.5 months **Year**: 2012-2013